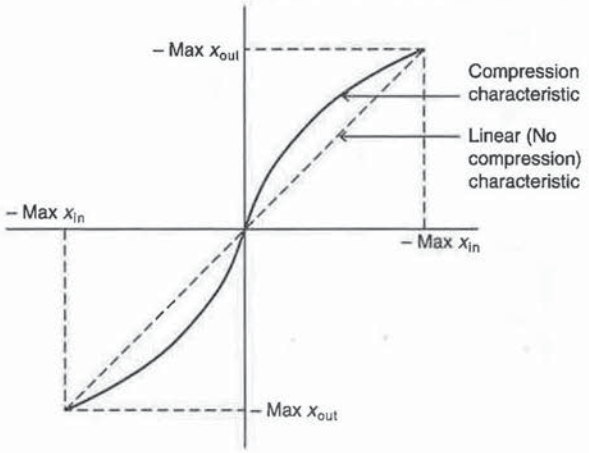
FIGURE 6.22 Input-output compression characteristic

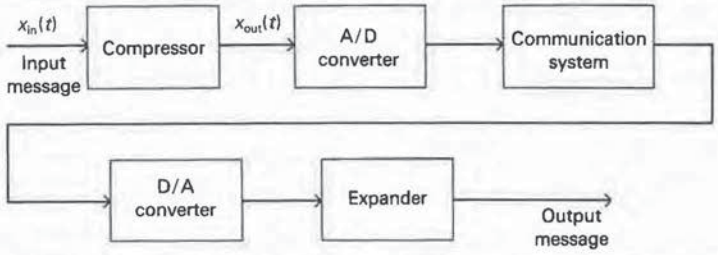


quantizer, in which the quantization steps are chosen so that the mean-square quantization error is minimized. The second technique, and the one of interest here, is to pass the analog signal through a nonlinear amplifier prior to the sampling process. The input-output characteristics of the amplifier are shown in Figure 6.22. For small values of the input x_{in}, the slope of the input-output characteristic is largest. A change in a low-amplitude signal will therefore force the signal through more quantization levels than the same change in a high-amplitude signal. This essentially yields smaller step sizes for small amplitude signals and therefore reduces the quantization error for small amplitude signals. It can be seen from Figure 6.22 that the peaks of the input signal are compressed. For this reason the characteristic shown in Figure 6.22 is known as a compressor.

The effect of the compressor must be compensated for when the signal is returned to analog form. This is accomplished by placing another nonlinear amplifier at the output of the D/A converter. This second nonlinear amplifier is known as an expander and is chosen so that the cascade combination of the compressor and expander yields a linear characteristic, as shown by the dashed line in Figure 6.22. The combination of a compressor and an expander is known as a compander. A companding system is shown in Figure 6.23.

The concept of predistorting a message signal in order to achieve better performance in the presence of noise, and then removing the effect of the predistortion, should remind us of the use of preemphasis and deemphasis filters in the implementation of FM systems.

FIGURE 6.23 Example of companding



SUMMARY

1. The signal-to-noise ratio at the output of a baseband communication system operating in an additive Gaussian noise environment is P_T/N_0W, where P_T is the signal power, N_0 is the single-sided power spectral density of the noise ($\frac{1}{2}N_0$ is the two-sided power spectral density), and W is the signal bandwidth.
2. A double-sideband (DSB) system has an output signal-to-noise ratio of P_T/N_0W assuming perfect phase coherence of the demodulation carrier and a bandwidth of W.
3. A single-sideband (SSB) system also has an output signal-to-noise ratio of P_T/N_0W assuming perfect phase coherence of the demodulation carrier and a bandwidth of W. Thus, under ideal conditions, both SSB and DSB have performance equivalent to the baseband system.
4. An amplitude modulation (AM) system with coherent demodulation achieves an output signal-to-noise ratio of $E(P_T/N_0W)$, where E is the efficiency of the system. An AM system with envelope detection achieves the same output signal-to-noise ratio as an AM system with coherent demodulation for a high signal-to-noise ratio. If the predetection signal-to-noise ratio is small, the signal and noise at the demodulation output become multiplicative rather than additive. The output exhibits severe loss of signal for a small decrease in the input signal-to-noise ratio. This is known as the threshold effect.
5. The square-law detector is a nonlinear system that can be analyzed for all values of P_T/N_0W. Since the square-law detector is nonlinear, a threshold effect is observed.
6. Using a quadrature double-sideband (QDSB) signal model, a generalized analysis is easily carried out to determine the combined effect of both additive noise and demodulation phase errors on a communication system. The result shows that SSB and QDSB are equally sensitive to

demodulation phase errors if the power in the two QDSB signals is equal. DSB is much less sensitive to demodulation phase errors than SSB or QDSB because SSB and QDSB both exhibit crosstalk between the quadrature channels for nonzero demodulation phase errors.

7. The analysis of angle modulation systems shows that the output noise is suppressed as the signal carrier amplitude is increased. Thus the demodulator noise power output is a function of the input signal power.
8. The demodulator output power spectral density is constant over the range $|f| < W$ for PM and is parabolic over the range $|f| < W$ for FM. The parabolic power spectral density for an FM system is due to the fact that FM demodulation is essentially a differentiation process.
9. The demodulated output signal-to-noise ratio is proportional to k_p^2 for PM, where k_p is the phase-deviation constant. The output signal-to-noise ratio is proportional to D^2 for an FM system, where D is the deviation ratio.
10. The use of preemphasis and deemphasis can significantly improve the noise performance of an FM system. Typical values result in a better than 10-dB improvement in the signal-to-noise ratio of the demodulated output.
11. As the input signal-to-noise ratio of an FM system is reduced, spike noise appears. The spikes are due to origin encirclements of the total (Gaussian plus spike) noise phasor. The area of the spikes is constant at 2π, and the power spectral density is proportional to the spike frequency. Since the predetection bandwidth must be increased as the modulation index is increased, resulting in a decreased predetection signal-to-noise ratio, the threshold value of P_T/N_0W increases as the modulation index increases.
12. Threshold extension can be achieved using a phase-lock loop or a frequency-compressive feedback loop.
13. An analysis of nonlinear analog pulse modulation shows that, like FM, a tradeoff exists between bandwidth and output signal-to-noise ratio. With pulse code modulation, the signal-to-noise ratio and the system bandwidth are determined by the number of quantizing levels.
14. A most important result for this chapter is the postdetection signal-to-noise ratios for various modulation methods. A summary of these results is given in Table 6.1. Given in this table is the postdetection SNR for each technique as well as the required transmission bandwidth. The tradeoff between postdetection SNR and transmission bandwidth is evident.

TABLE 6.1 Summary of Noise Performance Characteristics

System	Postdetection SNR	Transmission Bandwidth
Baseband	$\frac{P_T}{N_0 W}$	W
DSB with coherent demodulation	$\frac{P_T}{N_0 W}$	$2W$
SSB with coherent demodulation	$\frac{P_T}{N_0 W}$	W
AM with envelope detection (above threshold) or AM with coherent demodulation. *Note*: E is efficiency	$\frac{EP_T}{N_0 W}$	$2W$
AM with square-law detection	$2\left(\frac{a^2}{2+a^2}\right)^2 \frac{P_T/N_0 W}{1+(N_0 W/P_T)}$	$2W$
PM above threshold	$k_p^2 \overline{m^2} \frac{P_T}{N_0 W}$	$2(D+1)W$
FM above threshold (without preemphasis)	$3D^2 \overline{m_n^2} \frac{P_T}{N_0 W}$	$2(D+1)W$
FM above threshold (with preemphasis)	$\left(\frac{f_d}{f_3}\right)^2 \overline{m^2} \frac{P_T}{N_0 W}$	$2(D+1)W$

FURTHER READING

All the books cited at the end of Chapter 3 contain material about noise effects in the systems studied in this chapter. The books by Lathi (1983), Haykin (1989), and Shanmugam (1979) are especially recommended for their completeness. The book by Taub and Schilling (1986) contains excellent sections on both PCM systems and threshold effects in FM systems.

PROBLEMS

Section 6.1

6.1 A baseband system, as shown in Figure 6.1, uses an nth-order Butterworth lowpass filter to enhance the signal-to-noise ratio. The 3-dB frequency of the Butterworth filter is $W \ll B$. Assuming that the signal is completely passed by the filter, determine the signal-to-noise ratio at the lowpass filter output as a function of the filter order, n. Write the result in the form

$$\text{SNR} = f(n)\frac{P_T}{N_0 W}$$

and plot $f(n)$ for values of n in the range $1 \leq n \leq 6$.

6.2 Derive the equation for $y_D(t)$ for an SSB system assuming that the noise is expanded about the frequency $\omega_x = \omega_c \pm \frac{1}{2}(2\pi W)$. Derive the detection gain and $(\text{SNR})_D$. Determine and plot $S_{n_c}(f)$ and $S_{n_s}(f)$.

6.3 Derive an expression for the detection gain of a DSB system for the case in which the bandwidth of the bandpass predetection filter is B_T and the bandwidth of the lowpass postdetection filter is B_D. Let $B_T > 2W$ and let $B_D > W$ simultaneously, where W is the bandwidth of the modulation. (There are two reasonable cases to consider.)

6.4 Repeat Problem 6.3 for an AM signal.

6.5 Assume that an AM system operates with an index of 0.7 and that the message signal is $15 \cos 8\pi t$. Compute the efficiency, the detection gain in decibels, and the output signal-to-noise ratio in decibels relative to the baseband performance P_T/N_0W. Determine the improvement (in decibels) in the output signal-to-noise ratio that results if the modulation index is increased from 0.7 to 0.9.

6.6 An AM system has a message signal that has a zero-mean Gaussian amplitude distribution. The peak value of $m(t)$ is taken as that value that $|m(t)|$ exceeds 0.5% of the time. If the index is 0.5, what is the detection gain?

6.7 The threshold level for an envelope detector is sometimes defined as that value of $(\text{SNR})_T$ for which $A_c > r_n$ with probability 0.99. Assuming that $a^2\overline{m_n^2} \cong 1$, derive the signal-to-noise ratio at threshold, expressed in decibels.

6.8 An envelope detector operates above threshold. The modulating signal is a sinusoid. Plot $(\text{SNR})_D$ in decibels as a function of P_T/N_0W for the modulation index equal to 0.5, 0.7, and 0.9.

6.9 A square-law demodulator for AM is illustrated in Figure 6.24. Assuming that

$$x_c(t) = A_c[1 + am_n(t)] \cos \omega_c t$$

FIGURE 6.24

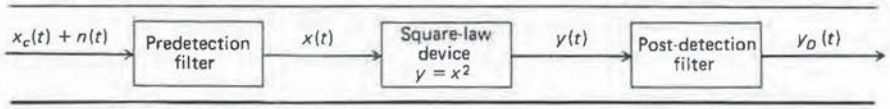
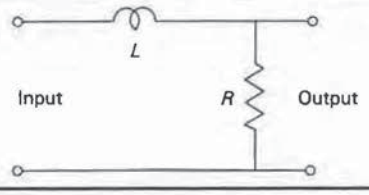


FIGURE 6.25



show that $y_D(t) = r^2(t)$, where $r^2(t)$ is defined by Equation (6.47). Let $m_n(t) = \cos \omega_m t$, and sketch the spectrum of each term that appears in $y_D(t)$. Do not neglect the noise power.

6.10 Compute $(\text{SNR})_D$ as a function of P_T/N_0W for a linear envelope detector assuming a high predetection SNR and a modulation index of unity. Compare this result to that for a square-law detector, and show that the square-law detector is inferior by approximately 1.8 dB.

6.11 The input to the filter shown in Figure 6.25 is $A \cos (2\pi f_c t)$ plus white noise with double-sided power spectral density $\frac{1}{2}N_0$. Compute the SNR at the filter output in terms of N_0, A, R, L, and f_c.

6.12 Repeat the preceding problem for the filter shown in Figure 6.26, writing the SNR in terms of N_0, A, R, C, and f_c.

6.13 Consider the system shown in Figure 6.27, in which an RC highpass filter is followed by an ideal lowpass filter having bandwidth W. Assume that the input to the system is $A \cos (2\pi f_c t)$, where $f_c < W$, plus white noise with double-sided power spectral density $\frac{1}{2}N_0$. Determine the SNR at the output of the ideal lowpass filter in terms of N_0, A, R, C, W, and f_c. What is the SNR in the limit as $W \to \infty$?

6.14 Compare the inprovement in $(\text{SNR})_D$ of a linear envelope detector over a square-law detector for a high-predetection SNR as the modulation index is varied. Assume a sinusoidal message signal.

FIGURE 6.26

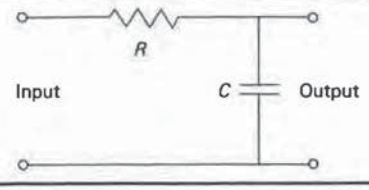
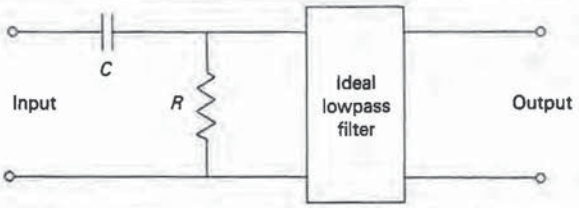


FIGURE 6.27



6.15 An AM system operates with a message signal that is a sample function of a zero-mean Gaussian process. The predetection signal-to-noise ratio is high, and envelope detection is used. The normalized message $m_n(t)$ is such that $|m_n(t)|$ exceeds 1 with probability 0.01. Determine the variance of $m_n(t)$, and plot $(\text{SNR})_D$ as a function of P_T/N_0W for index a in the range $0 \leq a \leq 1$.

Section 6.2

6.16 Assume that a linear modulation system has negligible noise in the passband of the predetection filter. Sketch the normalized mean-square error as a function of the phase-error variance of the demodulation carrier for SSB, QDSB, and DSB. Comment on the significance of these curves.

6.17 Starting with (6.68) derive an expression for the mean-square error at the output of a coherent demodulator in the presence of noise and demodulation phase errors. Expand $\cos\phi$, $\cos^2\phi$, and $\sin^2\phi$ using power series expansions and discard all terms involving ϕ^k for $k > 4$. Show that the result is

$$\overline{\epsilon^2} = \tfrac{3}{4}\sigma_{m_1}{}^2\sigma_\phi{}^2 + \sigma_{m_2}{}^2\sigma_\phi{}^2 - \sigma_{m_2}{}^2\sigma_\phi{}^4 + \sigma_n{}^4$$

Show that, under appropriate assumptions, this result implies (6.71) and (6.77).

6.18 An SSB system is to be operated with a normalized mean-square error of 0.1 or less. By making a plot of output SNR versus demodulation phase-error variance for the case in which normalized mean-square error is 0.1%, show the region of satisfactory system performance. Repeat for a DSB system. Plot both curves on the same set of axes.

6.19 A DSB communication system is implemented as shown in Figure 6.10. The pilot frequency is k times the carrier frequency. Let the

bandwidth of the predetection filter be α times the bandwidth of the pilot filter, and let ρ equal the pilot signal-to-noise ratio at the pilot filter output. Assume the pilot power is equal to the power in the modulating signal. Derive an expression for the normalized mean-square error of the system in terms of k, α, and ρ. Plot the normalized mean-square error as a function of α for ρ equal to 15 dB and k equal to 4.

6.20 It was shown in Chapter 2 that the output of a distortionless linear system is given by

$$y(t) = Ax(t - \tau)$$

where A is the gain of the system, τ is the system time delay, and $x(t)$ is the system input. It is often convenient to evaluate the performance of a linear system by comparing the system output with an amplitude-scaled and time-delayed version of the input. The mean-square error is then

$$\overline{\epsilon^2(A, \tau)} = \overline{[y(t) - Ax(t - \tau)]^2}$$

The values of A and τ that minimize this expression, denoted A_m and τ_m, respectively, are defined as the system gain and the system time delay. Show that, with these definitions, the system gain is

$$A_m = \frac{R_{xy}(\tau_m)}{R_x(0)}$$

and the resulting system mean-square error is

$$\overline{\epsilon^2(A_m, \tau_m)} = R_y(0) - \frac{R_{xy}^2(\tau_m)}{R_x(0)}$$

Also show that the signal power at the system output is

$$S_D = A_m^2 R_x(0) = \frac{R_{xy}^2(\tau_m)}{R_x(0)}$$

and the output signal-to-noise ratio is

$$\frac{S_D}{N_D} = \frac{R_{xy}^2(\tau_m)}{R_x(0)R_y(0) - R_{xy}^2(\tau_m)}$$

in which N_D is the mean-square error.*

* For a discussion of these techniques, see Houts and Simpson (1968).

6.21 A linear system has the input

$$x(t) = 6 \cos (20\pi t) + 3 \cos (40\pi t)$$

and the output

$$y(t) = 3 \cos \left(20\pi t - \frac{\pi}{2} \right) + 2 \cos \left(40\pi t - \frac{3\pi}{4} \right)$$

Using the definitions of system gain and system time delay given in the previous problem, determine the gain, A_m, and time delay, τ_m, of this system. Also, determine the signal-to-noise ratio, in decibels, at the system output using the system input, $x(t)$, as the reference.

Section 6.3

6.22 The process of stereophonic broadcasting was illustrated in Chapter 3. By comparing the noise power in the $l(t) - r(t)$ channel to the noise power in the $l(t) + r(t)$ channel, explain why stereophonic broadcasting is more sensitive to noise than nonstereophonic broadcasting.

6.23 An FDM communication system uses DSB modulation to form the baseband and FM modulation for transmission of the baseband. Assume that there are 8 channels and that all 8 message signals have equal power P_0 and equal bandwidth W. One channel does *not* use subcarrier modulation. The other channels use subcarriers of the form

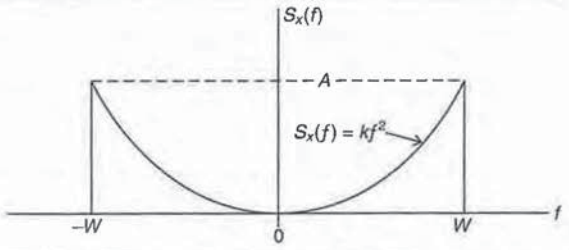
$$A_k \cos k\omega_1 t, \qquad 1 \leq k \leq 7$$

The width of the guardbands is $4W$. Sketch the power spectrum of the received *baseband* signal showing both the signal and noise components. Calculate the relationship between the values of A_k if the channels are to have equal signal-to-noise ratios.

6.24 Using Equation (6.130), derive an expression for the ratio of the noise power in $y_D(t)$ with deemphasis to the noise power in $y_D(t)$ without deemphasis. Plot this ratio as a funtion of W/f_3. Evaluate the ratio for the standard values of $f_3 = 2.1$ kHz and $W = 15$ kHz, and use the result to determine the improvement, in decibels, that results through the use of deemphasis. Compare the result with that found in Example 6.3.

6.25 White noise with two-sided power spectral density $\frac{1}{2}N_0$ is added to a signal having the power spectral density shown in Figure 6.28. The sum (signal plus noise) is filtered with an ideal lowpass filter with

FIGURE 6.28



unity passband gain and bandwidth $B > W$. Determine the signal-to-noise ratio at the filter output. By what factor will the signal-to-noise ratio increase if B is reduced to W?

6.26 Consider the system shown in Figure 6.29. The signal $x(t)$ is defined by

$$x(t) = A \cos 2\pi f_c t$$

The lowpass filter has unity gain in the passband and bandwidth W, where $f_c < W$. The noise $n(t)$ is white with two-sided power spectral density $\frac{1}{2}N_0$. The signal component of $y(t)$ is defined to be the component at frequency f_c. Determine the signal-to-noise ratio of $y(t)$.

6.27 Repeat the preceding problem for the system shown in Figure 6.30.

6.28 Consider the system shown in Figure 6.31. The noise is white with two-sided power spectral density $\frac{1}{2}N_0$. The power spectral density of the signal is

$$S_x(f) = \frac{A}{1 + (f/f_3)^2}, \qquad -\infty < f < \infty$$

FIGURE 6.29

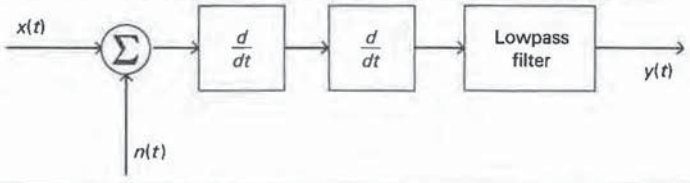
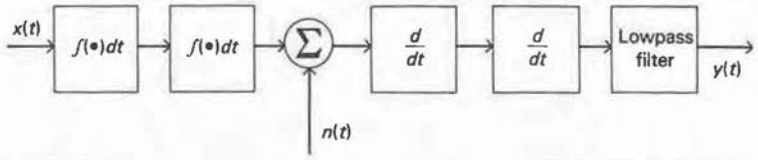


FIGURE 6.30



The parameter f_3 is the 3-dB frequency of the signal. The bandwidth of the lowpass filter is W. Determine the signal-to-noise ratio of $y(t)$. Plot the signal-to-noise ratio as a function of W/f_3.

Section 6.4

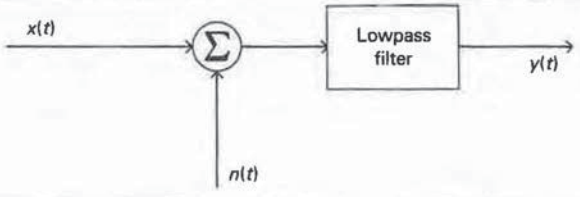
6.29 Derive an expression that illustrates the ratio of spike noise to Gaussian noise power at the output of an FM discriminator. Your answer should be a function of the deviation ratio D and P_T/N_0W. Assume an unmodulated carrier. Plot your answer as a function of P_T/N_0W for $D = 5$. At what value of P_T/N_0W does the spike noise power equal the Gaussian noise power? What happens to this value as D is changed?

6.30 Derive an expression, similar to Equation (6.155), that gives the output signal-to-noise ratio of an FM discriminator for the case in which the message signal is random with a Gaussian amplitude probability density function.

Section 6.5

6.31 Assume that a PPM system uses Nyquist rate sampling and that the minimum channel bandwidth is used for a given pulse duration. Show that the postdetection SNR can be written as

FIGURE 6.31



$$(\text{SNR})_D = K\left(\frac{B_T}{W}\right)^2 \frac{P_T}{N_0 W}$$

and evaluate K.

6.32 The message signal on the input to an analog-to-digital converter is a sinusoid of 15 V peak-to-peak. Compute the signal-to-quantization-noise power ratio as a function of the wordlength of the analog-to-digital converter. State any assumptions you make.



COMPUTER EXERCISES

6.1 Develop a set of performance curves, similar to those shown in Figure 6.9, that illustrate the performance of a coherent demodulator as a function of the phase error variance. Let the signal-to-noise ratio (SNR) be a parameter and express the SNR in decibels. As in Figure 6.9, assume a QDSB system. Repeat this exercise for a DSB system.

6.2 In many problems of practical interest it is important to know the total noise power at the output of an FM discriminator in which the discriminator input consists of an unmodulated sinusoid plus bandlimited white Gaussian noise. Give the expression for the noise power at the output of the postdetection filter as a function of B_T, W, P_T, and N_0, where each of these terms is defined in Section 6.3. Assume that the discriminator constant K_D is 1. Plot, on a log scale, the normalized noise power, N_D/B_T^2, as a function of the predetection SNR, $A_c^2/2N_0B_T$, expressed in decibels. Develop a second set of curves in which N_D/B_T^2 is shown as a function of P_T/N_0W, expressed in decibels. What do you conclude from the result of this exercise?

6.3 Develop a computer program to verify the FM discriminator performance characteristics illustrated in Figure 6.18. Use the resulting program to generate a set of performance curves for $\beta = 1$, 3, 5, 10, and 20. On a second set of axes plot the performance characteristic for $\beta = 0.01$. Is the threshold effect more or less pronounced? Why?

6.4 The value of the input signal-to-noise ratio at threshold is often defined as the value of P_T/N_0W at which the denominator of (6.155) is equal to 2. Note that this value yields a postdetection signal-to-noise ratio, $(\text{SNR})_D$, that is 3 dB below the value of $(\text{SNR})_D$ predicted by the above threshold (linear) analysis. Using this definition of threshold, plot the threshold value of P_T/N_0W, in decibels, as a function of β. What do you conclude?

6.5 In analyzing the performance of an FM discriminator, operating in the presence of noise, the postdetection signal-to-noise ratio, $(\text{SNR})_D$, is often determined using the approximation that the effect of modulation on $(\text{SNR})_D$ is negligible. In other words, $|\overline{\delta f}|$ is set equal to zero. Assuming sinusoidal modulation, investigate the error induced by making this approximation.

6.6 Develop a computer program to verify the performance curves shown in Figure 6.21. Compare the performance of the noncoherent FSK system to the performance of both coherent FSK and coherent PSK with a modulation index of 1. We will show in the following chapter that the bit-error probability for coherent FSK is

$$P_b = Q\left(\sqrt{\frac{P_T}{N_0 B_p}}\right)$$

and that the bit-error probability for coherent BPSK with a unity modulation index is

$$P_b = Q\left(\sqrt{\frac{2P_T}{N_0 B_p}}\right)$$

where B_p is the system bit-rate bandwidth. Compare the results of the three systems studied in this example for $n = 8$.

BINARY DATA TRANSMISSION 7

In Chapter 6 we studied the effects of noise in analog communication systems. We now consider a distinctly different situation. Instead of being concerned with continuous-time, continuous-level message signals, we are concerned with the transmission of information from sources that produce discrete symbols. That is, the input signal to the transmitter block of Figure 1.1 would be a signal that assumes only discrete values.

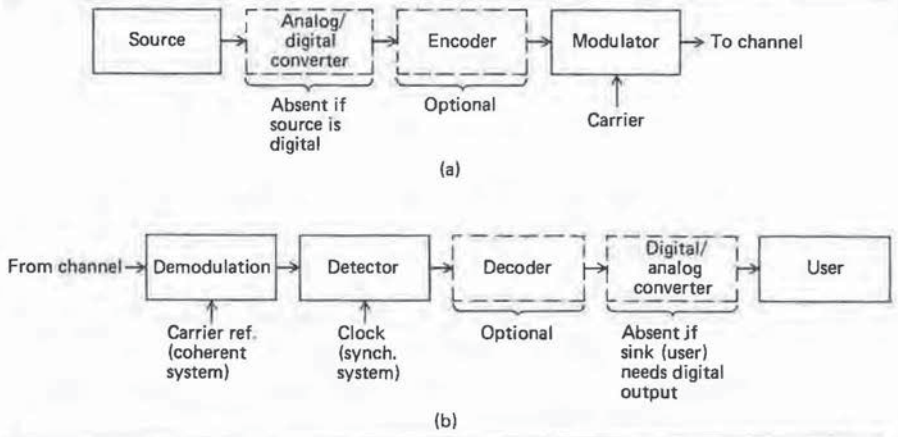
The purpose of this chapter is to consider various systems for the transmission of digital data and their relative performances. Before beginning, however, let us consider the block diagram of a digital data transmission system, shown in Figure 7.1, which is somewhat more detailed than Figure 1.1. The focus of our attention will be on the portion of the system between the optional blocks labeled *Encoder* and *Decoder*. In order to gain a better perspective of the overall problem of digital data transmission, we will briefly discuss the operations performed by the blocks shown as dashed lines.

While many sources result in message signals that are inherently digital, such as from computers, it is often advantageous to represent analog signals in digital form (referred to as *analog-to-digital conversion*) for transmission and then convert them back to analog form upon reception (referred to as *digital-to-analog conversion*), as discussed in the preceding chapter. Pulse code modulation (PCM), introduced in Chapter 3, is an example of a modulation technique that can be employed to transmit analog messages in digital form. The signal-to-noise ratio performance characteristics of a PCM system, which were presented in Chapter 6, show one advantage of this system to be the option of exchanging bandwidth for signal-to-noise ratio improvement.*

Regardless of whether a source is purely digital or an analog source that

* A device for converting voice signals from analog to digital and from digital to analog form is known as a *vocoder*. See, for example, Qualcomm's technical data sheet for the Q4400 variable rate vocoder. Qualcomm, Inc., VLSI Products, 10555 Sorrento Valley Road, San Diego, CA 92121-1617.

FIGURE 7.1 Block diagram of a digital data system. (a) Transmitter. (b) Receiver.



has been converted to digital, it may be advantageous to add or remove redundant digits to the digital signal. Such procedures, referred to as *coding*, are performed by the encoder-decoder blocks of Figure 7.1 and will be considered in Chapter 10.

We now consider the basic system in Figure 7.1, shown as the blocks with solid lines. If the digital signals at the modular input take on one of only two possible values, the communication system is referred to as *binary*. If one of $M > 2$ possible values is available, the system is referred to as *M-ary*. For long-distance transmission, these digital baseband signals from the source may modulate a carrier before transmission, as briefly mentioned in Chapter 3. The result is referred to as *amplitude-shift keying* (ASK), *phase-shift keying* (PSK), or *frequency-shift keying* (FSK) if it is amplitude, phase, or frequency, respectively, that is varied in accordance with the baseband signal. An important *M*-ary modulation scheme, *quadriphase-shift keying* (QPSK), is often employed in situations in which bandwidth efficiency is a consideration. Other schemes related to QPSK include offset QPSK and minimum-shift keying (MSK). These schemes will be discussed in Chapter 8.

A digital communication system is referred to as *coherent* if a local reference is available for demodulation that is in phase with the transmitted carrier (with fixed phase shifts due to transmission delays accounted for). Otherwise, it is referred to as *noncoherent*. Likewise, if a periodic signal is available at the receiver that is in synchronism with the transmitted sequence of digital signals (referred to as a *clock*), the system is referred to as *synchronous;* if a signaling technique is employed in which such a clock is unnecessary, the system is called *asynchronous*.

The primary measure of system performance for digital data communication systems is the probability of error P_E. In this chapter we will obtain expressions for P_E for various types of digital communication systems. We are, of course, interested in receiver structures that give minimum P_E for given conditions. Synchronous detection in a white Gaussian-noise background requires a correlation or a *matched filter* detector to give minimum P_E for fixed signal and noise conditions.

We begin our consideration of digital data transmission systems in Section 7.1 with the analysis of a simple, synchronous baseband system that employs a special case of the matched filter detector known as an *integrate-and-dump detector*. This analysis is then generalized in Section 7.2 to the matched-filter receiver. Section 7.3 contains several specializations of the results of Section 7.2 to common coherent digital signaling schemes, while noncoherent schemes are analyzed in Section 7.4. After analyzing these modulation schemes, which operate in an ideal environment in the sense that infinite bandwidth is available, we look at optimum signaling through bandlimited baseband channels in Section 7.5. In Sections 7.6 and 7.7, the effect of multipath interference and signal fading on data transmission is analyzed, and in Section 7.8, the use of equalizing filters to mitigate the effects of channel distortion is examined.

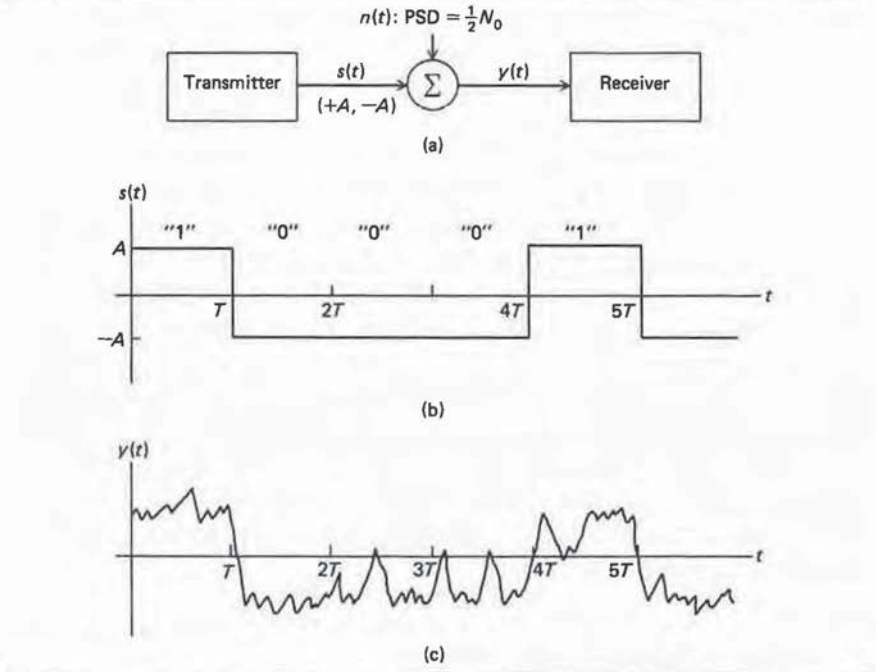
7.1 BASEBAND DATA TRANSMISSION IN WHITE GAUSSIAN NOISE

Consider the binary digital data communication system illustrated in Figure 7.2(a), in which the transmitted signal consists of a sequence of constant-amplitude pulses of either A or $-A$ units in amplitude and T seconds in duration. A typical transmitted sequence is shown in Figure 7.2(b). We may think of a positive pulse as representing a logic 1 and a negative pulse as representing a logic 0 from the data source. Each T-second pulse is called a *binit* for binary digit or, more simply, a *bit*. (In Chapter 10, the term *bit* will take on a new meaning.)

As in Chapter 6, the channel is idealized as simply adding white Gaussian noise with double-sided power spectral density $\frac{1}{2}N_0$ to the signal. A typical sample function of the received signal plus noise is shown in Figure 7.2(c). For sketching purposes, it is assumed that the noise is bandlimited, although it is modeled as white noise later when the performance of the receiver is analyzed. It is assumed that the starting and ending times of each pulse are known by the receiver. The problem of acquiring this information, referred to as *synchronization,* will not be considered at this time.

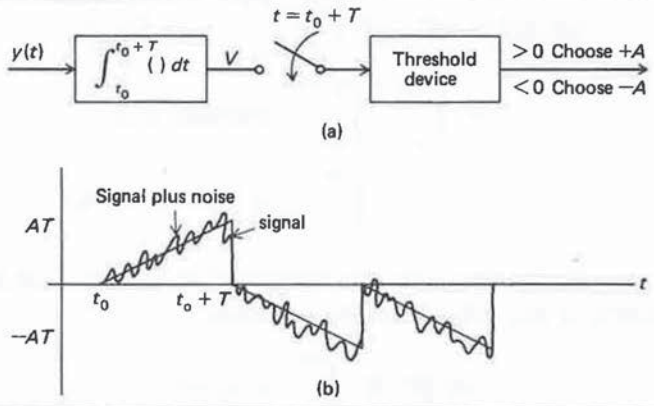
The function of the receiver is to decide whether the transmitted signal

FIGURE 7.2 System model and waveforms for synchronous baseband digital data transmission. (a) Baseband digital data communication system. (b) Typical transmitted sequence. (c) Received sequence plus noise.



was A or $-A$ during each bit period. A straightforward way of accomplishing this is to pass the signal plus noise through a lowpass predetection filter, sample its output at some time within each T-second interval, and determine the sign of the sample. If the sample is greater than zero, the decision is made that $+A$ was transmitted. If the sample is less than zero, the decision is that $-A$ was transmitted. With such a receiver structure, however, we do not take advantage of everything known about the signal. Since the starting and ending times of the pulses are known, a better procedure is to compare the area of the received signal-plus-noise waveform (data) with zero at the end of each signaling interval by integrating the received data over the T-second signaling interval. Of course, a noise component is present at the output of the integrator, but since the input noise has zero mean, it takes on positive and negative values with equal probability. Thus the output noise component has zero mean. The proposed receiver structure and a typical

FIGURE 7.3 Receiver structure and integrator output. (a) Integrate-and-dump receiver. (b) Output from the integrator.



waveform at the output of the integrator are shown in Figure 7.3 where t_0 is the start of an arbitrary signaling interval. For obvious reasons, this receiver is referred to as an integrate-and-dump detector.

The question to be answered is: How well does this receiver perform, and on what parameters does its performance depend? As mentioned previously, a useful criterion of performance is probability of error, and it is this we now compute. The output of the integrator at the end of a signaling interval is

$$\begin{aligned} V &= \int_{t_0}^{t_0+T} [s(t) + n(t)]\, dt \\ &= \begin{cases} +AT + N & \text{if } +A \text{ is sent} \\ -AT + N & \text{if } -A \text{ is sent} \end{cases} \end{aligned} \tag{7.1}$$

where N is a random variable defined as

$$N = \int_{t_0}^{t_0+T} n(t)\, dt \tag{7.2}$$

Since N results from a linear operation on a sample function from a Gaussian process, it is a Gaussian random variable. It has mean

$$E\{N\} = E\left\{\int_{t_0}^{t_0+T} n(t)\, dt\right\} = \int_{t_0}^{t_0+T} E\{n(t)\}\, dt = 0 \tag{7.3}$$

since $n(t)$ has zero mean. Its variance is therefore

$$\begin{aligned} \text{var}\,\{N\} &= E\{N^2\} = E\left\{\left[\int_{t_0}^{t_0+T} n(t)\,dt\right]^2\right\} \\ &= \int_{t_0}^{t_0+T}\int_{t_0}^{t_0+T} E\{n(t)n(\sigma)\}\,dt\,d\sigma \\ &= \int_{t_0}^{t_0+T}\int_{t_0}^{t_0+T} \tfrac{1}{2}N_0\,\delta(t-\sigma)\,dt\,d\sigma \end{aligned} \tag{7.4}$$

where we have made the substitution $E\{n(t)n(\sigma)\} = \frac{1}{2}N_0\,\delta(t-\sigma)$. Using the sifting property of the delta function, we obtain

$$\begin{aligned} \text{var}\,\{N\} &= \int_{t_0}^{t_0+T} \tfrac{1}{2}\,N_0\,d\sigma \\ &= \tfrac{1}{2}N_0T \end{aligned} \tag{7.5}$$

Thus the pdf of N is

$$f_N(\eta) = \frac{e^{-\eta^2/N_0T}}{\sqrt{\pi N_0 T}} \tag{7.6}$$

where η is used as the dummy variable for N to avoid confusion with $n(t)$.

There are two ways in which errors occur. If $+A$ is transmitted, an error occurs if $AT + N < 0$, that is, if $N < -AT$. From (7.6), the probability of this event is

$$P(\text{error}\,|\,A \text{ sent}) = P(E\,|\,A) = \int_{-\infty}^{-AT} \frac{e^{-\eta^2/N_0T}}{\sqrt{\pi N_0 T}}\,d\eta \tag{7.7}$$

which is the area to the left of $\eta = -AT$ in Figure 7.4. Letting $u = -\sqrt{2}\eta/\sqrt{N_0T}$, we can write this as*

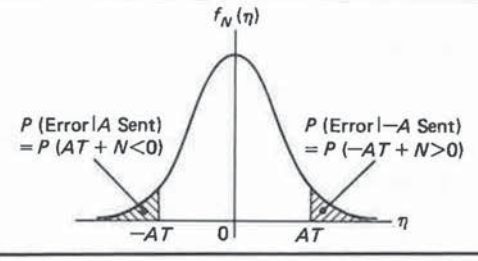
$$P(E\,|\,A) = \int_{\sqrt{2A^2T/N_0}}^{\infty} \frac{e^{-u^2/2}}{\sqrt{2\pi}}\,du \triangleq Q\left(\sqrt{\frac{2A^2T}{N_0}}\right) \tag{7.8}$$

The other way in which an error can occur is if $-A$ is transmitted and $-AT + N > 0$. The probability of this event is the same as the probability that $N > AT$, which can be written as

$$P(E\,|\,-A) = \int_{AT}^{\infty} \frac{e^{-\eta^2/N_0T}}{\sqrt{\pi N_0 T}}\,d\eta \triangleq Q\left(\sqrt{\frac{2A^2T}{N_0}}\right) \tag{7.9}$$

* See Appendix C.6 for a discussion and tabulation of the Q-function.

FIGURE 7.4 Illustration of error probabilities for binary signaling



which is the area to the right of $\eta = AT$ in Figure 7.4. The average probability of error is

$$P_E = P(E|+A)P(+A) + P(E|-A)P(-A) \tag{7.10}$$

Substituting (7.8) and (7.9) into (7.10) and noting that $P(+A) + P(-A) = 1$, we obtain

$$P_E = Q\left(\sqrt{\frac{2A^2T}{N_0}}\right) \tag{7.11}$$

Thus the important parameter is A^2T/N_0. We can interpret this ratio in two ways. First, since the energy in each signal pulse is

$$E_b = \int_{t_0}^{t_0+T} A^2\,dt = A^2T \tag{7.12}$$

we see that the ratio of signal energy per pulse to noise power spectral density is

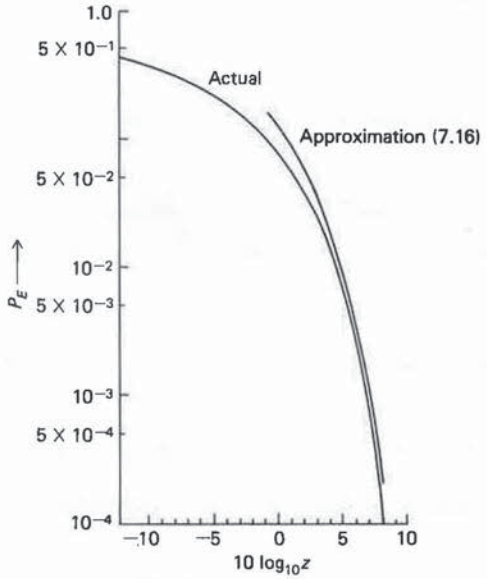
$$z = \frac{A^2T}{N_0} = \frac{E_b}{N_0} \tag{7.13}$$

where E_b is called the *energy per bit* because each signal pulse ($+A$ or $-A$) carries one *bit* of information. Second, we recall that a rectangular pulse of duration T seconds has amplitude spectrum AT sinc Tf and that $B_p = 1/T$ is a rough measure of its bandwidth. Thus

$$z = \frac{A^2}{N_0(1/T)} = \frac{A^2}{N_0B_p} \tag{7.14}$$

can be interpreted as the ratio of signal power to noise power in the signal bandwidth. The bandwidth B_p is sometimes referred to as the *bit-rate band-*

FIGURE 7.5 P_E for baseband signaling



width. We will refer to z as the signal-to-noise ratio (SNR). An often-used reference to this signal-to-noise ratio in the digital communications industry is "E_b-over-N_0."

A plot of P_E versus z is shown in Figure 7.5, where z is given in decibels. Also shown is an approximation for P_E using the asymptotic expansion for the Q-function [Equation (4.187)]:

$$Q(u) \cong \frac{e^{-u^2/2}}{u\sqrt{2\pi}}, \qquad u \gg 1 \tag{7.15}$$

Using this approximation,

$$P_E \cong \frac{e^{-z}}{2\sqrt{\pi z}}, \qquad z \gg 1 \tag{7.16}$$

which shows that P_E essentially decreases exponentially with increasing z. Figure 7.5 shows that the approximation of (7.16) is close to the true result of (7.11) for $z \gtrsim 3$ dB.

EXAMPLE 7.1 Digital data is to be transmitted through a baseband system with $N_0 = 10^{-7}$ W/Hz and the received signal amplitude $A = 20$ mV. (a) If 10^3 bits per second (bps) are transmitted, what is P_E? (b) If 10^4 bps are transmitted, to what value must A be adjusted in order to attain the same P_E as in part (a)?

SOLUTION To solve part (a), note that

$$z = \frac{A^2 T}{N_0} = \frac{(0.02)^2(10^{-3})}{10^{-7}} = 4 \tag{7.17}$$

Using (7.16), $P_E \cong e^{-4}/2\sqrt{4\pi} = 2.58 \times 10^{-3}$. Part (b) is solved by finding A such that $A^2(10^{-4})/(10^{-7}) = 4$, which gives $A = 63.2$ mV.

EXAMPLE 7.2 The conditions are the same as in the preceding example, but a bandwidth of 5000 Hz is available. (a) What is the maximum data rate that can be supported by the channel? (b) Find the transmitter power required to give a probability of error of 10^{-6} at the data rate found in part (a).

SOLUTION (a) Since a rectangular pulse has Fourier transform

$$\Pi(t/T) \leftrightarrow T \operatorname{sinc}(fT)$$

we take the signal bandwidth to be that of the first null of the sinc function. Therefore, $1/T = 5000$ Hz, which implies a maximum data rate of $R = 5000$ bps. (b) To find the transmitter power to give $P_E = 10^{-6}$, we solve

$$10^{-6} = Q\left[\sqrt{2A^2T/N_0}\right] = Q\left[\sqrt{2z}\right] \tag{7.18}$$

Using the approximation (7.15) for the error function, we need to solve

$$10^{-6} = \frac{e^{-z}}{2\sqrt{\pi z}}$$

iteratively. This gives the result

$$z \cong 10.54 \text{ dB} = 11.31 \text{ (ratio)}$$

Thus, $A^2T/N_0 = 11.31$, or

$$A^2 = (11.31)N_0/T = 5.65 \text{ mW (actually V}^2 \times 10^{-3}\text{)}$$

This corresponds to a signal amplitude of approximately 75.2 mV.

7.2 BINARY SYNCHRONOUS DATA TRANSMISSION WITH ARBITRARY SIGNAL SHAPES

In Section 7.1 we analyzed a simple baseband digital communication system. As in the case of analog transmission, it is often necessary to utilize modulation to condition a digital message signal so that it is suitable for transmission through a channel. Thus, instead of the constant-level signals considered in Section 7.1, we will let a logic 1 be represented by $s_1(t)$ and a logic 0 by $s_2(t)$. The only restriction on $s_1(t)$ and $s_2(t)$ is that they must have finite energy in a T-second interval. The energies of $s_1(t)$ and $s_2(t)$ are denoted by

$$E_1 \triangleq \int_{t_0}^{t_0+T} s_1^2(t)\, dt \tag{7.19a}$$

and

$$E_2 \triangleq \int_{t_0}^{t_0+T} s_2^2(t)\, dt \tag{7.19b}$$

respectively. In Table 7.1, several commonly used choices for $s_1(t)$ and $s_2(t)$ are given.

Receiver Structure and Error Probability

A possible receiver structure for detecting $s_1(t)$ or $s_2(t)$ in additive white Gaussian noise is shown in Figure 7.6. Since the signals chosen may have zero average value over a T-second interval (see the examples in Table 7.1), we can no longer employ an integrator followed by a threshold device as in the case of constant-amplitude signals. Instead of the integrator, we employ a filter with, as yet, unspecified impulse response $h(t)$ and corresponding transfer function $H(f)$. The received signal plus noise is either

$$y(t) = s_1(t) + n(t), \qquad t_0 \leq t \leq t_0 + T \tag{7.20a}$$

or

$$y(t) = s_2(t) + n(t), \qquad t_0 \leq t \leq t_0 + T \tag{7.20b}$$

where the noise, as before, is assumed to be white with power spectral density $\frac{1}{2}N_0$. We can assume that $t_0 \doteq 0$ without loss of generality; that is, the signaling interval under consideration is $0 \leq t \leq T$.

To find P_E, we again note that an error can occur in either one of two ways. Assume that $s_1(t)$ and $s_2(t)$ were chosen such that $s_{01}(T) < s_{02}(T)$, where $s_{01}(t)$ and $s_{02}(t)$ are the outputs of the filter due to $s_1(t)$ and $s_2(t)$,

TABLE 7.1 Possible Signal Choices for Binary Digital Signaling

Case	$s_1(t)$	$s_2(t)$	Type of Signaling
1	0	$A \cos \omega_c t$	Amplitude-shift keying
2	$A \sin (\omega_c t + \cos^{-1} m)$	$A \sin (\omega_c t - \cos^{-1} m)$	Phase-shift keying with carrier ($\cos^{-1} m \triangleq$ modulation index)
3	$A \cos \omega_c t$	$A \cos (\omega_c + \Delta\omega)t$	Frequency-shift keying

respectively, at the input. If not, the roles of $s_1(t)$ and $s_2(t)$ at the input can be reversed to ensure this. Referring to Figure 7.6, if $v(T) > k$, where k is the threshold, we decide that $s_2(t)$ was sent; if $v(T) < k$, we decide that $s_1(t)$ was sent. Letting $n_0(t)$ be the noise component at the filter output, an error is made if $s_1(t)$ is sent and $v(T) = s_{01}(T) + n_0(T) > k$; if $s_2(t)$ is sent, an error occurs if $v(T) = s_{02}(T) + n_0(T) < k$. Since $n_0(t)$ is the result of passing white Gaussian noise through a fixed linear filter, it is a Gaussian process. Its power spectral density is

$$S_{n_0}(f) = \tfrac{1}{2}N_0 |H(f)|^2 \tag{7.21}$$

Because the filter is fixed, $n_0(t)$ is a stationary process with mean zero and variance

$$\sigma_0^2 = \int_{-\infty}^{\infty} \tfrac{1}{2}N_0 |H(f)|^2 \, df \tag{7.22}$$

Since $n_0(t)$ is stationary, $N = n_0(T)$ is a random variable with mean zero and variance σ_0^2. Its pdf is

$$f_N(\eta) = \frac{e^{-\eta^2/2\sigma_0^2}}{\sqrt{2\pi\sigma_0^2}} \tag{7.23}$$

Given that $s_1(t)$ is transmitted, the sampler output is

$$V \triangleq v(T) = s_{01}(T) + N \tag{7.24}$$

FIGURE 7.6 A possible receiver structure for detecting binary signals in white Gaussian noise

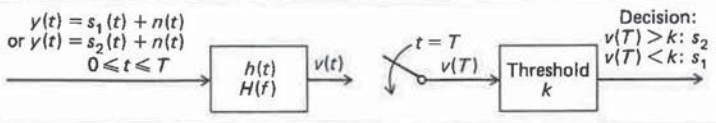
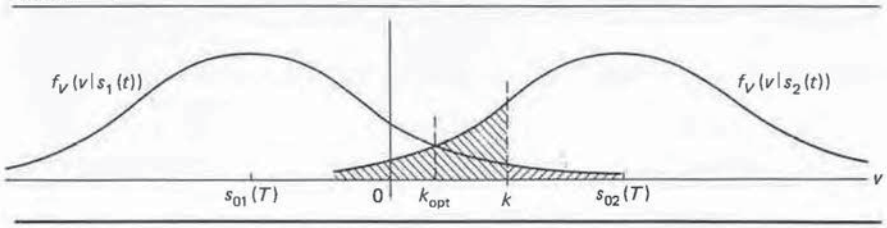


FIGURE 7.7 Conditional probability density functions of the filter output at time $t = T$



and if $s_2(t)$ is transmitted, the sampler output is

$$V \triangleq v(T) = s_{02}(T) + N \tag{7.25}$$

These are also Gaussian random variables, since they result from linear operations on Gaussian random variables. They have means $s_{01}(T)$ and $s_{02}(T)$, respectively, and the same variance as N, that is, σ_0^2. Thus the conditional pdf's of V given $s_1(t)$ is transmitted, $f_V(v|s_1(t))$, and given $s_2(t)$ is transmitted, $f_V(v|s_2(t))$, are as shown in Figure 7.7. Also illustrated is a decision threshold k.

From Figure 7.7, we see that the probability of error, given $s_1(t)$ is transmitted, is

$$\begin{aligned} P(E|s_1(t)) &= \int_k^\infty f_V(v|s_1(t))\, dv \\ &= \int_k^\infty \frac{e^{-[v-s_{01}(T)]^2/2\sigma_0^2}}{\sqrt{2\pi\sigma_0^2}}\, dv \end{aligned} \tag{7.26}$$

which is the area under $f_V(v|s_1(t))$ to the right of $v = k$. Similarly, the probability of error, given $s_2(t)$ is transmitted, which is the area under $f_V(v|s_2(t))$ to the left of $v = k$, is given by

$$P(E|s_2(t)) = \int_{-\infty}^k \frac{e^{-[v-s_{02}(T)]^2/2\sigma_0^2}}{\sqrt{2\pi\sigma_0^2}}\, dv \tag{7.27}$$

Assuming that $s_1(t)$ and $s_2(t)$ are *a priori* equally probable,* the average probability error is

$$P_E = \tfrac{1}{2}P[E|s_1(t)] + \tfrac{1}{2}P[E|s_2(t)] \tag{7.28}$$

The task now is to minimize this error probability by adjusting the threshold k and the impulse response $h(t)$.

* See Problem 7.8 for the case of unequal *a priori* probabilities.

Because of the equal *a priori* probabilities for $s_1(t)$ and $s_2(t)$ and the symmetrical shapes of $f_V(v \mid s_1(t))$ and $f_V(v \mid s_2(t))$, it is reasonable that the optimum choice for k is the intersection of the conditional pdf's, which is

$$k_{\text{opt}} = \tfrac{1}{2}[s_{01}(T) + s_{02}(T)] \tag{7.29}$$

The optimum threshold is illustrated in Figure 7.7 and can be derived by differentiating (7.28) with respect to k after substitution of (7.26) and (7.27). Because of the symmetry of the pdf's, the probabilities of either type of error, (7.26) or (7.27), are equal for this choice of k.

With this choice of k, the probability of error given by (7.28) reduces to

$$P_E = Q\left[\frac{s_{02}(T) - s_{01}(T)}{2\sigma_0}\right] \tag{7.30}$$

Thus we see that P_E is a function of the difference between the two output signals at $t = T$. Remembering that the Q-function decreases monotonically with u, we see that P_E decreases with increasing *distance* between the two output signals, a reasonable result. We will encounter this interpretation again in Chapter 9, where we discuss concepts of signal space.

We now consider the minimization of P_E by proper choice of $h(t)$. This will lead us to the matched filter.

The Matched Filter

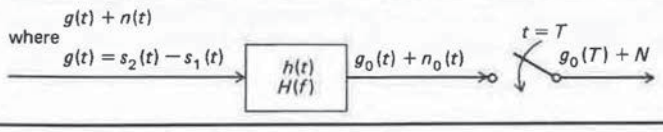
For a given choice of $s_1(t)$ and $s_2(t)$, we wish to determine an $H(f)$, or equivalently, an $h(t)$, that maximizes

$$\zeta = \frac{s_{02}(T) - s_{01}(T)}{\sigma_0} \tag{7.31}$$

Letting $g(t) = s_2(t) - s_1(t)$, the problem is to find the $H(f)$ that maximizes $\zeta = g_0(T)/\sigma_0$, where $g_0(t)$ is the signal portion of the output due to the input $g(t)$. This situation is illustrated in Figure 7.8. We can equally well consider the maximization of

$$\zeta^2 = \frac{g_0^2(T)}{\sigma_0^2} = \left.\frac{g_0^2(t)}{E\{n_0^2(t)\}}\right|_{t=T} \tag{7.32}$$

FIGURE 7.8 Choosing $H(f)$ to minimize P_E



Since the input noise is stationary,

$$E\{n_0^2(t)\} = E\{n_0^2(T)\} = \tfrac{1}{2}N_0 \int_{-\infty}^{\infty} |H(f)|^2 \, df \tag{7.33}$$

We can write $g_0(t)$ in terms of $H(f)$ and the Fourier transform of $g(t)$, $G(f)$, as

$$g_0(t) = \mathcal{F}^{-1}[G(f)H(f)] = \int_{-\infty}^{\infty} H(f)G(f)e^{j2\pi ft} \, df \tag{7.34}$$

Setting $t = T$ in (7.34) and using this result along with (7.33) in (7.32), we obtain

$$\zeta^2 = \frac{\left| \int_{-\infty}^{\infty} H(f)G(f)e^{j2\pi fT} \, df \right|^2}{\frac{1}{2}N_0 \int_{-\infty}^{\infty} |H(f)|^2 \, df} \tag{7.35}$$

To maximize this equation with respect to $H(f)$, we employ *Schwarz's inequality*. Schwarz's inequality is a generalization of the inequality

$$|\mathbf{A} \cdot \mathbf{B}| = |AB \cos \theta| \leq |\mathbf{A}||\mathbf{B}| \tag{7.36}$$

where **A** and **B** are ordinary vectors, with θ the angle between them, and $\mathbf{A} \cdot \mathbf{B}$ denotes their inner, or dot, product. Since $|\cos \theta|$ equals unity if and only if θ equals zero or an integer multiple of π, equality holds if and only if **A** equals $k\mathbf{B}$, where k is a constant. Considering the case of two complex functions $X(f)$ and $Y(f)$, and defining the inner product as

$$\int_{-\infty}^{\infty} X(f)Y^*(f) \, df$$

Schwarz's inequality assumes the form

$$\left| \int_{-\infty}^{\infty} X(f)Y^*(f) \, df \right|^2 \leq \int_{-\infty}^{\infty} |X(f)|^2 \, df \int_{-\infty}^{\infty} |Y(f)|^2 \, df \tag{7.37}$$

Equality holds if and only if $X(f) = kY(f)$ where k is, in general, complex. We will prove Schwarz's inequality in Chapter 9 with the aid of signal-space notation.

We now return to our original problem, that of finding the $H(f)$ that maximizes (7.35). We replace $X(f)$ in (7.37) with $H(f)$ and $Y^*(f)$ with $G(f)e^{j2\pi Tf}$. Thus

$$\zeta^2 = \frac{2}{N_0} \frac{\left| \int_{-\infty}^{\infty} X(f)Y^*(f)\, df \right|^2}{\int_{-\infty}^{\infty} |H(f)|^2\, df} \leq \frac{2}{N_0} \frac{\int_{-\infty}^{\infty} |H(f)|^2\, df \int_{-\infty}^{\infty} |G(f)|^2\, df}{\int_{-\infty}^{\infty} |H(f)|^2\, df} \tag{7.38}$$

Canceling the integral over $|H(f)|^2$ in the numerator and denominator, we find the maximum value of ζ^2 to be

$$\zeta^2_{\max} = \frac{2}{N_0} \int_{-\infty}^{\infty} |G(f)|^2\, df = \frac{2E_g}{N_0} \tag{7.39}$$

where $E_g = \int_{-\infty}^{\infty} |G(f)|^2\, df$ is the energy contained in $g(t)$, which follows by Rayleigh's energy theorem. Equality holds in (7.38) if and only if

$$H(f) = kG^*(f)e^{-j2\pi Tf} \tag{7.40}$$

where k is an arbitrary constant. Since k just fixes the gain of the filter, we can set it to unity. Thus the optimum choice for $H(f)$, $H_0(f)$, is

$$H_0(f) = G^*(f)e^{-j2\pi Tf} \tag{7.41}$$

The impulse response corresponding to this choice of $H_0(f)$ is

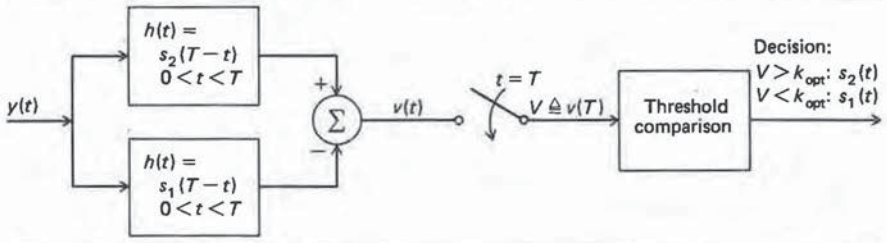
$$\begin{aligned} h_0(t) &= \mathcal{F}^{-1}[H_0(f)] \\ &= \int_{-\infty}^{\infty} G^*(f)e^{-j2\pi Tf}e^{j2\pi ft}\, df \\ &= \int_{-\infty}^{\infty} G(-f)e^{-j2\pi f(T-t)}\, df \\ &= \int_{-\infty}^{\infty} G(f')e^{j2\pi f'(T-t)}\, df' \end{aligned} \tag{7.42}$$

Recognizing this as the inverse Fourier transform of $g(t)$ with t replaced by $T - t$, we obtain

$$h_0(t) = s_2(T - t) - s_1(T - t) = g(T - t) \tag{7.43}$$

Thus, in terms of the original signals, the optimum receiver corresponds to passing the received signal plus noise through two parallel filters whose impulse responses are the time reverses of $s_1(t)$ and $s_2(t)$, respectively, and comparing the difference of their outputs at time T with the threshold given by (7.29). This operation is illustrated in Figure 7.9.

FIGURE 7.9 Matched filter receiver for binary signaling in white Gaussian noise



▼ EXAMPLE 7.3 Consider the pulse signal

$$s(t) = \begin{cases} A, & 0 \le t \le T \\ 0, & \text{otherwise} \end{cases} \tag{7.44}$$

A filter matched to this signal has the impulse response

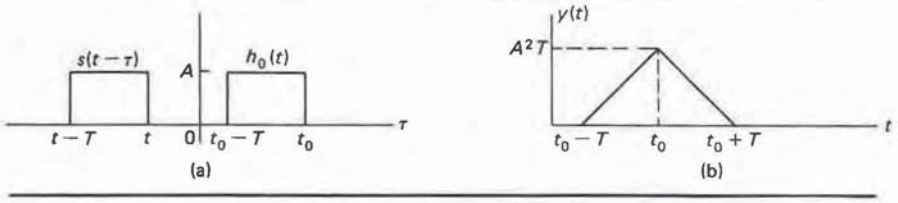
$$h_0(t) = s(t_0 - t) \tag{7.45}$$

where the parameter t_0 will be left to be fixed later. We note that if $t_0 < T$, the filter will be unrealizable, since it will have nonzero impulse response for $t < 0$. The response of the filter to $s(t)$ is

$$y(t) = h_0(t) * s(t) = \int_{-\infty}^{\infty} h_0(\tau)s(t - \tau)\, d\tau \tag{7.46}$$

The factors in the integrand are shown in Figure 7.10(a). The resulting integrations are familiar from our previous considerations of linear systems, and the filter output is easily found to be as shown in Figure 7.10(b). We note that the peak output signal occurs at $t = t_0$. This is also the time of peak-signal-to-rms-noise ratio, since the noise is stationary. Clearly, in digital signaling, we want $t_0 = T$. ▲

FIGURE 7.10 Signals pertinent to finding the matched-filter response of Example 7.3



EXAMPLE 7.4 For a given value of N_0, consider the peak-signal-to-rms-noise ratio at the output of a matched filter for the two pulses

$$g_1(t) = A\Pi\left(\frac{t - t_0}{T}\right) \tag{7.47}$$

and

$$g_2(t) = B\cos\left[\frac{2\pi(t - t_0)}{T}\right]\Pi\left(\frac{t - t_0}{T}\right) \tag{7.48}$$

Relate A and B such that both pulses provide the same signal-to-noise ratio at the matched filter output.

SOLUTION Since the signal-to-noise ratio at the matched filter output is $2E_g/N_0$ and N_0 is the same for both cases, we can obtain equal signal-to-noise ratios for both cases by computing the energy of each pulse and setting the two energies equal. The results are

$$E_{g_1} = \int_{t_0-T/2}^{t_0+T/2} A^2\,dt = A^2T \tag{7.49}$$

$$E_{g_2} = \int_{t_0-T/2}^{t_0+T/2} B^2\cos^2\left[\frac{2\pi(t - t_0)}{T}\right]dt = \frac{B^2T}{2} \tag{7.50}$$

Setting these equal, we have that $A = B/\sqrt{2}$ to give equal signal-to-noise ratios. The peak signal-squared-to-mean-square-noise ratio is

$$\frac{E_g}{N_0} = \frac{A^2T}{N_0} = \frac{B^2T}{2N_0} \tag{7.51}$$

Error Probability for the Matched-Filter Receiver

From (7.30), the error probability for the matched-filter receiver of Figure 7.9 is

$$P_E = Q\left(\frac{\zeta}{2}\right) \tag{7.52}$$

where ζ is the maximum value,

$$\zeta = \left[\frac{2}{N_0}\int_{-\infty}^{\infty}|G(f)|^2\,df\right]^{1/2} = \left[\frac{2}{N_0}\int_{-\infty}^{\infty}|S_2(f) - S_1(f)|^2\,df\right]^{1/2} \tag{7.53}$$

given by (7.39). Using Parseval's theorem, we can write ζ^2 in terms of $g(t) = s_2(t) - s_1(t)$ as

$$\zeta^2 = \frac{2}{N_0}\int_{-\infty}^{\infty}[s_2(t) - s_1(t)]^2\,dt$$
$$= \frac{2}{N_0}\left\{\int_{-\infty}^{\infty}s_2{}^2(t)\,dt + \int_{-\infty}^{\infty}s_1{}^2(t)\,dt - 2\int_{-\infty}^{\infty}s_1(t)s_2(t)\,dt\right\} \quad (7.54)$$

From (7.19), we see that the first two terms inside the braces are E_1 and E_2, respectively. We define

$$\rho_{12} = \frac{1}{\sqrt{E_1E_2}}\int_{-\infty}^{\infty}s_1(t)s_2(t)\,dt \quad (7.55)$$

as the correlation coefficient of $s_1(t)$ and $s_2(t)$. Just as for random variables, ρ_{12} is a measure of the similarity between $s_1(t)$ and $s_2(t)$ and is normalized such that $-1 \leq \rho_{12} \leq 1$ (ρ_{12} achieves the end points for $s_1(t) = \pm ks_2(t)$, where k is a constant). Thus

$$\zeta^2 = \frac{2}{N_0}(E_1 + E_2 - 2\sqrt{E_1E_2}\rho_{12}) \quad (7.56)$$

and the error probability is

$$P_E = Q\left[\sqrt{2}\left(\frac{E_1 + E_2 - 2\sqrt{E_1E_2}\rho_{12}}{N_0}\right)^{1/2}\right] \quad (7.57)$$

It is apparent from (7.57) that in addition to depending on the signal energies, as in the constant-signal case, P_E also depends on the similarity between the signals through ρ_{12}. We note that (7.56) takes on its maximum value of $(2/N_0)(\sqrt{E_1} + \sqrt{E_2})^2$ for $\rho_{12} = -1$, which gives the minimum value of P_E possible as $s_1(t)$ and $s_2(t)$ vary. This is reasonable, for then the transmitted signals are as dissimilar as possible.

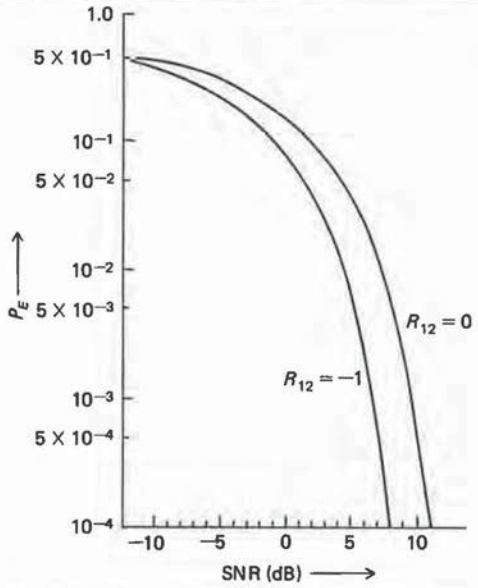
By noting that $E = \frac{1}{2}(E_1 + E_2)$ is the average received signal energy, since $s_1(t)$ and $s_2(t)$ are transmitted with equal *a priori* probability, we can write (7.57) as

$$P_E = Q[\sqrt{z(1 - R_{12})}] \quad (7.58)$$

where z is the average energy per bit divided by noise power spectral density E_b/N_0, as it was for baseband systems. The parameter R_{12} is defined as

$$R_{12} = \frac{2\sqrt{E_1E_2}}{E_1 + E_2}\rho_{12} = \frac{\sqrt{E_1E_2}}{E}\rho_{12} \quad (7.59)$$

FIGURE 7.11 Probability of error for arbitrary waveshape case with $R_{12} = 0$ and $R_{12} = -1$



and is a convenient parameter related to the correlation coefficient, but which should *not* be confused with a correlation function. The minimum value of R_{12} is -1, which is attained for $E_1 = E_2$ and $\rho_{12} = -1$. For this value of R_{12},

$$P_E = Q(\sqrt{2z}) \tag{7.60}$$

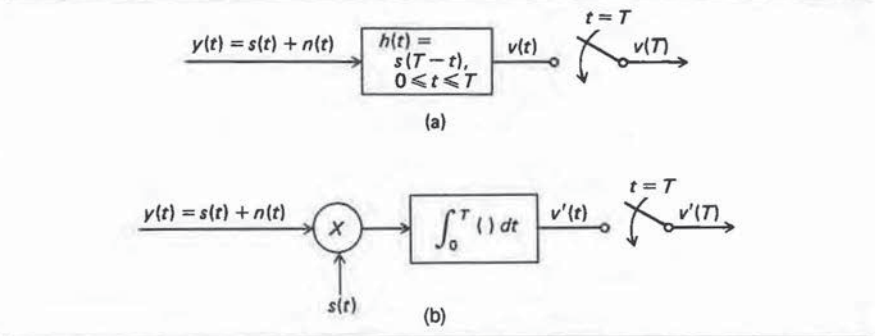
which is identical to (7.11), the result for the baseband system.

The probability of error versus the signal-to-noise ratio is compared in Figure 7.11 for $R_{12} = 0$ (orthogonal signals) and $R_{12} = -1$ (antipodal signals).

Correlator Implementation of the Matched-Filter Receiver

In Figure 7.9, the optimum receiver involves two filters with impulse responses equal to the time reverse of the respective signals being detected. An alternative receiver structure can be obtained by noting that the matched filter in Figure 7.12(a) can be replaced by a multiplier-integrator cascade as shown in Figure 7.12(b). Such a series of operations is referred to as *correlation detection.*

FIGURE 7.12 Equivalence of the matched-filter and correlator receivers. (a) Matched-filter sampler. (b) Correlator sampler.



To show that the operations given in Figure 7.12 are equivalent, we will show that $v(T)$ in Figure 7.12(a) is equal to $v'(T)$ in Figure 7.12(b). The output of the matched filter in Figure 7.12(a) is

$$v(t) = h(t) * y(t) = \int_0^T s(T - \tau)\, y(t - \tau)\, d\tau \tag{7.61}$$

which follows because $h(t) = s(T - t)$, $0 \leq t \leq T$, and zero otherwise. Letting $t = T$ and changing variables in the integrand to $\alpha = T - \tau$, we obtain

$$v(T) = \int_0^T s(\alpha)\, y(\alpha)\, d\alpha \tag{7.62}$$

Considering next the output of the correlator configuration in Figure 7.12(b), we obtain

$$v'(T) = \int_0^T y(t)s(t)\, dt \tag{7.63}$$

which is identical to (7.62). Thus the matched filters for $s_1(t)$ and $s_2(t)$ in Figure 7.9 can be replaced by correlation operations with $s_1(t)$ and $s_2(t)$, respectively, and the receiver operation will not be changed. We note that the integrate-and-dump receiver for the constant signal case of Section 7.1 is actually a correlation or, equivalently, a matched-filter receiver.

Optimum Threshold

The optimum threshold for binary signal detection is given by (7.29), where $s_{01}(T)$ and $s_{02}(T)$ are the outputs of the detection filter in Figure 7.6 at time

T due to the input signals $s_1(t)$ and $s_2(t)$, respectively. We now know that the optimum detection filter is a matched filter, matched to the difference of the input signals, and has impulse response given by (7.43). From the superposition integral, we have

$$\begin{aligned} s_{01}(T) &= \int_{-\infty}^{\infty} h(\lambda)s_1(T-\lambda)\,d\lambda \\ &= \int_{-\infty}^{\infty} [s_2(T-\lambda) - s_1(T-\lambda)]s_1(T-\lambda)\,d\lambda \\ &= \int_{-\infty}^{\infty} s_2(u)s_1(u)\,du - \int_{-\infty}^{\infty} [s_1(u)]^2\,du \\ &= \sqrt{E_1E_2}\,\rho_{12} - E_1 \end{aligned} \tag{7.64}$$

where the substitution $u = T - \lambda$ has been used to go from the second equation to the third, and the definition of the correlation coefficient (7.55) has been used to get the last equation along with the definition of energy of a signal. Similarly, it follows that

$$\begin{aligned} s_{02}(T) &= \int_{-\infty}^{\infty} [s_2(T-\lambda) - s_1(T-\lambda)]s_2(T-\lambda)\,d\lambda \\ &= \int_{-\infty}^{\infty} [s_2(u)]^2\,du - \int_{-\infty}^{\infty} s_2(u)s_1(u)\,du \\ &= E_2 - \sqrt{E_1E_2}\,\rho_{12} \end{aligned} \tag{7.65}$$

Substituting (7.64) and (7.65) into (7.29), we find the optimum threshold to be

$$k_{opt} = \tfrac{1}{2}(E_2 - E_1) \tag{7.66}$$

Note that equal energy signals will always result in an optimum threshold of zero. Also note that the waveshape of the signals, as manifested through the correlation coefficient, has no effect on the optimum threshold, but only the signal energies do.

Nonwhite (Colored) Noise Backgrounds

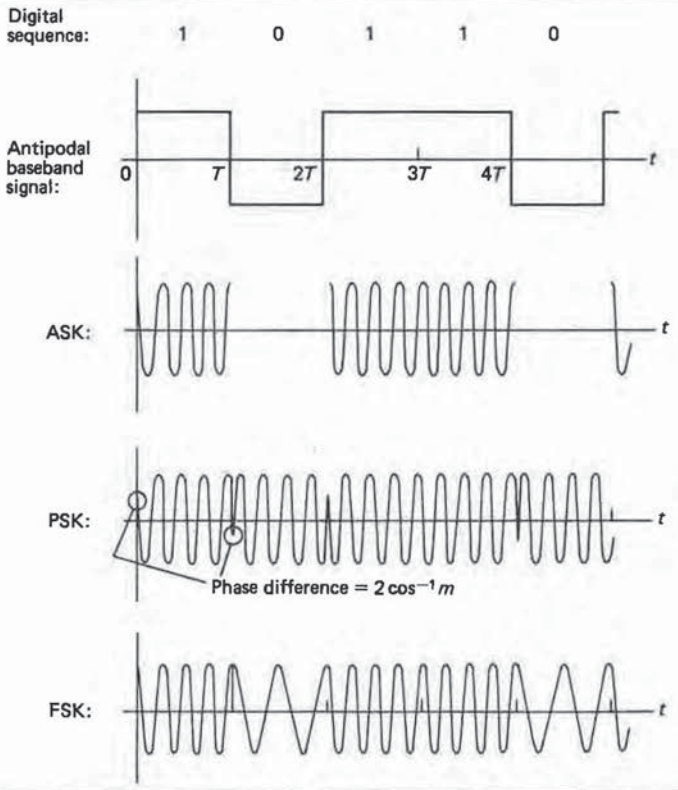
The question naturally arises about the optimum receiver for nonwhite noise backgrounds. Usually, the noise in a receiver system is generated primarily in the front-end stages and is due to thermal agitation of electrons in the electronic components (see Appendix A). This type of noise is well approx-

imated as white. If a bandlimited channel precedes the introduction of the white noise, then we need only work with modified transmitted signals. If, for some reason, a bandlimiting filter follows the introduction of the white noise (for example, an intermediate-frequency amplifier following the radio-frequency amplifier and mixers where most of the noise is generated in a heterodyne receiver), we can use a simple artifice to approximate the matched filter receiver. The colored noise plus signal is passed through a "whitening filter" with a transfer function that is the inverse square root of the noise spectral density. Thus, the output of this whitening filter is white noise plus a signal component that has been transformed by the whitening filter. We then build a matched filter receiver with impulse response that is the difference of the time-reverse of the "whitened" signals. The cascade of a whitening filter and matched filter (matched to the whitened signals) is called a *whitened matched filter*. This combination provides only an approximately optimum receiver for two reasons. Since the whitening filters will spread the received signals beyond the T-second signaling interval, two types of degradation will result: (1) the signal energy spread beyond the interval under consideration is not used by the matched filter in making a decision; (2) previous signals spread out by the whitening filter will interfere with the matched filtering operation on the signal on which a decision is being made. The latter is referred to as *intersymbol interference* and is explored further in Sections 7.6 and 7.8. It is apparent that degradation due to these effects is minimized if the signal *duration* is short compared with T, such as in a pulsed radar system. Finally, signal intervals adjacent to the interval being used in the decision process contain information that is relevant to making a decision on the basis of the correlation of the noise. In short, the whitened matched-filter receiver is nearly optimum if the signaling interval is large compared with the inverse bandwidth of the whitening filter. The question of bandlimited channels, and nonwhite background noise, is explored further in Section 7.5.

Receiver Implementation Imperfections

In the theory developed in this section, it is assumed that the signals are known *exactly* at the receiver. This is, of course, an idealized situation. Two possible deviations from this assumption are: (1) the phase of the receiver's replica of the transmitted signal may be in error, and (2) the exact arrival time of the received signal may be in error. These are called *synchronization* errors. The first case is explored in Section 7.3, and the latter is explored in the problems. Methods of synchronization are discussed in Chapter 8.

FIGURE 7.13 Waveforms for ASK, PSK, and FSK modulation



7.3 ERROR PROBABILITIES FOR COHERENT BINARY SIGNALING SCHEMES

We now compare the performance of several commonly used coherent binary signaling schemes. Then we will examine noncoherent systems. To obtain the error probability for coherent systems, the results of Section 7.2 will be applied directly. The three types of coherent systems to be considered in this section are amplitude-shift keyed (ASK), phase-shift keyed (PSK), and frequency-shift keyed (FSK). Typical transmitted waveforms for these three types of digital modulation are shown in Figure 7.13. We also will consider the effect of an imperfect phase reference on the performance of a coherent PSK system. Such systems are often referred to as partially coherent.

Amplitude-Shift Keying (ASK)

In Table 7.1, $s_1(t)$ and $s_2(t)$ for ASK are given as 0 and $A \cos \omega_c t$, where $f_c = \omega_c/2\pi$ is the carrier frequency. We note that the transmitter for such a system simply consists of an oscillator that is gated on and off; accordingly, ASK is often referred to as *on-off keying*. It is important to note that the oscillator runs continuously as the on-off gating is carried out.

The correlator realization for the optimum receiver consists of multiplication of the received signal plus noise by $A \cos \omega_c t$, integration over $(0, T)$, and comparison of the integrator output with the threshold $\frac{1}{4}A^2T$ as calculated from (7.66).

From (7.55) and (7.59), $R_{12} = \rho_{12} = 0$, and the probability of error, from (7.58), is

$$P_E = Q(\sqrt{z}) \tag{7.67}$$

Because of the lack of a factor $\sqrt{2}$ in the argument of the Q function, ASK is seen to be 3 dB worse in terms of signal-to-noise ratio than antipodal baseband signaling. The probability of error versus SNR corresponds to the curve for $R_{12} = 0$ in Figure 7.11.

Phase-Shift Keying (PSK)

From Table 7.1, the signals for PSK are

$$s_k(t) = A \sin [\omega_c t - (-1)^k \cos^{-1} m], \qquad 0 \leq t \leq T, k = 1, 2 \tag{7.68}$$

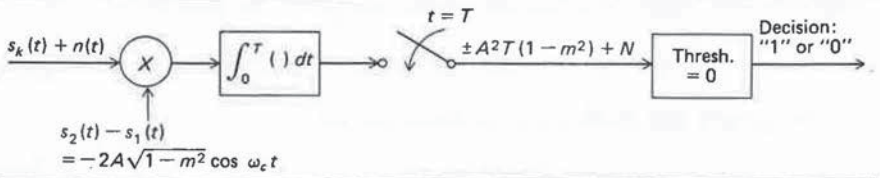
where $\cos^{-1} m$, the modulation index, is written in this fashion for future convenience. For simplicity, we assume that $\omega_c = 2\pi n/T$, where n is an integer. Using $\sin(-x) = -\sin x$ and $\cos(-x) = \cos(x)$, we can write (7.68) as

$$s_k(t) = Am \sin \omega_c t - (-1)^k A\sqrt{1 - m^2} \cos \omega_c t, \qquad 0 \leq t \leq T, k = 1, 2 \tag{7.69}$$

where we note that $\cos(\cos^{-1} m) = m$ and $\sin(\cos^{-1} m) = \sqrt{1 - m^2}$.

The first term on the right-hand side of (7.69) represents a carrier component included in some systems for synchronization of the local carrier reference at the receiver to the transmitted carrier. The power in the carrier component is $\frac{1}{2}(Am)^2$, and the power in the modulation component is $\frac{1}{2}A^2(1 - m^2)$. Thus m^2 is the fraction of the total power in the carrier. The correlator receiver is shown in Figure 7.14, where, instead of two correlators, only a single correlation with $s_2(t) - s_1(t)$ is used. The threshold, calculated from (7.66), is zero. We note that the carrier component of $s_k(t)$ is

FIGURE 7.14 Correlator realization of optimum receiver for PSK



of no consequence in the correlation operation because it is orthogonal to the modulation component over the bit interval. For PSK, $E_1 = E_2 = \frac{1}{2}A^2T$ and

$$\begin{aligned}\sqrt{E_1E_2}\rho_{12} &= \int_0^T s_1(t)s_2(t)\,dt \\ &= \int_0^T (Am\sin\omega_c t + A\sqrt{1 - m^2}\cos\omega_c t) \\ &\quad \cdot (Am\sin\omega_c t - A\sqrt{1 - m^2}\cos\omega_c t)\,dt \\ &= \tfrac{1}{2}A^2Tm^2 - \tfrac{1}{2}A^2T(1 - m^2) \\ &= \tfrac{1}{2}A^2T(2m^2 - 1) \end{aligned} \tag{7.70}$$

Thus R_{12}, from (7.59), is

$$\begin{aligned}R_{12} &= \frac{2\sqrt{E_1E_2}}{E_1 + E_2}\rho_{12} \\ &= 2m^2 - 1 \end{aligned} \tag{7.71}$$

and the probability of error for PSK is

$$P_E = Q[\sqrt{2(1 - m^2)z}] \tag{7.72}$$

The effect of allocating a fraction m^2 of the total transmitted power to a carrier component is to degrade P_E by $10\log_{10}(1 - m^2)$ decibels from the ideal $R_{12} = -1$ curve of Figure 7.11.

For $m = 0$, the resultant error probability is 3 dB better than ASK and corresponds to the $R_{12} = -1$ curve in Figure 7.11. We will refer to the case for which $m = 0$ as *biphase-shift keying* (BPSK) to avoid confusion with the case for which $m \neq 0$.

▼ **EXAMPLE 7.5** Consider PSK with $m = 1/\sqrt{2}$. (a) By how many degrees does the modulated carrier shift in phase each time the binary data changes? (b) What percent of the total power is in the carrier, and what percent is in the modulation component? (c) What value of $z = E_b/N_0$ is required to give $P_E = 10^{-6}$?

SOLUTION (a) Since the change in phase is from $-\cos^{-1} m$ to $\cos^{-1} m$ whenever the phase switches, the phase change of the modulated carrier is

$$2 \cos^{-1} m = 2 \cos^{-1} (1/\sqrt{2}) = 2(45°) = 90° \tag{7.73}$$

(b) The carrier and modulation components are

$$\text{carrier} = Am \sin (\omega_c t) \tag{7.74a}$$

and

$$\text{modulation} = \pm A\sqrt{1 - m^2} \cos (\omega_c t) \tag{7.74b}$$

respectively. Therefore, the power in the carrier component is

$$P_c = \frac{A^2 m^2}{2} \tag{7.75a}$$

and the power in the modulation component is

$$P_m = \frac{A^2(1 - m^2)}{2} \tag{7.75b}$$

Since the total power is $A^2/2$, the percent power in each of these components is

$$\%P_c = m^2 \times 100 = 50\% \quad \text{and} \quad \%P_m = (1 - m^2) \times 100 = 50\%$$

respectively.

(c) We have, for the probability of error,

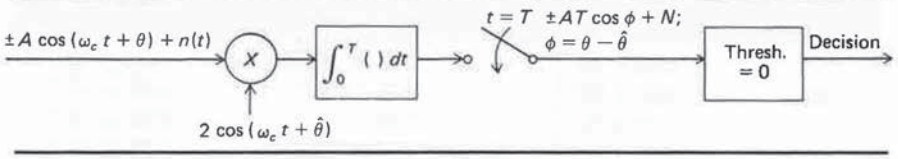
$$P_E = Q[\sqrt{2(1 - m^2)z}] \cong \frac{e^{-(1 - m^2)z}}{2\sqrt{\pi(1 - m^2)z}} \tag{7.76}$$

Solving this iteratively, we obtain, for $m = 0.5$, $z = 22.6$ or $E_b/N_0 = 13.54$ dB. Actually, we do not have to solve the error probability relationship iteratively again. From Example 7.2 we already know that $z = 10.54$ dB gives $P_E = 10^{-6}$ for PSK. In this example we simply note that the required power is twice as much as for BPSK, which is equivalent to adding 3 dB on to the 10.54 dB required in Example 7.2. ▲

Biphase-Shift Keying with Imperfect Reference

The results obtained earlier for PSK are for the case of a perfect reference at the receiver. If $m = 0$, it is simple to consider the case of an imperfect reference at the receiver as represented by an input of the form $\pm A \cos (\omega_c t + \theta) + n(t)$ and the reference by $A \cos (\omega_c t + \hat{\theta})$, where θ is an unknown carrier phase and $\hat{\theta}$ is the phase estimate at the receiver.

FIGURE 7.15 Effect of phase error in reference signal for correlation detection of BPSK



The correlator implementation for the receiver is shown in Figure 7.15. Using appropriate trigonometric identities, we find that the signal component of the correlator output at the sampling instant is $\pm AT \cos \phi$, where $\phi = \theta - \hat{\theta}$ is the phase error. It follows that the error probability *given* the phase error ϕ is

$$P_E(\phi) = Q(\sqrt{2z \cos^2 \phi}) \tag{7.77}$$

We note that the performance is degraded by $20 \log_{10} \cos \phi$ decibels compared with the perfect reference case.

If we assume ϕ to be fixed at some maximum value, we may obtain an upper bound on P_E due to phase error in the reference. However, a more exact model is often provided by approximating ϕ as a Gaussian random variable with the pdf

$$p(\phi) = \frac{e^{-\phi^2/2\sigma_\phi^2}}{\sqrt{2\pi\sigma_\phi^2}} \tag{7.78}$$

This is an especially appropriate model if the phase reference at the receiver is derived by means of a phase-locked loop operating with high signal-to-noise ratio at its input. If this is the case, σ_ϕ^2 is related to the signal-to-noise ratio at the input of the phase estimation device, whether it is a phase-locked loop or a bandpass-filter-limiter combination.

To find the error probability averaged over all possible phase errors, we simply find the expectation of $P(E|\phi)$ with respect to the phase-error pdf, $p(\phi)$, that is,

$$P_E = \int_{-\pi}^{\pi} P_E(\phi) p(\phi)\, d\phi \tag{7.79}$$

The resulting integral must be evaluated numerically for typical phase error pdf's.* Typical results are given in Table 7.2 for $p(\phi)$ Gaussian.

* See, for example, Van Trees (1968), Chapter 4.

TABLE 7.2 Effect of Gaussian Phase Reference Jitter on the Detection of BPSK

E/N_0, dB	P_E, $\sigma_\phi^2 = 0.01$ rad^2	P_E, $\sigma_\phi^2 = 0.05$ rad^2	P_E, $\sigma_\phi^2 = 0.1$ rad^2
9	3.68×10^{-5}	6.54×10^{-5}	2.42×10^{-4}
10	4.55×10^{-6}	1.08×10^{-5}	8.96×10^{-5}
11	3.18×10^{-7}	1.36×10^{-6}	3.76×10^{-5}
12	1.02×10^{-8}	1.61×10^{-7}	1.83×10^{-5}

Frequency-Shift Keying (FSK)

In Table 7.1, the signals for FSK are given as

$$\left.\begin{aligned} & s_1(t) = A \cos \omega_c t \\ \text{and} \quad & s_2(t) = A \cos (\omega_c + \Delta\omega)t \end{aligned}\right\} \quad 0 \leq t \leq T \tag{7.80}$$

For simplification, we assume that

$$\omega_c = \frac{2\pi n}{T} \tag{7.81a}$$

and

$$\Delta\omega = \frac{2\pi m}{T} \tag{7.81b}$$

where m and n are integers. This ensures that both $s_1(t)$ and $s_2(t)$ will go through an integer number of cycles in T seconds. As a result,

$$\begin{aligned} \sqrt{E_1 E_2}\rho_{12} &= \int_0^T A^2 \cos \omega_c t \cos (\omega_c + \Delta\omega)t \, dt \\ &= \tfrac{1}{2}A^2 \int_0^T [\cos \Delta\omega t + \cos (2\omega_c + \Delta\omega)t] \, dt \\ &= 0 \end{aligned} \tag{7.82}$$

and $R_{12} = 0$. Thus

$$P_E = Q(\sqrt{z}) \tag{7.83}$$

which is the same as for ASK. The error probability versus signal-to-noise ratio therefore corresponds to the curve $R_{12} = 0$ in Figure 7.11.

We note that the reason ASK and FSK have the same P_E versus SNR characteristics is that we are making our comparison on the basis of *average* signal power. If we constrain *peak* signal power to be equal, ASK will be 3 dB worse than FSK.

We denote the three schemes just considered as coherent, binary ASK, PSK, and FSK to indicate the fact that they are binary. We will consider M-ary ($M > 2$) schemes in Chapter 8.

EXAMPLE 7.6 Compare binary ASK, PSK, and FSK on the basis of E_b/N_0 required for $P_E = 10^{-6}$ and on the basis of transmission bandwidth for a constant data rate. Take the required bandwidth as the null-to-null bandwidth of the square-pulse modulated carrier. Assume the minimum bandwidth possible for BFSK.

SOLUTION From before, we know that to give $P_{E,\text{BPSK}} = 10^{-6}$, the required E_b/N_0 is 10.54 dB. ASK, on an average basis, and FSK require 3 dB more, or 13.54 dB, to give $P_E = 10^{-6}$. The Fourier transform of a square-pulse modulated carrier is

$$\Pi(t/T)\cos(2\pi f_c t) \leftrightarrow (T/2)\{\text{sinc}[T(f-f_c)] + \text{sinc}[T(f+f_c)]\}$$

The null-to-null bandwidth of the positive-frequency portion of this spectrum is

$$B_{RF} = \frac{2}{T}\ \text{Hz} \tag{7.84}$$

For binary ASK and PSK, the required bandwidth is

$$B_{\text{PSK}} = B_{\text{ASK}} = \frac{2}{T} = 2R\ \text{Hz} \tag{7.85}$$

where R is the data rate in bits per second. For FSK, the spectra for

$$s_1(t) = A\cos\omega_c t, \qquad 0 \le t \le T, \qquad \omega_c = 2\pi f_c$$

and

$$s_2(t) = A\cos(\omega_c t + \Delta\omega)t, \qquad 0 \le t \le T, \qquad \Delta\omega = 2\pi\,\Delta f$$

are assumed to be separated by $1/2T$ Hz, which is the minimum spacing for orthogonality of the signals. The required bandwidth is therefore

$$B_{\text{FSK}} = \underbrace{\frac{1}{T}}_{f_c\ \text{burst}} + \underbrace{\frac{1}{2T} + \frac{1}{T}}_{f_c + \Delta f\ \text{burst}} = \frac{2.5}{T} = 2.5R\ \text{Hz} \tag{7.86}$$

We often specify bandwidth efficiency R/B in terms of bits per second per hertz. For binary ASK and PSK the bandwidth efficiency is 0.5 bits/s/Hz, while for binary FSK it is 0.4 bits/s/Hz.

7.4 MODULATION SCHEMES NOT REQUIRING COHERENT REFERENCES

We now consider several modulation schemes that do not require the acquisition of a local reference signal in phase coherence with the received carrier. The first scheme to be considered is referred to as *differentially coherent phase-shift keying* (DPSK) and may be thought of as the noncoherent version of BPSK considered in Section 7.3. Also considered in this section will be noncoherent, binary FSK.

Differential Phase-Shift Keying (DPSK)

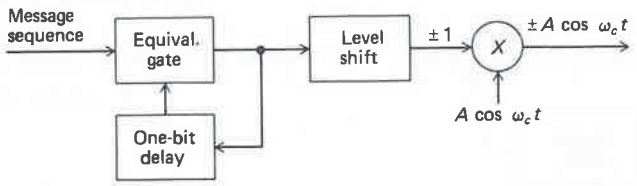
One way of obtaining a phase reference for the demodulation of BPSK is to use the carrier phase of the preceding signaling interval. The implementation of such a scheme presupposes two things: (1) The mechanism causing the unknown phase perturbation on the signal varies so slowly that the phase is essentially constant from one signaling interval to the next. (2) The phase during a given signaling interval bears a known relationship to the phase during the preceding signaling interval. The former is determined by the stability of the transmitter oscillator, time-varying changes in the channel, and so on. The latter requirement can be met by employing what is referred to as *differential encoding* of the message sequence at the transmitter.

Differential encoding of a message sequence is illustrated in Table 7.3. An arbitrary reference binary digit is assumed for the initial digit of the encoded sequence. In the example shown in Table 7.3, a 1 has been chosen. For each digit of the encoded sequence, the present digit is used as a reference for the following digit in the sequence. A 0 in the message sequence is encoded as a transition from the state of the reference digit to the opposite state in the encoded message sequence; a 1 is encoded as no change of state. In the example shown, the first digit in the message sequence is a 1,

TABLE 7.3 Differential Encoding Example

Message sequence:		1	0	0	1	1	1	0	0	0
Encoded sequence:	1	1	0	1	1	1	1	0	1	0
Reference digit	↑									
Transmitted phase:	0	0	π	0	0	0	0	π	0	π

FIGURE 7.16 Block diagram of a DPSK modulator



so no change in state is made in the encoded sequence, and a 1 appears as the next digit in the encoded sequence. This serves as the reference for the next digit to be encoded. Since the next digit appearing in the message sequence is a 0, the next encoded digit is the opposite of the reference digit, or a 0. The encoded message sequence then phase-shift keys a carrier with the phases 0 and π as shown in the table.

The block diagram in Figure 7.16 illustrates the generation of DPSK. The equivalence gate, which is the negation of an EXCLUSIVE-OR, is a logic circuit that performs the operations listed in Table 7.4. By a simple level shift at the output of the logic circuit, so that the encoded message is bipolar, the DPSK signal is produced by multiplication by the carrier, or double-sideband modulation.

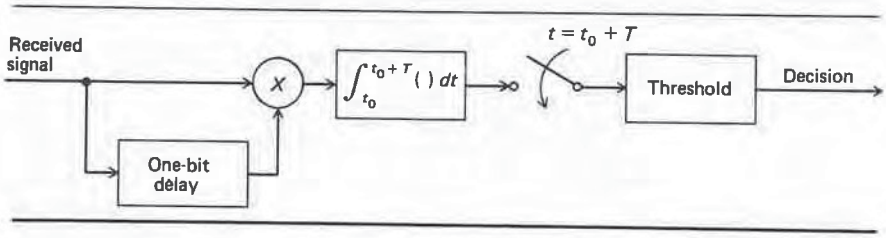
A possible implementation of a differentially coherent demodulator for DPSK is shown in Figure 7.17. The received signal plus noise is correlated bit by bit with a one-bit delayed version of the signal plus noise. The output of the correlator is then compared with a threshold set at zero, a decision being made in favor of a 1 or a 0, depending on whether the correlator output is positive or negative, respectively.

To illustrate that the received sequence will be correctly demodulated, consider the example given in Table 7.3, assuming no noise is present. After the first two bits have been received (the reference bit plus the first encoded

TABLE 7.4 Truth Table for the Equivalence Operation

Input 1 (Message)	Input 2 (Reference)	Output
0	0	1
0	1	0
1	0	0
1	1	1

FIGURE 7.17 Demodulation of DPSK



bit), the signal input to the correlator is $S_1 = A \cos \omega_c t$, and the reference, or delayed, input is $R_1 = A \cos \omega_c t$. The output of the correlator is

$$v_1 = \int_0^T A^2 \cos^2 \omega_c t \, dt = \tfrac{1}{2} A^2 T \tag{7.87a}$$

and the decision is that a 1 was transmitted. For the next bit interval, the inputs are $S_2 = -A \cos \omega_c t$ and $R_2 = S_1 = A \cos \omega_c t$, resulting in a correlator output of

$$v_2 = \int_0^T (-A^2 \cos^2 \omega_c t) \, dt = -\tfrac{1}{2} A^2 T \tag{7.87b}$$

and a decision that a 0 was transmitted is made. Continuing in this fashion, we see that the original message sequence is obtained if there is no noise at the input.

This detector, while simple to implement, is actually not optimum. The optimum detector for binary DPSK is shown in Figure 7.18. The test statistic for this detector is

$$\ell = x_k x_{k-1} + y_k y_{k-1} \tag{7.88}$$

If $\ell > 0$, the receiver chooses the signal sequence

$$s_1(t) = \begin{cases} A \cos(\omega_c t + \theta), & -T \le t < 0 \\ A \cos(\omega_c t + \theta), & 0 \le t < T \end{cases} \tag{7.89}$$

as having been sent. If $\ell < 0$, the receiver chooses the signal sequence

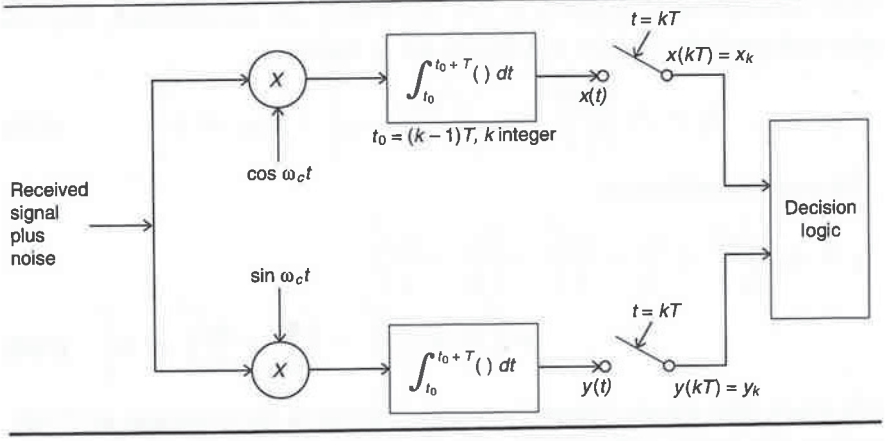
$$s_2(t) = \begin{cases} A \cos(\omega_c t + \theta), & -T \le t < 0 \\ -A \cos(\omega_c t + \theta), & 0 \le t < T \end{cases} \tag{7.90}$$

as having been sent.

Without loss of generality, we can choose $\theta = 0$ (the noise and signal orientations with respect to the sine and cosine mixers in Figure 7.18 are completely random). The probability of error can then be computed from

$$P_E = Pr(x_k x_{k-1} + y_k y_{k-1} < 0 \mid s_1 \text{ sent}, \theta = 0)$$

FIGURE 7.18 Optimum receiver for binary differential phase-shift keying



(it is assumed that s_1 and s_2 are equally likely). Assuming that the $\omega_c T$ is an integer multiple of 2π, we find the outputs of the integrators at time $t = 0$ to be

$$x_0 = \frac{AT}{2} + n_1 \qquad \text{and} \qquad y_0 = n_3 \tag{7.91}$$

where

$$n_1 = \int_{-T}^{0} n(t) \cos(\omega_c t)\, dt \tag{7.92a}$$

and

$$n_3 = \int_{-T}^{0} n(t) \sin(\omega_c t)\, dt \tag{7.92b}$$

Similarly, at time $t = T$, the outputs are

$$x_1 = \frac{AT}{2} + n_2 \qquad \text{and} \qquad y_1 = n_4 \tag{7.93}$$

where

$$n_2 = \int_{0}^{T} n(t) \cos(\omega_c t)\, dt \tag{7.94a}$$

and

$$n_4 = \int_{0}^{T} n(t) \sin(\omega_c t)\, dt \tag{7.94b}$$

It follows that n_1, n_2, n_3, and n_4 are uncorrelated, zero-mean Gaussian random variables with variances $N_0T/4$. Since they are uncorrelated, they are also independent, and the expression for P_E becomes

$$P_E = Pr\left[\left(\frac{AT}{2} + n_1\right)\left(\frac{AT}{2} + n_2\right) + n_3 n_4 < 0\right] \tag{7.95}$$

This can be rewritten as

$$P_E = Pr\left[\left(\frac{AT}{2} + \frac{n_1}{2} + \frac{n_2}{2}\right)^2 - \left(\frac{n_1}{2} - \frac{n_2}{2}\right)^2 + \left(\frac{n_3}{2} + \frac{n_4}{2}\right)^2 - \left(\frac{n_3}{2} - \frac{n_4}{2}\right)^2 < 0\right] \tag{7.96}$$

[To check this, simply square the separate terms in the argument of (7.96), collect like terms, and compare with the argument of (7.95).] Defining new Gaussian random variables as

$$\begin{aligned} w_1 &= \frac{n_1}{2} + \frac{n_2}{2} \\ w_2 &= \frac{n_1}{2} - \frac{n_2}{2} \\ w_3 &= \frac{n_3}{2} + \frac{n_4}{2} \\ w_4 &= \frac{n_3}{2} - \frac{n_4}{2} \end{aligned} \tag{7.97}$$

the probability of error can be written as

$$P_E = Pr\left[\left(\frac{AT}{2} + w_1^2\right)^2 + w_3^2 < w_2^2 + w_4^2\right] \tag{7.98}$$

The positive square roots of the quantities on either side of the inequality sign inside the brackets can be compared just as well as the quantities themselves. From the definitions of w_1, w_2, w_3, and w_4, it can be shown that they are uncorrelated with each other and all are zero mean with variances $N_0T/8$. Since they are uncorrelated and Gaussian, they are also independent. It follows that

$$R_1 = \sqrt{\left(\frac{AT}{2} + w_1\right)^2 + w_3^2} \tag{7.99}$$

is a Rician random variable (see Problem 5.33). It is also true that

$$R_2 = \sqrt{w_2^2 + w_4^2} \tag{7.100}$$

is a Rayleigh random variable. It follows that the probability of error can be written as the double integral

$$P_E = \int_0^\infty \left[\int_{r_2}^\infty f_{R_2}(r_2) \right] f_{R_1}(r_1)\, dr_1 \tag{7.101}$$

where $f_{R_1}(r_1)$ is a Rayleigh pdf and $f_{R_2}(r_2)$ is a Rician pdf. This double integral will arise later when we consider noncoherent FSK modulation. It is rather amazing that it evaluates to the simple result

$$P_E = \tfrac{1}{2} e^{-E_b/N_0} = \tfrac{1}{2} e^{-z} \tag{7.102}$$

It has been shown in the literature that the suboptimum integrate-and-dump detector of Figure 7.12 gives an approximate probability of error*

$$P_E \cong Q[\sqrt{E_b/N_0}] = Q[\sqrt{z}] \tag{7.103}$$

The result is about a 2-dB degradation in signal-to-noise ratio for a specified probability of error from that of the optimum detector.

Recalling the result for BPSK, (7.72) with $m = 0$, and using the asymptotic expression $Q(u) \cong e^{-u^2/2}/[(2\pi)^{1/2}u]$, we obtain the following result for BPSK valid for large z:

$$P_E \cong \frac{e^{-z}}{2\sqrt{\pi z}}, \qquad (BPSK;\ z \gg 1) \tag{7.104}$$

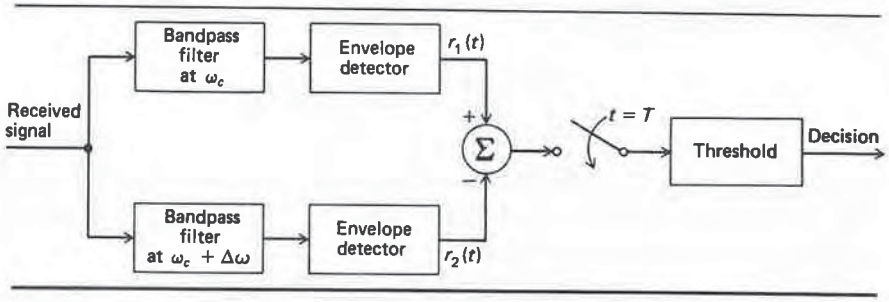
For large z, DPSK and BPSK differ only by the factor $(\pi z)^{1/2}$, or roughly a 1-dB degradation in signal-to-noise ratio of DPSK with respect to BPSK at low probability of error. This makes DPSK an extremely attractive solution to the problem of carrier reference acquisition required for demodulation of BPSK. The only significant disadvantages of DPSK are that the signaling rate is locked to the specific value dictated by the delay elements in the transmitter and receiver and that errors tend to occur in groups of two because of the correlation imposed between successive bits by the differential encoding process (the latter is the main reason for the 1-dB degradation in performance of DPSK over BPSK at high signal-to-noise ratios).

Noncoherent FSK

The computation of error probabilities for noncoherent systems is somewhat more difficult than it is for coherent systems. Since more is known about the received signal in a coherent system than in a noncoherent system, it is not surprising that the performance of the latter is worse than the corre-

* See J. H. Park, "On Binary DPSK Reception," *IEEE Transactions on Communications*, Vol. COM-26, April 1978, pp. 484–486.

FIGURE 7.19 Receiver for noncoherent FSK



sponding coherent system. Even with this loss in performance, noncoherent systems are often used when simplicity of implementation is a predominent consideration.

Only noncoherent FSK will be discussed here.* A truly noncoherent PSK system does not exist, but DPSK can be viewed as such.

For noncoherent FSK, the transmitted signals are

$$\text{and} \qquad \begin{aligned} s_1(t) &= A\cos(\omega_c t + \theta), \qquad 0 \le t \le T \\ s_2(t) &= A\cos[(\omega_c + \Delta\omega)t + \theta], \qquad 0 \le t \le T \end{aligned} \tag{7.105}$$

where $\Delta\omega$ is sufficiently large that $s_1(t)$ and $s_2(t)$ occupy different spectral regions. The receiver for FSK is shown in Figure 7.19; note that it consists of two receivers for noncoherent ASK in parallel. As such, calculation of the probability of error for FSK proceeds much the same way as for ASK, although we are not faced with the dilemma of a threshold that must change with signal-to-noise ratio. Indeed, because of the symmetries involved, an exact result for P_E can be obtained. Assuming $s_1(t)$ has been transmitted, the output of the upper detector at time T, $R_1 \triangleq r_1(T)$, has the Rician pdf

$$f_{R_1}(r_1) = \frac{r_1}{N} e^{-(r_1^2+A^2)/2N} I_0\left(\frac{Ar_1}{N}\right), \qquad r_1 > 0 \tag{7.106}$$

where $I_0(\cdot)$ is the modified Bessel function of the first kind of order zero and we have made use of Problem 5.33. The noise power is $N = N_0 B_T$. The output of the lower filter at time T, $R_2 \triangleq r_2(T)$, results from noise alone; its pdf is therefore Rayleigh:

$$f_{R_2}(r_2) = \frac{r_2}{N} e^{-r_2^2/2N}, \qquad r_2 > 0 \tag{7.107}$$

* See Problem 7.27 for a sketch of the derivation of P_E for noncoherent ASK.

It is a special case of the Rician pdf with $A = 0$. An error occurs if $R_2 > R_1$, which can be written as

$$P(E \mid s_1(t)) = \int_0^\infty f_{R_1}(r_1) \left[\int_{r_1}^\infty f_{R_2}(r_2)\, dr_2 \right] dr_1 \tag{7.108}$$

By symmetry, it follows that $P(E \mid s_1(t)) = P(E \mid s_2(t))$, so that (7.108) is the average probability of error. The inner integral in (7.108) integrates to $e^{-r_1^2/2N}$, which results in the expression

$$P_E = e^{-z} \int_0^\infty \frac{r_1}{N} I_0\left(\frac{Ar_1}{N}\right) e^{-r_1^2/N}\, dr_1 \tag{7.109}$$

where $z = A^2/2N$ as before. If we use a table of definite integrals, we can reduce (7.109) to

$$P_E = \tfrac{1}{2} e^{-z/2} \tag{7.110}$$

For coherent, binary FSK, the error probability for large signal-to-noise ratios, using the asymptotic expansion for the Q-function, is

$$P_E \cong \exp\left(-\tfrac{1}{2}z\right)/\sqrt{2\pi z} \qquad \text{for } z \gg 1 \tag{7.111}$$

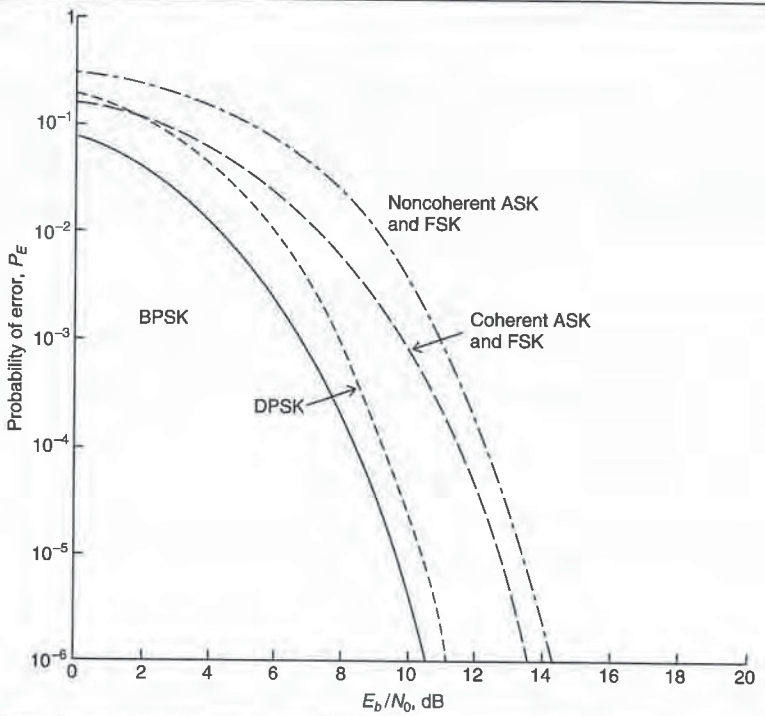
which indicates that *the power margin over noncoherent detection at large signal-to-noise ratios is inconsequential.* Thus, because of the comparable performance and the added simplicity of noncoherent FSK, it is employed almost exclusively in practice, instead of coherent FSK.

Comparison of Digital Modulation Systems

The binary digital modulation systems analyzed in this section and the preceding one are compared in Figure 7.20. We see that there is less than a 4-dB difference between the best (BPSK) and worst (noncoherent ASK and FSK) at high signal-to-noise ratios. This may seem to be a small price to pay for the simplicity in going from a coherent PSK system to a noncoherent FSK system. However, in some applications, even a 1-dB savings is worthwhile.

In addition to cost and complexity of implementation, there are many other considerations in choosing one type of digital data system over another. For some channels, where the channel gain or phase characteristics (or both) are perturbed by randomly varying propagation conditions, use of a noncoherent system may be dictated because of the near impossibility of establishing a coherent reference at the receiver under such conditions. Such channels are referred to as *fading*. In other situations, the choice of a coherent system may be demanded by considerations other than power savings.

FIGURE 7.20 Error probabilities for several binary digital signaling schemes



The following example illustrates some typical signal-to-noise ratio calculations for these digital modulation techniques.

▼ **EXAMPLE 7.7** Suppose a P_E of 10^{-4} is desired for a certain digital data transmission system. (a) Compare the necessary SNR's for BPSK, DPSK, noncoherent ASK, and noncoherent FSK. (b) If a PSK system is used with 10% of the transmitted signal power allocated to the carrier, how much must the SNR be increased to maintain $P_E = 10^{-4}$? (c) If BPSK is used and a maximum demodulator phase error of 10% is anticipated, what must the SNR power margin be to ensure that $P_E \leq 10^{-4}$?

SOLUTION For part (a), we use asymptotic expressions for P_E and neglect factors of $z^{-1/2}$. The error in doing so is less than 1 dB, as shown in Table 7.5.

TABLE 7.5 Comparison of Binary Modulation Schemes at $P_E = 10^{-4}$

Modulation Method	P_E A = Asymptotic E = Exact	Required SNR (Approx.) (dB)	Actual SNR (dB)
BPSK	$e^{-z}/2\sqrt{\pi}$ (A)	9.0	8.4
DPSK	$e^{-z}/2$ (E)	9.3	9.3
Noncoherent ASK	$e^{-z/2}/2$ (A)	12.3	—
Noncoherent FSK	$e^{-z/2}/2$ (E)	12.3	12.3

For part (b), $m^2 = 0.1$ and the degradation in SNR over a BPSK system is $10 \log_{10} (1 - m^2) = -0.46$ dB. Thus an SNR of $8.4 + 0.46 = 8.86$ dB is required to maintain $P_E = 10^{-4}$.

In part (c), the degradation is $20 \log_{10} \cos 10° = -0.133$ dB. Thus an SNR of $8.4 + 0.133 = 8.533$ dB will ensure that $P_E \leq 10^{-4}$. ▲

7.5 DIGITAL SIGNALING THROUGH BANDLIMITED CHANNELS

The analyses of the digital modulation techniques considered so far assumed the availability of an infinite-bandwidth channel. In practical applications, the channel bandwidth is never infinite. Two approaches to the finite-bandwidth channel case are the following:

1. Make use of one of the standard digital modulation schemes considered previously and simply transmit a higher-power signal than ideally required to compensate for the degradation imposed by the finite-bandwidth channel.
2. Choose designs for transmitter and receiver filters that shape the signal pulse-shape function so as to ideally eliminate interference between adjacent pulses.

To see how one might make use of the latter approach, we recall the sampling theorem, which gives a theoretical minimum spacing between samples to be taken from a signal with an ideal lowpass spectrum in order that the signal can be reconstructed exactly from the sample values. In particular, the transmission of a lowpass signal with bandwidth W can be viewed as sending $2W$ independent samples per second. If these $2W$ samples per second represent $2W$ independent pieces of data, this transmission can be viewed as sending $2W$ pulses per second through a channel represented by an ideal lowpass filter of bandwidth W. The transmission of the nth piece of information through the channel at time $t = nT = n/2W$ is accomplished by

sending an impulse of amplitude a_n. The output of the channel due to this impulse at the input is

$$y_n(t) = a_n \operatorname{sinc}\left[2W\left(t - \frac{n}{2W}\right)\right] \tag{7.112}$$

For an input consisting of a train of impulses spaced by $T = 1/2W$, the channel output is

$$y(t) = \sum_n y_n(t) = \sum_n a_n \operatorname{sinc}\left[2W\left(t - \frac{n}{2W}\right)\right] \tag{7.113}$$

If the channel output is sampled at time $t_m = m/2W$, the sample value is a_m because

$$\operatorname{sinc}(m - n) = \begin{cases} 1, & m = n \\ 0, & m \neq n \end{cases} \tag{7.114}$$

which results in all terms in (7.113) except the mth being zero. In other words, the mth sample value at the output is not affected by preceding or succeeding sample values; it represents an independent piece of information.

Note that the bandlimited channel implies that the time response due to the nth impulse at the input is infinite in extent; a waveform cannot be simultaneously bandlimited and time-limited. It is of interest to inquire if there are any other bandlimited waveforms other than sinc $(2Wt)$ that have the property of (7.114), that is, that their zero crossings are spaced by T seconds. One such family of pulses are those having *raised cosine spectra*. Their time response is given by

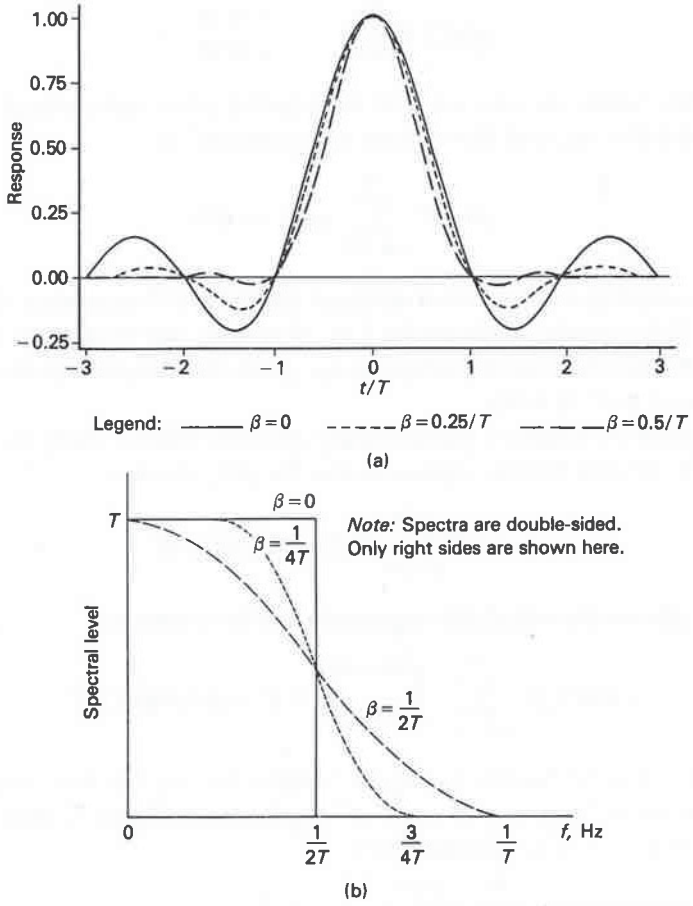
$$p(t) = \frac{\cos(2\pi\beta t)}{1 - (4\beta t)^2} \operatorname{sinc}\left(\frac{t}{T}\right) \tag{7.115}$$

and their spectra by

$$P(f) = \begin{cases} T, & |f| \leq 1/2T - \beta \\ \dfrac{T}{2}\left\{1 + \cos\left[\dfrac{\pi(|f| - 1/2T + \beta)}{2\beta}\right]\right\}, & 1/2T - \beta < |f| \leq 1/2T + \beta \\ 0, & |f| > 1/2T + \beta \end{cases} \tag{7.116}$$

Figure 7.21 shows this waveform and its spectra for several values of β. Note that zero crossings for $p(t)$ occur at least every T seconds. If $\beta = 1/2T$, the bandwidth of $P(f)$ is $1/T$ Hz, which is twice that of the sinc (t/T) pulse ($\beta = 0$). The increased bandwidth, however, results from a cosine rolloff with

FIGURE 7.21 (a) Pulse response for the raised cosine spectra shown in (b)



frequency of $P(f)$, which may be easier to realize in a practical filter. Also, $p(t)$ for $\beta = 1/2T$ has a narrow main lobe with very low side lobes. This is advantageous in that interference with neighboring pulses is minimized. Pulses with raised cosine spectra are used extensively in the design of digital communication systems.

Given a pulse-shape function $p(t)$, which has the Fourier transform $P(f)$ that satisfies the criterion

$$\sum_{k=-\infty}^{\infty} P\left(f + \frac{k}{T}\right) = T, \qquad |f| \leq \frac{1}{2T} \tag{7.117}$$

then

$$p(nT) = \begin{cases} 1, & n = 0 \\ 0, & n \neq 0 \end{cases} \tag{7.118}$$

Using this result, we can see that no adjacent pulse interference will be obtained if the received data stream is represented as

$$y(t) = \sum_{k=-\infty}^{\infty} a_k p(t - kT) \tag{7.119}$$

and the sampling at the receiver occurs at multiples of T seconds at the pulse epochs. For example, to obtain the $k = 10$ sample, one simply sets $t = 10T$ in (7.119), and the resulting sample is a_{10}, given that Nyquist's pulse-shaping criterion of (7.117) holds.

The proof of Nyquist's pulse-shaping criterion follows easily by making use of the inverse Fourier representation for $p(t)$, which is

$$p(t) = \int_{-\infty}^{\infty} P(f) \exp(j2\pi ft)\, df \tag{7.120}$$

For the nth sample value, this expression can be written as

$$p(nT) = \sum_{k=-\infty}^{\infty} \int_{(2k-1)/2T}^{(2k+1)/2T} P(f) \exp(j2\pi fnT)\, df \tag{7.121}$$

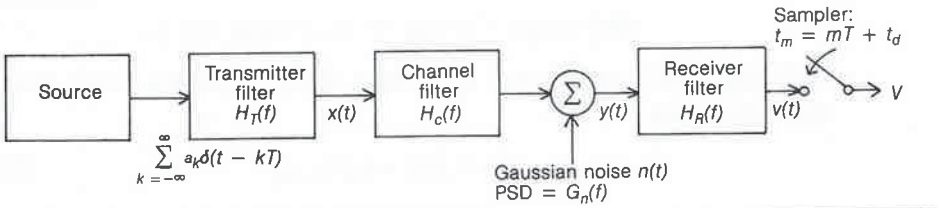
where the inverse Fourier transform integral for $p(t)$ has been broken up into contiguous frequency intervals of length $1/T$ Hz. By the change of variables $u = f - k/T$, (7.121) becomes

$$\begin{aligned} p(nT) &= \sum_{k=-\infty}^{\infty} \int_{-1/2T}^{1/2T} P\left(u + \frac{k}{T}\right) \exp(j2\pi nTu)\, du \\ &= \int_{-1/2T}^{1/2T} \sum_{k=-\infty}^{\infty} P\left(u + \frac{k}{T}\right) \exp(j2\pi nTu)\, du \end{aligned} \tag{7.122}$$

where the order of integration and summation has been reversed. By hypothesis, $\sum_{k=-\infty}^{\infty} P(u + k/T) = T$ between the limits of integration, so (7.122) becomes

$$\begin{aligned} p(nT) &= \int_{-1/2T}^{1/2T} T \exp(j2\pi nTu)\, du = \operatorname{sinc} n \\ &= \begin{cases} 1, & n = 0 \\ 0, & n \neq 0 \end{cases} \end{aligned} \tag{7.123}$$

FIGURE 7.22 Baseband system for signaling through a bandlimited channel



which completes the proof of Nyquist's pulse-shaping criterion. With the aid of this result, it is now apparent why the raised-cosine pulse family is free of interference, even though the family is by no means unique.

To use this result in designing digital communication systems for bandlimited channels, we consider a model for a baseband system such as is depicted in Figure 7.22. The transmitted signal is

$$\begin{aligned} x(t) &= \sum_{k=-\infty}^{\infty} a_k \delta(t - kT) * h_T(t) \\ &= \sum_{k=-\infty}^{\infty} a_k h_T(t - kT) \end{aligned} \tag{7.124}$$

where $h_T(t)$ is the impulse response of the transmitter filter that has the lowpass transfer function $H_T(f) = \mathcal{F}[h_T(t)]$. This signal passes through a bandlimited channel filter, after which Gaussian noise with power spectral density $G_n(f)$ is added to give the received signal

$$y(t) = x(t) * h_C(t) + n(t) \tag{7.125}$$

where $h_C(t) = \mathcal{F}^{-1}[H_C(f)]$ is the impulse response of the channel. Detection at the receiver is accomplished by passing $y(t)$ through a filter with impulse response $h_R(t)$ and sampling its output at intervals of T seconds. If we require that the cascade of transmitter, channel, and receiver filters satisfies Nyquist's pulse-shaping criterion, it then follows that the output sample at time $t = t_d$, where t_d is the delay imposed by the channel for the receiver filter, is

$$\begin{aligned} V &= Aa_0 p(0) + N \\ &= Aa_0 + N, \end{aligned} \tag{7.126}$$

where

$$Ap(t - t_d) = h_T(t) * h_C(t) * h_R(t) \tag{7.127}$$

or, by Fourier transforming both sides, we have

$$AP(f) \exp(-j2\pi f t_d) = H_T(f)H_C(f)H_R(f) \tag{7.128}$$

In (7.126), A is a scale factor, t_d is a time delay accounting for all delays in the system, and

$$N = n(t) * h_R(t)\big|_{t=t_d} \tag{7.129}$$

is the Gaussian noise component at the output of the detection filter at time $t = t_d$.

To analyze the probability of error for the performance of the system, we assume binary signaling ($a_m = +1$ or -1) so that the average probability of error is

$$\begin{aligned} P_E &= Pr(a_m = 1)Pr(Aa_m + N \leq 0 \quad \text{given } a_m = 1) \\ &\quad + Pr(a_m = -1)Pr(Aa_m + N \geq 0 \quad \text{given } a_m = -1) \end{aligned} \tag{7.130}$$

$$= Pr(Aa_m + N \leq 0 \quad \text{given } a_m = 1) = Pr(Aa_m + N \geq 0 \quad \text{given } a_m = -1) \tag{7.131}$$

where the latter two equations result by assuming $a_m = 1$ and $a_m = -1$ are equally likely. Taking the last equation of (7.131), it follows that

$$P_E = Pr(N \geq A) = \int_A^\infty \frac{\exp(-u^2/2\sigma^2)}{\sqrt{2\pi\sigma^2}}\, du = Q\left(\frac{A}{\sigma}\right) \tag{7.132}$$

where

$$\sigma^2 = \text{var}(N) = \int_{-\infty}^{\infty} G_n(f)|H_R(f)|^2 df \tag{7.133}$$

Because the Q-function is a monotonically decreasing function of its argument, it follows that the average probability of error can be minimized through proper choice of $H_T(f)$ and $H_R(f)$ [$H_C(f)$ is assumed to be fixed], by maximizing A/σ or by minimizing σ^2/A^2. The minimization can be carried out, subject to the constraint in (7.128), by applying Schwarz's inequality. The result* is

$$|H_R(f)|_{\text{opt}} = \frac{K|P(f)|^{1/2}}{G_n^{1/4}(f)|H_C(f)|^{1/2}} \tag{7.134}$$

* For a derivation, see Ziemer and Peterson (1992).

and

$$|H_T(f)|_{\text{opt}} = \frac{A}{K} |P(f)|^{1/2} G_n^{1/4}(f) / |H_C(f)|^{1/2} \tag{7.135}$$

where K is an arbitrary constant and any appropriate phase response can be used.

A special case of interest occurs when

$$G_n(f) = \frac{N_0}{2}, \qquad \text{all } f \quad \text{(white noise)} \tag{7.136}$$

and

$$H_C(f) = H_0, \qquad |f| \leq \frac{1}{2T} \tag{7.137}$$

The minimum probability of error then simplifies to

$$P_{E,\min} = Q(\sqrt{2E_T/N_0}) \tag{7.138}$$

where

$$E_T = \int_{-\infty}^{\infty} |H_T(f)|^2 df \tag{7.139}$$

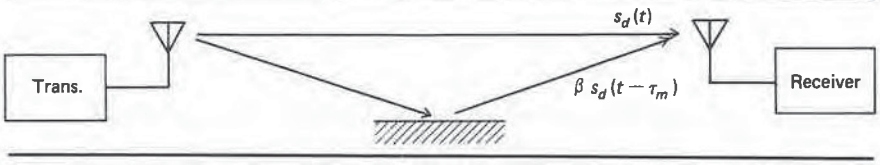
is the average transmitted signal energy. This result is identical to that obtained previously for binary signaling in an infinite bandwidth baseband channel.

7.6 MULTIPATH INTERFERENCE

The channel models that we have assumed so far have been rather idealistic in that the only signal perturbation considered was due to additive Gaussian noise. Although realistic for many situations, additive Gaussian-noise channel models do not accurately represent many transmission phenomena. Other important sources of degradation in many digital data systems are bandlimiting of the signal by the channel, as examined in the previous section; non-Gaussian noise, such as impulse noise due to lightning discharges or switches; radio frequency interference due to other transmitters; and multiple transmission paths due to stratifications in the transmission medium or reflecting objects.

In this section we consider the effects of multipath transmission because it is a fairly common transmission perturbation and its effects on digital data

FIGURE 7.23 Channel model for multipath transmission



transmission can, in the simplest form, be analyzed in a straightforward fashion.

We will limit our discussion to a two-ray multipath model as illustrated in Figure 7.23. In addition to the multiple transmission, the channel perturbs the signal with white Gaussian noise with double-sided power spectral density $\frac{1}{2}N_0$. Thus the received signal plus noise is given by

$$y(t) = s_d(t) + \beta s_d(t - \tau_m) + n(t) \tag{7.140}$$

where $s_d(t)$ is the received direct-path signal, β is the attenuation of the multipath component, and τ_m is its delay. For simplicity, only binary BPSK will be considered in the following analysis. Thus the direct-path signal can be represented as

$$s_d(t) = Ad(t) \cos \omega_c t \tag{7.141}$$

where $d(t)$, the data stream, is a sequence of plus or minus 1's, each one of which is T seconds in duration. Because of the multipath component, we must consider a sequence of bits at the receiver input. We will analyze the effect of the multipath component and noise on a correlation receiver as shown in Figure 7.24, which, we recall, detects the data in the presence of Gaussian noise alone with minimum probability of error. Writing the noise in terms of quadrature components $n_c(t)$ and $n_s(t)$, we find that the input to the integrator, ignoring double frequency terms, is

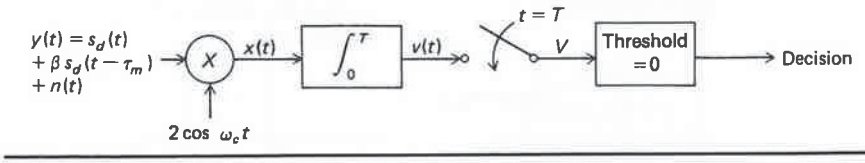
$$\begin{aligned} x(t) &= Lp[2y(t) \cos \omega_c t] \\ &= Ad(t) + \beta Ad(t - \tau_m) \cos \omega_c \tau_m + n_c(t) \end{aligned} \tag{7.142}$$

where $Lp[\ \ ]$ stands for the lowpass part of the bracketed quantity.

The second term in (7.142) represents interference due to the multipath. It is useful to consider two special cases:

1. $\tau_m/T \cong 0$, so that $d(t - \tau_m) \cong d(t)$. For this case, we assume $\omega_0 \tau_m$ is a uniformly distributed random variable in $(-\pi, \pi)$. This will be true if $\omega_c \tau_m$ fluctuates much faster than the carrier tracking loop time constant. The predominant effect of the multipath for this case will be fading of the signal component. This case will be analyzed in the next section.

FIGURE 7.24 Correlation receiver for BPSK with signal plus multipath at its input



2. $0 < \tau_m/T \leq 1$, so that successive bits of $d(t)$ and $d(t - \tau_m)$ overlap; in other words, we will have intersymbol interference. For this case, we will let $\delta = \beta \cos \omega_c \tau_m$ be a parameter in our analysis.

We now analyze the receiver performance for case 2, for which the effect of intersymbol interference is nonnegligible. To simplify notation, let

$$\delta = \beta \cos \omega_c \tau_m \tag{7.143}$$

so that (7.142) becomes

$$x(t) = Ad(t) + A\delta d(t - \tau_m) + n_c(t) \tag{7.144}$$

If $\tau_m/T \leq 1$, only adjacent bits of $Ad(t)$ and $A\delta d(t - \tau_m)$ will overlap. Thus we can compute the signal component of the integrator output in Figure 7.24 by considering the four combinations shown in Figure 7.25. Assuming 1's and 0's are equally probable, the four combinations shown in Figure 7.25 will occur with equal probabilities. Thus the average probability of error is

$$P_E = \tfrac{1}{4}[P(E|+\,+) + P(E|-\,+) + P(E|+\,-) + P(E|-\,-)] \tag{7.145}$$

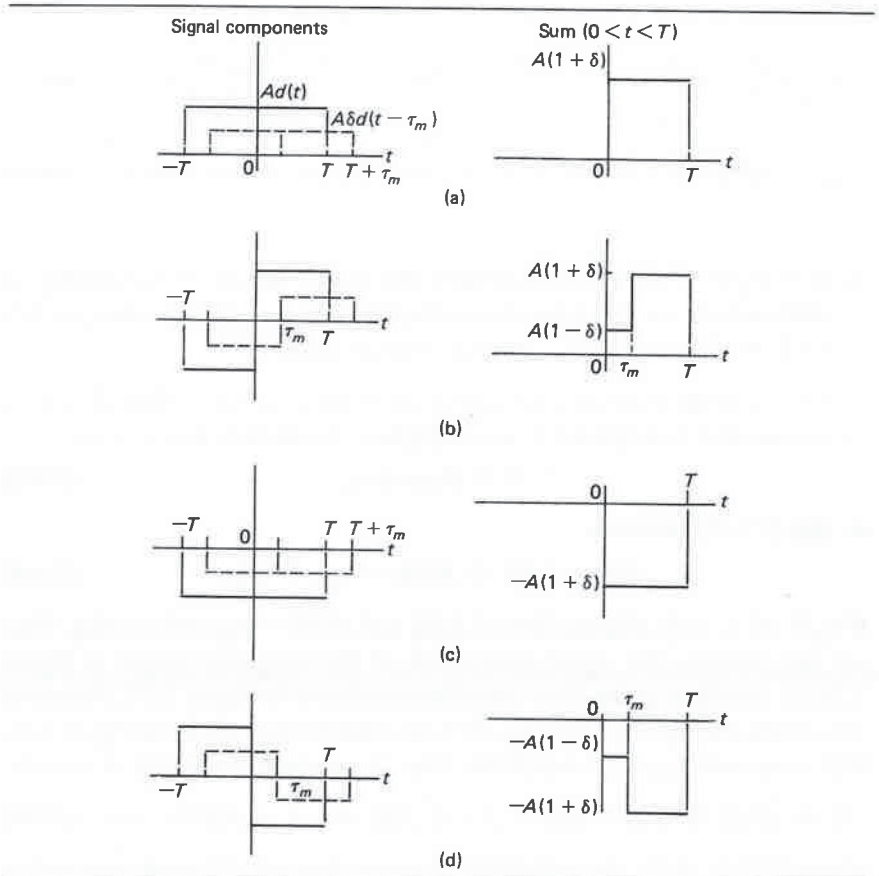
where $P(E|+\,+)$ is the probability of error given two 1's were sent, and so on. The noise component of the integrator output, namely

$$N = \int_0^T 2n(t) \cos \omega_c t \, dt \tag{7.146}$$

is Gaussian with zero mean and variance

$$\begin{aligned} \sigma_n^2 &= E\left\{4 \int_0^T \int_0^T n(t)n(\sigma) \cos \omega_c t \cos \omega_c \sigma \, dt \, d\sigma\right\} \\ &= 4 \int_0^T \int_0^T \frac{N_0}{2} \delta(t - \sigma) \cos \omega_c t \cos \omega_c \sigma \, d\sigma \, dt \\ &= 2N_0 \int_0^T \cos^2 \omega_c t \, dt \\ &= N_0 T \qquad (\omega_c T \text{ an integer multiple of } 2\pi) \end{aligned} \tag{7.147}$$

FIGURE 7.25 The various possible cases for intersymbol interference in multipath transmission



Because of the symmetry of the noise pdf and the symmetry of the signals in Figure 7.25, it follows that

$$P(E|++) = P(E|--) \quad \text{and} \quad P(E|-+) = P(E|+-) \tag{7.148}$$

so that we have to compute only two probabilities instead of four. From Figure 7.25, it follows that the signal component at the integrator output, given a 1-1 was transmitted, is

$$V_{++} = AT(1 + \delta) \tag{7.149}$$

and if a 0-1 was transmitted, it is

$$V_{-+} = AT(1 + \delta) - 2A\delta\tau_m = AT\left[(1 + \delta) - \frac{2\delta\tau_m}{T}\right] \tag{7.150}$$

The conditional error probability $P(E\,|\,+\ +)$ is therefore

$$P(E\,|\,+\ +) = P[AT(1 + \delta) + N < 0] = \int_{-\infty}^{-AT(1+\delta)} \frac{e^{-u^2/2N_0T}}{\sqrt{2\pi N_0 T}}\,du = Q\left[\sqrt{\frac{2E}{N_0}}(1 + \delta)\right] \tag{7.151}$$

where $E = \frac{1}{2}A^2T$ is the energy of the direct signal component. Similarly, $P(E\,|\,-\ +)$ is given by

$$P(E\,|\,-\ +) = P\left\{AT\left[(1 + \delta) - \frac{2\delta\tau_m}{T}\right] + N < 0\right\} = \int_{-\infty}^{-AT[(1+\delta)-2\delta\tau_m/T]} \frac{e^{-u^2/2N_0T}}{\sqrt{2\pi N_0 T}}\,du = Q\left\{\sqrt{\frac{2E}{N_0}}\left[1 + \delta - \frac{2\delta\tau_m}{T}\right]\right\} \tag{7.152}$$

Substituting these results into (7.145) and using the symmetry properties for the other conditional probabilities, we have the average probability of error

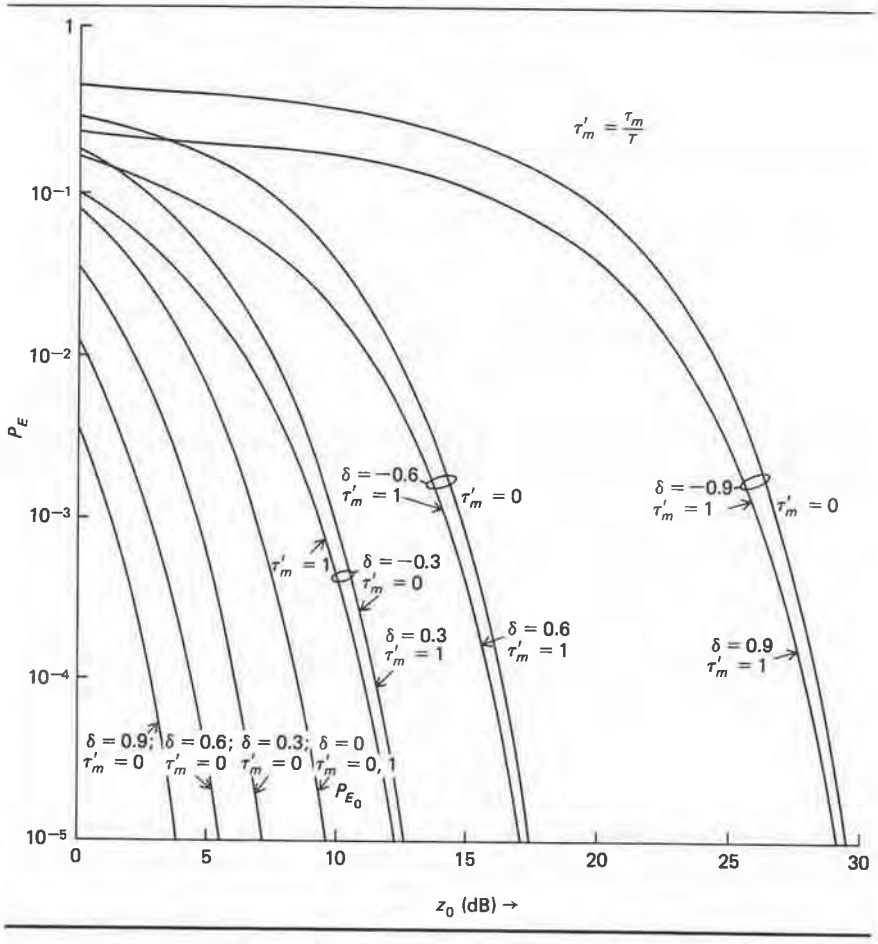
$$P_E = \tfrac{1}{2}Q\sqrt{2z_0}\,[(1 + \delta)] + \tfrac{1}{2}Q\{\sqrt{2z_0}\,[(1 + \delta) - 2\delta\tau_m/T]\} \tag{7.153}$$

where $z_0 \triangleq E/N_0 = A^2T/2N_0$ as before.

A plot of P_E versus z_0 for various values of δ and τ_m/T, as shown in Figure 7.26, gives an indication of the effect of multipath on signal transmission. A question arises as to which curve in Figure 7.26 should be used as a basis of comparison. The one for $\delta = \tau_m/T = 0$ corresponds to the error probability for BPSK signaling in a nonfading channel. However, we note that

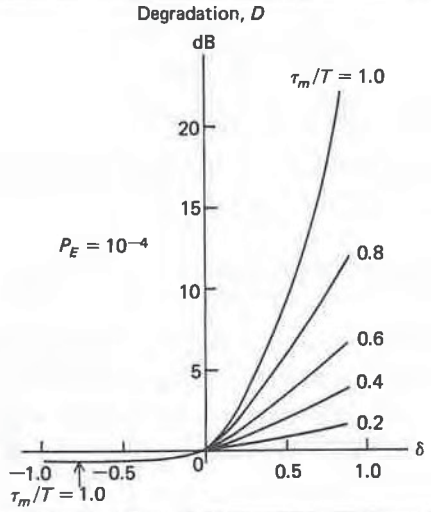
$$z_m = \frac{E(1 + \delta)}{N_0} = z_0(1 + \delta) \tag{7.154}$$

FIGURE 7.26 P_E versus z for various conditions of fading and intersymbol interference due to multipath



is the signal-to-noise ratio that results if the total effective received signal energy, including that of the indirect component, is used. Indeed, from (7.153) it follows that this is the curve for $\tau_m/T = 0$ for a given value of δ. Thus, if we use this curve for P_E as a basis of comparison for P_E with τ_m/T nonzero for each δ, we will be able to obtain the increase in P_E due to intersymbol interference alone. However, it is more useful for system design purposes to have degradation in SNR instead. That is, we want the increase in signal-to-noise ratio (or signal energy) necessary to maintain a given P_E in the presence of multipath relative to a channel with $\tau_m = 0$. Figure 7.27 shows typical results for $P_E = 10^{-4}$.

FIGURE 7.27 Degradation versus δ for correlation detection of BPSK in specular multipath for $P_E = 10^{-4}$



We note that the degradation is actually negative for $\delta < 0$; that is, the performance with intersymbol interference is better than for no intersymbol interference, provided the indirect received signal fades out of phase with respect to the direct component. This seemingly contradictory result is explained by consulting Figure 7.25, which shows that the direct and indirect received signal components being out of phase, as implied by $\delta < 0$, results in additional signal energy being received for cases (b) and (d) with $\tau_m/T > 0$ over what would be received if $\tau_m/T = 0$. On the other hand, the received signal energy for cases (a) and (c) is independent of τ_m/T.

Two interesting conclusions may be drawn from Figure 7.27. First, we note that when $\delta < 0$, the effect of *intersymbol interference* is negligible, since variation of τ_m/T has no significant effect on the degradation. The degradation is due primarily to the decrease in signal amplitude owing to the destructive interference because of the phase difference of the direct and indirect signal components. Second, when $\delta > 0$, the degradation shows a strong dependence on τ_m/T, indicating that intersymbol interference is the primary source of the degradation.

The adverse effects of intersymbol interference due to multipath can be combated by using an *equalization filter* that precedes detection of the received data.* To illustrate the basic idea of such a filter, we take the Fou-

* Equalization can be used to improve performance whenever intersymbol interference is a problem, for example, due to filtering.

rier transform of (7.140) with $n(t) = 0$ to obtain the transfer function of the channel, $H_C(f)$:

$$H_C(f) = \frac{\mathcal{F}[y(t)]}{\mathcal{F}[s_d(t)]} = 1 + \beta e^{-j2\pi\tau_m f} \tag{7.155}$$

If β and τ_m are known, the correlation receiver of Figure 7.24 can be preceded by a filter, referred to as an equalizer, with the transfer function

$$H_{eq}(f) = \frac{1}{H_C(f)} = \frac{1}{1 + \beta e^{-j2\pi\tau_m f}} \tag{7.156}$$

to fully compensate for the signal distortion introduced by the multipath. Since β and τ_m will not be known exactly, or may even change with time, provision must be made for adjusting the parameters of the equalization filter. Noise, although important, is neglected for simplicity.

7.7 FLAT FADING CHANNELS

Returning to (7.140), we assume that the delay of the multipath portion is small compared with a bit period so that we have as the approximate integrate-and-dump detector output

$$x(t) = A(1 + \beta)\, d(t) \cos \omega_c \tau_m + n_c(t) \tag{7.157}$$

Since the multipath channel is usually unknown, it is sensible to model β and $\omega_c\tau_m$ as random variables, assuming that the channel varies slowly relative to the bit duration. This is known as a slowly fading channel. If β and $\omega_c\tau_m$ vary quickly with respect to $d(t)$, the channel is said to be fast fading. This is a more difficult case to analyze than the slowly fading case, and we do not consider it here. A common model for the envelope of the received signal in the slowly fading case is a Rayleigh random variable, which is also the simplest case to analyze. Somewhat more general, but more difficult to analyze, is to model the envelope of the received signal as a Rician random variable. We illustrate the consideration of a BPSK signal received from a Rayleigh slowly fading channel as follows. Let the demodulated signal (7.157) be written in the simpler form

$$x(t) = R\, d(t) + n_c(t) \tag{7.158}$$

where R is a Rayleigh random variable with pdf given by (7.107). If R were a constant, we know that the probability of error is given by (7.72) with $m = 0$. In other words, *given* R, we have for the probability of error

$$P_E(R) = Q(\sqrt{2z}) \tag{7.159}$$

In order to find the average probability of error over the amplitude R, we average (7.159) with respect to the pdf of R, which is assumed to be Rayleigh in this case. However, R is not explicitly present in (7.159) because it is buried in z:

$$z = \frac{E_b}{N_0} = \frac{R^2 T_b}{2N_0} \tag{7.160}$$

Now if R is Rayleigh-distributed, it can be shown by transformation of pdf's that R^2, and therefore z, is exponentially distributed. Thus, the average of (7.159) is

$$P_E = \int_0^\infty Q(\sqrt{2z}) \frac{1}{\bar{z}} e^{-z/\bar{z}} \, dz \tag{7.161}$$

where $\bar{z}$ is the average signal-to-noise ratio. This integration can be carried out with the result that

$$P_E = \tfrac{1}{2}\left[1 - \sqrt{\frac{\bar{z}}{1 + \bar{z}}}\right] \qquad \text{BPSK} \tag{7.162}$$

A similar analysis for binary, coherent FSK results in the expression

$$P_E = \tfrac{1}{2}\left[1 - \sqrt{\frac{\bar{z}}{2 + \bar{z}}}\right] \qquad \text{coherent FSK} \tag{7.163}$$

Other modulation techniques that we can consider in a similar fashion are DPSK and noncoherent FSK. For these modulation schemes, we obtain

$$P_E = \frac{1}{2(1 + \bar{z})} \qquad \text{DPSK} \tag{7.164}$$

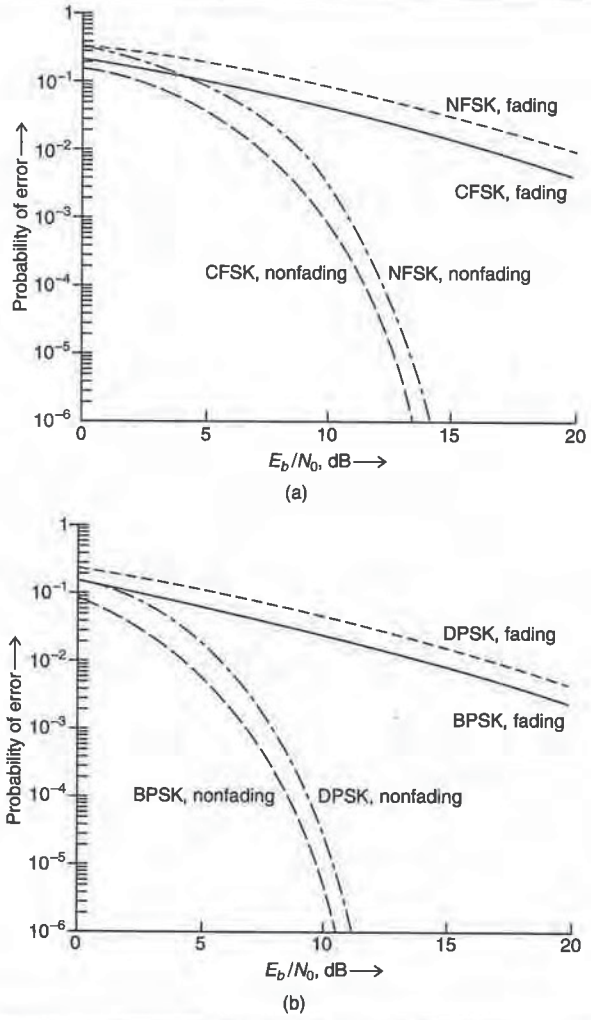
and

$$P_E = \frac{1}{2 + \bar{z}} \qquad \text{noncoherent FSK} \tag{7.165}$$

respectively. The derivations are left to the problems. These results are plotted in Fig. 7.28 and compared with the corresponding results for nonfading channels. Note that the penalty imposed by the fading is severe.

What can be done to combat the adverse effects of fading? We note that the degradation in performance due to fading results from the received signal amplitude being less than what it would be for a nonfading channel because of the factor $\beta \cos \phi$. If the transmitted signal power can be divided between two or more subchannels that fade independently of one another, then the degradation will most likely not be severe in all subchannels for

FIGURE 7.28 Error probabilities for various modulation schemes in flat fading Rayleigh channels. (a) Coherent and noncoherent FSK. (b) BPSK and DPSK.



the same binary digit. Then, if the outputs of these subchannels are recombined in the proper fashion, it seems reasonable that better performance can be obtained than that from using a single transmission path. The use of such multiple transmission paths to combat fading is referred to as *diversity transmission*. There are various ways to obtain the independent transmission paths; chief ones are by transmitting over spatially different paths (space diversity),

at different times (time diversity), with different carrier frequencies (frequency diversity), or with different polarizations of the propagating wave (polarization diversity).

In any case, an optimum number of subpaths exist that give the maximum improvement. The number of subpaths D employed is referred to as the *order of diversity*.

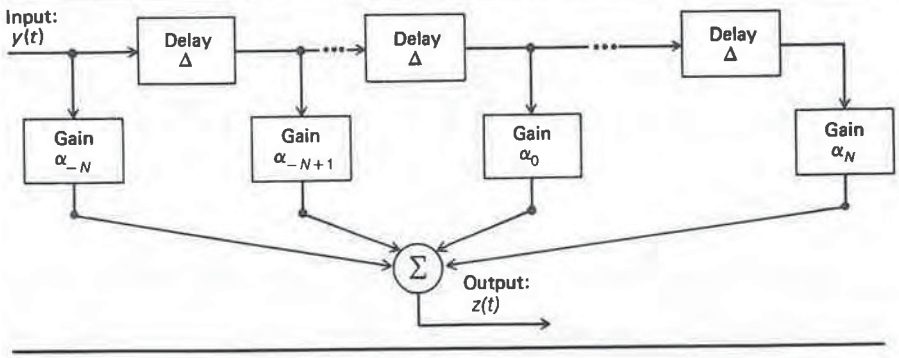
It is apparent that an optimum value of D exists. Increasing D provides additional diversity and decreases the probability that most of the subchannel outputs are badly faded. On the other hand, as D increases with total signal energy held fixed, the average signal-to-noise ratio per subchannel decreases, thereby resulting in a larger probability of error per subchannel. Clearly, therefore, a compromise between these two situations must be made. The problem of fading is again reexamined in Chapter 9 (Section 9.3), and the optimum selection of D is considered in Problem 9.17.

7.8 EQUALIZATION

As explained in Section 7.6, an equalization filter can be used to combat channel-induced distortion caused by perturbations such as multipath propagation or bandlimiting due to filters. According to (7.156), a simple approach to the idea of equalization leads to the concept of an inverse filter. In this section, we specialize our considerations of an equalization filter to a particular form—a transversal or tapped-delay-line filter. Figure 7.29 is a block diagram of such a filter.

There are at least two reasons for considering a transversal structure for the purpose of equalization. First, it is simple to analyze. Second, it is easy

FIGURE 7.29 Transversal filter implementation for equalization of intersymbol interference



to mechanize by means of *surface acoustic wave* (SAW) filters* at high frequencies and by digital signal processors and *charge-transfer devices*† (CTDs) at lower frequencies.

We can take two approaches to determining the tap weights, $\alpha_{-N}, \ldots, \alpha_0, \ldots, \alpha_N$, in Figure 7.29 for given channel conditions. One is *zero-forcing*, and the other is *minimization of mean-square error* (MMSE). Let us briefly discuss these two techniques.

Equalization by Zero-Forcing

Let the pulse response of the channel output be $p_c(t)$. The output of the equalizer in response to $p_c(t)$ is

$$p_{eq}(t) = \sum_{n=-N}^{N} \alpha_n p_c(t - n\Delta) \tag{7.166}$$

We want $p_{eq}(t)$ to satisfy Nyquist's pulse-shaping criterion, which we will call the *zero-ISI condition*. Since the output of the equalizer is sampled every T seconds, it is reasonable that the tap spacing be $\Delta = T$. The zero-ISI condition therefore becomes

$$\begin{aligned} p_{eq}(mT) &= \sum_{n=-N}^{N} \alpha_n p_{cl}[(m - n)T] \\ &= \begin{cases} 1, & m = 0 \\ 0, & m \neq 0 \end{cases} \qquad m = 0, \pm 1, \pm 2, \ldots, \pm N \end{aligned} \tag{7.167}$$

Note that the zero-ISI condition can be satisfied at only $2N + 1$ time instants because there are only $2N + 1$ coefficients to be selected in (7.167). Defining the matrices

$$[P_{eq}] = \begin{bmatrix} 0 \\ 0 \\ \vdots \\ 0 \\ 1 \\ 0 \\ 0 \\ \vdots \\ 0 \end{bmatrix} \begin{matrix} \left.\begin{matrix} \\ \\ \\ \end{matrix}\right\} N \text{ zeros} \\ \\ \left.\begin{matrix} \\ \\ \\ \end{matrix}\right\} N \text{ zeros} \end{matrix} \tag{7.168}$$

* See "SAW Bandpass Filters," Anderson Laboratories (1980), 1280 Blue Hill Avenue, Bloomfield, CT 06002.

† Allen Gersho, "Charge-Coupled Devices: The Analog Shift Register Comes of Age," *IEEE Communications Magazine*, Vol. 13, November 1975, pp. 27–32.

$$[A] = \begin{bmatrix} \alpha_{-N} \\ \alpha_{-N+1} \\ \vdots \\ \alpha_N \end{bmatrix} \tag{7.169}$$

and

$$[P_c] = \begin{bmatrix} p_c(0) & p_c(-T) & \cdots & p_c(-2NT) \\ p_c(T) & p_c(0) & \cdots & p_c[(-2N+1)T] \\ \vdots & & & \vdots \\ p_c(2NT) & & & p_c(0) \end{bmatrix} \tag{7.170}$$

it follows that (7.167) can be written in matrix form as

$$[P_{eq}] = [P_c][A] \tag{7.171}$$

The method of solution of the zero-forcing coefficients is now clear. Since $[P_{eq}]$ is specified by the zero-ISI condition, all we must do is find the inverse of $[P_c]$. The desired coefficient matrix $[A]$ is then the middle column of $[P_c]^{-1}$, which follows by multiplying $[P_c]^{-1}$ and $[P_{eq}]$.

▼ **EXAMPLE 7.8** Consider a channel for which the following sample values of the channel pulse response are obtained:

$$p_c(-2T) = -0.05 \qquad p_c(-T) = 0.2 \qquad p_c(0) = 1.0$$
$$p_c(T) = 0.3 \qquad p_c(2T) = -0.07$$

The matrix $[P_c]$ is

$$[P_c] = \begin{bmatrix} 1.0 & 0.2 & -0.05 \\ 0.3 & 1.0 & 0.2 \\ -0.07 & 0.3 & 1.0 \end{bmatrix} \tag{7.172}$$

and the inverse matrix is

$$[P_c]^{-1} = \begin{bmatrix} 1.0815 & -0.2474 & 0.1035 \\ -0.3613 & 1.1465 & -0.2474 \\ 0.1841 & -0.3613 & 1.0815 \end{bmatrix} \tag{7.173}$$

The zero-forcing tap coefficients are given by the middle column of this inverse matrix. Using these coefficients, the equalizer output is

$$p_{eq}(mT) = -0.2474p_c[(m+1)T] + 1.1465p_c(mT) - 0.3613p_c[(m-1)T] \tag{7.174}$$

▲ Note that $p_{eq}(0) = 1.0$ and that samples on either side of $p_{eq}(0)$ are zero.

Equalization by MMSE

Suppose that the desired output from the transversal filter equalizer of Figure 7.29 is $d(t)$. An MMSE criterion then seeks the tap weights that minimize the mean-square error between the desired output from the equalizer and its actual output. Since this output includes noise, we denote it by $z(t)$ to distinguish it from the pulse response of the equalizer. The MMSE criterion is therefore expressed as

$$\mathcal{E} = E\{[z(t) - d(t)]^2\} = \text{minimum} \tag{7.175}$$

where, if $y(t)$ is the equalizer input including noise, the equalizer output is

$$z(t) = \sum_{n=-N}^{N} \alpha_n y(t - n\Delta) \tag{7.176}$$

Since $\mathcal{E}$ is a concave function of the tap weights, a set of sufficient conditions for minimizing the tap weights is

$$\frac{\partial \mathcal{E}}{\partial \alpha_m} = 0 = 2E\left\{[z(t) - d(t)]\frac{\partial z(t)}{\partial \alpha_m}\right\}, \qquad m = 0, \pm 1, \ldots, \pm N \tag{7.177}$$

Substituting (7.176) in (7.177) and carrying out the differentiation, we obtain the conditions

$$E\{[z(t) - d(t)]y(t - m\Delta)\} = 0, \qquad m = 0, \pm 1, \pm 2, \ldots, \pm N \tag{7.178}$$

or

$$R_{yz}(m\Delta) = R_{yd}(m\Delta), \qquad m = 0, \pm 1, \pm 2, \ldots, \pm N \tag{7.179}$$

where

$$R_{yz}(\tau) = E[y(t)z(t + \tau)] \tag{7.180}$$

and

$$R_{yd}(\tau) = E[y(t)d(t + \tau)] \tag{7.181}$$

are the cross-correlations of the received signal with the equalizer output and with the data, respectively.

Using the expression in (7.176) for $z(t)$ in (7.179), these conditions can be expressed as the matrix equation

$$[R_{yy}][A] = [R_{yd}] \tag{7.182}$$

where

$$[R_{yy}] = \begin{bmatrix} R_{yy}(0) & R_{yy}(\Delta) & \cdots & R_{yy}(2N\Delta) \\ R_{yy}(-\Delta) & R_{yy}(0) & \cdots & R_{yy}[2(N-1)\Delta] \\ \vdots & & & \vdots \\ R_{yy}(-2N\Delta) & & \cdots & R_{yy}(0) \end{bmatrix} \tag{7.183}$$

and

$$[R_{yd}] = \begin{bmatrix} R_{yd}(-N\Delta) \\ R_{yd}[-(N-1)\Delta] \\ \vdots \\ R_{yd}(N\Delta) \end{bmatrix} \tag{7.184}$$

and $[A]$ is defined by (7.169). Note that these conditions for the optimum tap weights using the MMSE criterion are similar to the conditions for the zero-forcing weights, except correlation-function samples are used instead of pulse-response samples.

Two questions remain with regard to setting the tap weights. The first is what should be used for the desired response $d(t)$. In the case of digital signaling, one could use the detected data, even if the modem performance is very poor, since an error probability of only 10^{-2} still implies that $d(t)$ is correct for 99 out of 100 bits. Algorithms using the detected data as $d(t)$, the desired output, are called *decision-directed*.

The second question is what procedure should be followed if the sample values of the pulse needed in the zero-forcing criterion or the samples of the correlation function required for the MMSE criterion are not available. A useful strategy to follow in such cases is referred to as *adaptive equalization*. In this approach, known as the LMS algorithm, an initial guess for the coefficients is corrected according to the recursive relationship

$$\mathbf{A}(n+1) = \mathbf{A}(n) - K\epsilon(n)\mathbf{Y}(n) \tag{7.185}$$

where K is an adjustment parameter, $\mathbf{Y}(n)$ is a vector of received data samples,

$$\mathbf{Y}(n) = \begin{bmatrix} y(n\Delta) \\ y[(n-1)\Delta] \\ \vdots \\ y(2N\Delta) \end{bmatrix} \tag{7.185}$$

and $\epsilon(n)$ is the error $y(n) - d(n)$.

Much more could be said about equalization, but we will close here.*

SUMMARY

1. Binary baseband data transmission in additive white Gaussian noise with equally likely signals having constant amplitudes of $\pm A$ and of duration T results in an average error probability of

* For an excellent survey article dealing with equalization methods in part, see S. Qureshi "Adaptive Equalization," *IEEE Communications Magazine,* Vol. 20, March 1982, pp. 9–16.

$$P_E = Q\left(\sqrt{\frac{2A^2T}{N_0}}\right)$$

where N_0 is the single-sided power spectral density of the noise. The hypothesized receiver was the integrate-and-dump receiver, which turns out to be the optimum receiver in terms of minimizing the probability of error.

2. An important parameter in binary data transmission is $z = E_b/N_0$, the energy per bit divided by the noise power spectral density (single sided). For binary baseband signaling, it can be expressed in the following equivalent forms:

$$z = \frac{E_b}{N_0} = \frac{A^2T}{N_0} = \frac{A^2}{N_0(1/T)} = \frac{A^2}{N_0B_p}$$

where B_p is the "pulse" bandwidth, or roughly the bandwidth required to pass the baseband pulses. The latter expression then allows the interpretation that z is the signal power divided by the noise power in a pulse, or bit-rate, bandwidth.

3. For binary data transmission with arbitrary (finite energy) signal shapes, $s_1(t)$ and $s_2(t)$, the error probability for equally probable signals, was found to be

$$P_E = Q(\sqrt{w})$$

where

$$w = \frac{1}{2N_0}\int_{-\infty}^{\infty} |\mathcal{S}_1(f) - \mathcal{S}_2(f)|^2\, df = \frac{1}{2N_0}\int_{-\infty}^{\infty} |s_1(t) - s_2(t)|^2\, dt$$

in which $\mathcal{S}_1(f)$ and $\mathcal{S}_2(f)$ are the Fourier transforms of $s_1(t)$ and $s_2(t)$, respectively. This expression resulted from minimizing the average probability of error, assuming a linear-filter/threshold-comparison type of receiver. The receiver involves the concept of a matched filter; such a filter is matched to a specific signal pulse and maximizes peak signal divided by rms noise ratio at its output. In a matched filter receiver for binary signaling, two matched filters are used in parallel, each matched to one of the two signals, and their outputs are compared at the end of each signaling interval. The matched filters also can be realized as correlators.

4. The expression for the error probability of a matched-filter receiver also can be written as

$$P_E = Q\{[z(1 - R_{12})]^{1/2}\}$$

where $z = E/N_0$, E being the *average* signal energy given by $E = \frac{1}{2}(E_1 + E_2)$. R_{12} is a parameter that is a measure of the similarity of the two signals; it is given by

$$R_{12} = \frac{2}{E_1 + E_2} \int_{-\infty}^{\infty} s_1(t)s_2(t)\, dt$$

If $R_{12} = -1$, the signaling is termed *antipodal,* while if $R_{12} = 0$, the signaling is termed *orthogonal.*

5. Examples of coherent (that is, the signal arrival time and carrier phase are known at the receiver) signaling techniques at a carrier frequency ω_c rad/s are the following:

$$PSK: s_k(t) = A \sin [\omega_c t - (-1)^k \cos^{-1} m], \qquad nt_0 \leq t \leq nt_0 + T, \quad k = 1, 2$$

($\cos^{-1} m$ is called the *modulation index*)

$$ASK: s_1(t) = 0, \qquad nt_0 \leq t \leq nt_0 + T$$
$$s_2(t) = A \cos \omega_c t, \qquad nt_0 \leq t \leq nt_0 + T$$

$$FSK: s_1(t) = A \cos \omega_c t, \qquad nt_0 \leq t \leq nt_0 + T$$
$$s_2(t) = A \cos [(\omega_c + \Delta\omega)t], \qquad nt_0 \leq t \leq nt_0 + T$$

If $\Delta\omega = 2\pi\ell/T$ for FSK, where ℓ is an integer, it is an example of an orthogonal signaling technique. If $m = 0$ for PSK, it is an example of an antipodal signaling scheme. A value of E_b/N_0 of approximately 10.54 dB is required to achieve an error probability of 10^{-6} for PSK with $m = 0$; 3 dB more than this is required to achieve the same error probability for ASK and FSK.

6. Examples of signaling schemes not requiring coherent carrier references at the receiver are differential phase-shift keying (DPSK) and noncoherent FSK. Using ideal minimum-error-probability receivers, DPSK yields the error probability

$$P_E = \tfrac{1}{2} \exp (-E_b/N_0)$$

while noncoherent FSK gives the error probability

$$P_E = \tfrac{1}{2} \exp\left(-E_b/2N_0\right)$$

Noncoherent ASK is another possible signaling scheme with about the same error probability performance as noncoherent FSK.

7. In general, if a sequence of signals is transmitted through a bandlimited channel, adjacent signal pulses are smeared into each other by the transient response of the channel. Such interference between signals is termed *intersymbol interference*. By appropriately choosing transmitting and receiving filters, it is possible to signal through bandlimited channels while eliminating intersymbol interference. This signaling technique was examined by using Nyquist's pulse-shaping criterion and Schwarz's inequality. A useful family of pulse shapes for such signaling are those having raised cosine spectra.

8. One form of channel distortion is multipath interference. The effect of a simple two-ray multipath channel on binary data transmission is examined. Half of the time the received signal pulses interfere destructively, and the rest of the time they interfere constructively. The interference can be separated into intersymbol interference of the signaling pulses and cancelation due to the carriers of the direct and multipath components arriving out of phase.

9. Fading results from channel variations caused by propagation conditions. One of these conditions is multipath if the differential delay is short compared with the bit period but made up of many wavelengths. A commonly used model for a fading channel is one where the envelope of the received signal has a Rayleigh pdf. In this case, the signal power or energy has an exponential pdf, and the probability of error can be found by using the previously obtained error probability expressions for nonfading channels and averaging over the signal energy with respect to the assumed exponential pdf of the energy. Figure 7.28 compares the error probability for fading and nonfading cases for various modulation schemes. Fading results in severe degradation of the performance of a given modulation scheme. A way to combat fading is to use *diversity*.

10. Equalization can be used to remove a large part of the intersymbol interference introduced by channel filtering. Two techniques were briefly examined: zero-forcing and minimum-mean-squared error. Both can be realized by tapped delay-line filters. In the former technique, zero intersymbol interference is forced at sampling instants separated by multiples of a symbol period. If the tapped delay line is of length

$(2N + 1)T$, then N zeros can be forced on either side of the desired pulse. In a minimum mean-square-error equalizer, the tap weights are sought that give minimum mean square error between the desired output from the equalizer and the actual output. The resulting weights for either case can be precalculated and preset, or adaptive circuitry can be implemented to automatically adjust the weights. The latter technique can make use of a training sequence periodically sent through the channel, or it can make use of the received data itself in order to carry out the minimizing adjustment.

FURTHER READING

A number of excellent recently published textbooks deal exclusively with the subject of digital communications and treat the binary case in detail.

A very complete treatment of digital communications is contained in the book by Sklar (1989). Covered in this one volume are the concepts of basic modulation theory, error-correcting codes, link-power budget analysis, synchronization, and encryption. A very readable treatment of digital communications, although not as complete as the book by Sklar, is the volume by Haykin (1989).

The books by Proakis (1989) and Lee and Messerschmitt (1988) are other good treatments of digital communication systems. Proakis includes excellent treatments of the bandlimited channel problem and the problem of combating fading and multipath, which will be treated in Chapter 9. Proakis also includes a good introductory chapter on spread-spectrum communications, which will be treated in Chapter 8.

The book by Benedetto, Biglieri, and Castellani (1987) also provides an excellent overall treatment of the digital communication problem. They include a chapter on transmission over "real" channels and have good treatments of intersymbol interference, equalization, coding, and nonlinear channels.

The book by Ziemer and Peterson (1992) develops digital communication systems in more depth than in this chapter.

PROBLEMS

Section 7.1

7.1 A baseband digital transmission system that sends $\pm A$-valued rectangular pulses through a channel at a rate of 10,000 bps is to achieve an error probability of 10^{-5}. If the noise power spectral density is

$N_0 = 10^{-7}$ W/Hz, what is the required value of A? What is a rough estimate of the bandwidth required?

7.2 (a) Consider a baseband digital transmission system with noise level of $N_0 = 10^{-5}$ W/Hz. The signal bandwidth is defined to be that required to pass the main lobe of the signal spectrum. Fill in the following table with the required signal power and bandwidth to achieve the error probability/data rate combinations given.

Required Signal Power A^2 and Bandwidth

R, bps	$P_E = 10^{-3}$	$P_E = 10^{-4}$	$P_E = 10^{-5}$	$P_E = 10^{-6}$
1,000				
10,000				
100,000				

(b) Assume the noise level of part (a), but assume that the bandwidth is that required to pass the main lobe and the first side lobe of the signal spectrum. Recompute the preceding table.

7.3 A receiver for baseband digital data has a threshold set at ϵ instead of zero. Rederive (7.8), (7.9), and (7.10) taking this into account. If $P(+A) = P(-A) = \frac{1}{2}$, find E_b/N_0 in decibels as a function of ϵ for $0 \leq \epsilon/\sigma \leq 1$ to give $P_E = 10^{-6}$, where σ^2 is the variance of N.

7.4 With $N_0 = 10^{-6}$ W/Hz and $A = 20$ mV in a baseband data transmission system, what is the maximum data rate that will allow a P_E of 10^{-4} or less? 10^{-5}? 10^{-6}?

7.5 In a practical implementation of a baseband data transmission system, the sampler at the output of the integrate-and-dump detector requires 1 μs to sample the output. How much additional E_b/N_0, in decibels, is required to achieve a given P_E for a practical system over an ideal system for the following data rates? (a) 10 kbps; (b) 50 kbps; (c) 100 kbps.

7.6 (a) The received signal in a digital baseband system is either $+A$ or $-A$, equally likely, for T-second contiguous intervals. However, the timing is off at the receiver so that the integration starts ΔT seconds late (positive) or early (negative). Assume that the timing error is less than one signaling interval. By assuming a zero threshold and considering two successive intervals [i.e., $(+A$,

$+A$), $(+A, -A)$, $(-A, +A)$, $(-A, -A)$] obtain an expression for the probability of error as a function of ΔT. Show that it is

$$P_E = \tfrac{1}{2}Q\left(\sqrt{\frac{2E_b}{N_0}}\right) + \tfrac{1}{2}Q\left[\sqrt{\frac{2E_b}{N_0}}\left(1 - \frac{2|\Delta T|}{T}\right)\right]$$

Plot for $|\Delta T|/T = 0$, 0.1, 0.2, and 0.3.

(b) The degradation due to timing error in E_b/N_0 at a particular probability of error is the decibel difference between the curve for no timing error and that for a given timing error. Plot the degradation due to timing error at $P_E = 10^{-6}$ as a function of $|\Delta T|/T$. What is the additional amount of signal power (or energy) required to maintain an error probability of 10^{-6} for a timing error of 15%?

7.7 As an approximation to the integrate-and-dump detector in Figure 7.3(a), we replace the integrator with a lowpass RC filter with transfer function

$$H(f) = \frac{1}{1 + j(f/f_3)}$$

where f_3 is the 3-dB cutoff frequency.

(a) Find $s_0^2(T)/E\{n_0^2(t)\}$, where $s_0(T)$ is the value of the output signal at $t = T$ due to $+A$ being applied at $t = 0$, and $n_0(t)$ is the output noise. (Assume that the filter initial conditions are zero.)

(b) Find the relationship between T and f_3 such that the signal-to-noise ratio found in part (a) is maximized.

Section 7.2

7.8 Assume that the probabilities of sending the signals $s_1(t)$ and $s_2(t)$ are not equal, but are given by p and $q = 1 - p$, respectively. Derive an expression for P_E that replaces (7.30) that takes this into account. Show that the error probability is minimized by choosing the threshold to be

$$k_{\text{opt}} = \frac{\sigma_O^2}{s_{0_1}(T) - s_{0_2}(T)} \ln(p/q) + \frac{s_{0_1}(T) + s_{0_2}(T)}{2}$$

7.9 The general definition of a matched filter is a filter that maximizes *peak* signal-to-rms noise at some prechosen instant of time t_0.

(a) Assuming white noise at the input, use Schwarz's inequality to show that the transfer function of the matched filter is

$$H_m(f) = S^*(f) \exp(-j2\pi f t_0)$$

where $S(f) = \mathcal{F}[s(t)]$ and $s(t)$ is the signal to which the filter is matched.

(b) Show that the impulse response for the matched-filter transfer function found in part (a) is

$$h_m(t) = s(t_0 - t)$$

(c) If $s(t)$ is not zero for $t > t_0$, the matched-filter impulse response is nonzero for $t < 0$; that is, the filter is noncausal and cannot be physically realized because it responds before the signal is applied. If we want a realizable filter, we use

$$h_{mr}(t) = \begin{cases} s(t_0 - t), & t \geq 0 \\ 0, & t < 0 \end{cases}$$

Find the realizable matched-filter impulse response corresponding to the signal

$s(t) = A\Pi[(t - T/2)/T]$ and t_0 equal to 0, $T/2$, T, and $2T$.

(d) Find the peak output signal for all cases in part (c). Plot them versus t_0. What do you conclude about the relation between t_0 and the causality condition?

7.10 Referring to Problem 7.9 for the general definition of a matched filter, find the following in relation to the two signals shown in Figure 7.30.

(a) The causal matched-filter impulse responses. Sketch them.
(b) Relate the constants A and B so that both cases give the same peak-signal-to-rms noise ratio at the matched-filter output.

FIGURE 7.30

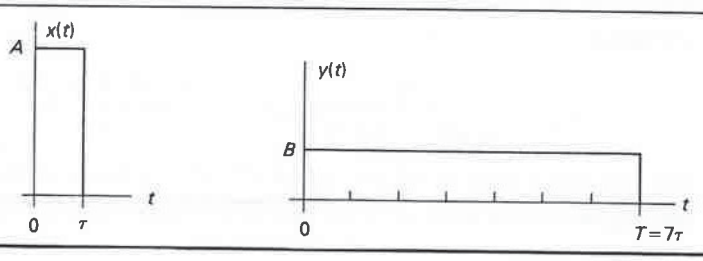
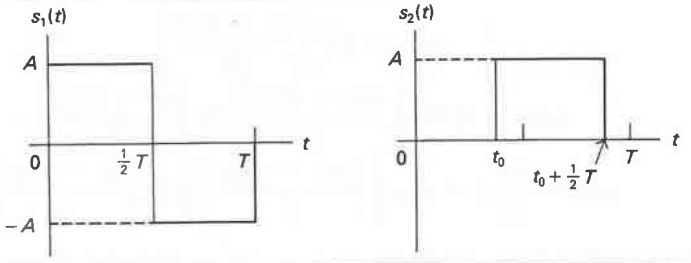


FIGURE 7.31



(c) Sketch the output of the matched filters as a function of time with signal only at the input.

(d) Comment on the ability of the two matched filters for these signals to provide an accurate measurement of time delay. What do you estimate the maximum error to be in so doing in each case?

(e) If *peak* transmitted power is a consideration, which waveform (and matched filter) is preferable?

7.11 (a) Find the optimum (matched) filter impulse response $h_0(t)$, as given by (7.43) for $s_1(t)$ and $s_2(t)$, shown in Figure 7.31.

(b) Find ζ^2 as given by (7.54). Plot ζ^2 versus t_0.

(c) What is the best choice for t_0 such that the error probability is minimized?

(d) Sketch a correlator receiver structure for these signals.

7.12 Find the peak-signal-squared-to-mean-squared-noise ratio for the output of a matched filter for each of the following signals in terms of A and T. Take the noise spectral density (single-sided) as N_0.

(a) $s_1(t) = A\Pi\left[\dfrac{(t - T/2)}{T}\right]$

(b) $s_2(t) = \dfrac{A}{2}\left\{1 + \cos\left[\dfrac{2\pi(t - T/2)}{T}\right]\right\}\Pi\left[\dfrac{(t - T/2)}{T}\right]$

(c) $s_3(t) = A\cos\left[\dfrac{\pi(t - T/2)}{T}\right]\Pi\left[\dfrac{(t - T/2)}{T}\right]$

(d) $s_4(t) = A\Lambda\left[\dfrac{(t - T/2)}{T}\right]$

The signals $\Pi(t)$ and $\Lambda(t)$ are the unit-rectangular and unit-triangular functions defined in Chapter 2.

7.13 Given these signals:

$$s_A(t) = A\Pi\left[\frac{(t - T/2)}{T}\right]$$

$$s_B(t) = B\cos\left[\frac{\pi(t - T/2)}{T}\right]\Pi\left[\frac{(t - T/2)}{T}\right]$$

$$s_C(t) = \frac{C}{2}\left\{1 + \cos\left[\frac{2\pi(t - T/2)}{T}\right]\right\}\Pi\left[\frac{(t - T/2)}{T}\right]$$

Assume that these signals are used in a binary digital data transmission system in the following combinations. In each case, calculate R_{12} in (7.59) in terms of A, B, C, and T. Write down an expression for P_E according to (7.58). What is the optimum threshold in each case?

(a) $s_1(t) = s_A(t)$; $s_2(t) = s_B(t)$
(b) $s_1(t) = s_A(t)$; $s_2(t) = s_C(t)$
(c) $s_1(t) = s_B(t)$; $s_2(t) = s_C(t)$
(d) $s_1(t) = s_B(t)$; $s_2(t) = -s_B(t)$
(e) $s_1(t) = s_C(t)$; $s_2(t) = -s_C(t)$

Section 7.3

7.14 Verify the numbers given in Table 7.2 by numerical integration. To evaluate $Q(x)$, use the rational approximation given in Appendix C.6.

7.15 Plot the results for P_E given in Table 7.2 versus $z = E_b/N_0$ in decibels with P_E plotted on a semilog axis. Estimate the additional E_b/N_0 at $P_E = 10^{-5}$ in decibels over the case for no phase error. Compare these results with that for constant phase error, as given by (7.77), of the same magnitude (ϕ for constant phase error equals σ_ϕ for the Gaussian phase-error case).

7.16 Find $z = E_b/N_0$ required to give $P_E = 10^{-7}$ for the following coherent digital modulation techniques: (a) binary ASK; (b) BPSK; (c) binary FSK; (d) BPSK with no carrier component but with a phase error of 5 degrees in the demodulator; (e) PSK with no phase error in demodulation, but with $m = 1/\sqrt{2}$; (f) PSK with $m = 1/\sqrt{2}$ and with a phase error of 5 degrees in the demodulator.

7.17 (a) Make a plot of degradation in decibels versus ϕ, the phase error in demodulation, for BPSK. Assume ϕ constant.

(b) Given that $z = 10.54$ dB is required to give $P_E = 10^{-6}$ for BPSK with no phase error in demodulation, what values of z in decibels are required to give $P_E = 10^{-6}$ for the following static phase errors in demodulation? (i) $\phi = 3$ degrees; (ii) $\phi = 5$ degrees; (iii) $\phi = 10$ degrees; (iv) $\phi = 15$ degrees.

7.18 (a) Plot the required signal-to-noise ratio $z = E_b/N_0$, in decibels, to give $P_E = 10^{-4}$ versus m for PSK with a carrier component for $0 \leq m \leq 1$.

(b) Repeat part (a) for $P_E = 10^{-5}$.

7.19 (a) Consider the transmission of digital data at a rate of $R = 50$ kbps and at an error probability of $P_E = 10^{-4}$. Using the bandwidth of the main lobe as a bandwidth measure, give an estimate of the required transmission bandwidth and signal-to-noise ratio in decibels required for the following coherent modulation schemes: (i) binary ASK; (ii) BPSK; (iii) binary coherent FSK (take the minimum spacing possible between the signal representing the logic 1 and that representing the logic 0).

(b) Consider the same question as in part (a), but with $R = 100$ kbps and $P_E = 10^{-5}$.

(c) Repeat part (a), but with $R = 25$ kbps and $P_E = 10^{-6}$.

7.20 Derive an expression for P_E for binary coherent FSK if the frequency separation of the two transmitted signals is chosen to give a *minimum* correlation coefficient between the two signals. How much improvement in SNR over the orthogonal-signal case is obtained?

Section 7.4

7.21 Differentially encode the following binary sequences. Arbitrarily choose a 1 as the reference bit to begin the encoding process. (*Note:* Spaces are used to add clarity.)

(a) 100 111 000 101
(b) 101 010 101 010
(c) 111 111 111 111
(d) 000 000 000 000
(e) 111 111 000 000

7.22 Consider the sequence to 110 111 001 010. Differentially encode it and assume that the differentially encoded sequence is used to biphase modulate a sinusoidal carrier of arbitrary phase. Prove that the demodulator of Figure 7.17 properly gives back the original sequence.

7.23 (a) In the analysis of the optimum detector for DPSK, show that the random variables n_1, n_2, n_3, and n_4 have zero means and variances $N_0T/4$.

(b) Show that w_1, w_2, w_3, and w_4 have zero means and variances $n_0T/8$.

7.24 Compare (7.102) and (7.103) to show that for large z, nonoptimum detection and optimum detection of DPSK differ by approximately 2 dB.

7.25 (a) Compute z in decibels required to give $P_E = 10^{-6}$ for noncoherent, binary FSK and DPSK. For the latter, carry out the computation for both the optimum and suboptimum detectors.
(b) Repeat part (a) for $P_E = 10^{-5}$.
(c) Repeat part (a) for $P_E = 10^{-4}$.

7.26 Compare bandwidth requirements for noncoherent FSK and for DPSK for the following data rates R. Use null-to-null RF bandwidths. Assume that the FSK "tones" must be separated by $2/T$ Hz.

(a) $R = 10$ kbps
(b) $R = 50$ kbps
(c) $R = 100$ kbps
(d) $R = 500$ kbps
(e) $R = 1$ Mbps

7.27 Find the probability of error for noncoherent ASK, with signal set

$$s_i(t) = \begin{cases} 0, & 0 \le t \le T,\ i = 1 \\ A\cos(\omega_c t + \theta), & 0 \le t \le T,\ i = 2 \end{cases}$$

where θ is a uniformly distributed random variable in $(0, 2\pi)$. White Gaussian noise is added to this signal in the channel. The receiver is a bandpass filter followed by an envelope detector followed by a sampler and threshold comparison. Show that the envelope detector output with signal 1 present (i.e., zero signal) is Rayleigh-distributed, and that the envelope detector output with signal 2 present is Rician-distributed. Assuming that the threshold is set at $A/2$, find an expression for the probability of error. You will not be able to integrate this expression. However, by making use of the approximation

$$I_0(v) \approx \frac{e^v}{\sqrt{2\pi v}}, \qquad v \gg 1$$

you will be able to approximate the pdf of the sampler output for large signal-to-noise ratio as Gaussian and express the probability of error in terms of a Q-function. (*Hint:* Neglect the $v^{-1/2}$ in the above approximation.) Plot the error probability versus the signal-to-noise ratio.

Section 7.5

7.28 Show that (7.115) and (7.116) are Fourier transform pairs.

7.29 Assume a raised-cosine pulse with $\beta = 1/2T$, additive noise with power spectral density

$$G_n(f) = \frac{2\sqrt{2}\sigma_n^2/\pi f_3}{1 + (f/f_3)^4}$$

and a channel filter with transfer-function-squared magnitude given by

$$|H_C(f)|^2 = \frac{1}{1 + (f/f_C)^2}$$

Find and sketch the optimum transmitter and receiver filters for binary signaling for the following cases:

(a) $f_3 = f_C = \frac{1}{2T}$ (b) $f_C = 2f_3 = \frac{1}{T}$ (c) $f_3 = 2f_C = \frac{1}{T}$

(d) $\frac{1}{2T} = f_3 = 2f_C$ (e) $\frac{1}{2T} = f_C = 2f_3$

7.30 By appropriate sketches, show that the raised-cosine spectra satisfy Nyquist's pulse-shaping criterion.

7.31 (a) Using (7.128), and (7.139), show that the transmitted signal energy is

$$E_T = A^2 \int_{-\infty}^{\infty} \frac{|P(f)|^2\, df}{|H_C(f)|^2 |H_R(f)|^2}$$

(b) Solving for A^2 in the result obtained for E_T above and using (7.129) to find var $(N) = \sigma^2$, show that

$$\frac{\sigma^2}{A^2} = \frac{1}{E_T} \int_{-\infty}^{\infty} G_n(f) |H_R(f)|^2\, df \int_{-\infty}^{\infty} \frac{|P(f)|^2\, df}{|H_C(f)|^2 |H_R(f)|^2}$$

(c) Use Schwarz's inequality to show that the minimum for σ^2/A^2 is

$$\left(\frac{\sigma}{A}\right)^2_{\min} = E_T^{-1} \left[\int_{-\infty}^{\infty} \frac{G_n^{1/2}(f) |P(f)|}{|H_C(f)|}\, df \right]^2$$

which is achieved for $|H_R(f)|_{opt}$ and $|H_T(f)|_{opt}$ given when (7.134) and (7.135) are used.

(d) Show the minimum error probability is given by

$$P_{E,\min} = Q\left\{\sqrt{E_T}\left[\int_{-\infty}^{\infty} \frac{G_n^{1/2}(f)|P(f)|}{|H_C(f)|}\,df\right]^{-1/2}\right\}$$

7.32 Data are to be transmitted through a bandlimited channel at a rate $R = 1/T = 9600$ bps. The channel filter has transfer function

$$H_C(f) = \frac{1}{1 + j(f/4800)}$$

The noise is white with power spectral density

$$\frac{N_0}{2} = 10^{-12} \text{ W/Hz}$$

Assume a received pulse with raised-cosine spectrum given by (7.116) with

$$\beta = \frac{1}{2T} = 4800 \text{ Hz}$$

is desired.

(a) Find the magnitudes of the transmitter and receiver filter transfer functions that give zero intersymbol interference and optimum detection.

(b) Using a table or the asymptotic approximation for the Q-function, find the value of A/σ required to give $P_{E,\min} = 10^{-4}$.

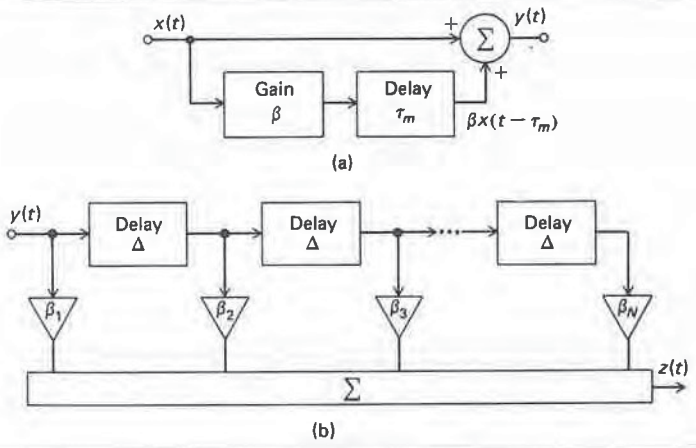
(c) Referring to Problem 7.31, find E_T to give this value of A/σ for the N_0, $G_n(f)$, $P(f)$, and $H_C(f)$ given above. (Numerical integration required.)

Section 7.6

7.33 Plot P_E from Equation (7.153) versus z_0 for $\delta = 0.5$ and $\tau_m/T = 0.2$, 0.6, and 1.0. Note that effective use can be made of Figure 7.26 by appropriately shifting the abscissa.

7.34 Redraw Figure 7.27 for $P_E = 10^{-5}$. For a rough plot, make use of Figure 7.26. For a more refined plot, write a Mathcad program using solve blocks to obtain the degradation for various values of δ and τ_m/T.

FIGURE 7.32



7.35 A simple model for a multipath communications channel is shown in Figure 7.32(a).

(a) Find $H_c(f) = Y(f)/X(f)$ for this channel and plot $|H_c(f)|$ for $\beta = 1$ and 0.5.

(b) In order to equalize, or undo, the channel-induced distortion, an equalization filter is used. Ideally, its transfer function should be

$$H_{eq}(f) = \frac{1}{H_c(f)}$$

if the effects of noise are ignored and only distortion caused by the channel is considered. A tapped delay-line or transversal filter, as shown in Figure 7.32(b), is commonly used to approximate $H_{eq}(f)$. Write down a series expression for $H'_{eq}(f) = Z(f)/Y(f)$.

(c) Using $(1 + x)^{-1} = 1 - x + x^2 - x^3 + \ldots$, $|x| < 1$, find a series expression for $1/H_c(f)$. Equating this with $H_{eq}(f)$ found in part (b), find the values for $\beta_1, \beta_2, \ldots, \beta_N$, assuming $\tau_m = \Delta$.

Section 7.7

7.36 Fading margin can be defined as the incremental E_b/N_0, in decibels, required to provide a certain desired error probability in a fading channel as could be achieved with the same modulation technique in a nonfading channel. Assume that a bit error probability of 10^{-2}

is specified. Find the fading margin required for the following cases: (a) BPSK; (b) DPSK; (c) coherent FSK; (d) noncoherent FSK.

7.37 Repeat Problem 7.36 for a specified error probability of 10^{-3}.

7.38 Carry out the integrations leading to (7.162), (7.163), (7.164), and (7.165) given that the signal-to-noise ratio pdf is given by

$$f_z(z) = \frac{1}{\bar{z}} e^{-z/\bar{z}}, \qquad z \geq 0$$

Section 7.8

7.39 Given the following channel pulse-response samples:

$p_c(-3T) = 0.001$ $p_c(-2T) = -0.01$ $p_c(-T) = 0.1$ $p_c(0) = 1.0$
$p_c(T) = 0.2$ $p_c(2T) = -0.02$ $p_c(3T) = 0.005$

(a) Find the tap coefficients for a three-tap zero-forcing equalizer.
(b) Find the output samples for $mT = -2T, -T, 0, T,$ and $2T$.

7.40 (a) Consider the design of an MMSE equalizer for a multipath channel whose output is of the form

$$y(t) = A\, d(t) + bA\, d(t - T_m) + n(t)$$

where the second term is a multipath component and the third term is noise independent of the data, $d(t)$. Assume $d(t)$ is a random (coin-toss) binary sequence with autocorrelation function $R_{dd}(\tau) = \Lambda(\tau/T)$. Let the noise have a lowpass-RC-filtered spectrum with 3-dB cutoff frequency $f_3 = 1/T$. Let the tap spacing be $\Delta = T_m = T$. Express the matrix $[R_{yy}]$ in terms of the signal-to-noise ratio $E_b/N_0 = A^2T/N_0$, where N_0 is the single-sided power spectral density of the noise into the lowpass RC filter that produced the noise into the equalizer.

(b) Obtain the optimum tap weights for a three-tap MMSE equalizer and at a signal-to-noise ratio of 10 dB.



COMPUTER EXERCISES*

7.1 Develop a computer simulation of an integrate-and-dump detector for antipodal baseband signaling. Generate Gaussian noise samples so that

* Computer exercises requiring a computer simulation, such as 7.1 and 7.4, are best done with a high-level programming language such as C or Fortran. Matlab may also suffice in these exercises.

white noise of two-sided spectral density $N_0/2$ is simulated. You can do this by drawing independent Gaussian random numbers with zero mean with variance σ^2 obeying*

$$\sigma^2 T_s = \frac{N_0}{2}$$

where T_s is the sample interval (this should be one-tenth the bit period or less). Obtain an estimate the probability of error versus E_b/N_0 by simulating the transmission of many bits into the receiver, counting the number of errors, and dividing by the total number of bits received for a number of values of E_b/N_0. Do your results check with Figure 7.5?

7.2 Write a computer program to evaluate the degradation imposed by bit timing error at a desired error probability as discussed in Problem 7.6.

7.3 Write a computer program to evaluate the degradation imposed by Gaussian phase jitter at a desired error probability as discussed in connection with the data presented in Table 7.2. This will require numerical integration.

7.4 Referring to Computer Exercise 7.1 and Problem 7.7, write a simulation of a receiver in which the integrate-and-dump detector is replaced by a first-order filter, thus verifying the theoretical result obtained in Problem 7.7. You will have to simulate the filter digitally. It is suggested that you use the bilinear-z transform realization method for the digital filter.†

7.5 Write a computer program to evaluate various digital modulation techniques:

(a) For a specified data rate and error probability, find the required bandwidth and E_b/N_0 in decibels. Corresponding to the data rate and required E_b/N_0, find the required received signal power for $N_0 = 1$ W/Hz.

(b) For a specified bandwidth and error probability find the allowed data rate and required E_b/N_0 in decibels. Corresponding to the data rate and required E_b/N_0, find the required received signal power for $N_0 = 1$ W/Hz.

7.6 Write a computer program to compute and plot the transfer functions of the optimum filters as specified by (7.134) and (7.135) for specified

* See Ziemer and Peterson, pp. 121–122.

† See, for example, Ziemer, Tranter, and Fannin, Chapter 9.

noise power spectral density and channel transfer function for raised cosine spectra.

7.7 Write a computer program to verify Figures 7.26 and 7.27.

7.8 Write a computer program to evaluate degradation due to fading at a specified error probability.

7.9 Write a computer program to design equalizers for specified channel conditions for: (a) the zero-forcing criterion; (b) the MMSE criterion.

8 ADVANCED DATA COMMUNICATIONS TOPICS

In this chapter we consider some topics on data transmission that are beyond the fundamental ones considered in Chapter 7. The first topic considered is that of M-ary digital modulation systems, where $M > 2$. We next examine bandwidth requirements for data transmission systems. An important consideration in any communications system is synchronization including carrier, symbol, and word. This is considered next. Following this, we look at modulation techniques that utilize bandwidths much larger than that required for data modulation itself. Such schemes are referred to as *spread-spectrum systems*. The final section deals with satellite communications links, which provides a specific example of the application of some of the digital communications topics considered in Chapters 7 and 8.

8.1 *M*-ARY DATA COMMUNICATIONS SYSTEMS

With the binary digital communications systems we have considered so far, one of only two possible signals can be transmitted during each signaling interval. In an M-ary system, one of M possible signals may be transmitted during each T_s-second signaling interval, where $M \geq 2$ (we now place a subscript s on the signaling interval T to denote "symbol"; we will place the subscript b on T to denote "bit" when $M = 2$). Thus binary data transmission is a special case of M-ary data transmission. We refer to each possible transmitted signal of an M-ary message sequence as a *character* or *symbol*. The rate at which M-ary symbols are transmitted through the channel is called the *baud rate* in bauds.

M-ary Schemes Based on Quadrature Multiplexing

In Section 3.6 we demonstrated that two different messages can be sent through the same channel by means of quadrature multiplexing. In a quadrature-multiplexed system, the messages $m_1(t)$ and $m_2(t)$ are used to double-

sideband modulate two carrier signals, which are in phase quadrature, to produce the modulated signal

$$x_c(t) = A[m_1(t) \cos \omega_c t - m_2(t) \sin \omega_c t]$$
$$\triangleq R(t) \cos [\omega_c t + \theta(t)] \tag{8.1}$$

Demodulation at the receiver is accomplished by coherent demodulation with two reference sinusoids that are ideally phase and frequency coherent with the quadrature carriers. This same principle can be applied to transmission of digital data and results in several modulation schemes, three of which will be described here: (1) quadriphase-shift keying (QPSK), (2) offset quadriphase-shift keying (OQPSK), and (3) minimum-shift keying (MSK).

In the analysis of these systems, we make use of the fact that coherent demodulation ideally results in the two messages $m_1(t)$ and $m_2(t)$ being separate at the outputs of the quadrature mixers. Thus these quadrature-multiplexed schemes can be viewed as two separate digital modulation schemes operating in parallel.

The block diagram of a parallel realization for a QPSK transmitter is shown in Figure 8.1, along with typical signal waveforms. In the case

FIGURE 8.1 Modulator and typical waveforms for QPSK

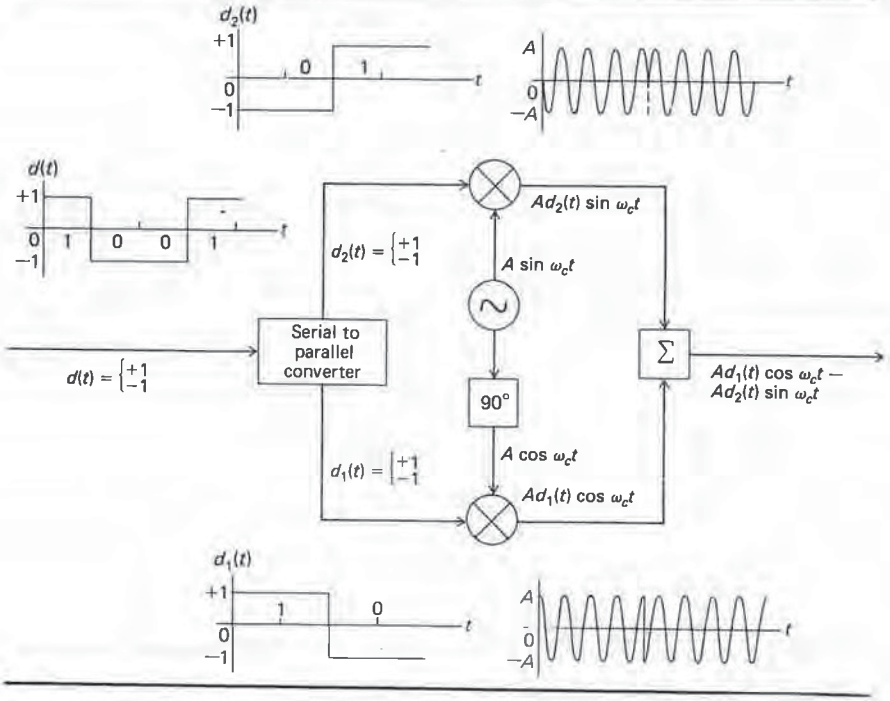
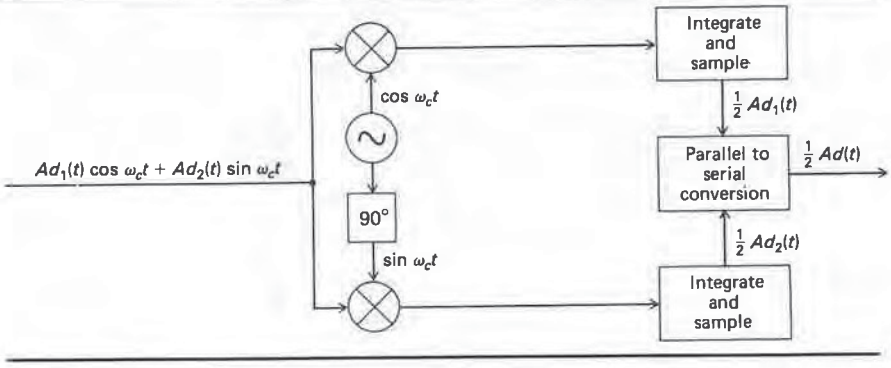


FIGURE 8.2 Detection of QPSK



of QPSK, we set $m_1(t) = d_1(t)$ and $m_2(t) = d_2(t)$, where d_1 and d_2 are ± 1-valued waveforms that have possible transitions each T_s seconds. Transitions are aligned. Note that we may think of $d_1(t)$ and $d_2(t)$, the bit streams that modulate the quadrature carriers, as being obtained by grouping the bits of a binary signal $d(t)$ with a bit period half the symbol period of $d_1(t)$ and $d_2(t)$, two bits at a time. Since the phase of the transmitted signal is

$$\theta_i = \tan^{-1}\left[\frac{-d_2(t)}{d_1(t)}\right] \tag{8.2}$$

we see that θ_i takes on the four possible values $\pm 45°$ and $\pm 135°$. Consequently, a QPSK transmitter can be realized in a serial fashion where $d_1(t)$ and $d_2(t)$ impose phase shifts on the carrier that are integer multiples of 90°.

Because the transmitted signal for a QPSK system can be viewed as two binary PSK signals summed as shown in Figure 8.1, it is reasonable that demodulation and detection involve two binary receivers in parallel, one for each quadrature carrier. The block diagram of such a system is shown in Figure 8.2. We note that a symbol in $d(t)$ will be correct only if the corresponding bits in both $d_1(t)$ and $d_2(t)$ are correct. Thus the probability of correct reception P_c for each bit of $d(t)$ is given by

$$P_c = (1 - P_{E_1})(1 - P_{E_2}) \tag{8.3}$$

where P_{E_j} is the probability of error for quadrature channel j, $j = 1$ or 2. In writing (8.3), it has been assumed that errors in the quadrature channels are independent. We will discuss this assumption shortly.

Turning now to the calculation of P_{E_j}, $j = 1, 2$, we note that because of

symmetry, $P_{E_1} = P_{E_2}$. Assuming that the input to the receiver is signal plus white Gaussian noise with double-sided power spectral density $\frac{1}{2}N_0$, that is,

$$y(t) = Ad_1(t) \cos \omega_c t - Ad_2(t) \sin \omega_c t + n(t) \tag{8.4}$$

we find that the output of the upper correlator in Figure 8.2 at the end of a signaling interval T_s is

$$V_1 = v_1(T_s) = \pm\tfrac{1}{2}AT_s + N_1 \tag{8.5}$$

where

$$N_1 = \int_0^{T_s} n(t) \cos \omega_c t \, dt \tag{8.6}$$

Similarly, the output of the lower correlator at $t = T_s$ is

$$V_2 = v_2(T_s) = \pm\tfrac{1}{2}AT_s + N_2 \tag{8.7}$$

where

$$N_2 = \int_0^{T_s} n(t) \sin \omega_c t \, dt \tag{8.8}$$

Errors at either correlator output will be independent if V_1 and V_2 are independent, which requires that N_1 and N_2 be independent. We can show that N_1 and N_2 are uncorrelated (Problem 8.4), and since they are Gaussian (why?), they are independent.

Returning to the calculation of P_{E_1}, we note that the problem is similar to the antipodal baseband case. The mean of N_1 is zero, and its variance is

$$\begin{aligned}
\sigma_1^2 = E\{N_1^2\} &= E\left\{\left[\int_0^{T_s} n(t) \cos \omega_c t \, dt\right]^2\right\} \\
&= \int_0^{T_s}\int_0^{T_s} E\{n(t)n(\alpha)\} \cos \omega_c t \cos \omega_c \alpha \, dt \, d\alpha \\
&= \int_0^{T_s}\int_0^{T_s} \frac{N_0}{2} \delta(t - \alpha) \cos \omega_c t \cos \omega_c \alpha \, d\alpha \, dt \\
&= \frac{N_0}{2}\int_0^{T_s} \cos^2 \omega_c t \, dt \\
&= \frac{N_0 T_s}{4}
\end{aligned} \tag{8.9}$$

Thus, following a series of steps similar to the case of binary antipodal signaling, we find that

$$\begin{aligned} P_{E_1} &= P(d_1 = +1)P(E_1 \mid d_1 = +1) + P(d_1 = -1)P(E_1 \mid d_1 = -1) \\ &= P(E_1 \mid d_1 = +1) = P(E_1 \mid d_1 = -1) \end{aligned} \tag{8.10}$$

where the latter equation follows by noting the symmetry of the pdf of V_1. But

$$\begin{aligned} P(E \mid d_1 = +1) &= P(\tfrac{1}{2}AT_s + N_1 < 0) = P(N_1 < -\tfrac{1}{2}AT_s) \\ &= \int_{-\infty}^{-AT_s/2} \frac{e^{-n_1^2/2\sigma_1^2}}{\sqrt{2\pi\sigma_1^2}}\, dn_1 \\ &= Q\left(\sqrt{\frac{A^2T_s}{N_0}}\right) \end{aligned} \tag{8.11}$$

Thus the probability of error for the upper channel in Figure 8.2 is

$$P_{E_1} = Q\left(\sqrt{\frac{A^2T_s}{N_0}}\right) \tag{8.12}$$

the same as P_{E_2}. Noting that $\frac{1}{2}A^2T_s$ is the average energy for *one* quadrature channel, we see that (8.12) is identical to binary PSK. Thus, considered on a *per channel* basis, QPSK performs identically to binary PSK.

However, if we consider the probability of error for a single phase of a QPSK system we obtain, from (8.3), the result

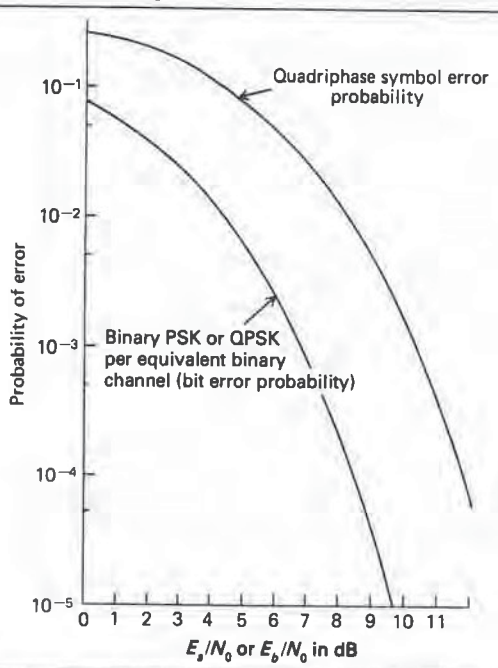
$$\begin{aligned} P_E &= 1 - P_c = 1 - (1 - P_{E_1})^2 \cong 2P_{E_1}, \qquad P_{E_1} \ll 1 \\ &= 2Q\left(\sqrt{\frac{A^2T_s}{N_0}}\right) \end{aligned} \tag{8.13}$$

Noting that the energy per symbol, or character, is $A^2T_s \triangleq E_s$ for the quadriphase signal, we may write (8.13) as

$$P_E = 2Q\left(\sqrt{\frac{E_s}{N_0}}\right) \tag{8.14}$$

If we compare QPSK and binary PSK on the basis of average energy-per-symbol-to-noise-spectral-density ratio, *QPSK is approximately 3 dB worse than binary PSK. However, we are transmitting twice as many bits with the QPSK system,*

FIGURE 8.3 Error probability for QPSK



assuming T_s the same. Comparing QPSK and binary PSK on the basis of the systems transmitting equal numbers of bits per second (two bits per QPSK phase), we find that the performances are the same. Binary PSK and QPSK are compared in Figure 8.3 on the basis of signal-to-noise ratio $z = E_s/N_0$, where E_s is the average energy per symbol. Note that the curve for QPSK approaches $\frac{3}{4}$ as the SNR approaches zero ($-\infty$ dB). This is reasonable because the receiver will, on average, make only one correct decision for every four signaling intervals (one of four possible phases) if the input is noise alone.

OQPSK Systems

Because the quadrature data streams $d_1(t)$ and $d_2(t)$ can switch signs simultaneously in a QPSK system, it follows that the data-bearing phase θ_i of the modulated signal can change by 180°. This can have an undesirable effect in terms of envelope deviation if the modulated signal is filtered, which is invariably the case in a practical system. To avoid the possibility of 180° phase switching, the switching instants of the quadrature-channel data signals $d_1(t)$ and $d_2(t)$ of a QPSK system can be offset by $T_s/2$ relative to each

other, where T_s is the signaling interval in either channel. The resulting modulation scheme is referred to as *offset QPSK*, which is abbreviated OQPSK; it is also sometimes called *staggered QPSK*. With the staggering or offsetting of quadrature data streams by $T_s/2$, the maximum phase change due to data modulation of the transmitted carrier is 90°. For an ideal system, the error probability performance of OQPSK is identical to that of QPSK. One limitation of an OQPSK system is that the data streams $d_1(t)$ and $d_2(t)$ *must have the same symbol durations*, whereas for QPSK they need not.

MSK Systems

In (8.1), suppose that message $m_1(t)$ is of the form

$$m_1(t) = d_1(t) \cos \omega_1 t \tag{8.15}$$

and message $m_2(t)$ is given by

$$m_2(t) = d_2(t) \sin \omega_1 t \tag{8.16}$$

where $d_1(t)$ and $d_2(t)$ are binary data signals taking on the value $+1$ or -1 in symbol intervals of length $T_s = 2T_b$ seconds, and ω_1 is the radian frequency of the weighting functions, $\cos \omega_1 t$ and $\sin \omega_1 t$, to be specified later. As in the case of QPSK, these data signals can be thought of as having been derived from a serial binary data stream whose bits occur each T_b seconds, with even-indexed bits used to produce $d_1(t)$ and odd-indexed bits used to produce $d_2(t)$, or vice versa. These binary data streams are weighted by a cosine or sine waveform as shown in Figure 8.4. If we substitute (8.15) and (8.16) into (8.1) and keep in mind that $d_1(t)$ and $d_2(t)$ are either $+1$ or -1, then, through the use of appropriate trigonometric identities, it follows that the modulated signal can be written as

$$x_c(t) = A \cos [\omega_c t + \theta_i(t)] \tag{8.17}$$

where

$$\theta_i(t) = -\tan^{-1}\left\{ \left[\frac{d_2(t)}{d_1(t)} \right] \tan (\omega_1 t) \right\} \tag{8.18}$$

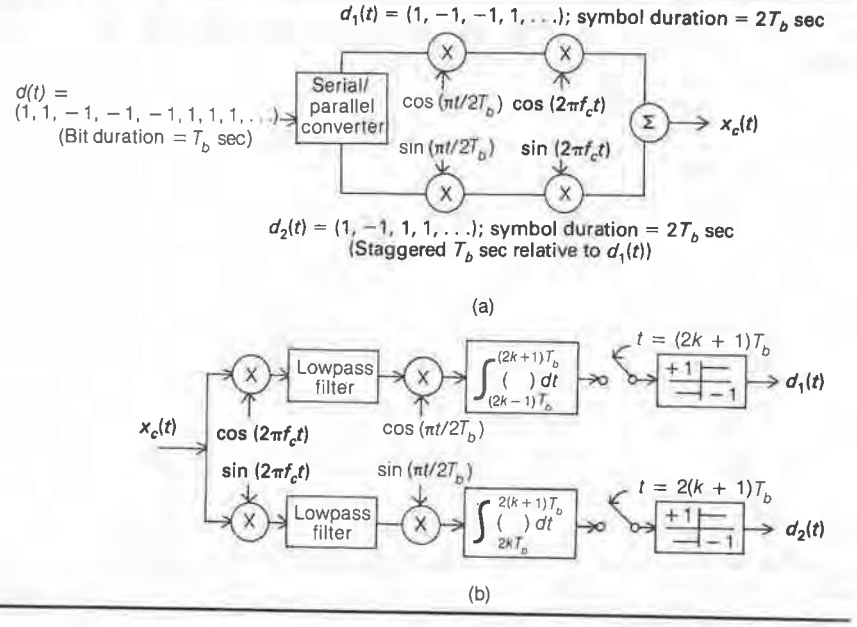
If $d_2(t) = d_1(t)$ (i.e., successive bits in the serial data stream are the same, either both logic 1's or both logic 0's), then

$$\theta_i(t) = -\omega_1 t \tag{8.19}$$

whereas, if $d_2(t) = -d_1(t)$ (i.e., successive bits in the serial data stream are different), then

$$\theta_i(t) = \omega_1 t \tag{8.20}$$

FIGURE 8.4 Block diagrams for parallel MSK modulator and demodulator. (a) Modulator. (b) Demodulator. (From R. E. Ziemer and C. R. Ryan, "Minimum-Shift Keyed Modem Implementations for High Data Rates," *IEEE Communications Magazine*, Vol. 21, October 1983. Copyright © 1983 IEEE. Reprinted with permission.)

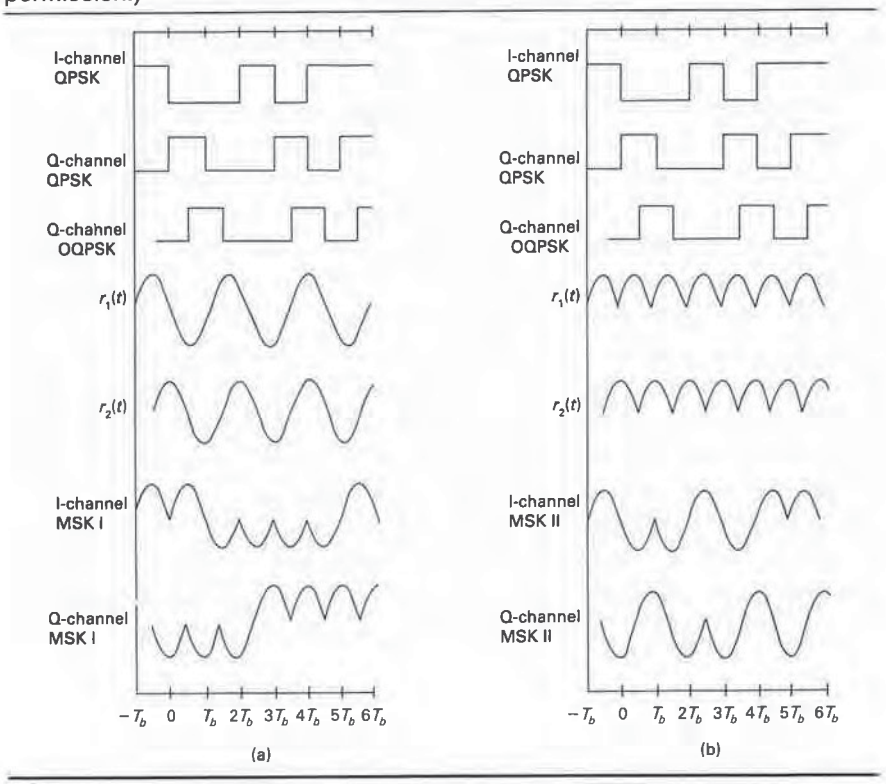


One form of minimum-shift keying (MSK) results if $\omega_1 = \pi/T_s = \pi/2T_b$. In this case, each symbol of the data signal $d_1(t)$ is multiplied or weighted by one-half cycle of a sine waveform, and each symbol of the data signal $d_2(t)$ is weighted by one-half cycle of a cosine waveform, as shown in Figure 8.5. This form of MSK, wherein the weighting functions for each symbol are alternating half cycles of sine or cosine waveforms, is referred to as *MSK type I*. *MSK type II* modulation results if the weighting is always a positive half-cosinusoid or half-sinusoid, depending on whether it is the upper or lower arm in Figure 8.4 being referred to. This type of MSK modulation, which is also illustrated in Figure 8.5, bears a closer relationship to OQPSK than to MSK type I.

Using $\omega_1 = \pi/2T_b$ in (8.18) and substituting the result into (8.19) gives

$$x_c(t) = A \cos\left[2\pi\left(f_c \pm \frac{1}{4T_b}\right)t + u_k\right] \tag{8.21}$$

FIGURE 8.5 (a) MSK type I modulation. (b) MSK type II modulation. (Adapted from Figure 3.6 of *Digital Communications by Satellite* by V. K. Bhargava et al. Copyright © 1981 John Wiley & Sons, Inc. Used with permission.)



where $f_c = \omega_c/2\pi$ and $u_k = 0$ or $u_k = k\pi$ modulo $\cdot\ 2\pi$, according to whether d_2/d_1 equals $+1$ or -1, respectively. From this form of an MSK-modulated signal, we can see that MSK can be viewed as frequency modulation in which the transmitted tones* are either one-quarter data rate $(1/4T_b)$ above or one-quarter data rate below the carrier f_c in instantaneous frequency (since the carrier is not actually transmitted, f_c is sometimes referred to as the *apparent carrier*). Note that the frequency spacing between the tones is $\Delta f = 1/2T_b$, which is the minimum frequency spacing required for the tones to be coherently orthogonal [that is, ρ_{12} of (7.57) is zero].

* One should not infer from this that the spectrum of the transmitted signal consists of impulses at frequencies $f_c \pm 1/4T_b$.

In neither MSK type I nor MSK type II modulation formats is there a one-to-one correspondence between the data bits of the serial bit stream and the instantaneous frequency of the transmitted signal. A modulation format in which this is the case, referred to as *fast frequency-shift keying (FFSK)*, can be obtained by differentially encoding the serial bit stream before modulation by means of an MSK type I modulator.

Viewing (8.21) as a phase-modulated signal, we note that the argument of the cosine can be separated into two phase terms, one due solely to the carrier frequency, or $2\pi f_c t$, and the other due to the modulation, or $\pm\pi(t/2T_b) + u_k$. The latter term is referred to as the *excess phase* and is conveniently portrayed by a trellis diagram, such as that in Figure 8.6, which shows the excess phase trajectories for all possible serial data sequences. Note that the excess phase changes by exactly $\pi/2$ radians each T_b seconds and that it is a continuous function of time. This results in even better envelope deviation characteristics than OQPSK when filtered. In the excess-phase trellis diagram, straight lines with positive slope correspond to alternating 1's and 0's in serial-data sequences, and straight lines with negative slope correspond to all 1's or all 0's in serial-data sequences.

The detector for MSK signals can be realized in parallel form in analogous fashion to QPSK or OQPSK, as shown in Figure 8.2, except that multiplication by $\cos(\pi t/2T_b)$ is required in the upper arm and multiplication by $\sin(\pi t/2T_b)$ is required in the lower arm in order to realize the optimum

FIGURE 8.6 MSK trellis diagram (From R. E. Ziemer and C. R. Ryan, "Minimum-Shift Keyed Modem Implementations for High Data Rates," *IEEE Communications Magazine*, Vol. 21, October 1983. Copyright © 1983 IEEE. Reprinted with permission.)

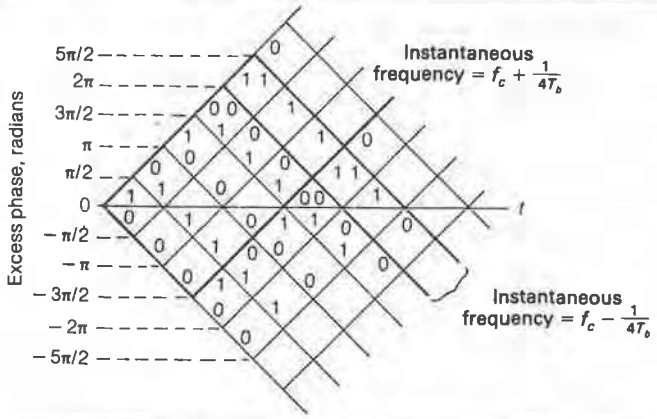
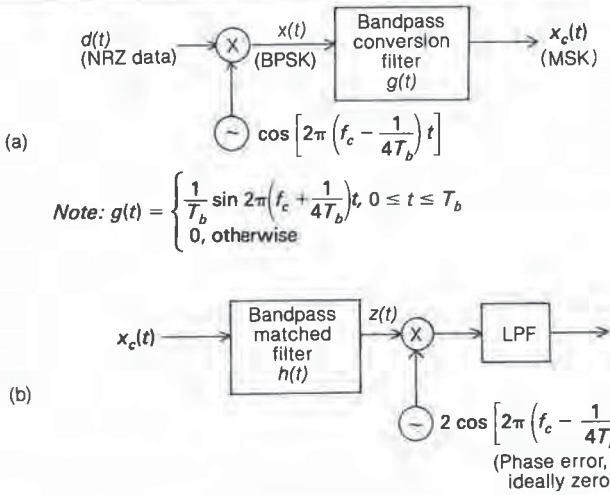


FIGURE 8.7 Block diagrams of serial MSK modulator and demodulator. (a) Serial MSK modulator. (b) Serial MSK demodulator. (From R. E. Ziemer and C. R. Ryan, "Minimum-Shift Keyed Modem Implementations for High Data Rates," *IEEE Communications Magazine*, Vol. 21, October 1983. Copyright © 1983 IEEE. Reprinted with permission.)



correlation detector for the two data signals $d_1(t)$ and $d_2(t)$. As in the case of QPSK (or OQPSK), it can be shown that the noise components at the integrator outputs of the upper and lower arms are uncorrelated. Except for a different scaling factor, the error probability analysis for MSK is identical to that for QPSK, and consequently, the error probability performance of MSK is identical to that of QPSK or OQPSK.

In the discussion of MSK so far, we have viewed the modulation and detection processes as being accomplished by parallel structures like those shown in Figures 8.1 and 8.2 for QPSK. It turns out that MSK can be processed in a serial fashion as well. The serial modulator structure, as shown in Figure 8.7(a), consists of a BPSK modulator with a conversion filter at its output with the transfer function

$$G(f) = \{\text{sinc}\,[(f - f_c)T_b - 0.25] + \text{sinc}\,[(f + f_c)T_b + 0.25]\}e^{-j2\pi f t_0} \tag{8.22}$$

where t_0 is an arbitrary filter delay and f_c is the apparent carrier frequency of the MSK signal. Note that the peak of the frequency response of the conversion filter is offset in frequency one-quarter data rate above the appar-

ent carrier. The BPSK signal, on the other hand, is offset one-quarter data rate below the desired apparent carrier of the MSK signal. Its power spectrum can be written as

$$S_{\text{BPSK}}(f) = (A^2T_b/2)\{\text{sinc}^2\,[(f - f_c)T_b + 0.25] + \text{sinc}^2\,[(f + f_c)T_b - 0.25]\} \quad (8.23)$$

The product of $|G(f)|^2$ and $S_{\text{BPSK}}(f)$ gives the power spectrum of the conversion filter output, which, after some simplification, can be shown to be

$$S_{\text{MSK}}(f) = \frac{32A^2T_b}{\pi^4}\left\{\frac{\cos^2 2\pi T_b(f - f_c)}{[1 - 16T_b^2(f - f_c)^2]^2} + \frac{\cos^2 2\pi T_b(f + f_c)}{[1 - 16T_b^2(f + f_c)^2]^2}\right\} \quad (8.24)$$

as illustrated graphically in Figure 8.8. This is the double-sided power spectrum of an MSK-modulated signal,* which demonstrates in the frequency domain the validity of the serial approach to the generation of MSK. Thus the parallel modulator structure can be replaced by a serial modulator structure, which means that the difficult task of producing amplitude-matched phase-quadrature signals in the parallel structure can be replaced by the perhaps easier task of generation of BPSK signals and synthesis of conversion filters.

At the receiver, essentially the reverse of the signal-processing procedure at the transmitter is carried out. The received signal is passed through a filter whose frequency response is proportional to the square root of the MSK spectrum. As shown in Figure 8.7(b), the filter is followed by a coherent demodulator, a sampler, and threshold comparison to carry out the data detection. Although the details will not be given here,† it can be shown that each symbol is sampled independently of those preceding or following it at the proper sampling instants.

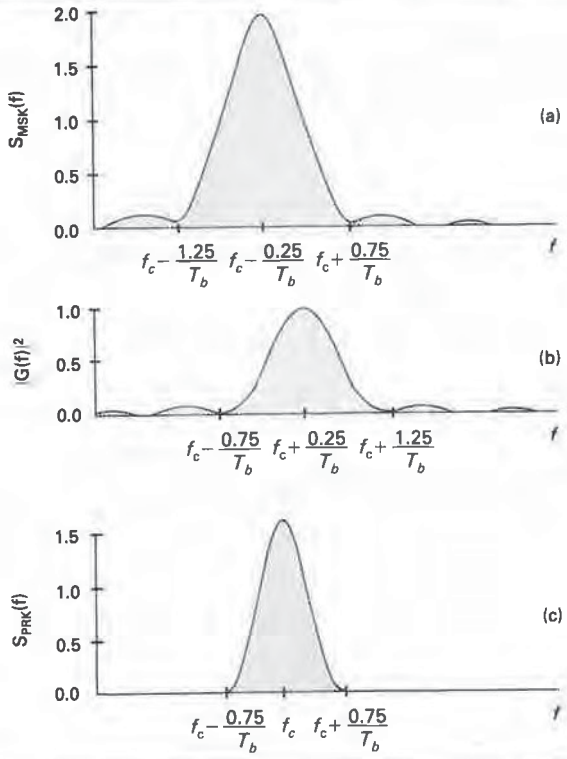
M-ary Data Transmission in Terms of Signal Space

A convenient framework for discussing *M*-ary data transmission systems is that of signal space. The approach used here in terms of justifying the receiver structure is heuristic. It is placed on a firm theoretical basis in Chapter 9, where optimum signal detection principles are discussed.

* This will be shown in Section 8.2.

† See F. Amoroso and J. A. Kivett, "Simplified MSK Signaling Technique," *IEEE Transactions on Communication,* Vol. COM-25, April 1977, pp. 433–441.

FIGURE 8.8 Spectra pertinent to producing serial MSK. (a) PRK power spectrum. (b) Frequency response of conversion filter magnitude squared. (c) MSK power spectrum. Only positive-frequency halves of double-sided spectra are shown. (From R. E. Ziemer and C. R. Ryan, "Minimum-Shift Keyed Modem Implementations for High Data Rates," *IEEE Communications Magazine*, Vol. 21, October 1983. Copyright © 1983 IEEE. Reprinted with permission.)



We consider coherent communication systems with signal sets of the form

$$s_i(t) = \sum_{j=1}^{K} a_{ij}\phi_j(t), \qquad 0 \le t \le T_s, \quad K \le M, \quad i = 1, 2, \ldots, M \tag{8.25}$$

where the functions $\phi_j(t)$ are orthonormal over the symbol interval. That is,

$$\int_0^{T_s} \phi_m(t)\phi_n(t)\,dt = \begin{cases} 1, & m = n \\ 0, & m \neq n \end{cases} \tag{8.26}$$

Based on (8.25), we can visualize the possible transmitted signals as points in a space with coordinate axes $\phi_1(t)$, $\phi_2(t)$, $\phi_3(t)$, . . . , $\phi_K(t)$, much as illustrated in Figure 2.5.

At the output of the channel it is assumed that signal plus additive white Gaussian noise is received; that is,

$$y(t) = s_i(t) + n(t), \qquad t_0 \leq t \leq t_0 + T_s,\ i = 1, \ldots, M \tag{8.27}$$

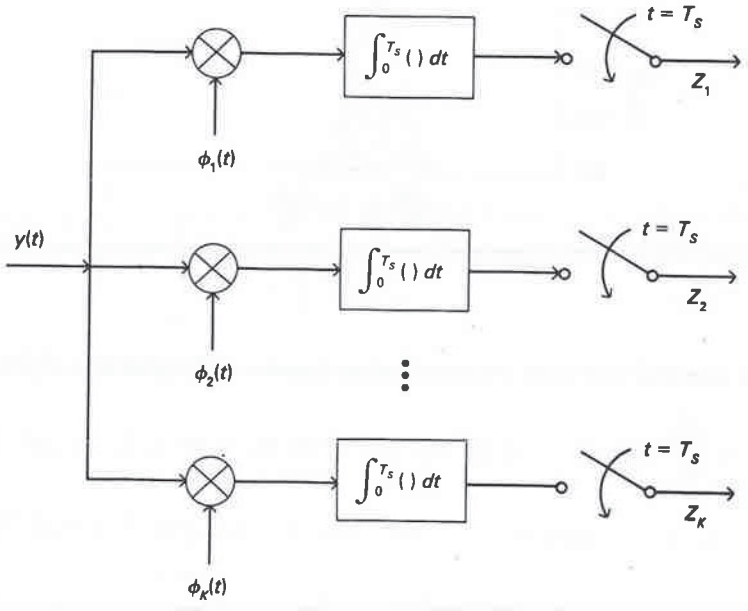
where t_0 is an arbitrary starting time equal to an integer times T_s. As shown in Figure 8.9, the receiver consists of a bank of K correlators, one for each orthonormal function. The output of the jth correlator is

$$Z_j = a_{ij} + N_j \tag{8.28}$$

where the noise component N_j is given by ($t_0 = 0$ for notational ease)

$$N_j = \int_0^{T_s} n(t)\phi_j(t)\, dt \tag{8.29}$$

FIGURE 8.9 Computation of signal-space coordinates



Note: $y(t) = s_i(t) + n(t)$ where $n(t)$ is white Gaussian noise.

Since $n(t)$ is Gaussian and white, the random variables $N_1, N_2, \ldots, N_K$ can be shown to be independent, zero-mean, Gaussian random variables with variances $N_0/2$, which is the two-sided spectral density of the noise.

It can be shown that this process preserves all the information required to make a minimum error-probability decision regarding which signal was transmitted. The next operation in the receiver is a decision box that performs the following function:

> Compare the received signal plus noise coordinates with the stored signal coordinates, a_{ij}. Choose as the transmitted signal that one closest to the received signal plus noise point with distance measured in the Euclidian sense; i.e., choose the transmitted signal as the one whose a_{ij}'s minimize $\sum_{j=1}^{K} [Z_j - a_{ij}]^2$.

This decision procedure will be shown in Chapter 9 to result in the minimum error probability possible.

▼ **EXAMPLE 8.1** Consider BPSK. Only one orthonormal function is required in this case, and it is

$$\phi(t) = \sqrt{\frac{2}{T_b}} \cos \omega_c t, \qquad 0 \leq t \leq T_b \tag{8.30}$$

The possible transmitted signals can be represented as

$$s_1(t) = \sqrt{E_b}\, \phi(t) \qquad \text{and} \qquad s_2(t) = -\sqrt{E_b}\, \phi(t) \tag{8.31}$$

▲ where E_b is the bit energy.

QPSK in Terms of Signal Space

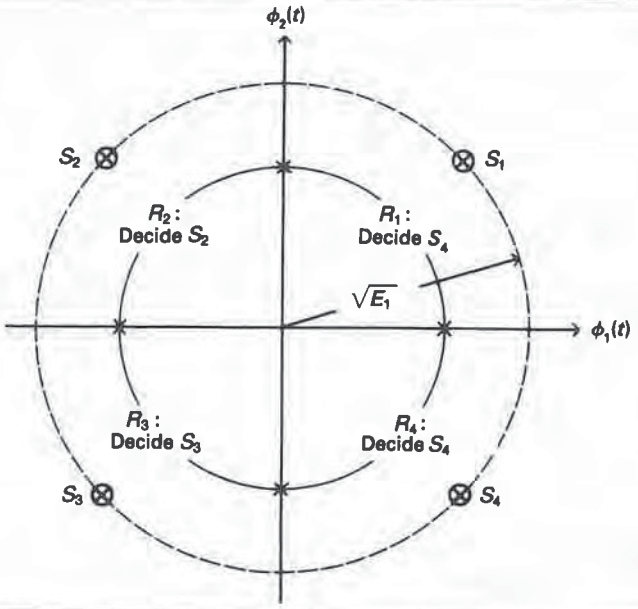
From Figures 8.9 and 8.2 we see that the receiver for QPSK consists of a bank of two correlators. Thus the received data can be represented in a two-dimensional signal space as shown in Figure 8.10. The transmitted signals can be represented in terms of two orthonormal functions $\phi_1(t)$ and $\phi_2(t)$ as

$$x_c(t) = s_i(t) = \sqrt{E_s}\, [d_1(t)\phi_1(t) - d_2(t)\phi_2(t)] = \sqrt{E_s}\, [\pm\phi_1(t) \pm \phi_2(t)] \tag{8.32}$$

where

$$\phi_1(t) = \sqrt{\frac{2}{T_s}} \cos \omega_c t, \qquad 0 \leq t \leq T_s \tag{8.33}$$

FIGURE 8.10 Signal space for QPSK



and

$$\phi_2(t) = \sqrt{\frac{2}{T_s}} \sin \omega_c t, \qquad 0 \leq t \leq T_s \tag{8.34}$$

E_s is the energy contained in $x_c(t)$ in one symbol interval. The resulting regions for associating a received data point with a possible signal point are also illustrated in Figure 8.10. It can be seen that the coordinate axes provide the boundaries of the regions that determine the signal point to be associated with a received data point. For example, if the received data point is in the first quadrant (region R_1), the decision is made that $d_1 = 1$ and $d_2 = -1$ (this will be denoted as signal point S_1 in the signal space). A simple bound on symbol error probability can be obtained by noting that

$$\begin{aligned} P_E &= Pr(Z \in R_2 \text{ or } R_3 \text{ or } R_4 | S_1 \text{ sent}) \\ &\leq Pr(Z \in R_2 \text{ or } R_3 | S_1 \text{ sent}) + Pr(Z \in R_3 \text{ or } R_4 | S_1 \text{ sent}) \end{aligned} \tag{8.35}$$

The two probabilities on the right-hand side of (8.35) can be shown to be equal. Thus,

$$\begin{aligned} P_E \leq 2Pr(Z \in R_2 \text{ or } R_3) &= 2Pr(\sqrt{E_s/2} + N_\perp < 0) \\ &= 2Pr(N_\perp < -\sqrt{E_s/2}) \end{aligned} \tag{8.36}$$

where $N_\perp$, as shown in Figure 8.11, is the noise component perpendicular to the decision boundary between R_1 and R_2. It can be shown that it has zero mean and variance $N_0/2$. Thus,

$$P_E \leq 2\int_{-\infty}^{-\sqrt{E_s/2}} \frac{e^{-u^2/N_0}}{\sqrt{\pi N_0}}\,du = 2\int_{\sqrt{E_s/2}}^{\infty} \frac{e^{-u^2/N_0}}{\sqrt{\pi N_0}}\,du \tag{8.37}$$

Making the change of variables $\mu = v/\sqrt{N_0/2}$, we can reduce this to the form

$$P_E = 2Q(\sqrt{E_s/N_0}) \tag{8.38}$$

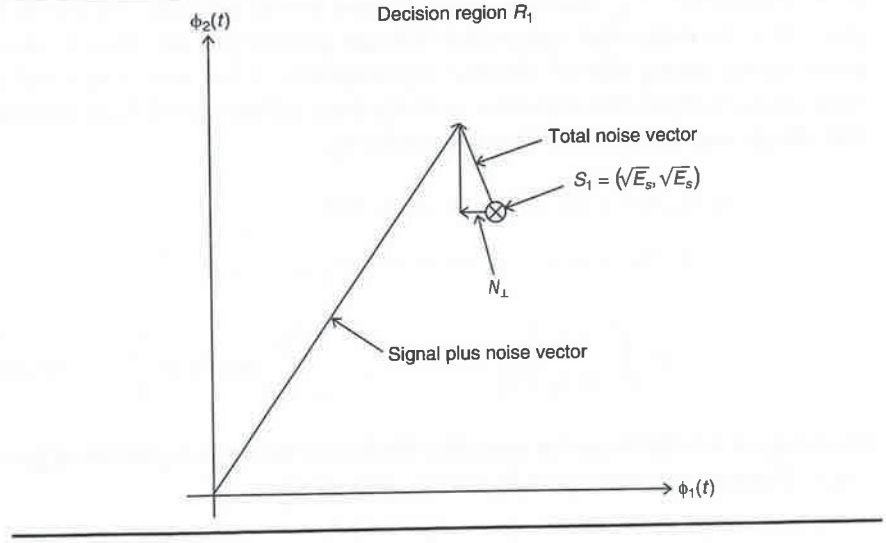
This is identical to (8.14), which resulted in neglecting the square of P_{E_1} in (8.13).

M-ary Phase-Shift Keying

The signal set for QPSK can be generalized to an arbitrary number of phases. The modulated signal takes the form

$$s_i(t) = \sqrt{\frac{2E_s}{T_s}} \cos\left[\omega_c t + \frac{2\pi(i-1)}{M}\right], \quad 0 \leq t \leq T_s, \quad i = 1, 2, \ldots, M \tag{8.39}$$

FIGURE 8.11 Representation of signal plus noise in signal space, showing $N_\perp$, the noise component that can cause the received data vector to land in R_2



Using trigonometric identities, this can be expanded as

$$s_i(t) = \sqrt{E_s}\left[\cos\left(\frac{2\pi(i-1)}{M}\right)\sqrt{\frac{2}{T_s}}\cos\omega_c t - \sin\left(\frac{2\pi(i-1)}{M}\right)\sqrt{\frac{2}{T_s}}\sin\omega_c t\right]$$

$$= \sqrt{E_s}\left[\cos\left(\frac{2\pi(i-1)}{M}\right)\phi_1(t) - \sin\left(\frac{2\pi(i-1)}{M}\right)\phi_2(t)\right] \qquad (8.40)$$

where $\phi_1(t)$ and $\phi_2(t)$ are the orthonormal functions defined by (8.33) and (8.34).

A plot of the signal points S_i, $i = 1, 2, \ldots, M$ along with the optimum decision regions is shown in Figure 8.12(a). The probability of error can be overbounded by noting from Figure 8.12(b) that the total area represented by the two half planes D_1 and D_2 is greater than the total shaded area in Figure 8.12(b), and thus the probability of symbol error is overbounded by the probability that the received data point Z lies in either half plane. Because of symmetry of the noise distribution, both probabilities are equal. Consider a single half plane along with a single signal point, which is at a minimum distance of

$$d = \sqrt{E_s}\sin(\pi/M) \qquad (8.41)$$

away from the boundary of the half plane. As in Figure 8.11, consider the noise component $N_\perp$, which is perpendicular to the boundary of the half plane. It is the only noise component that can possibly put the received data point on the wrong side of the decision boundary; it has zero mean and a variance $N_0/2$. From this discussion and referring to Figure 8.12(b), it follows that the probability of error is overbounded by

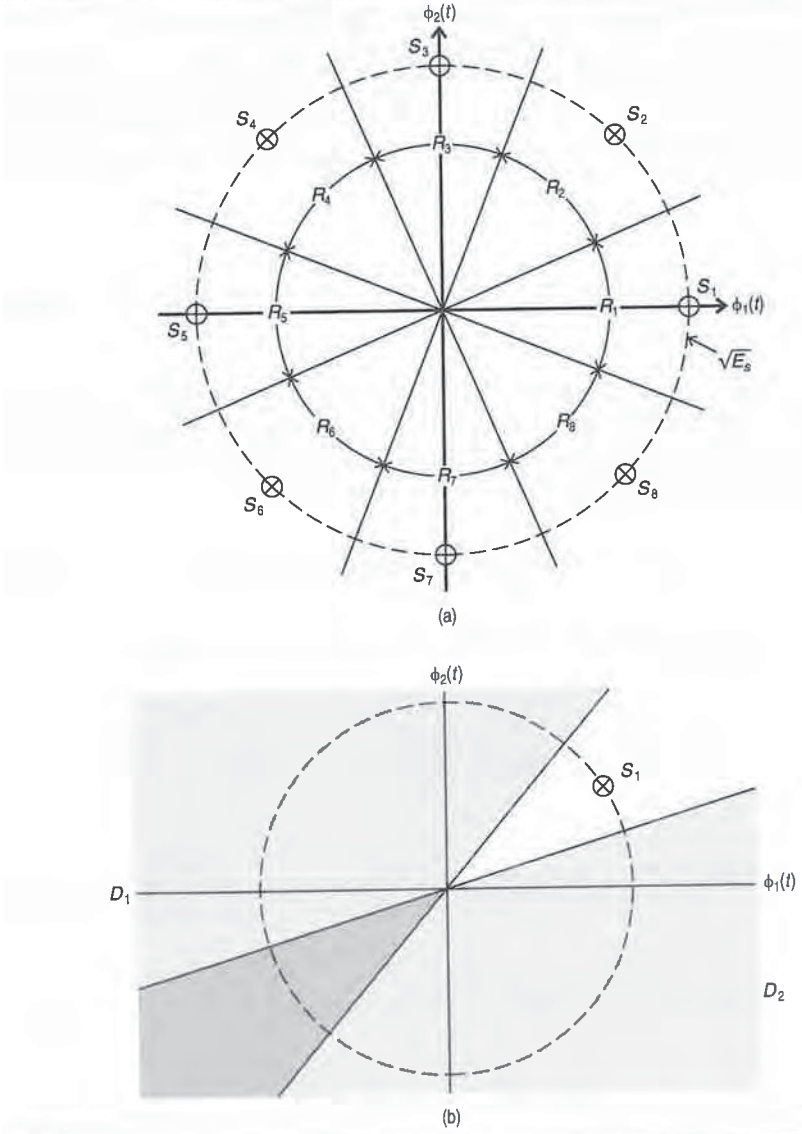
$$P_E < Pr(Z \in D_1 \text{ or } D_2) = 2Pr(Z \in D_1)$$

$$= 2Pr(d + N_\perp < 0) = 2Pr(N_\perp < -d)$$

$$= 2\int_{-\infty}^{-d} \frac{e^{-u^2/N_0}}{\sqrt{\pi N_0}}\,du = 2Q\left(\sqrt{\frac{2E_s}{N_0}}\sin(\pi/M)\right) \qquad (8.42)$$

From Figure 8.12(b) it can be seen that the bound becomes tighter as M gets larger (because the overlap of D_1 and D_2 gets smaller).

FIGURE 8.12 (a) Signal space for M-ary PSK with $M = 8$. (b) Signal space for M-ary PSK showing two half-planes that can be used to overbound P_E.



Quadrature-Amplitude-Shift Keying (QASK)

Another signaling scheme that allows multiple signals to be transmitted using quadrature carriers is *quadrature-amplitude-shift keying* (QASK), which is also referred to as *quadrature-amplitude modulation* (QAM). For example, M-QASK utilizes a signal structure similar to that of (8.32) but with the data sequences d_1 and d_2 each taking on $\sqrt{M}$ different possible levels. Thus, for example, we represent the transmitted signal in an arbitrary signaling interval for 16-QASK as

$$s_i(t) = \sqrt{\frac{2E_s}{T_s}}(A_i \cos \omega_c t + B_i \sin \omega_c t), \qquad 0 \leq t \leq T_s \tag{8.43}$$

where A_i and B_i take on the possible values $\pm a$ and $\pm 3a$ with equal probability. A signal-space representation for 16-QASK is shown in Figure 8.13(a), and the receiver structure is shown in Figure 8.13(b). The probability of symbol error for 16-QASK can be shown to be

$$P_E = 1 - [\tfrac{1}{4}P(C\,|\,\mathrm{I}) + \tfrac{1}{2}P(C\,|\,\mathrm{II}) + \tfrac{1}{4}P(C\,|\,\mathrm{III})] \tag{8.44}$$

where the probabilities $P(C\,|\,\mathrm{I})$, $P(C\,|\,\mathrm{II})$, and $P(C\,|\,\mathrm{III})$ are given by

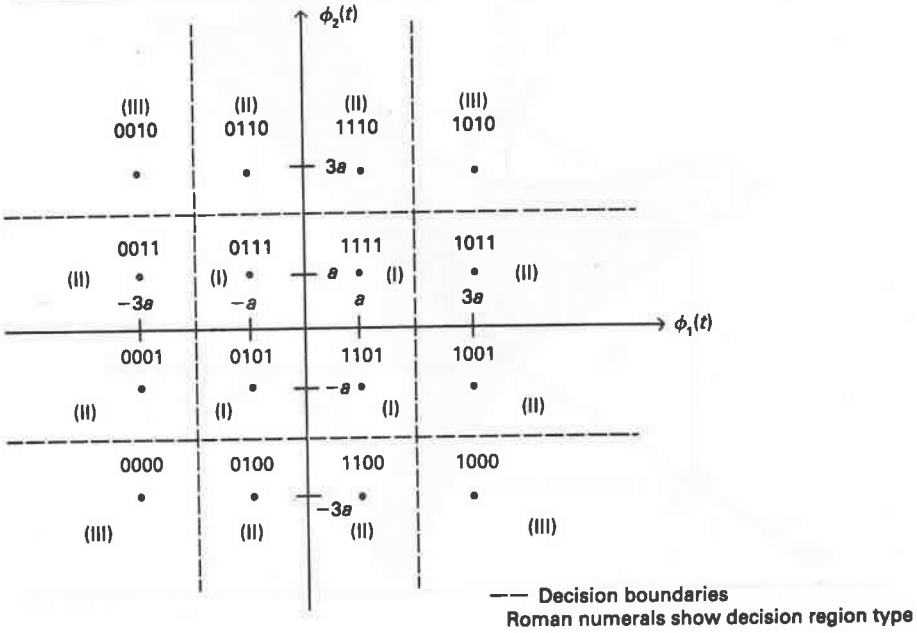
$$P(C\,|\,\mathrm{I}) = \left[1 - 2Q\left(\sqrt{\frac{2a^2}{N_0}}\right)\right]^2 \tag{8.45a}$$

$$P(C\,|\,\mathrm{II}) = \left[1 - 2Q\left(\sqrt{\frac{2a^2}{N_0}}\right)\right]\left[1 - Q\left(\sqrt{\frac{2a^2}{N_0}}\right)\right] \tag{8.45b}$$

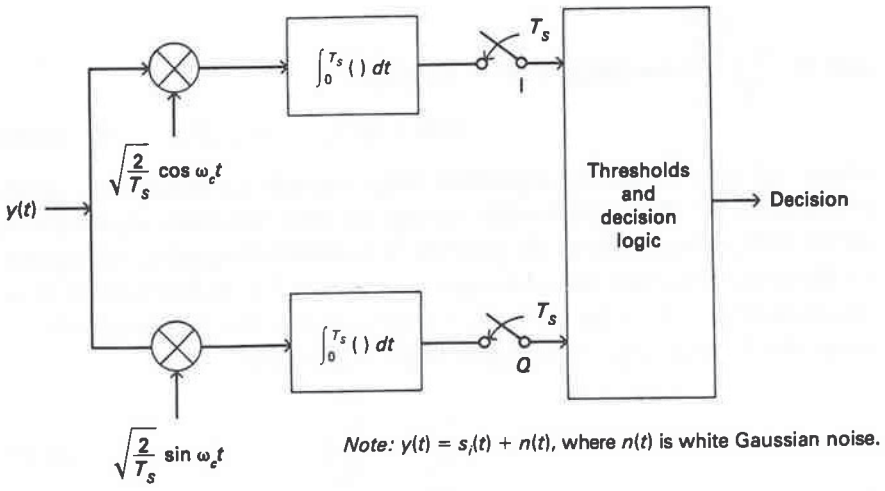
$$P(C\,|\,\mathrm{III}) = \left[1 - Q\left(\sqrt{\frac{2a^2}{N_0}}\right)\right]^2 \tag{8.45c}$$

In the preceding equations $a^2 = E_s/10$, where E_s is the average energy per symbol. The notation I, II, or III denotes that the particular probability refers to the probability of correct reception for the three types of decision regions shown in Figure 8.13(a). This error probability will be compared with that for M-ary PSK later. The error probability for 64-QASK or 256-QASK also can be obtained in a straightforward, but tedious, manner.

FIGURE 8.13 Signal space and detector structure for 16-QASK. (a) Signal constellation and decision regions for 16-QASK. (b) Detector structure for 16-QASK. (Binary representations for signal points are Gray encoded.)



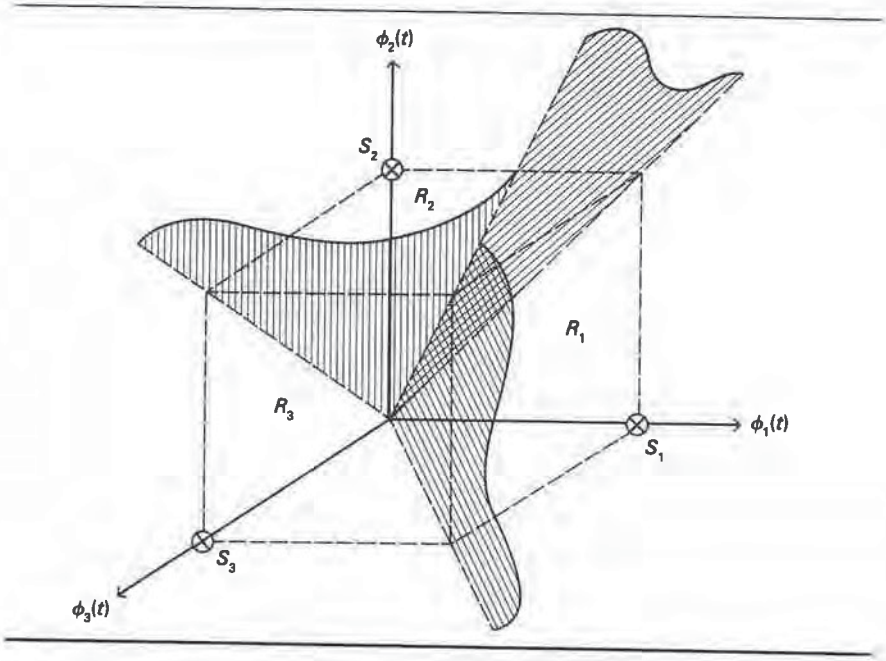
(a)



Note: $y(t) = s_i(t) + n(t)$, where $n(t)$ is white Gaussian noise.

(b)

FIGURE 8.14 Signal space showing decision regions for 3-ary coherent FSK



Coherent Frequency-Shift Keying

The error probability for M-ary FSK will be derived in Chapter 9. The transmitted signals have the form

$$s_i(t) = \sqrt{\frac{2E_s}{T_s}} \cos\{2\pi[f_c + (i-1)\Delta f]t\},$$

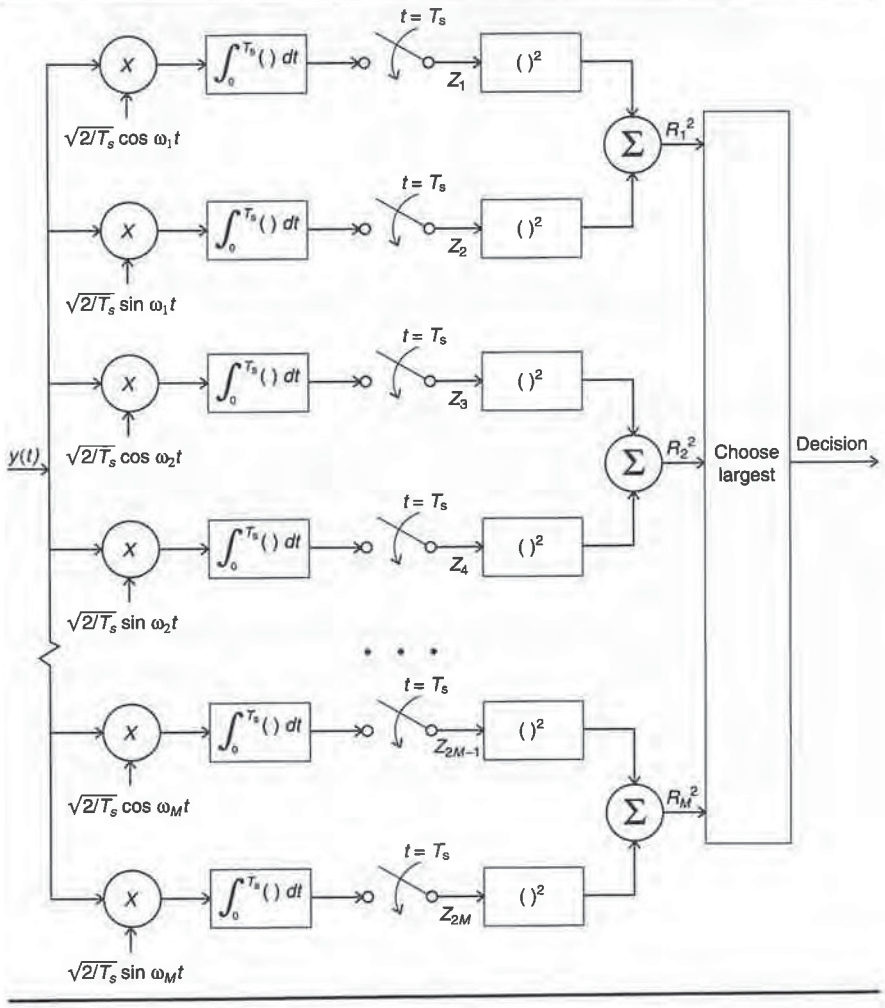
$$0 \le t \le T_s, \quad i = 1, 2, \ldots, M \qquad (8.46)$$

where Δf is a frequency separation large enough to make the signals represented by (8.46) coherently orthogonal (the minimum separation is $\Delta f = 1/2T_s$). Since each of the possible M transmitted signals is orthogonal to the rest, it follows that the signal space must be M-dimensional. It is shown in Figure 8.14 for $M = 3$. An upper bound for the probability of error that becomes tighter as M gets larger is given by*

$$P_E \le M\,Q\left(\sqrt{\frac{E_s}{N_0}}\right) \qquad (8.47)$$

*See Ziemer and Peterson (1992), Chapter 4.

FIGURE 8.15 Receiver for noncoherent FSK



Note: $y(t) = s_1(t) + n(t)$, where $n(t)$ is white Gaussian noise.

Noncoherent Frequency-Shift Keying

Noncoherent M-ary FSK employs the same signal set as coherent FSK; however, a receiver structure is used that does not require the acquisition of a coherent carrier reference. A block diagram of a suitable receiver structure is shown in Figure 8.15. The symbol error probability can be shown to be*

$$P_E = \sum_{k=1}^{M-1} \binom{M-1}{k} \frac{(-1)^{k+1}}{k+1} \exp\left(-\frac{k}{k+1}\frac{E_s}{N_0}\right) \tag{8.48}$$

*See Ziemer and Peterson (1992), Chapter 4.

TABLE 8.1 Gray Code Illustration

Digit	Binary Code	Gray Code
0	000	000
1	001	001
2	010	011
3	011	010
4	100	110
5	101	111
6	110	101
7	111	100

Note: See problem 8.14 for the encoding algorithm.

Bit Error Probability from Symbol Error Probability

If one of M possible symbols is transmitted, the number of bits required to specify this symbol is $\log_2 M$. It is possible to number the signal points using a binary code such that only one bit changes in going from a signal point to an adjacent signal point. Such a code is a *Gray code* and is given in Table 8.1 for $M = 8$.

Since mistaking an adjacent signal point for a given signal point is the most probable error, we assume that only such errors occur and that Gray encoding has been used so that a symbol error corresponds to a single bit error. We may then write the bit error probability in terms of the symbol error probability for an M-ary communications system for which these assumptions are valid as

$$P_{E,\text{bit}} = \frac{P_{E,\text{symbol}}}{\log_2 M} \tag{8.49}$$

Since we neglect probabilities of symbol errors where the symbols are further away than adjacent symbols, this result gives a *lower bound* for the bit error probability.

A second way that we can relate bit error probability to symbol error probability is as follows. Consider an M-ary modulation scheme for which $M = 2^n$. Then each symbol (M-ary signal) can be represented by an n-bit binary number, for example, the binary representation of the signal's index minus one. Such a representation is given in Table 8.2 for $M = 8$.
Take any column, say the last, which is enclosed by a box. In this column, there are $M/2$ zeros and $M/2$ ones. If a symbol (M-ary signal) is received in error, then for any given bit position of the binary representation (in this example, we are considering the right-most bit), there are $M/2$ of a possible

TABLE 8.2 Computation of Bit Error Probability for Orthogonal Signaling

M-ary Signal	Binary Representation
1 (0)	0 0 0
2 (1)	0 0 1
3 (2)	0 1 0
4 (3)	0 1 1
5 (4)	1 0 0
6 (5)	1 0 1
7 (6)	1 1 0
8 (7)	1 1 1

$M - 1$ ways that the chosen bit can be in error (one of the M total possibilities is correct). Therefore, the probability of a given data bit being in error, given that a signal (symbol) was received in error, is

$$P(B \mid S) = \frac{M/2}{M - 1} \tag{8.50}$$

Since a symbol is in error if a bit in the binary representation of it is in error, it follows that the probability $P(S \mid B)$ of a symbol error given a bit error is unity. Employing Bayes' rule, we find the equivalent bit error probability of an M-ary system can be approximated by

$$P_{E,\text{bit}} = \frac{P(B \mid S)P_{E,\text{symbol}}}{P(S \mid B)} = \frac{M}{2(M - 1)} P_{E,\text{symbol}} \tag{8.51}$$

This result is especially useful for orthogonal signaling schemes such as FSK.

One more thing must be accomplished before we can compare communications systems using a different number of symbols on an equivalent basis. This is that the energies must be equivalent. For this purpose, we note that the energy per bit E_b in terms of the energy per symbol E_s is

$$E_b = \frac{E_s}{\log_2 M} \tag{8.52}$$

▼ **EXAMPLE 8.2** Compare the performances of noncoherent and coherent FSK on the basis of E_b/N_0 required to provide a bit error probability of 10^{-6} for various values of M.

TABLE 8.3 Power Efficiencies for Noncoherent and Coherent FSK

	E_b/N_0 for $P_{E,\text{bit}} = 10^{-6}$	
M	Noncoherent	Coherent
2	14.2	13.6
4	11.3	10.8
8	9.7	9.3
16	8.7	8.2

SOLUTION Using (8.47), (8.48), (8.51), and (8.52), the results in Table 8.3 can be obtained with the aid of the asymptotic approximation for the Q-function: ▲

Comparison of M-ary Communications Systems

Figure 8.16 compares different M-ary PSK systems on the basis of bit error probability versus E_b/N_0. This figure shows that the bit error probability gets

FIGURE 8.16 Bit error probability versus E_b/N_0 for M-ary PSK and 16-QASK

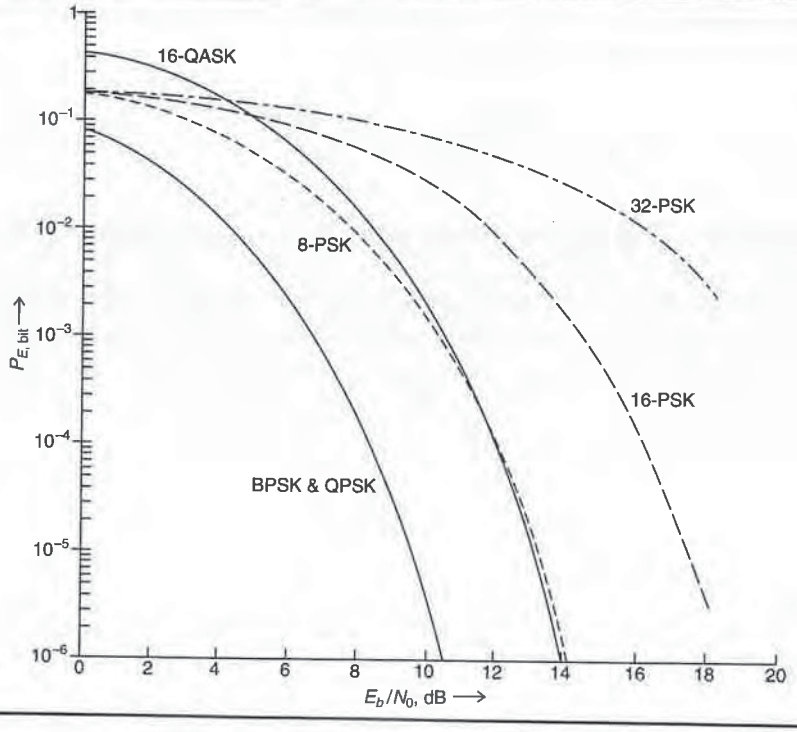
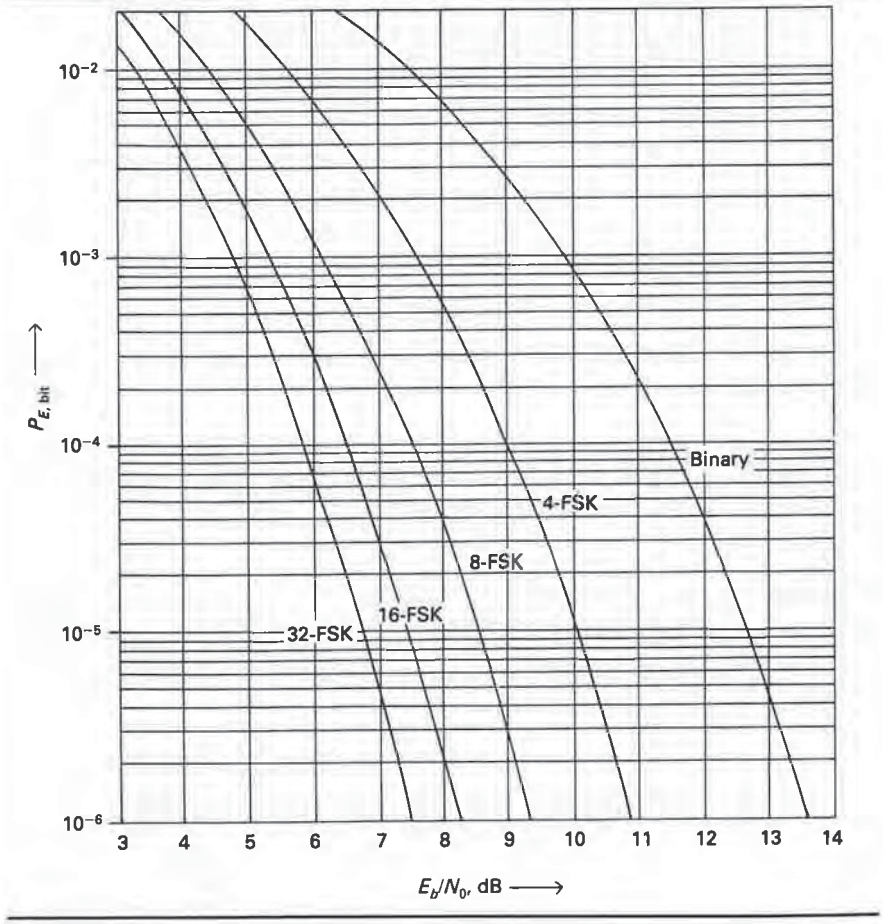


FIGURE 8.17 Bit error probability versus E_b/N_0 for coherent M-ary FSK



worse as M gets larger. This can be attributed to the signal points being crowded closer together in the two-dimensional signal space as M gets larger. Not all M-ary digital modulation schemes exhibit this undesirable behavior. We have seen that M-ary FSK is a signaling scheme in which the number of dimensions in the signal space grows directly with M. This means that the bit error probability for M-ary FSK *decreases* as M increases. This is illustrated in Figure 8.17, which compares bit error probability for coherent FSK for various values of M. Unfortunately, the bandwidth required for this signaling scheme grows larger directly with M, whereas this is not the case for M-ary PSK.

If one considers the required bandwidth to be that required to pass the main lobe of the signal spectrum (null to null), it follows that the *bandwidth*

TABLE 8.4 Bandwidth Efficiencies of Various M-ary Digital Modulation Schemes[a]

M-ary Scheme	Bandwidth Efficiency (bits/s/Hz)
PSK, QASK	$0.5 \log_2 M$
Coherent FSK	$\frac{2 \log_2 M}{M + 3}$ (Assumes tone spacing of $1/2T_s$ Hz)
Noncoherent FSK	$\frac{\log_2 M}{2M}$ (Assumes tone spacing of $2/T_s$ Hz)

[a] For justification, see Ziemer and Peterson (1992), Chapter 4.

efficiencies of the various *M*-ary schemes that we have just considered are as given in Table 8.4.

EXAMPLE 8.3 Compare bandwidth efficiencies on a mainlobe spectrum basis for PSK, QASK, and FSK for various *M*.

SOLUTION Bandwidth efficiencies in bits per second per hertz for various values of *M* are as follows. Note that for QASK, *M* must be a power of 4. Also note that the bandwidth efficiency of *M*-ary PSK *goes up* with increasing *M* while that for FSK *goes down*.

M	QASK	PSK	Coh. FSK	Noncoh. FSK
2		0.5	0.4	0.25
4	1	1.0	0.57	0.25
8		1.5	0.55	0.19
16	2	2.0	0.42	0.13
32		2.5	0.29	0.08

8.2 BANDWIDTH EFFICIENCIES OF DIGITAL MODULATION FORMATS

Our principal measure of performance for the various modulation schemes considered so far has been probability of error. Actually, this measure tells only half the story of how well a given modulation scheme performs, the other half being given by the bandwidth occupancy of the modulated signal. Specifically, we are interested in the data rate in bits per second that can be achieved by a given modulation scheme through a channel of a given band-

width in hertz. Theoretically, of course, an infinite bandwidth may be required, depending on the signal pulse shape used to represent a symbol. Consequently, a definition of bandwidth is required that, for purposes of this discussion, is based on the criterion of fractional power of the signal within a certain specified bandwidth. That is, if $S(f)$ is the double-sided power spectrum of a given modulation format, the fraction of total power in a bandwidth B is given by

$$\Delta P_{IB} = 2P_T^{-1} \int_{f_c - B/2}^{f_c + B/2} S(f)\, df \tag{8.53}$$

where the factor of 2 is used since we only integrate over positive frequencies,

$$P_T = \int_{-\infty}^{\infty} S(f)\, df \tag{8.54}$$

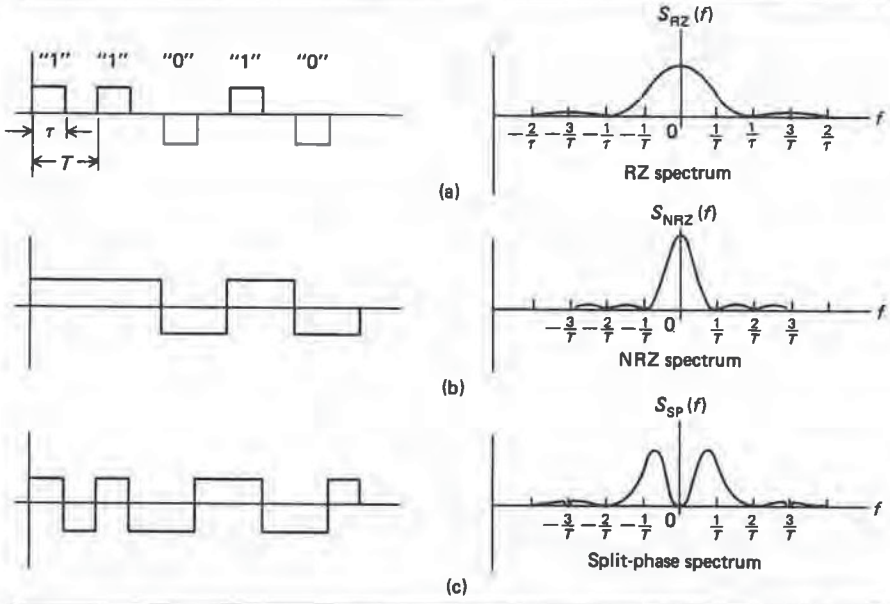
is the total power, and f_c is the "center" frequency of the spectrum (usually the carrier frequency, apparent or otherwise). The percent out-of-band power ΔP_{OB} is defined as

$$\Delta P_{OB} = (1 - \Delta P_{IB}) \times 100\% \tag{8.55}$$

The definition of modulated signal bandwidth is conveniently given by setting ΔP_{OB} equal to some acceptable value, say 0.01 or 1%, and solving for the corresponding bandwidth. A curve showing ΔP_{OB}, in decibels, versus bandwidth is a convenient tool for carrying out this procedure, since the 1% out-of-band power criterion for bandwidth corresponds to the bandwidth at which the out-of-band power curve has a value of -20 dB. Later we will present several examples to illustrate this procedure. First, however, we will discuss the spectra for various baseband data formats and for the digital modulation schemes considered so far.

The spectrum of a digitally modulated signal is influenced both by the particular baseband data format used to represent the digital data and by the type of modulation scheme used to prepare the signal for transmission. Several commonly used baseband data formats are illustrated in Figure 8.18. These data formats are referred to as *return-to-zero* (RZ), *non-return-to-zero* (NRZ), and *split-phase* (or *Manchester*). Split-phase, we note, is obtained from NRZ by multiplication by a squarewave clock waveform with a period equal to the bit duration. Typical power spectra are also shown in Figure 8.18 for these three modulation formats, assuming a random (coin toss) bit sequence.

FIGURE 8.18 Typical digital data waveforms and corresponding power spectra. (a) Return-to-zero (RZ) waveform. (b) Non-return-to-zero (NRZ) waveform. (c) Split-phase (Manchester) waveform.



The spectra are derived using the techniques of Chapter 5, in particular, of Example 5.6, and using appropriate expressions for the pulse-shape function $p(t)$. None of these formats results in power spectra with significant frequency content at multiples of the bit rate $1/T_b$. Thus, for the purpose of bit synchronization, nonlinear operations are required to generate power at a frequency of $1/T_b$ Hz or multiples thereof. Both the RZ and split-phase formats guarantee at least one zero crossing per bit interval, but both require twice the transmission bandwidth of NRZ. Around 0 Hz, NRZ and RZ possess significant energy content and therefore may have an adverse effect on carrier-acquisition devices.

These data formats have no memory between symbols. Other data formats are possible in which memory is introduced between symbols for various reasons, including spectral shaping (refer to Example 5.6, Case 2).

In order to obtain the spectrum of a BPSK-modulated signal using any of these data formats, the appropriate spectrum shown in Figure 8.18 is simply shifted up in frequency and centered around the carrier (assuming a single-sided spectrum). An analysis similar to that carried out in Example 5.6 can be used to obtain the spectrum of a quadrature-modulated waveform of the

form given by (8.1), where $m_1(t) = d_1(t)$ and $m_2(t) = d_2(t)$ are random (coin toss) waveforms of the forms

$$d_1(t) = \sum_{k=-\infty}^{\infty} a_k p(t - kT_s - \Delta_1) \tag{8.56}$$

and

$$d_2(t) = \sum_{k=-\infty}^{\infty} b_k q(t - kT_s - \Delta_2) \tag{8.57}$$

with

$$E\{a_k\} = E\{b_k\} = 0, \qquad E\{a_k^2\} = A^2, \qquad E\{b_k^2\} = B^2$$

The pulse-shape functions $p(t)$ and $q(t)$ in (8.56) and (8.57) may be the same, or one of them may be zero. It is left to the problems to show that the double-sided spectrum of (8.1), with (8.56) and (8.57) substituted, is

$$S(f) = G(f - f_c) + G(f + f_c) \tag{8.58}$$

where

$$G(f) = \frac{A^2|P(f)|^2 + B^2|Q(f)|^2}{T_s} \tag{8.59}$$

in which $P(f)$ and $Q(f)$ are the Fourier transforms of $p(t)$ and $q(t)$, respectively.

This result can be applied to BPSK, for example, by letting $q(t) = 0$ and $p(t) = \Pi(t/T_b)$. The resulting baseband spectrum is

$$G_{\text{PRK}}(f) = A^2 T_b \operatorname{sinc}^2 (T_b f) \tag{8.60}$$

The spectrum for QPSK follows by letting

$$p(t) = q(t) = \frac{1}{\sqrt{2}} \Pi\left(\frac{t}{2T_b}\right) \tag{8.61}$$

and $A = B$. The result for $G(f)$ is

$$G_{\text{QPSK}}(f) = 2A^2 T_b \operatorname{sinc}^2 (2T_b f) \tag{8.62}$$

This result also holds for OQPSK because the pulse-shape function $q(t)$ differs from $p(t)$ only by a time shift that results in a factor of $\exp(-j2\pi T_b f)$ in the amplitude spectrum $Q(f)$ (its magnitude is unity).

The baseband spectrum for MSK is found by choosing the pulse-shape functions

$$p(t) = q(t - T_b) = \cos\left(\frac{\pi t}{2T_b}\right)\Pi\left(\frac{t}{2T_b}\right) \tag{8.63}$$

and by letting $A = B$. It can be shown (see Problem 8.25) that

$$\mathcal{F}\left\{\cos\left(\frac{\pi t}{2T_b}\right)\Pi\left(\frac{t}{2T_b}\right)\right\} = \frac{4T_b\cos(2\pi T_b f)}{\pi[1 - (4T_b f)^2]} \tag{8.64}$$

which results in the baseband spectrum for MSK,

$$G_{\text{MSK}}(f) = \frac{16A^2T_b\cos^2(2\pi T_b f)}{\pi^2[1 - (4T_b f)^2]^2} \tag{8.65}$$

Using these results for the baseband spectra of BPSK, QPSK (or OQPSK), and MSK in the definition of percent out-of-band power, Equation (8.55), results in the set of plots shown in Figure 8.19. From this figure, it follows that the bandwidths containing 90% of the power for these modulation formats are approximately

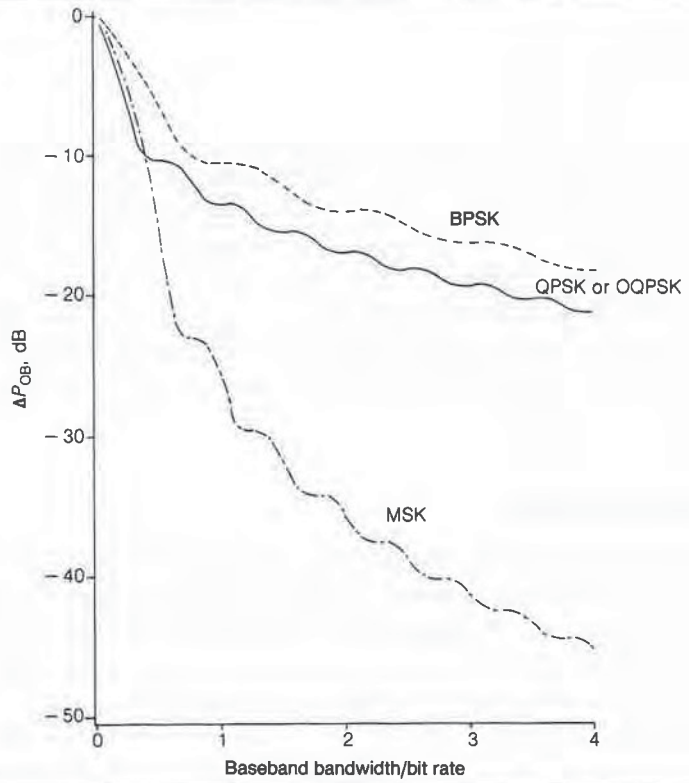
$$\begin{aligned} B_{90\%} &= \frac{1}{T_b}\text{ Hz} \qquad \text{(QPSK, OQPSK, MSK)} \\ B_{90\%} &= \frac{2}{T_b}\text{ Hz} \qquad \text{(BPSK)} \end{aligned} \tag{8.66}$$

These are obtained by noting the bandwidths on the curves corresponding to $\Delta P_{\text{OB}} = -10$ dB and doubling these values, since the plots are for baseband bandwidths.

Because the MSK out-of-band power curve rolls off at a much faster rate than do the curves for BPSK or QPSK, a more stringent in-band power specification, such as 99%, results in a much smaller containment bandwidth for MSK than for BPSK or QPSK. The bandwidths containing 99% of the power are

$$\begin{aligned} B_{99\%} &= \frac{1.2}{T_b} \qquad \text{(MSK)} \\ B_{99\%} &= \frac{8}{T_b} \qquad \text{(QPSK or OQPSK)} \end{aligned} \tag{8.67}$$

FIGURE 8.19 Fractional out-of-band power for BPSK, QPSK or OQPSK, and MSK



For binary FSK, the following formula can be used to compute the power spectrum if the phase is continuous:*

$$G(f) = G_+(f) + G_-(f) \tag{8.68a}$$

where

$$G_\pm(f) = \frac{A^2 \sin^2 [\pi(f \pm f_1)T_b \sin^2 [\pi(f \pm f_2)T_b]}{2\pi^2 T_b\{1 - 2\cos [2\pi(f \pm \alpha)T_b] \cos (2\pi\beta T_b) + \cos^2 (2\pi\beta T_b)\}} \times \left[\frac{1}{f \pm f_1} - \frac{1}{f \pm f_2}\right]^2 \tag{8.68b}$$

* See W. R. Bennett and J. R. Davey, *Data Transmission* (New York: McGraw-Hill, 1965).

In (8.68b), the following definitions are used:

$$f_1, f_2 = \text{the signaling frequencies in hertz (that is, } f_c \text{ and } f_c + \Delta f)$$
$$\alpha = \tfrac{1}{2}(f_1 + f_2)$$
$$\beta = \tfrac{1}{2}(f_2 - f_1)$$

Equation (8.58) is used to get the bandpass (modulated) signal spectrum.

The preceding approach to determining bandwidth occupancy of digitally modulated signals provides one criterion for selecting modulation schemes based on bandwidth considerations. It is not the only approach by any means. Another important criterion is adjacent channel interference. In other words, what is the degradation imposed on a given modulation scheme by channels adjacent to the channel of interest? In general, this is a difficult problem. For one approach, the reader is referred to a series of papers on the concept of crosstalk.*

8.3 SYNCHRONIZATION

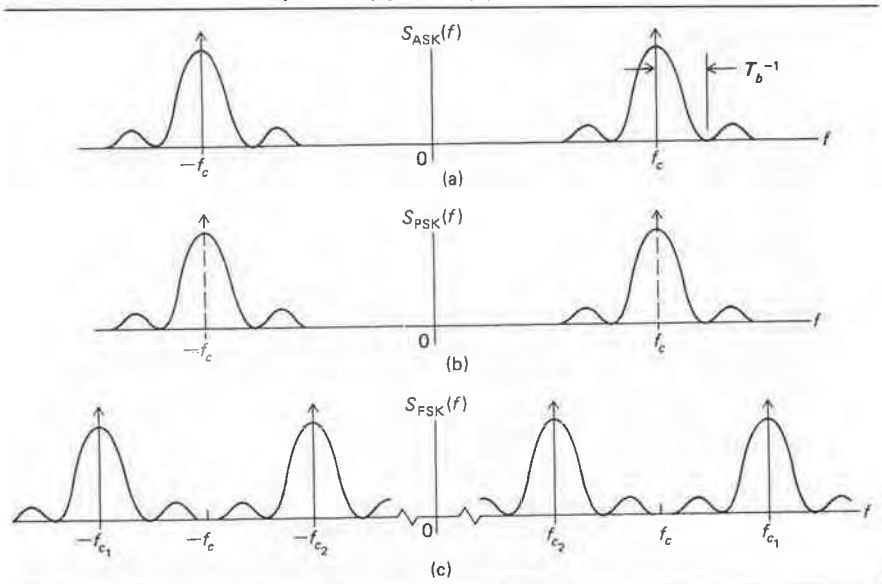
We have seen that at least two levels of synchronization are necessary in a coherent communication system. For the known-signal-shape receiver considered in Section 7.2, the beginning and ending times of the signals had to be known. When specialized to the case of ASK, PSK, or FSK, knowledge was needed not only of the bit timing but of carrier phase as well. In addition, if the bits are grouped into words, the starting and ending times of the words are also required. In this section we will look at methods for achieving synchronization at these three levels. In order of consideration, we will look at methods for (1) carrier synchronization, (2) bit synchronization, and (3) word synchronization. There are also other levels of synchronization in some communication systems that will not be considered here.

Carrier Synchronization

The three main types of digital modulation methods considered were ASK, PSK, and FSK. Typical power spectra for ASK, FSK, and PSK, assuming a random NRZ data sequence, are illustrated in Figure 8.20. In each case, impulses are shown at $f = \pm f_c$ Hz corresponding to the carrier. For PSK, the impulses are dashed, signifying that they are absent for BPSK. Assuming the presence of a carrier component in the modulated signal spectrum, car-

* See I. Kalet, "A Look at Crosstalk in Quadrature-Carrier Modulation Systems," *IEEE Transactions on Communications*, Vol. COM-25, September 1977, pp. 884–892.

FIGURE 8.20 Power spectra. (a) ASK. (b) PSK. (c) FSK.



rier coherence is very simply obtained by locking onto the carrier component with a phase-locked loop. To minimize the adverse effects of modulation power on the loop, a split-phase modulation format is typically used. (See Problem 8.24 for derivations of these spectra.)

If a carrier component is not present, as in BPSK, two alternatives that may be employed are squaring and Costas loops, as discussed in Chapter 3 for double-sideband modulation.* When used for digital data demodulation, however, these loop mechanizations introduce a problem that was not present for demodulation of analog message signals. We note that either loop will lock if we assume $\pm d(t) \cos \omega_c t$ at the loop input. Some method is usually required to resolve this sign ambiguity at the demodulator output. One method of doing so is to differentially encode the data stream before modulation and differentially decode it at the detector output with a resultant small loss in signal-to-noise ratio. This is referred to as *coherent detection* of differentially encoded BPSK and is different from differentially coherent detection of BPSK.

Circuits similar to the Costas and squaring loops may be constructed for four-phase PSK or QPSK.

* The decision-feedback loop is yet another alternative. See Lindsey and Simon (1973).

TABLE 8.5 Tracking Loop Error Variances

No modulation (PLL)	$\sigma_\phi^2 = \frac{N_0 B_L}{P_c}$
PSK (squaring or Costas loop)	$\sigma_\phi^2 = \frac{1}{L}\left(\frac{1}{z} + \frac{1}{2z^2}\right); z = E_s/N_0; L = \frac{1}{B_L T_s} \propto \frac{B_s}{B_L} = \frac{T_L}{T_s}$
QPSK (quadrupling or data estimation loop)	$\sigma_\phi^2 = \frac{1}{L}\left(\frac{1}{z} + \frac{9}{2}\frac{1}{z^2} + \frac{6}{z^3} + \frac{3}{2}\frac{1}{z^4}\right)$

Definitions: T_s = symbol duration
B_L = single-sided loop bandwidth
N_0 = single-sided noise spectral density
$T_L = B_L^{-1}$ = loop memory time
L = effective number of symbols used by loop in making phase estimate
P_c = signal power (carrier component only)
$B_s = T_s^{-1}$ = symbol bandwidth (bit-rate bandwidth for binary case)
E_s = symbol energy

The question naturally arises as to the effect of noise on these phase-tracking devices. The *phase error,* that is, the difference between the input signal phase and the VCO phase, can be shown to be approximately Gaussian with zero mean at high signal-to-noise ratios at the loop input. Table 8.5 summarizes the phase-error variance for these various cases.* When used with equations such as (7.79), these results provide a measure for the average performance degradation due to an imperfect phase reference. Note that in all cases, σ_ϕ^2 is inversely proportional to the signal-to-noise ratio raised to integer powers and to the effective number L of symbols remembered by the loop in making the phase estimate. (See Problem 8.28.)

We next look at methods for acquiring bit synchronization.

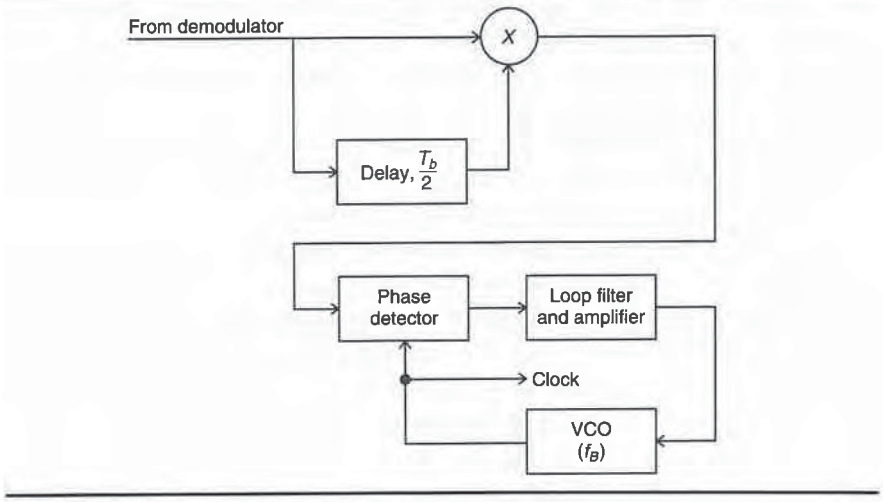
Bit Synchronization†

Three general methods by which bit synchronization can be obtained are (1) derivation from a primary or secondary standard (for example, transmitter and receiver slaved to a master timing source), (2) utilization of a separate synchronization signal (pilot clock), and (3) derivation from the modulation itself, referred to as *self-synchronization,* as illustrated in Figure 8.21. Because

* Stiffler (1971), Equation (8.3.13).

† See Stiffler (1971) or Lindsey and Simon (1973) for a more extensive discussion.

FIGURE 8.21 Block diagram of a system for deriving a clock that is coherent with a random-bit stream



of the nonlinear operation provided by the delay-and-multiply operation (almost any even-order nonlinearity will do), energy is produced at twice the bit frequency, which permits the acquisition of a clock by locking a phase-locked loop to this frequency component and dividing it by two. This loop configuration is analogous to the squaring loop for carrier acquisition from a BPSK waveform. Loop configurations for acquiring bit synchronization that are similar in form to the Costas loop are also possible but will not be discussed here.*

The analysis of bit synchronizer performance in noise proceeds similarly to the analysis of carrier acquisition devices, and expressions may be derived for the timing-error variance similar to the expressions given in Table 8.5 for phase-error variance.†

Word Synchronization

The same principles used for bit synchronization may be applied to word synchronization. These are (1) derivation from a primary or secondary standard, (2) utilization of a separate synchronization signal, and (3) self-synchronization.

Only the second method will be discussed here. The third method involves the utilization of self-synchronizing codes. It is clear that such

* Again, see Stiffler (1971) or Lindsey and Simon (1973).

† See Stiffler (1971) or Lindsey and Simon (1973).

codes, which consist of sequences of 1's and 0's in the binary case, must be such that no shift of an arbitrary sequence of code words produces another code word. If this is the case, proper alignment of the code words at the receiver is accomplished simply by comparing all possible time shifts of a received digital sequence with all code words in the code dictionary (assumed available at the receiver) and choosing the shift and code word having maximum correlation. For long code words, this could be very time-consuming. Furthermore, the construction of good codes is not a simple task and requires computer search procedures in some cases.*

When a separate synchronization signal is employed, this signal may be transmitted over a channel separate from the one being employed for data transmission, or over the data channel by inserting the synchronization signal periodically between data words. If the first alternative is employed, the synchronizing waveform should have small cross correlation with its own cyclic permutations. The second alternative is often accomplished by inserting a known sequence, referred to as a *prefix*, in front of each data word. In this case, the synchronization waveform employed should have small aperiodic cross correlation with its cyclic permutations. Waveforms having such properties will be discussed shortly. In both the case of a separate channel and the case of employment of a prefix, it should be noted that power is wasted in achieving synchronization. Thus the self-synchronization approach is preferable in cases in which power is at a premium. For example, self-synchronizing codes were used in the deep space missions by NASA.

To see how the second method can be implemented, we digress briefly to discuss pseudo-noise sequences.

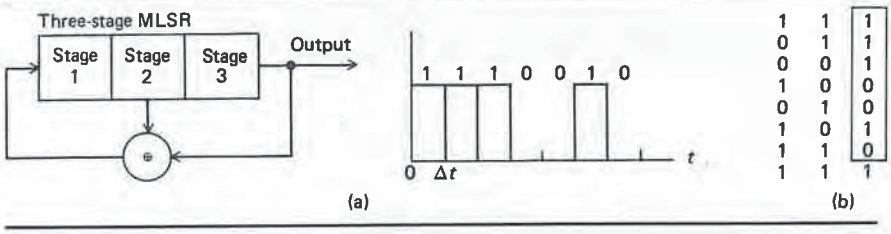
Pseudo-Noise (PN) Sequences

Pseudo-noise (PN) codes are binary-valued, noiselike sequences; they approximate a sequence of coin tossings for which a 1 represents a head and a 0 represents a tail. However, their primary advantages are that they are deterministic, being easily generated by feedback shift registers, and they have a correlation function that is highly peaked for zero delay and approximately zero for other delays. Thus they find application wherever waveforms at remote locations must be synchronized. These applications include not only word synchronization but also the determination of range between two points and the measurement of the impulse response of a system by cross-correlation of input with output, as discussed in Chapter 5 (Example 5.7).

Figure 8.22 illustrates the generation of a PN code of length $2^3 - 1 =$

* See Stiffler (1971) or Lindsey and Simon (1973).

FIGURE 8.22 Generation of a 7-bit PN sequence. (a) Generation. (b) Shift register contents.



7, which is accomplished with the use of a shift register three stages in length. After each shift of the contents of the shift register to the right, the contents of the second and third stages are used to produce an input to the first stage through an EXCLUSIVE-OR (XOR) operation (that is, a binary add without carry). The logical operation performed by the XOR circuit is given in Table 8.6. Thus, if the initial contents of the shift register are 1 1 1, as shown in the first row of Figure 8.22(b), the contents for seven more successive shifts are given by the remaining rows of this table. Therefore, the shift register again returns to the 1 1 1 state after $2^3 - 1 = 7$ more shifts, which is also the length of the output sequence taken at the third stage. By using an n-stage shift register with proper feedback connections, PN sequences of length $2^n - 1$ may be obtained. Proper feedback connections for several values of n are given in Table 8.7.

Considering next the autocorrelation function of the periodic waveform (normalized to a peak value of unity) obtained by letting the shift register in Figure 8.22(a) run indefinitely, we see that its values for integer multiples of the output pulse width $\Delta = n\Delta t$ are given by

$$R(\Delta) = \frac{N_A - N_U}{\text{sequence length}} \tag{8.69}$$

where N_A is the number of like digits of the sequence and a sequence shifted by n pulses and N_U is the number of unlike digits of the sequence and a sequence shifted by n pulses. This equation is a direct result of the definition of the autocorrelation function for a periodic waveform, given by Equation

TABLE 8.6 Truth Table for the XOR Operation

Input 1	Input 2	Output
1	1	0
1	0	1
0	1	1
0	0	0

TABLE 8.7 Feedback Connections for Generation of PN Codes[a]

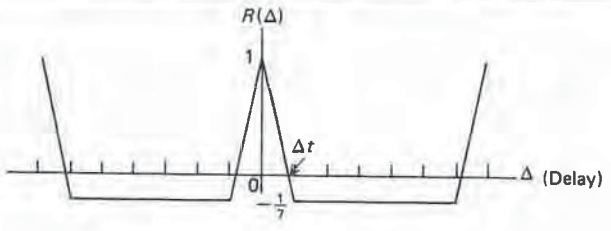
n	Sequence Length	Sequence (Initial State: All Ones)	Feedback Digit
2	3	110	$x_1 \oplus x_2$
3	7	11100 10	$x_2 \oplus x_3$
4	15	11110 00100	$x_3 \oplus x_4$
		11010	
5	31	11111 00110	$x_2 \oplus x_5$
		10010 00010	
		10111 01100 0	

[a] See R. E. Ziemer and R. L. Peterson (1992), Chapter 8, for additional sequences and proper feedback connections.

(2.150), and the binary-valued nature of the shift register output if the peak value is normalized to unity. Thus the autocorrelation function for the sequence generated by the feedback shift register of Figure 8.22(a) is as shown in Figure 8.23, as you may readily verify. Applying the definition of the autocorrelation function, given by Equation (2.150), we could also easily show that the shape for noninteger values of delay is as shown in Figure 8.23. In general, for a sequence of length N, the minimum correlation is $-1/N$. Because the correlation function of a PN sequence consists of a narrow triangle around zero delay and is essentially zero otherwise, it resembles white noise when used to drive any system whose bandwidth is small compared with the inverse pulse width. This explains the reason for the name "pseudo-noise."

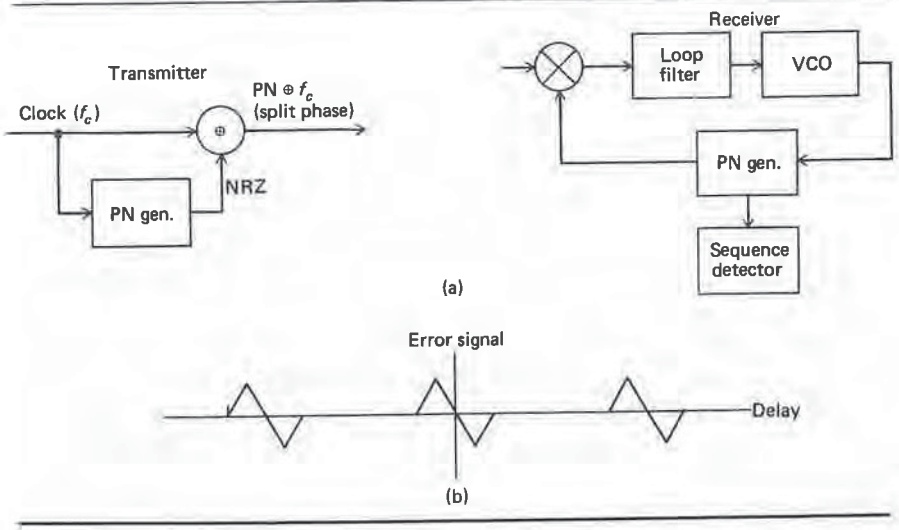
Returning to our original problem, that of synchronization of waveforms

FIGURE 8.23 Correlation function of a PN code



Code to be shifted	1	1	1	0	0	1	0							
Code plus one repetition	1	1	1	0	0	1	0	1	1	1	0	0	1	0

FIGURE 8.24 Synchronization by PN code. (a) PN transmitter-receiver portion for synchronization. (b) Error signal at VCO.



at remotely located points, consider the system illustrated in Figure 8.24(a). Assume that the transmitter transmits a PN sequence (with levels $+1$ and -1 instead of 1 and 0) that has been split-phase encoded. We recall that split-phase encoding can be thought of as multiplication of the sequence by a squarewave clock with period equal to the pulse width of the PN sequence. For simplicity, the operations of modulation and coherent demodulation, which would be performed in most systems, are not shown, and we view the system as operating at baseband. Initially, suppose that the transmitter and receiver clocks are unsynchronized but operating near the same frequency. Thus the PN sequence generated at the receiver will slowly slide by the received split-phase-encoded PN sequence. If the received sequence were *not* split-phase encoded, the output of the loop filter would be essentially the autocorrelation function of the sequence with the delay proportional to time because of the sequences sliding by each other. However, because of the multiplication of the transmitted sequence by the clock, an error signal at the loop filter output, as shown in Figure 8.24(b), will result. Eventually, the input to the voltage-controlled oscillator (VCO) will be the negative-slope portion of this error signal, and the frequency of the VCO will be driven in the proper direction so that the loop will lock at zero delay (with the delay due to the transmission path excluded). At this point, the VCO output will be locked to the transmitter clock, and the PN sequences at transmitter and receiver will be time-coincident if the channel delay is

TABLE 8.8 The Barker Sequences

+−
++−
++−+
+++−+
+++−−+−
+++−−−+−−+−
+++++−−++−+−+

excluded. More general schemes exist for the synchronization of PN sequences.*

It is not difficult to see how the system just described could be used for measuring the range between two points if the transmitter and receiver were colocated and a transponder at a remote location simply retransmitted whatever it received. This is, in fact, the technique used for the Global Positioning System (GPS).

To use this system for word synchronization, all that would be necessary would be to insert the split-phase-encoded PN sequence at the beginning of each word. The PN sequence generated at the receiver would, on average, have low correlation with the data. It is clear that if the PN sequence is inserted as a prefix before each data word, it is not the periodic correlation function that is important, but the *aperiodic* correlation function obtained by sliding the sequence past itself rather than past its periodic extension as in Figure 8.23. Sequences with good aperiodic correlation properties are the Barker codes.† Unfortunately the longest known Barker code is of length 13. Table 8.8 lists all known Barker sequences. (See Problem 8.31.) Other digital sequences with good correlation properties can be constructed from Hadamard matrices.‡

8.4 SPREAD-SPECTRUM COMMUNICATION SYSTEMS

We next consider a special class of modulation technique referred to as *spread-spectrum modulation*. In general, spread-spectrum modulation refers to any modulation technique in which the bandwidth of the modulated signal

* For techniques that will work with data present, see Ziemer and Peterson (1992), Chapter 8.

† See Skolnik (1970), Chapter 20.

‡ See Lindsey and Simon (1973). Also, see *IEEE Transactions on Communications*, August 1980 (special issue on synchronization).

is spread well beyond the bandwidth of the modulating signal, independently of the modulating signal bandwidth. The following are reasons for employing spread-spectrum modulation:

1. To provide resistance to intentional jamming by another source
2. To provide a means for masking the transmitted signal in the background noise and prevent another party from eavesdropping
3. To provide resistance to the degrading effects of multipath transmission
4. To provide a means for more than one user to use the same transmission channel
5. To provide range-measuring capability

The two most common techniques for effecting spread-spectrum modulation are referred to as *direct sequence* (DS) and *frequency hopping* (FH). Figures 8.25 and 8.26 are block diagrams of these generic systems. Variations and combinations of these two basic systems are also employed.

FIGURE 8.25 Block diagram of a DS spread-spectrum communication system. (a) Transmitter. (b) Receiver.

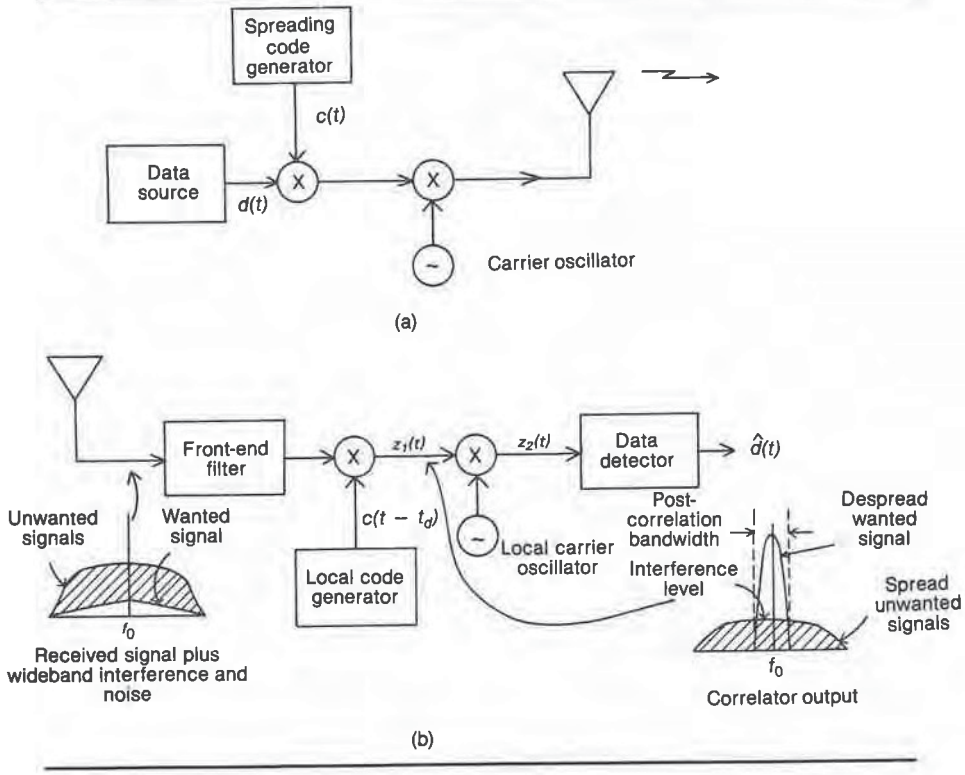
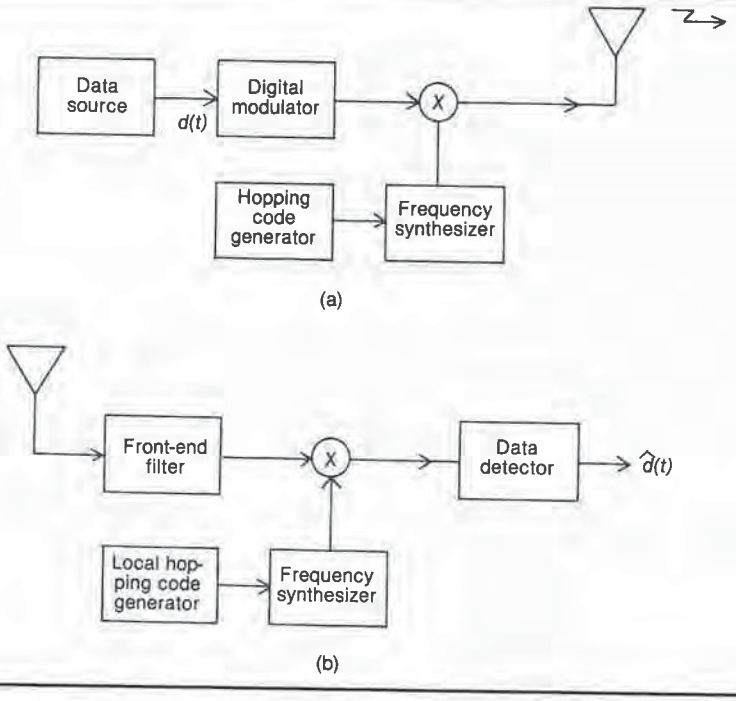


FIGURE 8.26 Block diagram of an FH spread-spectrum communication system. (a) Transmitter. (b) Receiver.



Direct-Sequence Spread Spectrum

In a *direct-sequence spread-spectrum* (DSSS) communication system, the modulation format may be almost any of the coherent digital techniques discussed previously, although BPSK, QPSK, and MSK are the most common. Figure 8.25 illustrates the use of BPSK. The spectrum spreading is effected by multiplying the data $d(t)$ by the spreading code $c(t)$. In this case, both are assumed to be binary sequences taking on the values $+1$ and -1. The duration of a data symbol is T_b, and the duration of a spreading-code symbol, called a *chip period,* is T_c. There are usually many chips per bit, so that $T_c \ll T_b$. In this case, it follows that the spectrum of the modulated signal is essentially dependent only on the inverse chip period. The spreading code is chosen to have the properties of a random binary sequence; an often-used choice for $c(t)$ is a PN sequence, as described in the previous section. Often, however, a sequence generated using nonlinear generation techniques is used for security reasons. It is also advantageous, from the standpoint of security, to use the same clock for both the data and spreading code so that

the data changes sign coincident with a sign change for the spreading code. This is not necessary for proper operation of the system, however.

In the system illustrated in Figure 8.25, BPSK data modulation is used. Typical spectra are shown directly below the corresponding blocks. At the receiver, it is assumed that a replica of the spreading code is available and is time-synchronized with the incoming code used to multiply the BPSK-modulated carrier. This synchronization procedure is composed of two steps, called *acquisition* and *tracking*. A very brief discussion of methods for acquisition will be given later. For a fuller discussion and analyses of both procedures, the student is referred to Peterson, Ziemer, and Borth (1995).

A rough approximation to the spectrum of a DSSS signal employing BPSK data modulation can be obtained by representing the modulated carrier as

$$x_c(t) = A\, d(t)c(t) \cos(\omega_c t + \theta) \tag{8.70}$$

where it is assumed that θ is a random phase uniformly distributed in $(0, 2\pi)$ and $d(t)$ and $c(t)$ are independent, random binary sequences (if derived from a common clock, the independence assumption for $d(t)$ and $c(t)$ is not strictly valid). With these assumptions, the autocorrelation function for $x_c(t)$ is

$$R_{x_c}(\tau) = \frac{A^2}{2} R_d(\tau) R_c(\tau) \cos(\omega_c \tau) \tag{8.71}$$

where $R_d(\tau)$ and $R_c(\tau)$ are the autocorrelation functions of the data and spreading code, respectively. If they are modeled as random "coin toss" sequences as considered in Example 5.6, their autocorrelation functions are given by

$$R_d(\tau) = \Lambda(\tau/T_b) \tag{8.72a}$$

and

$$R_c(\tau) = \Lambda(\tau/T_c) \tag{8.72b}$$

respectively. Their corresponding power spectral densities are

$$S_d(f) = T_b \operatorname{sinc}^2(T_b f) \tag{8.73}$$

and

$$S_c(f) = T_c \operatorname{sinc}^2(T_c f) \tag{8.74}$$

respectively, where the width of the main lobe of (8.73) is T_b^{-1} and that for (8.74) is T_c^{-1}.

The power spectral density of $x_c(t)$ can be obtained by taking the Fourier transform of (8.71):

$$S_{x_c}(f) = \frac{A^2}{2} S_d(f) * S_c(f) * \mathcal{F}[\cos(\omega_c \tau)] \tag{8.75}$$

Since the spectral width of $S_d(f)$ is much less than that for $S_c(f)$, the convolution of these two spectra is approximately $S_c(f)$. Thus the spectrum of the DSSS modulated signal is very closely approximated by

$$\begin{aligned} S_{x_c}(f) &= \frac{A^2}{4}[S_c(f - f_c) + S_c(f + f_c)] \\ &= \frac{A^2 T_c}{4}\{\text{sinc}^2[T_c(f - f_c)] + \text{sinc}^2[T_c(f + f_c)]\} \end{aligned} \tag{8.76}$$

The spectrum, as stated above, is approximately independent of the data spectrum and has a null-to-null bandwidth around the carrier of $2/T_c$ Hz.

We next look at the error probability performance. First, assume a DSSS signal plus additive white Gaussian noise is present at the receiver. Ignoring propagation delays, the output of the local code multiplier at the receiver (see Fig. 8.25) is

$$z_1(t) = A\, d(t)c(t)c(t - \Delta)\cos(\omega_c t + \theta) + n(t)c(t - \Delta) \tag{8.77}$$

where Δ is the misalignment of the locally generated code at the receiver with the code on the received signal. Assuming perfect code synchronization ($\Delta = 0$), the output of the coherent demodulator is

$$z_2(t) = A\, d(t) + n'(t) + \text{double frequency terms} \tag{8.78}$$

where

$$n'(t) = 2n(t)c(t)\cos(\omega_c t + \theta) \tag{8.79}$$

is a new Gaussian random process with zero mean. Passing $z_2(t)$ through an integrate-and-dump circuit, we have for the signal component at the output

$$V_0 = \pm AT_b \tag{8.80}$$

where the sign depends on the sign of the bit at the input. The noise component at the integrator output is

$$N_g = \int_0^{T_b} 2n(t)c(t)\cos(\omega_c t + \theta)\, dt \tag{8.81}$$

Since $n(t)$ has zero mean, N_g has zero mean. Its variance, which is the same as its second moment, can be found by squaring the integral, writing it as an iterated integral, and taking the expectation inside the double integral—a procedure that has been used several times before in this chapter and the previous one. The result is

$$\text{var}\,(N_g) = E(N_g^2) = N_0 T_b \tag{8.82}$$

where N_0 is the single-sided power spectral density of the input noise. This, together with the signal component of the integrator output, allows us to write down an expression similar to the one obtained for the baseband receiver analysis carried out in Section 7.1 (the only difference is that the signal power is $A^2/2$ here, whereas it was A^2 for the baseband signal considered there). The result for the probability of error is

$$P_E = Q(\sqrt{A^2 T_b/N_0}) = Q(\sqrt{2E_b/N_0}) \tag{8.83}$$

With Gaussian noise alone, DSSS performs the same as BPSK without the spread-spectrum modulation.

Consider next a cw interference component. Now, the input to the integrate-and-dump detector, excluding double frequencies, is

$$z_2'(t) = A\,d(t) + n'(t) + A_I \cos[(\omega_c + \Delta\omega)t + \phi][2\cos(\omega_c t + \theta)] \tag{8.84}$$

where A_I is the amplitude of the interference component and $\Delta\omega$ is its offset frequency from the carrier frequency. It is assumed that $\Delta\omega < 2\pi/T_c$. The output of the integrate-and-dump detector is

$$V_0' = \pm AT_b + N_g + N_I \tag{8.85}$$

The first two terms are the same as obtained before. The last term is the result of interference and is given by

$$\begin{aligned} N_I &= \int_0^{T_b} c(t) A_I \cos[(\omega_0 + \Delta\omega)t + \phi][2\cos(\omega_0 t + \theta)]\,dt \\ &= \int_0^{T_b} A_I c(t) \cos(\Delta\omega t + \theta - \phi)\,dt \end{aligned} \tag{8.86}$$

Because of the multiplication by the wideband spreading code $c(t)$ and the subsequent integration, we approximate this term by an equivalent Gaussian random variable (the integral is a sum of a large number of random variables). Its mean is zero, and for $\Delta\omega \ll 2\pi/T_c$, its variance can be shown to be

$$\text{var}\,(N_I) = \frac{T_c T_b A_I^2}{2} \tag{8.87}$$

With this Gaussian approximation for N_I, the probability of error can be shown to be

$$P_E = Q\left(\sqrt{\frac{A^2 T_b^2}{\sigma_T^2}}\right) \tag{8.88}$$

where

$$\sigma_T^2 = N_0 T_b + \frac{T_c T_b A_I^2}{2} \tag{8.89}$$

is the total variance of the noise plus interference components at the integrator output. The quantity under the square root can be further manipulated as

$$\frac{A^2 T_b^2}{2\sigma_T^2} = \frac{A_I^2/2}{N_0/T_b + (T_c/T_b)(A_I^2/2)} = \frac{P_s}{P_n + P_I/G_p} \tag{8.90a}$$

where

$P_s = A^2/2$ is the signal power at the input

$P_n = N_0/T_b$ is the Gaussian noise power in the bit-rate bandwidth

$P_I = A_I^2/2$ is the power of the interfering component at the input

$G_p = T_b/T_c$ is the processing gain of the DSSS system.

It is seen that the effects of the interfering component is decreased by the processing gain G_p. Equation (8.90a) can be rearranged as

$$\frac{A^2 T_b^2}{2\sigma_T^2} = \frac{\text{SNR}}{1 + \dfrac{(\text{SNR})(\text{JSR})}{G_p}} \tag{8.90b}$$

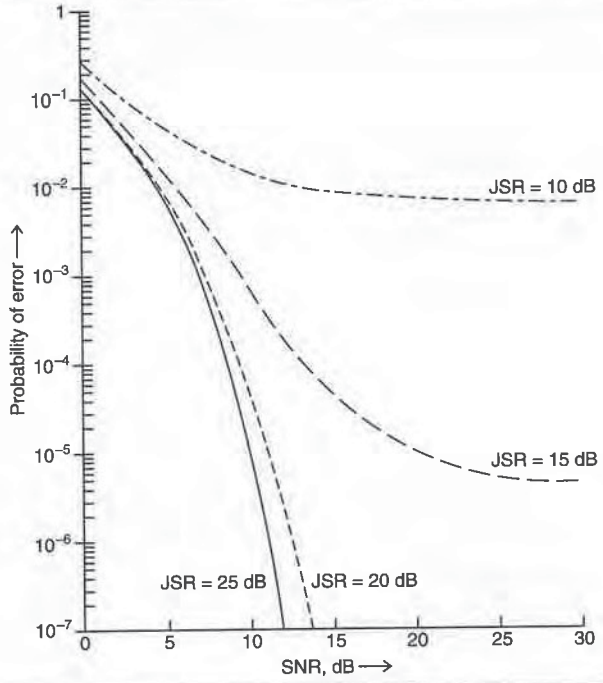
where

SNR $= P_s/P_n$ is the signal-to-noise ratio

JSR $= P_I/P_s$ is the jamming-to-signal ratio

Figure 8.27 shows P_E versus the SNR for several values of JSR/G_p.

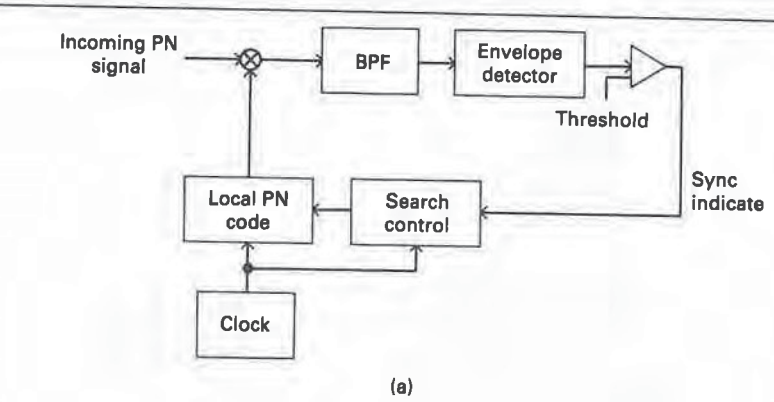
FIGURE 8.27 P_E versus SNR for DSSS with G_p = 30 dB for (a) JSR = 25 dB, (b) JSR = 20 dB, (c) JSR = 15 dB, and (d) JSR = 10 dB



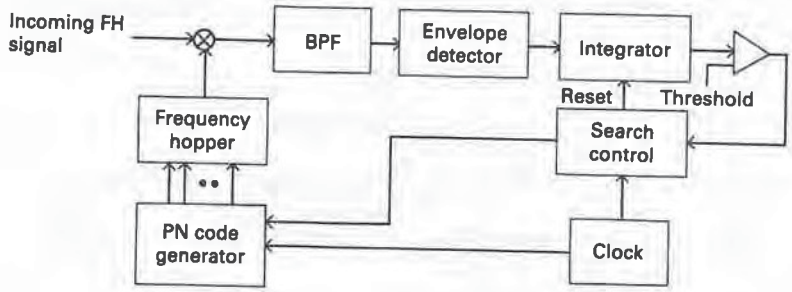
Frequency-Hop Spread Spectrum

In the case of *frequency-hop spread spectrum* (FHSS), the modulated signal is hopped in a pseudorandom fashion among a set of frequencies so that a potential eavesdropper does not know in what band to listen or jam. Consequently, the eavesdropper must listen or jam in the full bandwidth in which the signal is hopped. Current FHSS systems may be classified as *fast hop* or *slow hop,* depending on whether one (or less) or several data bits are included in a hop. The data modulator for either is usually a noncoherent type such as FSK or DPSK, since frequency synthesizers are not usually coherent from hop to hop. Even if one goes to the expense of building a coherent frequency synthesizer, the channel may not preserve the coherency property of the synthesizer output. At the receiver, as shown in Figure 8.26, a replica of the hopping code is produced and synchronized with the hopping pattern of the received signal. One possible circuit for achieving this synchronization process is shown later.

FIGURE 8.28 Code acquisition circuits for (a) DSSS and (b) FHSS using serial search



(a)



(b)

Code Synchronization

Only a brief discussion of code synchronization will be given here. For detailed discussions and analyses of such systems, the reader is referred to Ziemer and Petersen (1985).*

Figure 8.28(a) shows a serial-search acquisition circuit for DSSS. A replica of the spreading code is generated at the receiver and multiplied by the incoming spread-spectrum signal (the carrier is assumed absent in Figure 8.28 for simplicity). Of course, the code epoch is unknown, so an arbitrary local code delay relative to the incoming code is tried. If it is within $\pm\frac{1}{2}$

* For an excellent tutorial paper on acquisition and tracking, see S. S. Rappaport and D. M. Grieco, "Spread-Spectrum Signal Acquisition: Methods and Technology," *IEEE Communications Magazine*, Vol. 22, No. 6, June 1984, pp. 6–21.

chip of the correct code epoch, the output of the multiplier will be despread data and its spectrum will pass through the bandpass filter whose bandwidth is of the order of the data bandwidth. If the code delay is not correct, the output of the multiplier remains spread and little power passes through the bandpass filter. The envelope of the bandpass filter output is compared with a threshold—a value below threshold denotes an unspread condition at the multiplier output and, hence, a delay that does not match the delay of the spreading code at the receiver input, while a value above threshold indicates that the codes are approximately aligned. If the latter condition holds, the synchronization indicator stops the code search and a tracking mode is entered. If the below-threshold condition holds, the codes are assumed to be not aligned, so the search control steps to the next code delay (usually a half chip) and the process is repeated. It is apparent that such a process can take a relatively long time to achieve lock. The mean time to acquisition is given by

$$T_{\text{acq}} = \frac{nN_cT_e}{2(1 - P_{FH})} \frac{2 - P_H}{P_H} \tag{8.91}$$

where

T_e = examination time for each cell
n = number of cells examined per chip
N_c = initial number of chips to be searched
P_{FH} = probability of false threshold crossing at the end of an examination interval
P_H = probability of threshold crossing when correct alignment exists

Other techniques are available that speed up the acquisition, but at the expense of more hardware or special code structures.

A synchronization scheme for FHSS is shown in Figure 8.28(b). The discussion of its operation would be similar to that for acquisition in DSSS except that the correct frequency pattern for despreading is sought.

Conclusion

From the preceding discussions and the block diagrams of the DS and FH spread-spectrum systems, you can see that *nothing is gained by using a spread-spectrum system in terms of performance in an additive white Gaussian noise channel.* Indeed, using such a system may result in more degradation than using a conventional system, owing to the additional operations required. The

advantages of spread-spectrum systems accrue in environments that are hostile to digital communications—environments such as those in which multipath transmission or intentional jamming of channels exist. In addition, since the signal power is spread over a much wider bandwidth than it is in an ordinary system, it follows that the average power density of the transmitted spread-spectrum signal is much lower than the power density when the spectrum is *not* spread. This lower power density gives the sender of the signal a chance to mask the transmitted signal by the background noise and thereby lower the probability that anyone may intercept the signal.

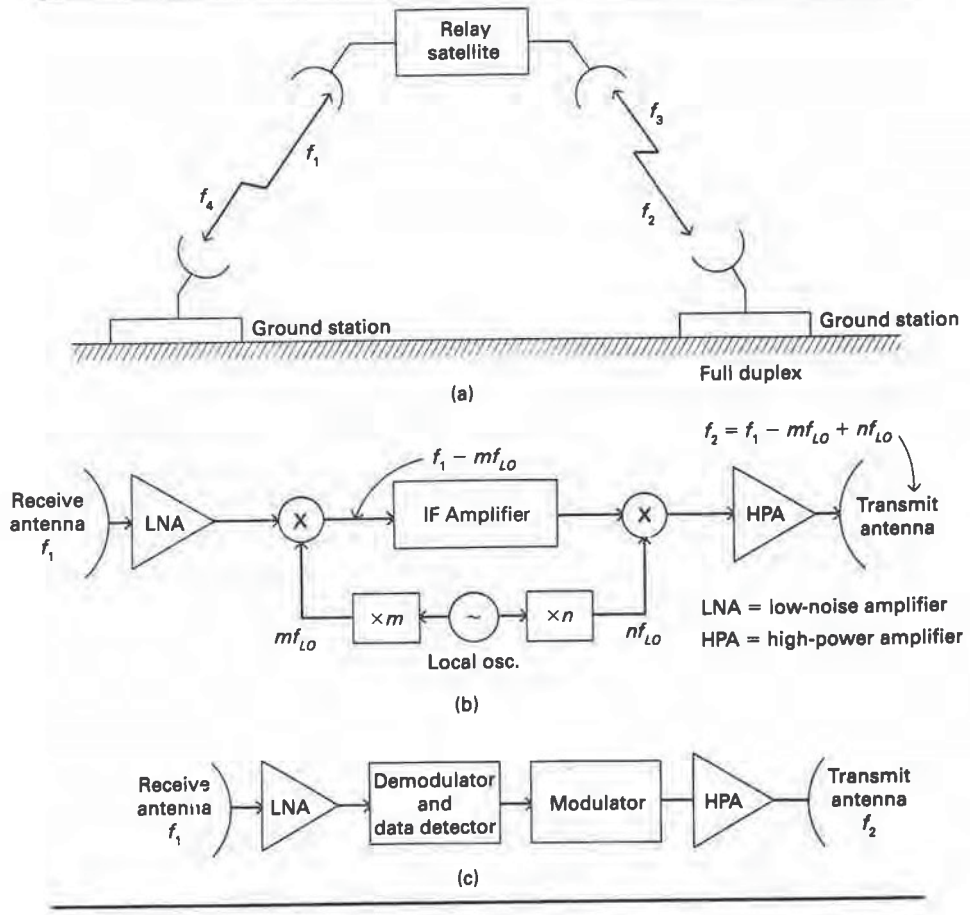
One last point is perhaps worth making: It is knowledge of the structure of the signal that allows the intended receiver to pull the received signal out of the noise. The use of correlation techniques is indeed powerful.

8.5 SATELLITE COMMUNICATIONS

In this section we look at the special application area of satellite communications to illustrate the use of some of the error probability results derived in this chapter. Satellite communications were first conceived in the 1950s. The first communications satellite was Echo I, a passive reflecting sphere, which was launched in 1956. The first active satellite, Courier, where "active" refers to the satellite's ability to receive, amplify, and retransmit signals, was launched in 1960. It had only two transmitters and had a launch weight of only 500 pounds. (Score was launched in 1958, but transmitted a prerecorded message.) In contrast, Intelsat VI, launched in 1986, has 77 transmitters and weighs 3600 pounds. Figure 8.29(a) shows a typical satellite repeater link, and Figure 8.29(b) shows a frequency-translating "bent-pipe" satellite communications system. Frequency translation is necessary to separate the receive and transmit frequencies and thus prevent "ring-around." Another type of satellite communication system, known as a *demod/remod system* (also referred to as on board processing, or OBP), is shown in Figure 8.29(c). In such a satellite repeater, the data are actually demodulated and subsequently remodulated onto the downlink carrier. In addition to the relay communications system on board the satellite, other communications systems include ranging (to provide a range measurement to the satellite), command (to receive commands from an earth station to control the satellite), and telemetry (to relay data about the satellite's condition back to the earth).

Early satellite transmissions took place in the UHF, C, or X bands. Because of the subsequent crowding of these bands, additional frequency allocations were added at K, V, and Q bands. Services are classified as *fixed-point* (communications between a satellite and fixed ground station), *broadcast* (trans-

FIGURE 8.29 Various satellite relay link communications configurations. (a) Satellite repeater link. (b) Frequency-translation satellite communications relay. (c) Demod/remod satellite communications relay.



mission to many receivers), and *mobile* (e.g., communications to aircraft, ships, and land vehicles). *Intersatellite* refers to communications between satellites.

It is important that satellites be stabilized so that the antennas can be pointed to predetermined points on the earth's surface. Early satellites were *spin-stabilized,* which means that the satellites were physically spun about an axis that kept them oriented in a particular relationship to the earth as a result of the gyroscopic effect. Because of the difficulty in despinning ever-more-complicated antenna systems, present-day satellites are almost all

three-axis stabilized. This means that a three-axis gyroscope system is on board to sense deviations from the desired orientation, and the resulting control signals derived from them are used to turn thruster jets on and off in order to maintain the desired orientation.

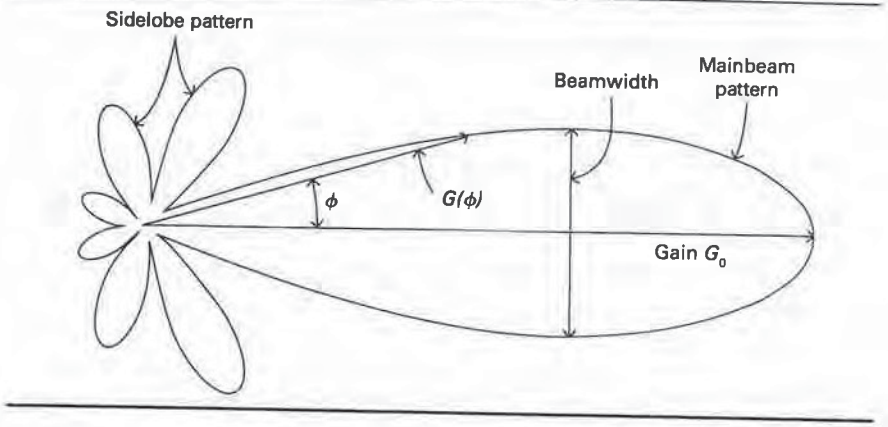
Satellites can be in low-earth orbits (LEO), medium-earth orbits (MEO), geostationary orbits, or interplanetary orbits. A geostationary orbit is one such that the satellite is at an altitude over the equator so that its angular rotation rate exactly matches that of the earth's, and it therefore appears to be stationary with respect to the earth. Geostationary altitude is 35,784 km or 22,235 statute miles (1 mile is approximately 1.6 km).

Antenna Coverage

Coverage of the earth by an antenna mounted on a satellite can be hemispherical, continental, or zonal depending on the antenna design. Antenna designs are now possible that cover several zones or spots simultaneously on the earth's surface. Such designs allow *frequency reuse*, in that the same band of frequencies can be reused in separate beams, which effectively multiplies the bandwidth of the satellite transponder available for communications by the reuse factor. Figure 8.30 shows a typical antenna gain pattern in polar coordinates. The maximum gain can be roughly calculated from

$$G_0 = \rho_a \left(\frac{4\pi}{\lambda^2}\right) A \tag{8.92a}$$

FIGURE 8.30 Polar representation of a general antenna gain function



where

ρ_a = antenna efficiency (≤ 1)
λ = wavelength
A = aperture area

For a circular aperture of diameter d, this expression becomes

$$G_0 = \rho_a \left(\frac{\pi d}{\lambda}\right)^2 \tag{8.92b}$$

The half-power beamwidth in radians can be approximated as

$$\phi_{3\text{dB}} = \frac{\lambda}{d\sqrt{\rho_a}} \tag{8.93}$$

A convenient approximation for the antenna pattern of a parabolic reflector antenna for small angles off boresight (such that the gain is within 6 dB of the maximum value) is

$$G(\phi) = \rho_a \left(\frac{\pi d}{\lambda}\right)^2 \exp\left[-2.76(\phi/\phi_{3\text{dB}})^2\right] \tag{8.94}$$

▼ **EXAMPLE 8.4** Find the aperture diameter and maximum gain for a transmit frequency of 10 GHz and $\rho_a = 0.8$ if, from geosynchronous altitude, the following coverages are desired: (a) hemispherical, (b) continental United States (CONUS), and (c) a 150-mile-diameter spot.

SOLUTION The wavelength at 10 GHz is

$$\lambda = \frac{3 \times 10^8 \text{ m/s}}{10 \times 10^9 \text{ Hz}} = 0.03 \text{ m}$$

$$= \frac{0.03 \text{ m}}{0.3048 \text{ m/ft}} = 0.0984 \text{ ft}$$

(a) Geosynchronous altitude is 22,235 statute miles, and the earth's radius is 3963 miles. The angle subtended by the earth from geosynchronous altitude is

$$\phi_{\text{hemis}} = \frac{2(3963)}{22{,}235} = 0.356 \text{ rad}$$

Equating this to ϕ_{3dB} in (8.93) and solving for d, we have

$$d = \frac{0.0984}{(0.356)\sqrt{0.8}} = 0.31 \text{ ft}$$

(b) The angle subtended by CONUS from geosynchronous altitude is

$$\phi_{CONUS} = \frac{4000}{22{,}235} = 0.18 \text{ rad}$$

Thus,

$$d = \frac{0.0984}{(0.18)\sqrt{0.8}} = 0.61 \text{ ft}$$

(c) A 150-mile-diameter spot on the earth's surface directly below the satellite subtends an angle of

$$\phi_{150} = \frac{150}{22{,}235} = 0.0067 \text{ rad}$$

from geosynchronous orbit. The diameter of an antenna with this beamwidth is

$$d = \frac{0.0984}{0.0067\sqrt{0.8}} = 16.3 \text{ ft}$$

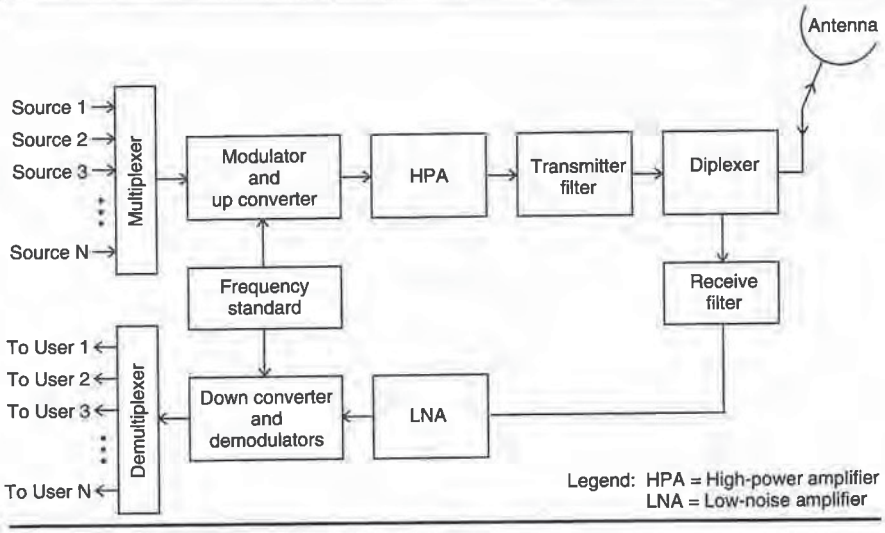
▲ Note that doubling the frequency to 20 GHz would halve these diameters.

Earth Stations and Transmission Methods

Figure 8.31 shows a block diagram of the transmitter and receiving end of an earth station. Signals from several sources enter the earth station (e.g., telephone, television, etc.), whereupon two transmission options are available. First, the information from a single source can be placed on a single carrier. This is referred to as *single-channel-per-carrier* (SCPC). Second, information from several sources can be multiplexed together and placed onto contiguous intermediate frequency carriers, the sum translated to radio frequency, power amplified, and transmitted. At the receiving end, the reverse process takes place.

At this point, it is useful to draw a distinction between *multiplexing* and *multiple access*. Multiple access (MA), like multiplexing, involves sharing of a common communications resource between several users. However, whereas multiplexing involves a fixed assignment of this resource at a local level, MA involves the remote sharing of a resource, and this sharing may under certain

FIGURE 8.31 Satellite ground station receiver/transmitter configuration. The command transmitter and telemetry receivers are not shown.



circumstances change dynamically under the control of a system controller. There are three main techniques in use for utilizing the bandwidth resources of a remote resource, such as a relay satellite. These are

1. Frequency division multiple access (FDMA), wherein the resource is divided up in frequency
2. Time division multiple access (TDMA), wherein the resource is divided up in time
3. Code division multiple access (CDMA), wherein a unique code is assigned to each intended user and the separate transmissions are separated by correlation with the code of the desired transmitting party

Figure 8.32 illustrates these three accessing schemes. In FDMA, signals from various users are stacked up in frequency, just as for frequency division multiplexing, as shown in Figure 8.32(a). Guard bands are maintained between adjacent signal spectra to minimize crosstalk between channels. If frequency slots are assigned permanently to the users, the system is referred to as *fixed-assigned multiple-access* (FAMA). If some type of dynamic allocation scheme is used to assign frequency slots, it is referred to as a *demand-assigned multiple-access* (DAMA) system.

In TDMA, the messages from various users are interlaced in time, just as for TDM, as shown in Figure 8.32(b). As illustrated in Figure 8.33, the data

from each user are conveyed in time intervals called *slots*. A number of slots make up a frame. Each slot is made up of a preamble plus information bits. The functions of the preamble are to provide identification and allow synchronization of the slot at the intended receiver. Guard times are utilized between each user's transmission to minimize crosstalk between channels.

FIGURE 8.32 Illustration of multiple-access techniques. (a) FDMA. (b) TDMA. (c) CDMA using frequency-hop modulation (numbers denote hopping sequences for channels 1, 2, and 3).

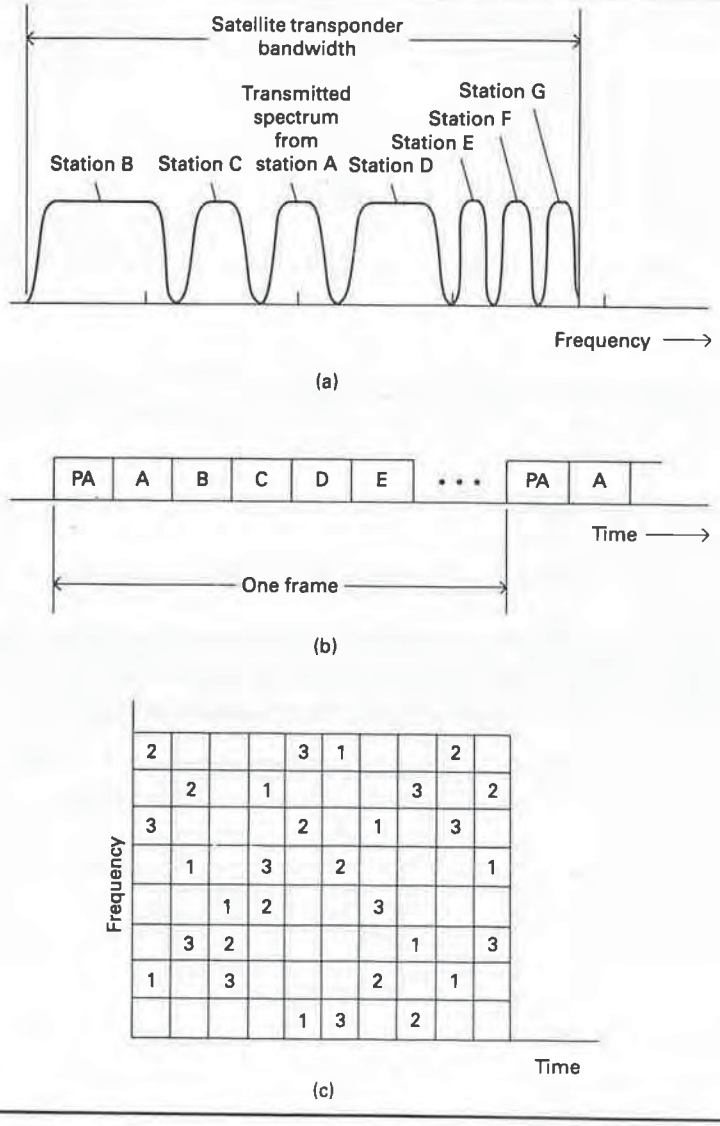
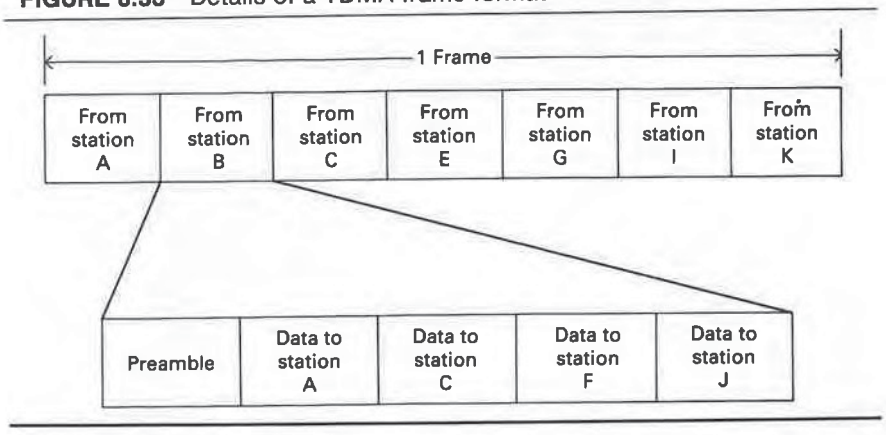


FIGURE 8.33 Details of a TDMA frame format



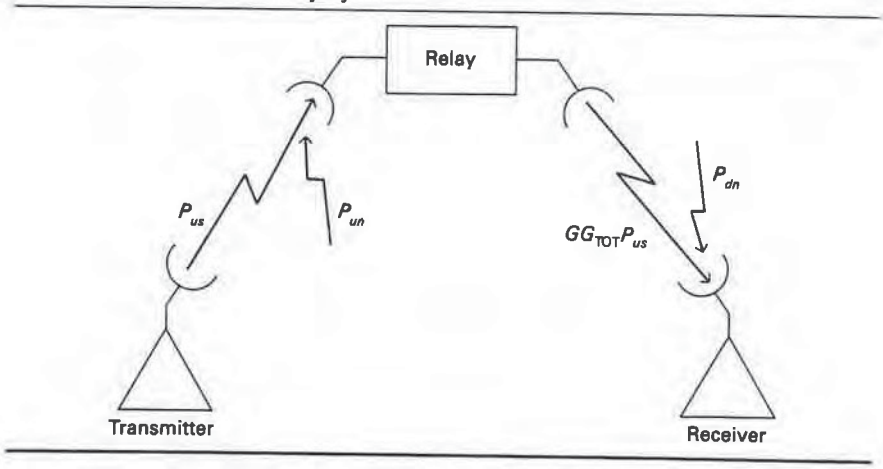
It is necessary to maintain overall network synchronization in TDMA, unlike FDMA. If, in a TDMA system, the time slots that make up each frame are preassigned to specific sources, it is referred to as FAMA; if time slots are not preassigned, but assigned on a dynamic basis, the technique is referred to as DAMA. DAMA schemes require a central network controller and a separate low-information-rate channel between each user and the controller to carry out the assignments. A DAMA TDMA system is more efficient in the face of bursty traffic than a FAMA system.

In CDMA, each user is assigned a code that ideally does not correlate with the codes assigned to other users, and the transmissions of a desired user are separated from those of all other users at a given receiving site through correlation with a locally generated replica of the desired user's code. Two ways that the messages can be modulated with the code for a given user is through direct-sequence spread spectrum or frequency-hop spread spectrum (see Section 8.4). Although CDMA schemes can be operated with network synchronization, it is obviously more difficult to do this than to operate the system asychronously, and therefore asynchronous operation is the preferred mode. When operated asynchronously, one must account for multiple access noise, which is a manifestation of the partial correlation of a desired user's code with all other users' codes present on the system.

Link Analysis: Bent-Pipe Relay

In Appendix A, a single one-way link budget is considered for a satellite communications system. Consider now the situation depicted in Figure 8.34. A transmitted signal from a ground station is broadcast to a satellite with power P_{us}, where the subscript u stands for "uplink." Noise referred to

FIGURE 8.34 Signal and noise powers in the uplink and downlink portions of a bent-pipe satellite relay system



the satellite input has power P_{un}. The sum of the signal and noise is amplified by the satellite repeater to give a transmitted power from the satellite of

$$P_T = G(P_{us} + P_{un}) \tag{8.95}$$

where G is the gain of the satellite repeater. The received signal power from the satellite at the receiving ground station is

$$P_{rs} = GG_{TOT}P_{us} \tag{8.96}$$

where G_{TOT} represents total system losses and gains on the downlink. It can be expressed as

$$G_{TOT} = \frac{G_t G_r}{L_a L_p} \tag{8.97}$$

where

G_t = gain of the satellite transmitter antenna
L_a = atmospheric losses on the downlink
L_p = propagation losses on the downlink
G_r = gain of the ground station receive antenna

The uplink noise power transmitted by the satellite repeater and appearing at the ground station input is

$$P_{ru} = GP_{un}G_{TOT} \tag{8.98}$$

Additional noise generated by the ground station itself is added to this noise at the ground station. The ratio of P_{rs} to total noise is the downlink carrier-to-noise power ratio. It is given by

$$(\text{CNR})_r = \frac{P_{rs}}{P_{ru} + P_{rd}} \tag{8.99}$$

Substituting previously derived expressions for each of the powers appearing on the right side of (8.99), we obtain

$$\begin{aligned}(\text{CNR})_r &= \frac{GG_{\text{TOT}}P_{us}}{GP_{un}G_{\text{TOT}} + P_{dn}} \\ &= \frac{1}{\dfrac{P_{un}}{P_{us}} + \dfrac{P_{dn}}{GG_{\text{TOT}}P_{us}}} \\ &= \frac{1}{(\text{CNR})_u^{-1} + (\text{CNR})_d^{-1}}\end{aligned} \tag{8.100}$$

where

$$(\text{CNR})_u = \frac{P_{us}}{P_{un}} = \text{carrier-to-noise power ratio on the uplink}$$

$$(\text{CNR})_d = \frac{GG_{\text{TOT}}P_{us}}{P_{dn}} = \text{carrier-to-noise power ratio on the downlink}$$

Note that the weakest of the two CNRs affects the overall carrier-to-noise power ratio the most. The overall carrier-to-noise power ratio cannot be better than the worse of two carrier-to-noise ratios that make it up. To obtain $(\text{CNR})_u$ and $(\text{CNR})_d$, we use the link equations developed in Appendix A.

To relate carrier-to-noise ratio to E_s/N_0 in order to calculate the error probability, we note that

$$\text{CNR} = \frac{P_c}{N_0 B_{RF}} \tag{8.101}$$

where

P_c = average carrier power

N_0 = noise power spectral density

B_{RF} = modulated signal (radio frequency) bandwidth

Multiplying numerator and denominator by the symbol duration T_s, we note that $P_c T_s = E_s$ is the symbol energy and obtain

$$\text{CNR} = \frac{E_s}{N_0 B_{RF} T_s}$$

or, solving for E_s/N_0,

$$\frac{E_s}{N_0} = (\text{CNR}) B_{RF} T_s \tag{8.102}$$

Given a modulation scheme, we can use a suitable bandwidth criterion to determine $B_{RF}T_s$. For example, using the null-to-null bandwidth for BPSK as B_{RF}, we have $B_{RF} = 2/T_b$ or $T_b B_{RF} = 2$, where $T_s = T_b$, since we are considering binary signaling.

Because the CNR is related to E_s/N_0 by the constant $B_{RF}T_s$, we can write (8.100) as

$$\left(\frac{E_s}{N_0}\right)_r = \frac{1}{(E_s/N_0)_u^{-1} + (E_s/N_0)_d^{-1}} \tag{8.103}$$

where

$(E_s/N_0)_u$ = symbol-energy-to-noise-spectral-density ratio on the uplink

$(E_s/N_0)_d$ = symbol-energy-to-noise-spectral-density ratio on the downlink

▼ EXAMPLE 8.5 Compute the relationship between $(E_s/N_0)_u$ and $(E_s/N_0)_d$ required to yield an error probability of $P_E = 10^{-6}$ on a bent-pipe satellite relay communications link if BPSK modulation is used.

SOLUTION For BPSK, $(E_b/N_0)_r \cong 10.54$ dB gives $P_E = 10^{-6}$. Thus (8.103) becomes

$$\frac{1}{(E_b/N_0)_u^{-1} + (E_b/N_0)_d^{-1}} = 10^{1.054} \cong 11.324 \tag{8.104}$$

Solving for $(E_b/N_0)_d$ in terms of $(E_b/N_0)_u$, we have the relationship

$$\left(\frac{E_b}{N_0}\right)_d = \frac{1}{0.0883 - (E_b/N_0)_u^{-1}} \tag{8.105}$$

▲ Several values are given in Table 8.9.

A curve showing the graphical relationship between the uplink and downlink values of E_b/N_0 will be shown later in conjunction with another exam-

TABLE 8.9 Uplink and Downlink Values of E_b/N_0 Required for $P_E = 10^{-6}$

$(E_s/N_0)_u$, dB	$(E_s/N_0)_d$, dB
20.0	11.06
15.0	12.47
14.0	13.14
13.55	13.55
12.0	15.98
11.0	20.52

ple. Note that the received E_b/N_0 is never better than the uplink or downlink values of E_b/N_0. For $(E_b/N_0)_u = (E_b/N_0)_d \cong 13.55$ dB, the value of $(E_b/N_0)_r$ is 10.54, which is that value required to give $P_E = 10^{-6}$. Note that as either $(E_b/N_0)_u$ or $(E_b/N_0)_d$ approaches infinity, the other energy-to-noise-spectral-density ratio approaches 10.54 dB.

Link Analysis: OBP Digital Transponder

Consider a satellite relay link in which the modulation is digital binary and detection takes place on board the satellite with subsequent remodulation of the detected bits on the downlink carrier and subsequent demodulation and detection at the receiving ground station. This situation can be illustrated in terms of bit errors as shown in Figure 8.35.

The channel is considered symmetrical in that errors for 1's and 0's are equally likely. It is also assumed that errors on the downlink are statistically independent of errors on the uplink and that errors in both links are independent of each other. From Figure 8.35, it follows that the overall probability of no error given that a 1 is transmitted is

$$P(C \mid 1) = q_u q_d + p_u p_d \tag{8.106}$$

where

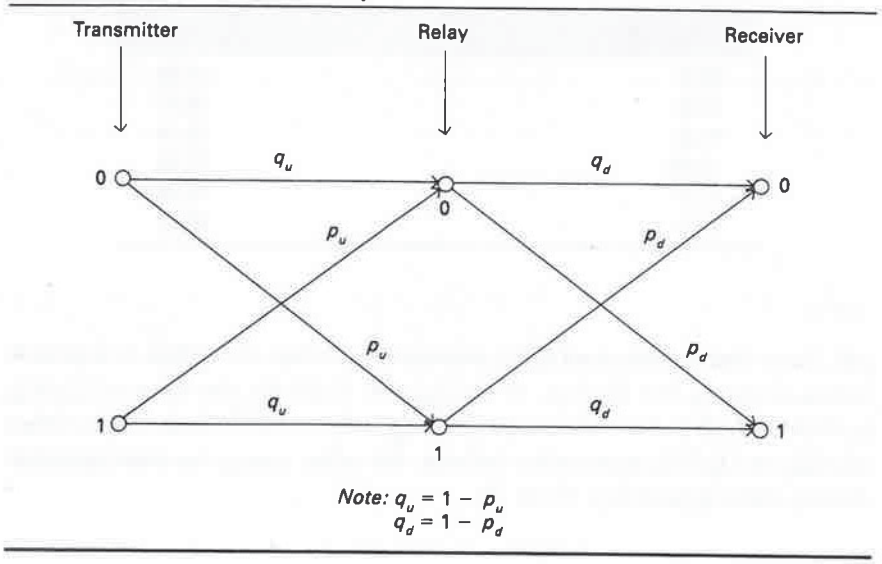
$q_u = 1 - p_u$ is the probability of no error on the uplink

$q_d = 1 - p_d$ is the probability of no error on the downlink

A similar expression holds for the probability $P(C \mid 0)$ of correct transmission through the channel given that a 0 is transmitted, and it therefore follows that the probability of correct reception averaged over both 1's and 0's is

$$P(C) = P(C \mid 1) = P(C \mid 0) \tag{8.107}$$

FIGURE 8.35 Transition probability diagram for uplink and downlink errors on a demod/remod satellite relay



The average probability of error is

$$\begin{aligned} P_E &= 1 - P(C) \\ &= 1 - (q_u q_d + p_u p_d) \\ &= 1 - (1 - p_u)(1 - p_d) - p_u p_d \\ &= p_u + p_d - 2p_u p_d \end{aligned} \tag{8.108}$$

The following example illustrates how to obtain the uplink and downlink signal energy-to-noise-spectral-density ratios required for an overall desired P_E for a given modulation technique.

▼ **EXAMPLE 8.6** Consider an OBP satellite communications link where BPSK is used on the uplink and the downlink. For this modulation technique,

$$p_u = Q(\sqrt{2(E_b/N_0)_u}) \cong \frac{e^{-(E_b/N_0)_u}}{2\sqrt{\pi(E_b/N_0)_u}}, \qquad (E_b/N_0)_u > 3 \tag{8.109}$$

with a similar expression for p_d. Say we want the error probability for the overall link to be 10^{-6}. Thus, from (8.108), we have

$$10^{-6} = p_u + p_d - 2p_u p_d \tag{8.110}$$

TABLE 8.10 E_b/N_0 Values for the Uplink and Downlink Required in an OBP Satellite Communications Link to Give $P_E = 10^{-6}$

p_u	$(E_b/N_0)_u$, dB	p_d	$(E_b/N_0)_d$, dB
10^{-7}	11.31	9×10^{-7}	10.58
5×10^{-7}	10.79	5×10^{-7}	10.79
6×10^{-7}	10.73	4×10^{-7}	10.87
7×10^{-7}	10.67	3×10^{-7}	10.96

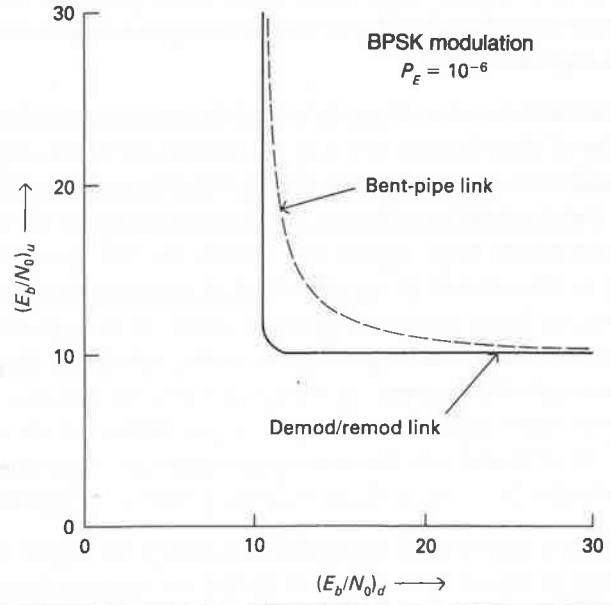
Solving for p_d in terms of p_u, we have

$$p_d = \frac{10^{-6} - p_u}{1 - 2p_u} \tag{8.111}$$

A table of values of p_d can be made up versus values of p_u and the corresponding required values of $(E_b/N_0)_u$ can then be calculated from (8.109) with a similar procedure followed for $(E_b/N_0)_d$. Such a table of values is presented as Table 8.10.

Figure 8.36 shows $(E_b/N_0)_u$ versus $(E_b/N_0)_d$ for both the bent-pipe and

FIGURE 8.36 Comparison of bent-pipe and OBP relay characteristics



demod/remod satellite relays for an overall bit error probability of 10^{-6}. Curves for other values of P_E or other digital modulation schemes can be obtained in a similar manner. This is left to the problems.

SUMMARY

1. When dealing with M-ary digital communications systems, with $M \geq 2$, it is important to distinguish between a bit and a symbol or character. A symbol conveys $\log_2(M)$ bits. The symbol rate in symbols per second is called the band rate in bauds. We must also distinguish between bit error probability and symbol error probability.

2. M-ary schemes based on quadrature multiplexing include quadrature phase-shift keying (QPSK), offset QPSK (OQPSK), and minimum-shift keying (MSK). All have a bit error rate performance that is essentially the same as binary BPSK if precoding is used to ensure that only one bit error results from mistaking one phase for an adjacent phase.

3. MSK can be produced by quadrature modulation or by serial modulation. In the latter case, MSK is produced by filtering BPSK with a properly designed conversion filter. At the receiver, serial MSK can be recovered by first filtering it with a bandpass matched filter and performing coherent demodulation with a carrier at $f_c + 1/4T_b$ (i.e., at the carrier plus a quarter data rate). Serial MSK performs identically to quadrature-modulated MSK and has advantageous implementation features at high data rates.

4. It is convenient to view M-ary data modulation in terms of signal space. Examples of data formats that can be considered in this way are M-ary PSK, quadrature-amplitude-shift keying (QASK), and M-ary FSK. For the former two modulation schemes, the dimensionality of the signal space stays constant as more signals are added; for the latter, it increases directly as the number of signals added. A constant-dimensional signal space means signal points are packed closer as the number of signal points is increased, thus degrading the error probability; the bandwidth remains essentially constant. In the case of FSK, with increasing dimensionality as more signals are added, the signal points are not compacted, and the error probability decreases for a constant signal-to-noise ratio; the bandwidth increases with an increasing number of signals, however.

5. A convenient measure of bandwidth occupancy for digital modulation is in terms of out-of-band power or power-containment bandwidth. An ideal brickwall containment bandwidth that passes 90% of the signal

power is approximately $1/T_b$ Hz for QPSK, OQPSK, and MSK, and about $2/T_b$ Hz for BPSK.

6. The different types of synchronization that may be necessary in a digital modulation system are carrier (only for coherent systems), symbol or bit, and possibly word. Carrier and symbol synchronization can be carried out by an appropriate nonlinearity followed by a narrowband filter or phase-lock loop. Alternatively, appropriate feedback structures may be used.

7. A pseudo-noise sequence resembles a random "coin toss" sequence but can be generated easily with linear feedback shift-register circuits. They have a narrow correlation peak for zero delay and low sidelobes for nonzero delay, a property that makes them ideal for synchronization of words or measurement of range.

8. Spread-spectrum communications systems are useful for providing resistance to jamming, to provide a means for masking the transmitted signal from unwanted interceptors, to provide resistance to multipath, to provide a way for more than one user to use the same time-frequency allocation, and to provide range-measuring capability.

9. The two major types of spread-spectrum systems are direct-sequence spread-spectrum (DSSS) and frequency-hop spread-spectrum (FHSS). In the former, a spreading code with rate much higher than the data rate multiplies the data sequence, thus spreading the spectrum, while for FHSS, a synthesizer driven by a pseudorandom code generator provides a carrier that hops around in a pseudorandom fashion. A combination of these two schemes, referred to as *hybrid spread spectrum,* is also another possibility.

10. Spread spectrum performs identically to whatever data-modulation scheme is employed without the spectrum spreading as long as the background is additive white Gaussian noise and synchronization is perfect.

11. The performance of a spread-spectrum system in interference is determined in part by its processing gain, which can be defined as the ratio of bandwidth of the spread system to that for an ordinary system employing the same type of data modulation as the spread-spectrum system. For DSSS the processing gain is the ratio of the data bit duration to the spreading code bit (or chip) duration.

12. An additional level of synchronization, referred to as *code synchronization,* is required in a spread-spectrum system. The serial search method is

perhaps the simplest in terms of hardware and to explain, but it is relatively slow in achieving synchronization.

13. Satellite communications systems provide a realistic example to which the digital modulation schemes considered in this chapter can be applied. Two general types of relay satellite configurations were considered in the last section of this chapter: bent-pipe and OBP. In the OBP system, the data on the uplink are demodulated and detected and then used to remodulate the downlink carrier. In the bent-pipe relay, the uplink transmissions are translated in frequency, amplified, and retransmitted on the downlink. Performance characteristics of both types of links were considered by example.

FURTHER READING

In addition to the references given in Chapter 7, for a fuller discussion and in-depth treatment of the digital modulation techniques presented here, see Ziemer and Peterson (1992), and Peterson, Ziemer, and Borth (1995).

PROBLEMS

Section 8.1

8.1 An M-ary communication system transmits at a rate of 1000 symbols per second. What is the equivalent bit rate in bits per second for $M = 4$? $M = 8$? $M = 64$?

8.2 A serial bit stream, proceeding at a rate of 10 kbps from a source, is given as

110 011 100 101 (spacing for clarity)

Number the bits from left to right starting with 1 and going through 12 for the right-most bit. Associate the odd-indexed bits with $d_1(t)$ and the even-indexed bits with $d_2(t)$ in Figure 8.1.

(a) What is the symbol rate for d_1 and d_2?
(b) What are the successive values of θ_i given by (8.2) assuming QPSK modulation? At what time intervals may θ_i switch?
(c) What are the successive values of θ_i given by (8.2) assuming OQPSK modulation? At what time intervals may θ_i switch values?

8.3 QPSK is used to transmit data through a channel that adds Gaussian noise with power spectral density $N_0 = 10^{-12}$ V^2/Hz. What are the

values of the quadrature-modulated carrier amplitudes required to give $P_{E,\text{symbol}} = 10^{-4}$ for the following data rates?

(a) 10 kbps (c) 1 Mbps
(b) 100 kbps (d) 1 Gbps

8.4 Show that the noise components N_1 and N_2 for QPSK, given by Equations (8.6) and (8.8), are uncorrelated.

8.5 (a) Given the following values for the transmitted signal phase, θ, in QPSK, from Figure 8.1 and the text, tell whether $d_1(t)$ and $d_2(t)$ are $+1$ or -1 for the following cases:
(1) $\theta_i = 45°$ (2) $\theta_i = 135°$ (3) $\theta_i = -45°$ (4) $\theta_i = -135°$
(b) For the results obtained in part (a) assume that an error is made in detecting $d_2(t)$ What is the corresponding $\hat{\theta}$?
(c) Same question as part (b), but an error is made in $d_1(t)$.

8.6 (a) A BPSK system and a QPSK system are designed to transmit at equal rates; that is, two bits are transmitted with the BPSK system for each phase in the QPSK system. Compare their *symbol* error probabilities versus SNR.
(b) A BPSK system and a QPSK system are designed to have equal transmission bandwidths. Compare their symbol error probabilities versus SNR.
(c) On the basis of parts (a) and (b), what do you conclude about the deciding factor(s) in choosing BPSK versus QPSK?

8.7 Compare P_E as computed from Equation (8.14) with the exact result for SNR's of $E_s/N_0 = 0$, 3, 6, and 9 dB.

8.8 Given the serial data sequence

1 1 1 0 0 1 0 1 1 1 0 0 1 0 0 0 0 1 1

associate every other bit with the upper and lower data streams of the block diagrams of Figures 8.2 and 8.4. Draw on the same time scale (one below the other) the quadrature waveforms for the following data modulation schemes: QPSK, OQPSK, MSK type I, and MSK type II.

8.9 Sketch an excess phase trellis diagram for each of the cases of Problem 8.8. Show as a heavy line the actual path through the trellis represented by the data sequence given.

8.10 Derive Equation (8.24) for the spectrum of an MSK signal, assuming that the block diagram of Figure 8.7(a) is correct. That is, show that serial modulation of MSK works from the standpoint of spectral argu-

ments. (*Hint:* Work only with the positive-frequency portions of the spectrum.)

8.11 An MSK system has a carrier frequency of 100 MHz and transmits data at a rate of 100 kbps.

(a) For the data sequence 1010101010 . . . , what is the instantaneous frequency?
(b) For the data sequence 000000000 . . . , what is the instantaneous frequency?

8.12 Sketch the signal space with decision regions for 16-ary PSK [see (8.39)].

8.13 Using (8.49) and appropriate bounds for $P_{E,\text{symbol}}$, obtain E_b/N_0 required for achieving $P_{E,\text{bit}} = 10^{-4}$ for M-ary PSK with $M = 8, 16, 32, 64$. Repeat for 16-GASK.

8.14 Gray encoding of decimal numbers ensures that only one bit changes when the decimal number changes by one unit. Let $b_1b_2b_3 \ldots b_n$ represent an ordinary binary representation of a number, with b_1 being the most significant bit. Let the corresponding Gray code digits be $g_1g_2g_3 \ldots g_n$. Then the Gray code representation is obtained by the algorithm

$$g_i = b_1$$
$$g_n = b_n \oplus b_{n-1}$$

where $\oplus$ denotes modulo-2 addition (i.e., $0 \oplus 0 = 0$, $0 \oplus 1 = 1$, $1 \oplus 0 = 1$, and $1 \oplus 1 = 0$). Find the Gray code representation for the decimal numbers 0 through 16.

8.15 Derive the three equations numbered (8.45) for 16-QASK.

8.16 Using (8.51) and (8.47), obtain E_b/N_0 required for achieving $P_{E,\text{bit}} = 10^{-4}$ for M-ary coherent FSK for $M = 8, 16, 32, 64$.

8.17 Repeat Problem 8.16 for noncoherent M-ary FSK for $M = 2, 4, 8$.

8.18 Sketch the signal space for binary coherent FSK showing the decision regions.

8.19 On the basis of null-to-null bandwidths, give the required transmission bandwidth to achieve a bit rate of 10 kbps for the following:

(a) 16-QASK or 16-PSK
(b) 8-PSK
(c) 32-PSK
(d) 8-FSK, coherent
(e) 16-FSK, coherent
(f) 32-FSK, coherent

Section 8.2

8.20 On the basis of 90% power-containment bandwidth, give the required transmission bandwidth to achieve a bit rate of 10 kbps for

(a) BPSK
(b) QPSK or OQPSK
(c) MSK

8.21 Repeat Problem 8.20, but use a 99% power-containment bandwidth. (Hint: For BPSK, use an appropriate reinterpretation of the abscissa of the curve for QPSK to extend the curve.)

8.22 Generalize the results for power-containment bandwidth for quadrature-modulation schemes given in Section 8.2 to M-ary PSK. With appropriate reinterpretation of the abscissa of Figure 8.19 and using the 90% power containment bandwidth, obtain the required transmission bandwidth to support a bit rate of 10 kbps for

(a) 8-PSK
(b) 16-PSK
(c) 32-PSK

8.23 Note that an NRZ waveform can be converted to split phase by multiplying the NRZ waveform by a squarewave with period equal to the bit period. Assume a random (coin-toss) NRZ bit stream with the autocorrelation function

$$R(\tau) = \left\{ \begin{array}{ll} 1 - \left|\frac{\tau}{T}\right|, & \left|\frac{\tau}{T}\right| \leq 1 \\ 0, & \text{otherwise} \end{array} \right\} = \Lambda\left(\frac{\tau}{T}\right)$$

Obtain a series expression for the power spectral density using the Fourier series expansion for a squarewave and the modulation theorem. Sketch the result, using the first few terms of the series.

8.24 Assume that a data stream $d(t)$ consists of a random (coin toss) sequence of $+1$ and -1 that is T seconds in duration. The autocorrelation function for such a sequence is

$$R_d(\tau) = \left\{ \begin{array}{ll} 1 - \left|\frac{\tau}{T}\right|, & \left|\frac{\tau}{T}\right| \leq 1 \\ 0, & \text{otherwise} \end{array} \right.$$

(a) Find and sketch the power spectral density for an ASK-modulated signal given by

$$s_{ASK}(t) = \tfrac{1}{2}A[1 + d(t)] \cos(\omega_c t + \theta)$$

where θ is a uniform random variable in $(0, 2\pi)$.

(b) Compute and sketch the power spectral density of a PSK-modulated signal given by

$$s_{PSK}(t) = A \sin[\omega_c t + \cos^{-1} m\, d(t) + \theta]$$

for the three cases $m = 0$, 0.5, and 1. (*Hint:* Expand $s_{PSK}(t)$ into its carrier and modulation components.)

8.25 Derive the Fourier transform pair in Equation (8.64).

8.26 Derive Equation (8.59), given Equations (8.56) and (8.57) and assuming that Δ_1 and Δ_2 are independent and uniformly distributed in the interval $(0, T)$.

8.27 Accurately plot spectra for BPSK, QPSK, and MSK. Use the independent variable $T_b f$.

Section 8.3

8.28 Plot σ_ϕ^2 versus z for the various cases given in Table 8.5. Assume 10% of the signal power is in the carrier for the PLL and all signal power is in the modulation for the Costas and data estimation loops. Assume values of $L = 100, 10, 5$.

8.29 Consider a 15-bit, maximal-length PN code. It is generated by feeding back the last two stages of a four-stage shift register. Assuming a 1 1 1 1 initial state, find all the other possible states of the shift register. What is the sequence? Find and plot its periodic autocorrelation function.

8.30 Repeat Problem 8.29 for a 31-bit maximal-length PN code.

8.31 The aperiodic autocorrelation function of a binary code is important for word synchronization. In computing it, the code is not assumed to periodically repeat itself, but each end is padded with zeros.

(a) Find the aperiodic autocorrelation function for the 7-bit sequence of Figure 8.22. What is the maximum of the absolute value of the autocorrelation function for nonzero delay? This is a Barker sequence.

(b) Compute the aperiodic autocorrelation function of the 15-bit PN sequence found in Problem 8.29 and compare with the result of part (a). Note from Table 8.4 that this is *not* a Barker sequence.

Section 8.4

8.32 Show that the variance of N_g as given by (8.81) is N_0T_b.

8.33 Show that the variance of N_I as given by (8.86) is approximated by the result given by (8.87). (*Hint:* You will have to make use of the fact that $T_c^{-1}\Lambda(\tau/T_c)$ is approximately a delta function for small T_c.)

8.34 A DSSS system employing BPSK data modulation operates with a data rate of 1 Mbps. A processing gain of 100 (20 dB) is desired.

(a) Find the required chip rate.
(b) What is the RF transmission bandwidth required (null-to-null)?
(c) An SNR of 10 dB is employed. What is P_E for the following JSRs? 5 dB; 10 dB; 15 dB; 30 dB.

8.35 Repeat Problem 8.34 for $G_p = 1000$ (30 dB).

8.36 Given a sequential search code acquisition system with $n = 2$ cells per chip, $N_c = 1000$ chips, $T_e = 1$ ms, $P_{FH} = 10^{-3}$, and $P_H = 0.9$. Find T_{acq}.

Section 8.5

8.37 Rederive the curves shown in Figure 8.36, assuming BPSK modulation, for an overall P_E of (a) 10^{-5}; (b) 10^{-4}.

8.38 Rederive the curves shown in Figure 8.36, assuming $P_E = 10^{-6}$, if the modulation technique used on the uplink and downlink is (a) binary noncoherent FSK; (b) binary DPSK.

8.39 Rederive the curves shown in Figure 8.36, assuming $P_{E,\text{bit}} = 10^{-6}$, if the modulation technique is changed to M-ary coherent FSK for (a) $M = 4$; (b) $M = 8$; (c) $M = 16$.



COMPUTER EXERCISES

8.1 Use a computer mathematics package to plot curves of P_b versus E_b/N_0 for

(a) M-ary PSK (use the upper-bound expression as an approximation to the actual error probability)

(b) Coherent M-ary FSK (again, use the upper bound as an approximation)
(c) Noncoherent M-ary FSK

Compare your results with Figures 8.16 and 8.17.

8.2 Use a computer mathematics package to plot out-of-band power for M-ary PSK, QPSK (or OQPSK), and MSK. Compare with Figure 8.19.

8.3 Approximate the power spectrum of coherent M-ary FSK by adding voltage spectra of sinusoidal bursts of duration T_b and of the appropriate frequency coherently, and then plotting the magnitude squared. What is the minimum spacing of the "tones" in order to maintain them coherently orthogonal? Write a program to evaluate and plot (8.68b). Compare with the spectrum found in the first part of this exercise.

8.4 Use a computer mathematics package to plot curves like those shown in Figure 8.27. Use a solve routine to find the processing gain required to give a desired probability of bit error for a given JSR and SNR. Note that your program should check to see if the desired bit error probability is possible for the given JSR and SNR.

8.5 Given a satellite altitude and desired illumination spot diameter on the earth's surface, use a computer mathematics package to determine the antenna aperture diameter and maximum gain to give the desired spot diameter.

8.6 Use a computer mathematics package to plot Figure 8.36 for a given probability of bit error, and

(a) M-ary PSK
(b) Coherent M-ary FSK
(c) Noncoherent M-ary FSK

9 OPTIMUM RECEIVERS AND SIGNAL-SPACE CONCEPTS

For the most part, this book has been concerned with the *analysis* of communication systems. An exception occurred in Chapter 7, where we sought the best receiver in terms of minimum probability of error for binary digital signals of known shape. In this chapter we deal with the *optimization* problem; that is, we wish to find the communication system for a given task that performs the *best,* within a certain class, of all possible systems. In taking this approach, we are faced with three basic problems:

1. What is the optimization criterion to be used?
2. What is the optimum structure for a given problem under this optimization criterion?
3. What is the performance of the optimum receiver?

We will consider the simplest type of problem of this nature possible—that of fixed transmitter and channel structure with only the receiver to be optimized.

We have two purposes for including this subject in our study of information transmission systems. First, in Chapter 1 we stated that the application of probabilistic systems analysis techniques coupled with statistical optimization procedures has led to communication systems distinctly different in character from those of the early days of communications. The material in this chapter will, we hope, give you an indication of the truth of this statement, particularly when you see that some of the optimum structures considered here are building blocks of systems analyzed in earlier chapters. Additionally, the signal-space techniques to be further developed later in this chapter provide a unification of the performance results for the analog and digital communication systems that we have obtained so far.

9.1 BAYES OPTIMIZATION

Signal Detection Versus Estimation

Based on our considerations in Chapters 7 and 8, we see that it is perhaps advantageous to separate the signal-reception problem into two domains.

The first of these we shall refer to as *detection,* for we are interested merely in detecting the presence of a particular signal, among other candidate signals, in a noisy background. The second is referred to as *estimation,* in which we are interested in estimating some characteristic of a signal that is assumed to be present in a noisy environment. The signal characteristic of interest may be a time-independent parameter such as a constant (random or nonrandom) amplitude or phase or an estimate (past, present, or future value) of the waveform itself (or a functional of the waveform). The former problem is usually referred to as *parameter estimation.* The latter is referred to as *filtering.* We see that demodulation of analog signals (AM, DSB, and so on), if approached in this fashion, would be a signal-filtering problem.*

While it is often advantageous to categorize signal-reception problems as either detection or estimation, both are usually present in practical cases of interest. For example, in the detection of phase-shift-keyed signals, it is necessary to have an estimate of the signal phase available to perform coherent demodulation. In some cases, we may be able to ignore one of these aspects, as in the case of noncoherent digital signaling, in which signal phase was of no consequence. In other cases, the detection and estimation operations may be inseparable. However, we will look at signal detection and estimation as separate problems in this chapter.

Optimization Criteria

In Chapter 7, the optimization criterion that was employed to find the matched filter receiver for binary signals was *minimum average probability of error.* In this chapter we will generalize this idea somewhat and seek signal detectors or estimators that *minimize average cost.* Such devices will be referred to as *Bayes* receivers for reasons that will become apparent later.

Bayes Detectors

To illustrate the use of minimum average cost optimization criteria to find optimum receiver structures, we will first consider detection. For example, suppose we are faced with a situation in which the presence or absence of a constant signal of value k is to be detected in the presence of an additive Gaussian noise component N (for example, as would result by taking a single

* See Van Trees (1968), Vol. 1, for a consideration of filtering theory applied to optimal demodulation.

sample of a signal plus noise waveform). Thus we may hypothesize two situations for the observed data Z:

Hypothesis 1 (H_1): $Z = N$ (noise alone) $P(H_1 \text{ true}) = p_0$
Hypothesis 2 (H_2): $Z = k + N$ (signal plus noise) $P(H_2 \text{ true}) = 1 - p_0$

Assuming the noise to have zero mean and variance σ_n^2, we may write down the pdf's of Z given hypotheses H_1 and H_2, respectively. Under hypothesis H_1, Z is Gaussian with mean zero and variance σ_n^2. Thus

$$f_Z(z \mid H_1) = \frac{e^{-z^2/2\sigma_n^2}}{\sqrt{2\pi\sigma_n^2}} \tag{9.1}$$

Under hypothesis H_2, since the mean is k,

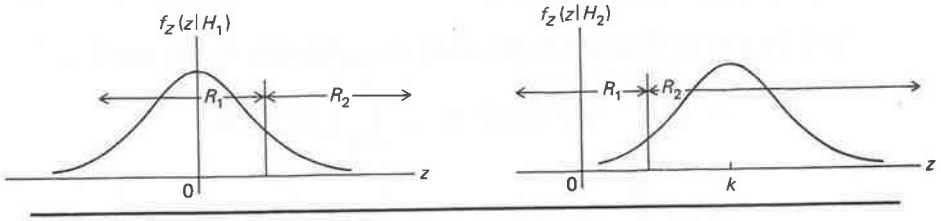
$$f_Z(z \mid H_2) = \frac{e^{-(z-k)^2/2\sigma_n^2}}{\sqrt{2\pi\sigma_n^2}} \tag{9.2}$$

These conditional pdf's are illustrated in Figure 9.1. We note in this example that Z, the observed data, can range over the real line $-\infty < Z < \infty$. Our objective is to partition this one-dimensional observation space into two regions R_1 and R_2 such that if Z falls into R_1, we decide hypothesis H_1 is true, while if Z is in R_2, we decide H_2 is true. We wish to accomplish this in such a manner that the average cost of making a decision is minimized. It may happen, in some cases, that R_1 or R_2 or both will consist of multiple segments of the real line. (See Problem 9.2.)

Taking a general approach to the problem, we note that four *a priori* costs are required, since there are four types of decisions that we can make. These costs are

c_{11}—the cost of deciding in favor of H_1 when H_1 is actually true
c_{12}—the cost of deciding in favor of H_1 when H_2 is actually true

FIGURE 9.1 Conditional pdf's for a two-hypothesis detection problem



c_{21}—the cost of deciding in favor of H_2 when H_1 is actually true
c_{22}—the cost of deciding in favor of H_2 when H_2 is actually true

Given that H_1 was actually true, the conditional average cost of making a decision, $C(D \mid H_1)$, is

$$C(D \mid H_1) = c_{11}P[\text{decide } H_1 \mid H_1 \text{ true}] + c_{21}P[\text{decide } H_2 \mid H_1 \text{ true}] \quad (9.3)$$

In terms of the conditional pdf of Z given H_1, we may write

$$P[\text{decide } H_1 \mid H_1 \text{ true}] = \int_{R_1} f_Z(z \mid H_1)\, dz \quad (9.4)$$

and

$$P[\text{decide } H_2 \mid H_1 \text{ true}] = \int_{R_2} f_Z(z \mid H_1)\, dz \quad (9.5)$$

where the one-dimensional regions of integration are as yet unspecified.

We note that Z must lie in either R_1 or R_2, since we are forced to make a decision. Thus

$$P[\text{decide } H_1 \mid H_1 \text{ true}] + P[\text{decide } H_2 \mid H_1 \text{ true}] = 1$$

or if expressed in terms of the conditional pdf $f_Z(z \mid H_1)$, we obtain

$$\int_{R_2} f_Z(z \mid H_1)\, dz = 1 - \int_{R_1} f_Z(z \mid H_1)\, dz \quad (9.6)$$

Thus, combining (9.3) through (9.6), the conditional average cost given H_1, $C(D \mid H_1)$, becomes

$$C(D \mid H_1) = c_{11} \int_{R_1} f_Z(z \mid H_1)\, dz + c_{21} \left[1 - \int_{R_1} f_Z(z \mid H_1)\, dz \right] \quad (9.7)$$

In a similar manner, the average cost of making a decision given that H_2 is true, $C(D \mid H_2)$, can be written as

$$\begin{aligned} C(D \mid H_2) &= c_{12}P[\text{decide } H_1 \mid H_2 \text{ true}] + c_{22}P[\text{decide } H_2 \mid H_2 \text{ true}] \\ &= c_{12} \int_{R_1} f_Z(z \mid H_2)\, dz + c_{22} \int_{R_2} f_Z(z \mid H_2)\, dz \\ &= c_{12} \int_{R_1} f_Z(z \mid H_2)\, dz + c_{22} \left[1 - \int_{R_1} f_Z(z \mid H_2)\, dz \right] \end{aligned} \quad (9.8)$$

To find the average cost without regard to which hypothesis is actually true, we must average (9.7) and (9.8) with respect to the prior probabilities of hypotheses H_1 and H_2, $p_0 = P[H_1 \text{ true}]$ and $q_0 = 1 - p_0 = P[H_2 \text{ true}]$. The average cost of making a decision is then

$$C(D) = p_0 C(D \mid H_1) + q_0 C(D \mid H_2) \tag{9.9}$$

Substituting (9.7) and (9.8) into (9.9) and collecting terms, we obtain

$$\begin{aligned} C(D) = {} & p_0 \left\{ c_{11} \int_{R_1} f_Z(z \mid H_1)\, dz + c_{21} \left[1 - \int_{R_1} f_Z(z \mid H_1)\, dz \right] \right\} \\ & + q_0 \left\{ c_{12} \int_{R_1} f_Z(z \mid H_2)\, dz + c_{22} \left[1 - \int_{R_1} f_Z(z \mid H_2)\, dz \right] \right\} \end{aligned} \tag{9.10}$$

for the average cost, or risk, in making a decision. Collection of all terms under a common integral that involves integration over R_1 results in

$$\begin{aligned} C(D) = {} & [p_0 c_{21} + q_0 c_{22}] \\ & + \int_{R_1} \{[q_0(c_{12} - c_{22}) f_Z(z \mid H_2)] - [p_0(c_{21} - c_{11}) f_Z(z \mid H_1)]\}\, dz \end{aligned} \tag{9.11}$$

The first term in brackets represents a fixed cost once p_0, q_0, c_{21}, and c_{22} are specified. The value of the integral is determined by those points which are assigned to R_1. Since wrong decisions should be more costly than right decisions, it is reasonable to assume that $c_{12} > c_{22}$ and $c_{21} > c_{11}$. Thus the two bracketed terms within the integral are positive because q_0, p_0, $f_Z(z \mid H_2)$, and $f_Z(z \mid H_1)$ are probabilities. Hence all values of z that give a larger value for the second term in brackets within the integral than for the first term in brackets should be assigned to R_1 because they contribute a negative amount to the integral. Values of z that give a larger value for the first bracketed term than for the second should be assigned to R_2. In this manner, $C(D)$ will be minimized. Mathematically, the preceding discussion can be summarized by the pair of inequalities

$$q_0(c_{12} - c_{22}) f_Z(Z \mid H_2) \underset{H_1}{\overset{H_2}{\gtrless}} p_0(c_{21} - c_{11}) f_Z(Z \mid H_1)$$

or

$$\frac{f_Z(Z \mid H_2)}{f_Z(Z \mid H_1)} \underset{H_1}{\overset{H_2}{\gtrless}} \frac{p_0(c_{21} - c_{11})}{q_0(c_{12} - c_{22})} \tag{9.12}$$

which are interpreted as follows: If an observed value for Z results in the left-hand ratio of pdf's being greater than the right-hand ratio of constants, choose H_2; if not, choose H_1. The left-hand side of (9.12), denoted by $\Lambda(Z)$,

$$\Lambda(Z) \triangleq \frac{f_Z(Z \mid H_2)}{f_Z(Z \mid H_1)} \tag{9.13}$$

is called the *likelihood ratio*. The right-hand side of (9.12),

$$\eta \triangleq \frac{p_0(c_{21} - c_{11})}{q_0(c_{12} - c_{22})} \tag{9.14}$$

is called the *threshold* of the test. Thus the Bayes criterion of minimum average cost has resulted in a test of the likelihood ratio, which is a random variable, against the threshold value η. Note that the development has been general, in that no reference has been made to the particular form of the conditional pdf's in obtaining (9.12). We now return to the specific example that resulted in the conditional pdf's of (9.1) and (9.2).

▼ **EXAMPLE 9.1** Consider the pdf's of (9.1) and (9.2). Let the costs for a Bayes test be $c_{11} = c_{22} = 0$ and $c_{21} = c_{12}$.

(a) Find $\Lambda(Z)$.
(b) Write down the likelihood ratio test for $p_0 = q_0 = \frac{1}{2}$.
(c) Compare the result of part (b) with the case $p_0 = \frac{1}{4}$ and $q_0 = \frac{3}{4}$.

SOLUTION

(a) $$\Lambda(Z) = \frac{\exp\left[-(Z-k)^2/2\sigma_n^2\right]}{\exp\left(-Z^2/2\sigma_n^2\right)} = \exp\left[\frac{2kZ - k^2}{2\sigma_n}\right] \tag{9.15}$$

(b) For this case $\eta = 1$, which results in the test

$$\exp\left[\frac{2kZ - k^2}{2\sigma_n^2}\right] \underset{H_1}{\overset{H_2}{\gtrless}} 1 \tag{9.16a}$$

Taking the natural logarithm of both sides [this is permissible because $\ln(x)$ is a monotonic function of x] and simplifying, we obtain

$$Z \underset{H_1}{\overset{H_2}{\gtrless}} \tfrac{1}{2}k \tag{9.16b}$$

which states that if the noisy received data are less than half the signal amplitude, the decision that minimizes risk is that the signal was absent, which is reasonable.

(c) For this situation, $\eta = \frac{1}{3}$, and the likelihood ratio test is

$$\exp\left[(2kZ - k^2)/2\sigma_n^2\right] \underset{H_1}{\overset{H_2}{\gtrless}} \frac{1}{3} \tag{9.17a}$$

or, simplifying,

$$Z \underset{H_1}{\overset{H_2}{\gtrless}} \frac{k}{2} - \frac{\sigma_n^2}{k} \ln 3 < \frac{k}{2} \tag{9.17b}$$

Thus, if the prior probability of a signal being present in the noise is increased, the optimum threshold is decreased so that the signal-present hypothesis (H_2) will be chosen with higher probability. ▲

Performance of Bayes Detectors

Since the likelihood ratio is a function of a random variable, it is itself a random variable. Thus, whether we compare the likelihood ratio $\Lambda(Z)$ with the threshold η or we simplify the test to a comparison of Z with a modified threshold as in Example 9.1, we are faced with the prospect of making wrong decisions. The average cost of making a decision, given by (9.11), can be written in terms of the conditional probabilities of making wrong decisions, of which there are two.* These are given by

$$P_F = \int_{R_2} f_Z(z \mid H_1)\, dz \tag{9.18}$$

and

$$\begin{aligned} P_M &= \int_{R_1} f_Z(z \mid H_2)\, dz \\ &= 1 - \int_{R_2} f_Z(z \mid H_2)\, dz = 1 - P_D \end{aligned} \tag{9.19}$$

The subscripts F, M, and D stand for "false alarm," "miss," and "detection," respectively, a terminology that grew out of the application of detection theory to radar. (It is implicitly assumed that hypothesis H_2 corresponds to the signal-present hypothesis and that hypothesis H_1 corresponds to noise-

* As will be apparent soon, the probability of error introduced in Chapter 7 can be expressed in terms of P_M and P_F. Thus these conditional probabilities provide a complete performance characterization of the detector.

alone when this terminology is used.) When (9.18) and (9.19) are substituted into (9.11), the risk per decision becomes

$$C(D) = p_0c_{21} + q_0c_{22} + q_0(c_{12} - c_{22})P_M - p_0(c_{21} - c_{11})(1 - P_F) \quad (9.20)$$

Thus it is seen that if the probabilities P_F and P_M (or P_D) are available, the Bayes risk can be computed.

Alternative expressions for P_F and P_M can be written in terms of the conditional pdf's of the likelihood ratio given H_1 and H_2 as follows: Given that H_2 is true, an erroneous decision is made if

$$\Lambda(Z) < \eta \quad (9.21)$$

for the decision, according to (9.12), is in favor of H_1. The probability of inequality (9.21) being satisfied, given H_2 is true, is

$$P_M = \int_0^{\eta} f_\Lambda(\lambda \mid H_2)\, d\lambda \quad (9.22)$$

where $f_\Lambda(\lambda \mid H_2)$ is the conditional pdf of $\Lambda(Z)$ given that H_2 is true. The lower limit of the integral in (9.22) is $\eta = 0$ since $\Lambda(Z)$ is nonnegative, being the ratio of pdfs. Similarly,

$$P_F = \int_{\eta}^{\infty} f_\Lambda(\lambda \mid H_1)\, d\lambda \quad (9.23)$$

because, given H_1, an error occurs if

$$\Lambda(Z) > \eta \quad (9.24)$$

[The decision is in favor of H_2 according to (9.12).] The conditional probabilities $f_\Lambda(\lambda \mid H_2)$ and $f_\Lambda(\lambda \mid H_1)$ can be found, in principle at least, by transforming the pdf's $f_Z(z \mid H_2)$ and $f_Z(z \mid H_1)$ in accordance with the transformation of random variables defined by (9.13). Thus two ways of computing P_M and P_F are given by using either (9.18) and (9.19) or (9.22) and (9.23). Often, however, P_M and P_F are computed by using a monotonic function of $\Lambda(Z)$ that is convenient for the particular situation being considered, as in Example 9.2.

A plot of $P_D = 1 - P_M$ versus P_F is called the *operating characteristic* of the likelihood ratio test, or the *receiver operating characteristic* (ROC). It provides all the information necessary to evaluate the risk through (9.20), provided the costs c_{11}, c_{12}, c_{21}, and c_{22} are known. To illustrate the calculation of an ROC, we return to the example involving detection of a constant in Gaussian noise.

▼ **EXAMPLE 9.2** Consider the conditional pdf's of (9.1) and (9.2). For an arbitrary threshold η, the likelihood ratio test of (9.12), after taking the natural logarithm of both sides, reduces to

$$\frac{2kZ - k^2}{2\sigma_n^2} \underset{H_1}{\overset{H_2}{\gtrless}} \ln \eta \qquad \text{or} \qquad \frac{Z}{\sigma_n} \underset{H_1}{\overset{H_2}{\gtrless}} \left(\frac{\sigma_n}{k}\right) \ln \eta + \frac{k}{2\sigma_n} \tag{9.25}$$

Defining the new random variable $X \triangleq Z/\sigma_n$ and the parameter $d \triangleq k/\sigma_n$, we can further simplify the likelihood ratio test to

$$X \underset{H_1}{\overset{H_2}{\gtrless}} d^{-1} \ln \eta + \tfrac{1}{2}d \tag{9.26}$$

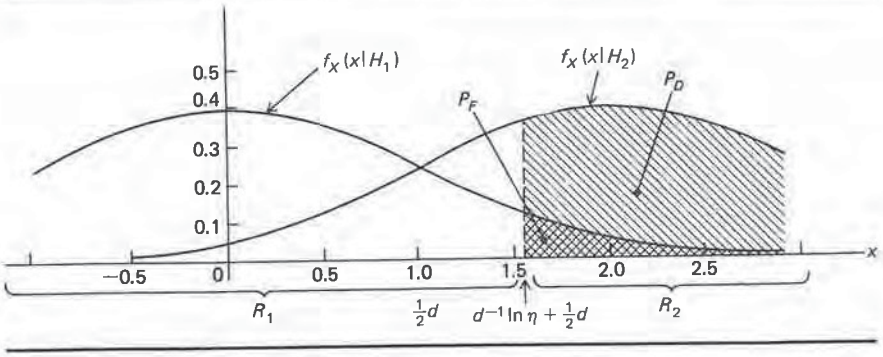
Expressions for P_F and P_M can be found once $f_X(x \mid H_1)$ and $f_X(x \mid H_2)$ are known. Because X is obtained from Z by scaling by σ_n, we see from (9.1) and (9.2) that

$$f_X(x \mid H_1) = \frac{e^{-x^2/2}}{\sqrt{2\pi}} \qquad \text{and} \qquad f_X(x \mid H_2) = \frac{e^{-(x-d)^2/2}}{\sqrt{2\pi}} \tag{9.27}$$

That is, under either hypothesis H_1 or hypothesis H_2, X is a unity variance Gaussian random variable. These two conditional pdf's are shown in Figure 9.2. A false alarm occurs if, given H_1,

$$X > d^{-1} \ln \eta + \tfrac{1}{2}d \tag{9.28}$$

FIGURE 9.2 Conditional probability density functions and decision regions for the problem of detecting a constant signal in zero-mean Gaussian noise



The probability of this happening is

$$P_F = \int_{d^{-1} \ln \eta + d/2}^{\infty} f_X(x \mid H_1)\, dx = \int_{d^{-1} \ln \eta + d/2}^{\infty} \frac{e^{-x^2/2}}{\sqrt{2\pi}}\, dx = Q(d^{-1} \ln \eta + d/2) \tag{9.29}$$

which is the area under $f_X(x \mid H_1)$ to the right of $d^{-1} \ln \eta + \frac{1}{2}d$ in Figure 9.2. Detection occurs if, given H_2,

$$X > d^{-1} \ln \eta + \tfrac{1}{2}d \tag{9.30}$$

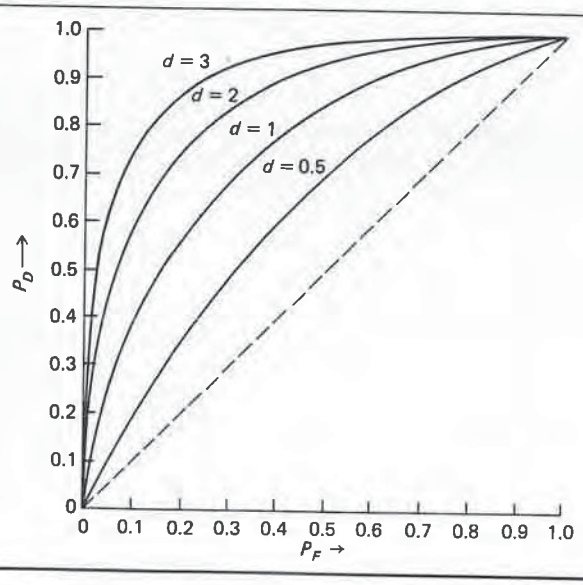
The probability of this happening is

$$P_D = \int_{d^{-1} \ln \eta + d/2}^{\infty} f_X(x \mid H_2)\, dx = \int_{d^{-1} \ln \eta + d/2}^{\infty} \frac{e^{-(x-d)^2/2}}{\sqrt{2\pi}}\, dx = Q(d^{-1} \ln \eta - d/2) \tag{9.31}$$

Thus P_D is the area under $f_X(x \mid H_2)$ to the right of $d^{-1} \ln \eta + \frac{1}{2}d$ in Figure 9.2.

The ROC is obtained by plotting P_D versus P_F for various values of d, as shown in Figure 9.3. The curves are obtained by varying η from 0 to ∞. For

FIGURE 9.3 Receiver operating characteristic for detecting a constant signal in zero-mean Gaussian noise



$\eta = 0$, $\ln \eta = -\infty$ and the detector always chooses H_2 ($P_F = 1$). For $\eta = \infty$, $\ln \eta = \infty$ and the detector always chooses H_1 ($P_D = P_F = 0$).

The Neyman-Pearson Detector

The design of a Bayes detector requires knowledge of the costs and *a priori* probabilities. If these are unavailable, a simple optimization procedure is to fix P_F at some tolerable level, say α, and maximize P_D (or minimize P_M) subject to the constraint $P_F \leq \alpha$. The resulting detector is known as the *Neyman-Pearson detector*. It can be shown that the Neyman-Pearson criterion leads to a likelihood ratio test identical to that of (9.12), except that the threshold η is determined by the allowed value of probability of false alarm α. This value of η can be obtained from the ROC for a given value of P_F, for it can be shown that the slope of a curve of an ROC at a particular point is equal to the value of the threshold η required to achieve the P_D and P_F of that point.*

Minimum Probability of Error Detectors

From (9.11) it follows that if $c_{11} = c_{22} = 0$ (zero cost for making right decision) and $c_{12} = c_{21} = 1$ (equal cost for making either type of wrong decision), then the risk reduces to

$$\begin{aligned} C(D) &= p_0 \left[1 - \int_{R_1} f_Z(z \mid H_1)\, dz \right] + q_0 \int_{R_1} f_Z(z \mid H_2)\, dz \\ &= p_0 \int_{R_2} f_Z(z \mid H_1)\, dz + q_0 \int_{R_1} f_Z(z \mid H_2)\, dz \\ &= p_0 P_F + q_0 P_M \end{aligned} \tag{9.32}$$

where we have used (9.6), (9.18), and (9.19). However, (9.32) is the probability of making a wrong decision, averaged over both hypotheses, which is the same as the probability of error used as the optimization criterion in Chapter 7. Thus Bayes receivers with this special cost assignment are minimum-probability-of-error receivers.

The Maximum a Posteriori (MAP) Detector

Letting $c_{11} = c_{22} = 0$ and $c_{21} = c_{12}$ in (9.12), we can rearrange the equation in the form

$$\frac{f_Z(Z \mid H_2) P(H_2)}{f_Z(Z)} \underset{H_1}{\overset{H_2}{\gtrless}} \frac{f_Z(Z \mid H_1) P(H_1)}{f_Z(Z)} \tag{9.33}$$

* Van Trees (1968), Vol. 1.

where the definitions of p_0 and q_0 have been substituted, both sides of (9.12) have been multiplied by $P(H_2)$, and both sides have been divided by

$$f_Z(Z) \triangleq f_Z(Z \mid H_1)P(H_1) + f_Z(Z \mid H_2)P(H_2) \tag{9.34}$$

Using Bayes' rule, as given by Equation (4.7), (9.34) becomes

$$P(H_2 \mid Z) \underset{H_1}{\overset{H_2}{\gtrless}} P(H_1 \mid Z) \qquad (c_{11} = c_{22} = 0;\ c_{12} = c_{21}) \tag{9.35}$$

Equation (9.35) states that the most probable hypothesis, given a particular observation Z, is to be chosen in order to minimize the risk, which, for the special cost assignment assumed, is equal to the probability of error. The probabilities $P(H_1 \mid Z)$ and $P(H_2 \mid Z)$ are called *a posteriori* probabilities, for they give the probability of a particular hypothesis *after* the observation of Z, in contrast to $P(H_1)$ and $P(H_2)$, which give us the probabilities of the same events *before* observation of Z. Because the hypothesis corresponding to the maximum *a posteriori* probability is chosen, such detectors are referred to as *maximum a posteriori* (MAP) *detectors*. Minimum-probability-of-error detectors and MAP detectors are therefore equivalent.

Minimax Detectors

The minimax decision rule corresponds to the Bayes decision rule, where the *a priori* probabilities have been chosen to make the Bayes risk a maximum. For further discussion of this decision rule, see Weber (1987).

The M-ary Hypothesis Case

The generalization of the Bayes decision criterion to M hypotheses, where $M > 2$, is straightforward but unwieldy. For the M-ary case, M^2 costs and M *a priori* probabilities must be given. In effect, M likelihood ratio tests must be carried out in making a decision. If attention is restricted to the special cost assignment used to obtain the MAP detector for the binary case (that is, right decisions cost zero and wrong decisions are all equally costly), then a MAP decision rule results that is easy to visualize for the M-hypothesis case. Generalizing from (9.35), we have the MAP decision rule for the M-hypothesis case:

Compute the M posterior probabilities $P(H_i \mid Z)$, $i = 1, 2, \ldots, M$, and choose as the correct hypothesis the one corresponding to the largest posterior probability.

This decision criterion will be used when M-ary signal detection is considered.

Decisions Based on Vector Observations

If, instead of a single observation Z, we have N observations $Z \triangleq (Z_1, Z_2, \ldots, Z_N)$, all of the preceding results hold with the exception that the N-fold joint pdf's of Z, given H_1 and H_2, are to be used. If $Z_1, Z_2, \ldots, Z_N$ are conditionally independent, these joint pdf's are easily written down, since they are simply the N-fold products of the marginal pdf's of $Z_1, Z_2, \ldots, Z_N$, given H_1 and H_2. We will make use of this generalization when the detection of arbitrary finite energy signals in white Gaussian noise is discussed. We will find the optimum Bayes detectors for such problems by resolving the possible transmitted signals into a finite dimensional *signal space*. In the next section, therefore, we continue the discussion of vector space representation of signals begun in Chapter 2, Section 2.3.

9.2 VECTOR SPACE REPRESENTATION OF SIGNALS

We recalled, in Section 2.3, that any vector in three-dimensional space can be expressed as a linear combination of any three linearly independent vectors. Recall that such a set of three linearly independent vectors is said to *span* three-dimensional vector space and is referred to as a *basis-vector set* for the space. A basis set of unit-magnitude, mutually perpendicular vectors is called an *orthonormal basis set.*

Two geometrical concepts associated with vectors are magnitude of a vector and angle between two vectors. Both are described by the scalar (or dot) product of any two vectors $\mathbf{A}$ and $\mathbf{B}$ having magnitudes A and B, defined as

$$\mathbf{A} \cdot \mathbf{B} = AB \cos \theta \tag{9.36}$$

where θ is the angle between $\mathbf{A}$ and $\mathbf{B}$. Thus

$$A = \sqrt{\mathbf{A} \cdot \mathbf{A}} \qquad \text{and} \qquad \cos \theta = \frac{\mathbf{A} \cdot \mathbf{B}}{AB} \tag{9.37}$$

Generalizing these concepts to signals in Section 2.3, we expressed a signal $x(t)$ with finite energy in an interval $(t_0, t_0 + T)$ in terms of a complete set of orthonormal basis functions $\phi_1(t), \phi_2(t), \ldots$ as the series

$$x(t) = \sum_{n=1}^{\infty} X_n \phi_n(t) \tag{9.38}$$

where

$$X_n = \int_{t_0}^{t_0+T} x(t)\phi_n^*(t)\,dt \tag{9.39}$$

which is a special case of Equation (2.32) with $c_n = 1$ because the $\phi_n(t)$'s are assumed orthonormal on the interval $(t_0, t_0 + T)$. This representation provided the alternative representation for $x(t)$ as the infinite dimensional vector $(X_1, X_2, \ldots)$.

To set up a geometric structure on such a vector space, which will be referred to as *signal space*, we must first establish the linearity of the space by listing a consistent set of properties involving the members of the space and the operations between them. Second, we must establish the geometric structure of the space by generalizing the concept of scalar product, thus providing generalizations for the concepts of magnitude and angle.

Structure of Signal Space

We begin with the first task. Specifically, a collection of signals composes a linear signal space $\mathcal{S}$ if, for any pair of signals $x(t)$ and $y(t)$ in $\mathcal{S}$, the operations of addition (commutative and associative) of two signals and multiplication of a signal by a scalar are defined and obey the following axioms:

1. The signal $\alpha_1 x(t) + \alpha_2 y(t)$ is in the space for any two scalars α_1 and α_2 (establishes $\mathcal{S}$ as linear).
2. $\alpha[x(t) + y(t)] = \alpha x(t) + \alpha y(t)$ for any scalar α.
3. $\alpha_1[\alpha_2 x(t)] = (\alpha_1\alpha_2)x(t)$.
4. The product of $x(t)$ and the scalar 1 reproduces $x(t)$.
5. The space contains a unique zero element such that $x(t) + 0 = x(t)$.
6. To each $x(t)$ there corresponds a unique element $-x(t)$ such that $x(t) + [-x(t)] = 0$.

In writing relations such as the preceding, it is convenient to suppress the independent variable t, and this will be done from now on.

Scalar Product

The second task, that of establishing the geometric structure, is accomplished by defining the scalar product, denoted (x, y), as a scalar-valued function of two signals $x(t)$ and $y(t)$ (in general complex functions), with the following properties:

1. $(x, y) = (y, x)^*$
2. $(\alpha x, y) = \alpha(x, y)$

3. $(x + y, z) = (x, z) + (y, z)$
4. $(x, x) > 0$ unless $x \equiv 0$, in which case $(x, x) = 0$

The particular definition used for the scalar product depends on the application and the type of signals involved. Because we wish to include both energy and power signals in our future considerations, at least two definitions of scalar product are required. If $x(t)$ and $y(t)$ are both of the same class, a convenient choice is

$$(x, y) \triangleq \begin{cases} \lim_{T' \to \infty} \int_{-T'}^{T'} x(t)y^*(t)\, dt & \text{(energy signals)} \quad (9.40a) \\ \lim_{T' \to \infty} \frac{1}{2T'} \int_{-T'}^{T'} x(t)y^*(t)\, dt & \text{(power signals)} \quad (9.40b) \end{cases}$$

where T' has been used to avoid confusion with the signal observation interval T. In particular, for $x(t) = y(t)$, we see that (9.40a) is the total energy contained in $x(t)$ and (9.40b) corresponds to the average power. We note that the coefficients in the series of (9.38) can be written as

$$X_n = (x, \phi_n) \tag{9.41}$$

If the scalar product of two signals $x(t)$ and $y(t)$ is zero, they are said to be *orthogonal,* just as two ordinary vectors are said to be orthogonal if their dot product is zero.

Norm

The next step in establishing the structure of a linear signal space is to define the length, or norm $\|x\|$, of a signal. A particularly suitable choice, in view of the preceding discussion, is

$$\|x\| = (x, x)^{1/2} \tag{9.42}$$

More generally, the norm of a signal is any nonnegative real number satisfying the following properties:

1. $\|x\| = 0$ if and only if $x \equiv 0$
2. $\|x + y\| \leq \|x\| + \|y\|$ (known as the *triangle inequality*)
3. $\|\alpha x\| = |\alpha|\, \|x\|$, where α is a scalar

Clearly, the choice $\|x\| = (x, x)^{1/2}$ satisfies these properties, and we will employ it from now on.

A measure of the distance between, or dissimilarity of, two signals x and y is provided by the norm of their difference $\|x - y\|$.

Schwarz's Inequality

An important relationship between the scalar product of two signals and their norms is Schwarz's inequality, which was used in Chapter 7 without proof. For two signals $x(t)$ and $y(t)$, it can be written as

$$|(x, y)| \leq \|x\| \, \|y\| \tag{9.43}$$

with equality if and only if x or y is zero or if $x(t) = \alpha y(t)$ where α is a scalar.

To prove (9.43), we consider the nonnegative quantity $\|x + \alpha y\|^2$ where α is as yet an unspecified constant. Expanding it by using the properties of the scalar product, we obtain

$$\begin{aligned} \|x + \alpha y\|^2 &= (x + \alpha y, x + \alpha y) \\ &= (x, x) + \alpha^*(x, y) + \alpha(x, y)^* + |\alpha|^2(y, y) \\ &= \|x\|^2 + \alpha^*(x, y) + \alpha(x, y)^* + |\alpha|^2\|y\|^2 \end{aligned} \tag{9.44}$$

Choosing $\alpha = -(x, y)/\|y\|^2$, which is permissible since α is arbitrary, we find that the last two terms of (9.44) cancel, yielding

$$\|x + \alpha y\|^2 = \|x\|^2 - \frac{|(x, y)|^2}{\|y\|^2} \tag{9.45}$$

Since $\|x + \alpha y\|^2$ is nonnegative, rearranging (9.45) gives Schwarz's inequality. Furthermore, noting that $\|x + \alpha y\| = 0$ if and only if $x + \alpha y = 0$, we establish a condition under which equality holds in (9.43). Equality also holds, of course, if one or both signals are identically zero.

▼ **EXAMPLE 9.3** A familiar example of a space that satisfies the preceding properties is ordinary two-dimensional vector space. Consider two vectors with real components,

$$\mathbf{A}_1 = a_1\hat{i} + b_1\hat{j} \quad \text{and} \quad \mathbf{A}_2 = a_2\hat{i} + b_2\hat{j} \tag{9.46}$$

where $\hat{i}$ and $\hat{j}$ are the usual orthogonal unit vectors. The scalar product is taken as the vector dot product

$$(\mathbf{A}_1, \mathbf{A}_2) = a_1a_2 + b_1b_2 = \mathbf{A}_1 \cdot \mathbf{A}_2 \tag{9.47}$$

and the norm is taken as

$$\|\mathbf{A}_1\| = (\mathbf{A}_1, \mathbf{A}_1)^{1/2} = \sqrt{a_1^2 + b_1^2} \tag{9.48}$$

which is just the length of the vector. Addition is defined as vector addition,

$$\mathbf{A}_1 + \mathbf{A}_2 = (a_1 + a_2)\hat{i} + (b_1 + b_2)\hat{j} \tag{9.49}$$

which is commutative and associative. The vector $\mathbf{C} \triangleq \alpha_1\mathbf{A}_1 + \alpha_2\mathbf{A}_2$, where α_1 and α_2 are real constants, is also a vector in two-space (axiom 1, page 617). The remaining axioms follow as well, with the zero element being $0\hat{i} + 0\hat{j}$.

The properties of the scalar product (pages 617 and 618) are satisfied by the vector dot product.

The properties of the norm also follow, with property 2 taking the form

$$\sqrt{(a_1 + a_2)^2 + (b_1 + b_2)^2} \leq \sqrt{a_1^2 + b_1^2} + \sqrt{a_2^2 + b_2^2} \tag{9.50}$$

which is simply a statement that the length of the hypotenuse of a triangle is shorter than the sum of the lengths of the other two sides—hence the name *triangle inequality*. Schwarz's inequality squared is

$$(a_1a_2 + b_1b_2)^2 \leq (a_1^2 + b_1^2)(a_2^2 + b_2^2) \tag{9.51}$$

which simply states that $|\mathbf{A}_1 \cdot \mathbf{A}_2|^2$ is less than or equal to the length squared of $\mathbf{A}_1$ times the length squared of $\mathbf{A}_2$.

Scalar Product of Two Signals in Terms of Fourier Coefficients

Expressing two energy or power signals $x(t)$ and $y(t)$ in the form given in (9.38), we may show that

$$(x, y) = \sum_{m=1}^{\infty} X_m Y_m^* \tag{9.52a}$$

Letting $y = x$ results in Parseval's theorem, which is

$$\|x\|^2 = \sum_{m=1}^{\infty} |X_m|^2 \tag{9.52b}$$

To indicate the usefulness of the shorthand vector notation just introduced, we will carry out the proof of (9.52) using it. Let $x(t)$ and $y(t)$ be written in terms of their respective orthonormal expansions:

$$x(t) = \sum_{m=1}^{\infty} X_m\phi_m(t) \quad \text{and} \quad y(t) = \sum_{n=1}^{\infty} Y_n\phi_n(t) \tag{9.53}$$

where, in terms of the scalar product,

$$X_m = (x, \phi_m) \quad \text{and} \quad Y_n = (y, \phi_n) \tag{9.54}$$

Thus

$$(x, y) = \left(\sum_m X_m \phi_m, \sum_n Y_n \phi_n \right) = \sum_m X_m \left(\phi_m, \sum_n Y_n \phi_n \right) \tag{9.55}$$

by virtue of properties 2 and 3 of the scalar product. Applying property 1, we obtain

$$(x, y) = \sum_m X_m \left(\sum_n Y_n \phi_n, \phi_m \right)^* = \sum_m X_m \left[\sum_n Y_n^* (\phi_n, \phi_m)^* \right] \tag{9.56}$$

the last step of which follows by virtue of another application of properties 2 and 3. But the ϕ_n's are orthonormal; that is, $(\phi_n, \phi_m) = \delta_{nm}$, where δ_{nm} is the Kronecker delta. Thus

$$(x, y) = \sum_m X_m \left[\sum_n Y_n^* \delta_{nm} \right] = \sum_m X_m Y_m^* \tag{9.57}$$

which proves (9.52a).

▼ EXAMPLE 9.4 Consider a signal $x(t)$ and the approximation to it $x_a(t)$ of Example 2.5. Both x and x_a are in the signal space consisting of all finite energy signals. All the addition and multiplication properties for signal space hold for x and x_a. Because we are considering finite energy signals, the scalar product defined by (9.40) applies. The scalar product of x and x_a is

$$\begin{aligned}(x, x_a) &= \int_0^2 \sin \pi t \left[\frac{2}{\pi} \phi_1(t) - \frac{2}{\pi} \phi_2(t) \right] dt \\ &= \left(\frac{2}{\pi} \right)^2 - \left(\frac{2}{\pi} \right) \left(-\frac{2}{\pi} \right) = 2 \left(\frac{2}{\pi} \right)^2 \end{aligned} \tag{9.58}$$

The norm of their difference squared is

$$\begin{aligned}\|x - x_a\|^2 = (x - x_a, x - x_a) &= \int_0^2 \left[\sin \pi t - \frac{2}{\pi} \phi_1(t) + \frac{2}{\pi} \phi_2(t) \right]^2 dt \\ &= 1 - \frac{8}{\pi^2} \end{aligned} \tag{9.59}$$

which is just the minimum integral-squared error between x and x_a.

The norm squared of x is

$$\|x\|^2 = \int_0^2 \sin^2 \pi t \, dt = 1 \tag{9.60}$$

and the norm squared of x_a is

$$\|x_a\|^2 = \int_0^2 \left[\frac{2}{\pi}\phi_1(t) - \frac{2}{\pi}\phi_2(t)\right]^2 dt = 2\left(\frac{2}{\pi}\right)^2 \tag{9.61}$$

which follows from the orthonormality of ϕ_1 and ϕ_2. Thus Schwarz's inequality for this case is

$$2\left(\frac{2}{\pi}\right)^2 < 1 \cdot \sqrt{2}\left(\frac{2}{\pi}\right) \tag{9.62a}$$

which is equivalent to

$$\sqrt{2} < \tfrac{1}{2}\pi \tag{9.62b}$$

▲ Since x is not a scalar multiple of x_a, we must have strict inequality.

Choice of Basis Function Sets—The Gram-Schmidt Procedure

The question naturally arises as to how we obtain suitable basis sets. For energy or power signals, with no further restrictions imposed, we require infinite sets of functions. Suffice it to say that many suitable choices exist, depending on the particular problem and the interval of interest. These include not only the sines and cosines, or complex exponentials, of harmonically related frequencies, but also the Legendre functions, Hermite functions, and Bessel functions, to name only a few. All these are complete.

A technique referred to as the *Gram-Schmidt procedure* is often useful for obtaining basis sets, especially in the consideration of M-ary signal detection. This procedure will now be described.

Consider the situation in which we are given a finite set of signals $s_1(t)$, $s_2(t)$, . . . , $s_M(t)$ defined on some interval $(t_0, t_0 + T)$, and our interest is in all signals that may be written as linear combinations of these signals:

$$x(t) = \sum_{n=1}^{M} X_n s_n(t), \qquad t_0 \le t \le t_0 + T \tag{9.63}$$

The set of all such signals forms an M-dimensional signal space if the $s_n(t)$'s are linearly independent [that is, no $s_n(t)$ can be written as a linear combination of the rest]. If the $s_n(t)$'s are not linearly independent, the dimension of the space is less than M. An orthonormal basis for the space can be

obtained by using the Gram-Schmidt procedure, which consists of the following steps:

1. Set $v_1(t) = s_1(t)$ and $\phi_1(t) = v_1(t)/\|v_1\|$.
2. Set $v_2(t) = s_2(t) - (s_2, \phi_1)\phi_1$ and $\phi_2(t) = v_2(t)/\|v_2\|$ [$v_2(t)$ is the component of $s_2(t)$ that is linearly independent of $s_1(t)$].
3. Set $v_3(t) = s_3(t) - (s_3, \phi_2)\phi_2(t) - (s_3, \phi_1)\phi_1(t)$ and $\phi_3(t) = v_3(t)/\|v_3\|$ [$v_3(t)$ is the component of $s_3(t)$ linearly independent of $s_1(t)$ and $s_2(t)$].
4. Continue until all the $s_n(t)$'s have been used. If the $s_n(t)$'s are not linearly independent, then one or more steps will yield $v_n(t)$'s for which $\|v_n\| = 0$. These signals are omitted whenever they occur so that a set of K orthonormal functions is finally obtained where $K \leq M$.

The resulting set forms an orthonormal basis set for the space since, at each step of the procedure, we ensure that

$$(\phi_n, \phi_m) = \delta_{nm} \tag{9.64}$$

where δ_{nm} is the Kronecker delta defined in Chapter 2, and we use all signals in forming the orthonormal set.

▼ **EXAMPLE 9.5** Consider the set of three finite-energy signals

$$\begin{aligned} s_1(t) &= 1, & 0 \leq t \leq 1 \\ s_2(t) &= \cos 2\pi t, & 0 \leq t \leq 1 \\ s_3(t) &= \cos^2 \pi t, & 0 \leq t \leq 1 \end{aligned} \tag{9.65}$$

We desire an orthonormal basis for the signal space spanned by these three signals.

SOLUTION We let $v_1(t) = s_1(t)$ and compute

$$\phi_1(t) = \frac{v_1(t)}{\|v_1\|} = 1, \qquad 0 \leq t \leq 1 \tag{9.66}$$

Next, we compute

$$(s_2, \phi_1) = \int_0^1 1 \cos 2\pi t \, dt = 0 \tag{9.67}$$

and we set

$$v_2(t) = s_2(t) - (s_2, \phi_1)\phi_1 = \cos 2\pi t, \qquad 0 \leq t \leq 1 \tag{9.68}$$

The second orthonormal function is found from

$$\phi_2(t) = \frac{v_2}{\|v_2\|} = \sqrt{2}\cos 2\pi t, \qquad 0 \le t \le 1 \tag{9.69}$$

To check for another orthonormal function, we require the scalar products

$$(s_3, \phi_2) = \int_0^1 \sqrt{2}\cos 2\pi t \cos^2 \pi t \, dt = \tfrac{1}{4}\sqrt{2} \tag{9.70a}$$

and

$$(s_3, \phi_1) = \int_0^1 \cos^2 \pi t \, dt = \tfrac{1}{2} \tag{9.70b}$$

Thus

$$\begin{aligned} v_3(t) &= s_3(t) - (s_3\,\phi_2)\phi_2 - (s_3, \phi_1)\phi_1 \\ &= \cos^2 \pi t - (\tfrac{1}{4}\sqrt{2})\sqrt{2}\cos 2\pi t - \tfrac{1}{2} = 0 \end{aligned} \tag{9.70c}$$

▲ so that the space is two-dimensional.

Signal Dimensionality as a Function of Signal Duration

The sampling theorem, proved in Chapter 2, provides a means of representing strictly bandlimited signals, with bandwidth W, in terms of the infinite basis function set $\text{sinc}(f_s t - n)$, $n = 0, \pm 1, \pm 2, \ldots$, from Equation (2.246). Because $\text{sinc}(f_s t - n)$ is not time-limited, we suspect that a strictly bandlimited signal cannot also be of finite duration (that is, time-limited). However, practically speaking, a time-bandwidth dimensionality can be associated with a signal provided the definition of bandlimited is relaxed. The following theorem, given without proof, provides an upper bound for the dimensionality of time-limited and bandwidth-limited signals.*

▷**DIMENSIONALITY THEOREM**

Let $\{\phi_k(t)\}$ denote a set of orthogonal waveforms, all of which satisfy the following requirements:

1. They are identically zero outside a time interval of duration T, for example, $|t| \le \frac{1}{2}T$.

* This theorem is taken from Wozencraft and Jacobs (1965), p. 294, where it is also given without proof. However, a discussion of the equivalence of this theorem to the original ones due to Shannon and to Landau and Pollak is also given.

2. None has more than $\frac{1}{12}$ of its energy outside the frequency interval $-W < f < W$.

Then the number of waveforms in the set $\{\phi_k(t)\}$ is conservatively overbounded by $2.4TW$ when TW is large.

EXAMPLE 9.6 Consider the orthogonal set of waveforms

$$\phi_k(t) = \Pi\left[\frac{t - k\tau}{\tau}\right] = \begin{cases} 1, & \frac{1}{2}(2k-1)\tau \le t \le \frac{1}{2}(2k+1)\tau, \quad k = 0, \pm 1, \pm 2, \pm K \\ 0, & \text{otherwise} \end{cases} \tag{9.71}$$

where $(2K + 1)\tau = T$. The Fourier transform of $\phi_k(t)$ is

$$\Phi_k(f) = \tau \operatorname{sinc} \tau f\, e^{-j2\pi k\tau f} \tag{9.72}$$

The total energy in $\phi_k(t)$ is τ, and the energy for $|f| \le W$ is

$$E_W = \int_{-W}^{W} \tau^2 \operatorname{sinc}^2 \tau f\, df = \int_{-W}^{W} \tau^2 \frac{\sin^2 \pi\tau f}{(\pi\tau f)^2}\, df = \frac{2\tau}{\pi}\int_0^{\pi\tau W} \frac{\sin^2 u}{u^2}\, du \tag{9.73}$$

where the substitution $u = \pi\tau f$ has been made in the integral and the integration is carried out only over positive values of u, owing to the evenness of the integrand. Integrating by parts once, we obtain

$$E_W = -\frac{2\tau}{\pi}\frac{\sin^2 u}{u}\bigg|_0^{\tau\pi W} + \frac{2\tau}{\pi}\int_0^{2\pi\tau W} \frac{\sin \alpha}{\alpha}\, d\alpha \tag{9.74}$$

The second term can be written in terms of the sine-integral function Si (z), defined as

$$\text{Si}\,(z) = \int_0^z \frac{\sin \alpha}{\alpha}\, d\alpha \tag{9.75}$$

which is a tabulated function.* Letting $z = 2\pi\tau W$, we obtain

$$\frac{E_W}{E} = -2\tau W \operatorname{sinc}^2 (\tau W) + \frac{2}{\pi}\,\text{Si}\,(2\pi\tau W) \tag{9.76}$$

* M. Abramowitz and I. Stegun, *Handbook of Mathematical Functions* (New York: Dover, 1972).

We want to choose τW such that $E_W/E \geq \frac{11}{12} = 0.9167$. Using tables for the sinc and Si functions, we can compute the following values for E_W/E:

τW	E_W/E
1.0	0.9027
1.1	0.9033
1.2	0.9064
1.3	0.9130
1.4	0.9218
1.5	0.9312

Thus $\tau W = 1.4$ will ensure that none of the $\phi_k(t)$'s has more than $\frac{1}{12}$ of its energy outside the frequency interval $-W < f < W$.

Now $N = [T/\tau]$ orthogonal waveforms occupy the interval $(-\frac{1}{2}T, \frac{1}{2}T)$ where [ ] signifies the integer part of T/τ. Letting $\tau = 1.4W^{-1}$, we obtain

$$N = \left[\frac{TW}{1.4}\right] = [0.714TW] \tag{9.77}$$

▲ which satisfies the bound given by the theorem.

9.3 MAP RECEIVERS FOR DIGITAL DATA TRANSMISSION

We now apply the detection theory and signal-space concepts just developed to digital data transmission. We will consider examples of coherent and noncoherent systems.

Decision Criteria for Coherent Systems in Terms of Signal Space

In the analysis of QPSK systems in Chapter 8, the received signal plus noise was resolved into two components by the correlators comprising the receiver. This made simple the calculation of the probability of error. The QPSK receiver essentially computes the coordinates of the received signal plus noise in a signal space. The basis functions for this signal space are $\cos \omega_c t$ and $\sin \omega_c t$, $0 \leq t \leq T$, with the scalar product defined by

$$(x_1, x_2) = \int_0^T x_1(t)x_2(t)\, dt \tag{9.78}$$

which is a special case of (9.40a). These basis functions are orthogonal if $\omega_c T$ is an integer multiple of 2π, but are not normalized.

Recalling the Gram-Schmidt procedure, we see how this viewpoint might be generalized to M signals $s_1(t), s_2(t), \ldots, s_M(t)$ that have finite energy but are otherwise arbitrary. Thus, consider an M-ary communication system, depicted in Figure 9.4, wherein one of M possible signals of known form $s_i(t)$ associated with a message m_i is transmitted each T seconds. The receiver is to be constructed such that the probability of error in deciding which message was transmitted is minimized; that is, it is a MAP receiver. For simplicity, we assume that the messages are produced by the information source with equal *a priori* probability.

Ignoring the noise for the moment, we note that the ith signal can be expressed as

$$s_i(t) = \sum_{j=1}^{K} A_{ij}\phi_j(t), \qquad i = 1, 2, \ldots, M, \quad K \leq M \tag{9.79}$$

where the $\phi_j(t)$'s are orthonormal basis functions chosen according to the Gram-Schmidt procedure. Thus

$$A_{ij} = \int_0^T s_i(t)\phi_j(t)\, dt = (s_i, \phi_j) \tag{9.80}$$

and we see that the receiver structure shown in Figure 9.5, which consists of a bank of correlators, can be used to compute the generalized Fourier coefficients for $s_i(t)$. Thus we can represent each possible signal as a point in a K-dimensional signal space with coordinates $(A_{i1}, A_{i2}, \ldots, A_{iK})$, for $i = 1, 2, \ldots, M$.

FIGURE 9.4 *M*-ary communication system

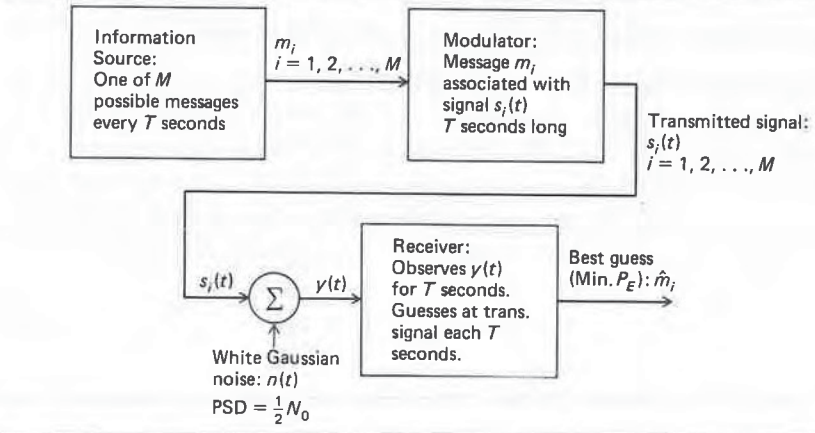
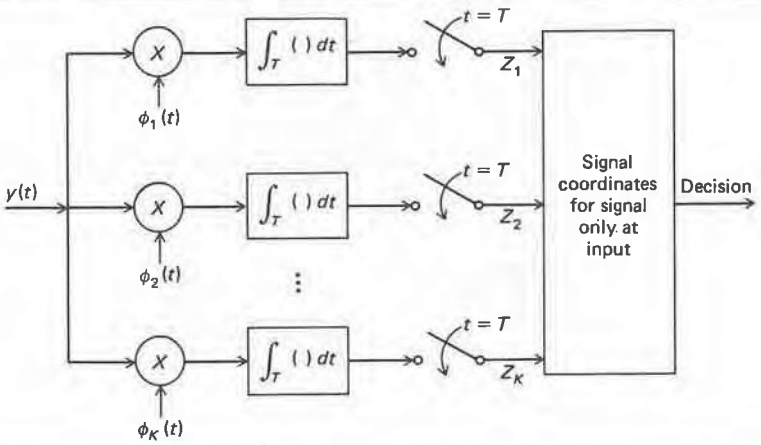


FIGURE 9.5 Receiver structure for resolving signals into K-dimensional signal space



Knowing the coordinates of $s_i(t)$ is as good as knowing $s_i(t)$, since it is uniquely specified through (9.79). The difficulty is, of course, that we receive the signals in the presence of noise. Thus, instead of the receiver providing us with the actual signal coordinates, it provides us with noisy coordinates $(A_{i1} + N_1, A_{i2} + N_2, \ldots, A_{iK} + N_K)$, where

$$N_i \triangleq \int_0^T n(t)\phi_j(t)\, dt = (n, \phi_j) \tag{9.81}$$

We refer to the vector $\mathbf{Z}$ having components

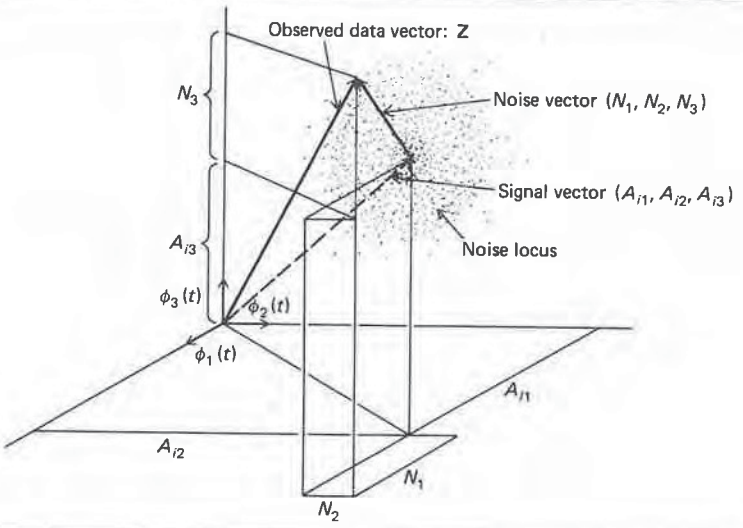
$$Z_j \triangleq A_{ij} + N_j, \qquad j = 1, 2, \ldots, K \tag{9.82}$$

as the *data vector*, and the space of all possible data vectors as the *observation space*. Figure 9.6 illustrates a typical situation for $K = 3$.

The decision-making problem we are therefore faced with is one of associating sets of noisy signal points with each possible transmitted signal point in a manner that will minimize the average error probability. That is, the observation space must be partitioned into M regions R_i, one associated with each transmitted signal, such that if a received data point falls into region R_ℓ, the decision "$s_\ell(t)$ transmitted" is made with minimum probability of error.

In Section 9.1, the minimum-probability-of-error detector was shown to

FIGURE 9.6 A three-dimensional observation space



correspond to a MAP decision rule. Thus, letting hypothesis H_ℓ be "signal $s_\ell(t)$ transmitted," we want to implement a receiver that computes

$$P(H_\ell | Z_1, Z_2, \ldots, Z_K), \qquad \ell = 1, 2, \ldots, M \tag{9.83}$$

and chooses the largest.* To compute the posterior probabilities of (9.83), we use Bayes' rule and assume that

$$P(H_1) = P(H_2) = \cdots = P(H_M) \tag{9.84}$$

Application of Bayes' rule results in

$$P(H_\ell | z_1, \ldots, z_K) = \frac{f_Z(z_1, \ldots, z_K | H_\ell) P(H_\ell)}{f_Z(z_1, \ldots, z_K)} \tag{9.85}$$

However, since the factors $P(H_\ell)$ and $f_Z(z_1, \ldots, z_K)$ do not depend on ℓ, the detector can compute $f_Z(z_1, \ldots, z_K | H_\ell)$ and choose the H_ℓ corresponding to the largest. The Z_j's given by (9.82) are the results of linear operations on a Gaussian process and are therefore Gaussian random variables. All that

* Capital letters are used to denote components of data vectors because they represent coordinates of an observation that is *random*.

is required to write their joint pdf, given H_ℓ, are their means, variances, and covariances. Their means, given hypothesis H_ℓ, are

$$E\{Z_j | H_\ell\} = E\{A_{\ell j} + N_j\} = A_{\ell j} + \int_0^T E\{n(t)\}\phi_j(t)\, dt$$
$$= A_{\ell j}, \qquad j = 1, 2, \ldots, K \tag{9.86}$$

Their variances, given hypothesis H_ℓ, are

$$\text{var}\,\{Z_j | H_\ell\} = E\{[(A_{\ell j} + N_j) - A_{\ell j}]^2\} = E\{N_j^2\}$$
$$= E\left\{\int_0^T n(t)\phi_j(t)\, dt \int_0^T n(t')\phi_j(t')\, dt'\right\}$$
$$= \int_0^T \int_0^T E\{n(t)n(t')\}\phi_j(t)\phi_j(t')\, dt\, dt'$$
$$= \int_0^T \int_0^T \frac{N_0}{2}\,\delta(t - t')\phi_j(t)\phi_j(t')\, dt\, dt'$$
$$= \int_0^T \frac{N_0}{2}\,\phi_j^2(t)\, dt = \tfrac{1}{2}N_0, \qquad j = 1, 2, \ldots, K \tag{9.87}$$

where the orthonormality of the ϕ_j's has been used. In a similar manner, it can be shown that the covariance of Z_j and Z_k, for $j \neq k$, is zero. Thus Z_1, $Z_2, \ldots, Z_K$ are uncorrelated Gaussian random variables and, hence, are statistically independent. Thus

$$f_Z(z_1, \ldots, z_K | H_\ell) = \prod_{j=1}^{K} \frac{\exp\,[-(z_j - A_{\ell j})^2/N_0]}{\sqrt{\pi N_0}}$$
$$= \frac{\exp\,[-\sum_{j=1}^{K} (z_j - A_{\ell j})^2/N_0]}{(\pi N_0)^{K/2}}$$
$$= \frac{\exp\,\{-\|z - s_\ell\|^2/N_0\}}{(\pi N_0)^{K/2}} \tag{9.88}$$

where

$$z = z(t) = \sum_{j=1}^{K} z_j\phi_j(t) \tag{9.89}$$

and

$$s_\ell = s_\ell(t) = \sum_{j=1}^{K} A_{\ell j}\phi_j(t) \tag{9.90}$$

Except for a factor independent of ℓ (9.88) is the posterior probability $P(H_\ell | z_1, \ldots, z_K)$ as obtained by applying Bayes' rule. Hence, choosing H_ℓ corresponding to the maximum posterior probability is the same as choosing the signal with coordinates $A_{\ell 1}, A_{\ell 2}, \ldots, A_{\ell K}$ so as to maximize (9.88) or, equivalently, so as to minimize the exponent. But $\|z - s_\ell\|$ is the distance between $z(t)$ and $s_\ell(t)$. Thus it has been shown that the decision criterion that minimizes the average probability of error is to choose as the transmitted signal the one whose signal point is closest to the received data point in observation space, distance being defined as the square root of the sum of the squares of the differences of the data and signal vector components. That is, choose H_ℓ such that*

$$\begin{aligned}(\text{Distance})^2 = d^2 &= \sum_{j=1}^{K} (Z_j - A_{\ell j})^2 \\ &= \|z - s_\ell\|^2 = \text{minimum}, \qquad \ell = 1, 2, \ldots, M\end{aligned} \tag{9.91}$$

which is exactly the operation to be performed by the receiver structure of Figure 9.5. We illustrate this procedure with the following example.

▼ **EXAMPLE 9.7** In this example we consider M-ary coherent FSK in terms of signal space. The transmitted signal set is

$$s_i(t) = A \cos \{2\pi[f_c + (i - 1)\Delta f]t\}, \qquad 0 \leq t \leq T_s \tag{9.92}$$

where

$$\Delta f = \frac{m}{2T_s}, \qquad m \text{ an integer, } i = 1, 2, \ldots, M$$

For mathematical simplicity, we assume that $f_c T_s$ is an integer. The orthonormal basis set can be obtained by applying the Gram-Schmidt procedure. Choosing

$$v_1(t) = s_1(t) = A \cos (2\pi f_c t), \qquad 0 \leq t \leq T_s \tag{9.93}$$

we have

$$\|v_1\|^2 = \int_0^{T_s} A^2 \cos^2 (2\pi f_c t)\, dt = \frac{A^2 T_s}{2} \tag{9.94}$$

* Again, Z_j is the jth coordinate of an observation $z(t)$ that is random; (9.91) is referred to as a *decision rule.*

so that

$$\phi_1(t) = \frac{v_1}{\|v_1\|} = \sqrt{\frac{2}{T_s}} \cos(2\pi f_c t), \qquad 0 \leq t \leq T_s \tag{9.95}$$

It can be shown in a straightforward fashion that $(s_2, \phi_1) = 0$ if $\Delta f = m/(2T_s)$, so that the second orthonormal function is

$$\phi_2(t) = \sqrt{\frac{2}{T_s}} \cos[2\pi(f_c + \Delta f)t], \qquad 0 \leq t \leq T_s \tag{9.96}$$

and similarly for $M - 2$ other orthonormal functions up to $\phi_M(t)$. Thus the number of orthonormal functions is the same as the number of possible signals; the ith signal can be written in terms of the ith orthonormal function as

$$s_i(t) = \sqrt{E_s}\, \phi_i(t) \tag{9.97}$$

We let the received signal plus noise waveform be represented as $y(t)$. When projected into the observation space, $y(t)$ has M coordinates, the ith one of which is given by

$$Z_i = \int_0^{T_s} y(t)\phi_i(t)\, dt \tag{9.98}$$

where $y(t) = s_i(t) + n(t)$. If $s_\ell(t)$ is transmitted, the decision rule (9.91) becomes

$$d^2 = \sum_{j=1}^{M} (Z_j - \sqrt{E_s}\, \delta_{\ell j})^2 = \text{minimum over } \ell = 1, 2, \ldots, M \tag{9.99}$$

Taking the square root and writing the sum out, this can be expressed as

$$d = \sqrt{Z_1^2 + Z_2^2 + \cdots + (Z_\ell - \sqrt{E_s})^2 + \cdots + Z_M^2}$$
$$= \text{minimum} \tag{9.100}$$

For two dimensions (binary FSK), the signal points lie on the two orthogonal axes at a distance $\sqrt{E_s}$ out from the origin. The decision space consists of the first quadrant, and the optimum (minimum error probability) partition is a line at 45° bisecting the right angle made by the two coordinate axes.

For M-ary FSK transmission, an alternative way of viewing the decision rule can be obtained by squaring the ℓth term in (9.99) so that we have

$$d^2 = \sum_{j=1}^{M} Z_j^2 + E_s - 2\sqrt{E_s}\, Z_\ell = \text{minimum} \tag{9.101}$$

Since the sums over j and E_s are independent of ℓ (a constant), d^2 can be minimized with respect to ℓ by choosing as the possible transmitted signal the one that will maximize the last term; that is, the decision rule becomes: Choose the possible transmitted signal $s_\ell(t)$ such that

$$\sqrt{E_s}\, Z_\ell = \text{maximum} \quad \text{or} \quad Z_\ell = \int_0^{T_s} y(t)\phi_\ell(t)\, dt = \text{maximum with respect to } \ell \tag{9.102}$$

In other words, we look at the output of the bank of correlators shown in Figure 9.5 at time $t = T_s$ and choose the one with the largest output as corresponding to the most probable transmitted signal.

Sufficient Statistics

To show that (9.91) is indeed the decision rule corresponding to a MAP criterion, we must clarify one point. In particular, the decision is based on the noisy signal

$$z(t) = \sum_{j=1}^{K} Z_j \phi_j(t) \tag{9.103}$$

Because of the noise component $n(t)$, this is *not* the same as $y(t)$, since an infinite set of basis functions would be required to represent all possible $y(t)$'s. However, we may show that only K coordinates, where K is the signal-space dimension, are required to provide all the information that is relevant to making a decision.

Assuming a complete orthonormal set of basis functions, $y(t)$ can be expressed as

$$y(t) = \sum_{j=1}^{\infty} Y_j \phi_j(t) \tag{9.104}$$

where the first K of the ϕ_j's are chosen using the Gram-Schmidt procedure for the given signal set. Given that hypothesis H_ℓ is true, the Y_j's are given by

$$Y_j = \begin{cases} Z_j = A_{\ell j} + N_j, & j = 1, 2, \ldots, K \\ N_j, & j = K+1, K+2, \ldots \end{cases} \tag{9.105}$$

where Z_j, $A_{\ell j}$, and N_j are as defined previously. Using a procedure identical to the one used in obtaining (9.86) and (9.87), we can show that

$$E\{Y_j\} = \begin{cases} A_{ij}, & j = 1, 2, \ldots, K \\ 0, & j > K \end{cases} \tag{9.106a}$$

$$\text{var}\{Y_j\} = \tfrac{1}{2}N_0, \qquad \text{all } j \tag{9.106b}$$

with cov $\{Y_j Y_k\} = 0$, $j \neq k$. Thus the joint pdf of $Y_1, Y_2, \ldots$, given H_ℓ, is of the form

$$\begin{aligned} f_Y(y_1, y_2, \ldots, y_K, \ldots | H_\ell) &= C \exp\left\{ -\frac{1}{N_0}\left[\sum_{j=1}^{K} (y_j - A_{\ell j})^2 + \sum_{j=K+1}^{\infty} y_j^2 \right] \right\} \\ &= C^1 \exp\left(-\frac{1}{N_0} \sum_{j=K+1}^{\infty} y_j^2 \right) f_Z(y_1, \ldots, y_K | H_\ell) \end{aligned} \tag{9.107}$$

where C^1 are constants. Since this pdf factors, $Y_{K+1}, Y_{K+2}, \ldots$ are independent of $Y_1, Y_2, \ldots, Y_K$ and the former provide no information for making a decision. Thus d^2 given by (9.101) is known as a *sufficient statistic.*

Detection of M-ary Orthogonal Signals

As a more complex example of the use of signal-space techniques, let us consider an M-ary signaling scheme for which the signal waveforms have equal energies and are orthogonal over the signaling interval. Thus

$$\int_0^{T_s} s_i(t) s_j(t)\, dt = \begin{cases} E_s, & i = j \\ 0, & i \neq j,\ i = 1, 2, \ldots, M \end{cases} \tag{9.108}$$

where E_s is the energy of each signal in $(0, T_s)$.

A practical example of such a signaling scheme is the signal set for M-ary coherent FSK given by (9.92). The decision rule for this signaling scheme was considered in Example 9.7. It was found that $K = M$ orthonormal functions are required, and the receiver shown in Figure 9.5 involves M corre-

lators. The output of the jth correlator at time T_s is given by (9.82). The decision criterion is to choose the signal point $i = 1, 2, \ldots, M$ such that d^2 given by (9.91) is minimized or, as shown in Example 9.7, such that

$$Z_\ell = \int_0^{T_s} y(t)\phi_\ell(t)\, dt = \text{maximum with respect to } \ell \tag{9.109}$$

That is, the signal is chosen that has the maximum correlation with the received signal plus noise. To compute the probability of symbol error, we note that

$$\begin{aligned} P_E &= \sum_{i=1}^{M} P[E \mid s_i(t) \text{ sent}]P[s_i(t) \text{ sent}] \\ &= \frac{1}{M}\sum_{i=1}^{M} P[E \mid s_i(t) \text{ sent}] \end{aligned} \tag{9.110}$$

where each signal is assumed *a priori* equally probable. We may write

$$P[E \mid s_i(t) \text{ sent}] = 1 - P_{ci} \tag{9.111}$$

where P_{ci} is the probability of a correct decision given that $s_i(t)$ was sent. Since a correct decision results only if

$$Z_j = \int_0^{T_s} y(t)s_j(t)\, dt < \int_0^{T_s} y(t)s_i(t)\, dt = Z_i \tag{9.112}$$

for all $j \neq i$, we may write P_{ci} as

$$P_{ci} = P\,(\text{all } Z_j < Z_i, \quad j \neq i) \tag{9.113}$$

If $s_i(t)$ is transmitted, then

$$\begin{aligned} Z_i &= \int_0^{T_s} [\sqrt{E_s}\,\phi_i(t) + n(t)]\phi_i(t)\, dt \\ &= \sqrt{E_s} + N_i \end{aligned} \tag{9.114}$$

where

$$N_i = \int_0^{T_s} n(t)\phi_i(t)\, dt \tag{9.115}$$

Since $Z_j = N_j$, $j \neq i$, given $s_i(t)$ was sent, it follows that (9.113) becomes

$$P_{ci} = P(\text{all } N_j < \sqrt{E_s} + N_i, \quad j \neq i) \tag{9.116}$$

Now N_i is a Gaussian random variable (a linear operation on a Gaussian process) with zero mean and variance

$$\text{var}\,[N_i] = E\left\{\left[\int_0^{T_s} n(t)\phi_j(t)\,dt\right]^2\right\} = \frac{N_0}{2} \tag{9.117}$$

Furthermore, N_i and N_j, for $i \neq j$, are independent, since

$$E[N_iN_j] = 0 \tag{9.118}$$

Given a particular value of N_i, (9.116) becomes

$$\begin{aligned} P_{ci}(N_i) &= \prod_{\substack{j=1\\ j\neq i}}^{M} P[N_j < \sqrt{E_s} + N_i] \\ &= \left(\int_{-\infty}^{\sqrt{E_s}+n_i} \frac{e^{-n_j^2/N_0}}{\sqrt{\pi N_0}}\,dn_j\right)^{M-1} \end{aligned} \tag{9.119}$$

which follows because the pdf of N_j is $n(0, \sqrt{N_0/2})$. Averaged over all possible values of N_i, (9.119) gives

$$\begin{aligned} P_{ci} &= \int_{-\infty}^{\infty} \frac{e^{-n_i^2/N_0}}{\sqrt{\pi N_0}} \left(\int_{-\infty}^{\sqrt{E_s}+n_i} \frac{e^{-n_j^2/N_0}}{\sqrt{\pi N_0}}\,dn_j\right)^{M-1} dn_i \\ &= (\pi)^{-M/2} \int_{-\infty}^{\infty} e^{-y^2} \left(\int_{-\infty}^{\sqrt{E_s/N_0}+y} e^{-x^2}\,dx\right)^{M-1} dy \end{aligned} \tag{9.120}$$

where the substitutions $x = n_j/\sqrt{N_0}$ and $y = n_i/\sqrt{N_0}$ have been made.

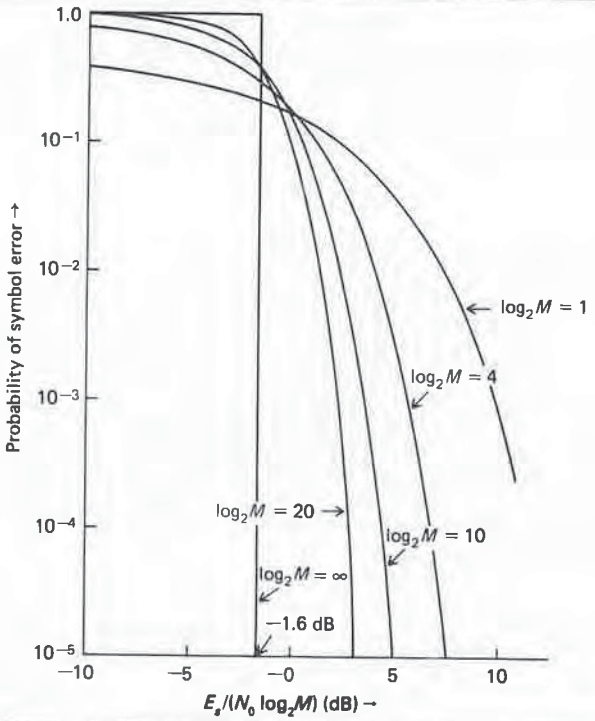
Since P_{ci} is independent of i, it follows that the probability of error is

$$P_E = 1 - P_{ci} \tag{9.121}$$

With (9.120) substituted in (9.121), a nonintegrable M-fold integral for P_E results, and one must resort to numerical integration to evaluate it.* Curves showing P_E versus $E_s/(N_0 \log_2 M)$ are given in Figure 9.7 for several values of M. We note a rather surprising behavior: As $M \to \infty$, error-free transmission can be achieved as long as $E_s/(N_0 \log_2 M) > \ln 2 = -1.59$ dB. This error-free transmission is achieved at the expense of infinite bandwidth, however, since $M \to \infty$ means that an infinite number or orthonormal functions are required. We will discuss this behavior further in Chapter 10.

* See Lindsey and Simon (1973), pp. 199ff, for tables giving P_E.

FIGURE 9.7 Probability of symbol error for coherent detection of M-ary orthogonal signals



A Noncoherent Case

To illustrate the application of signal-space techniques to noncoherent digital signaling, let us consider the following binary hypothesis situation:

$$H_1: y(t) = G\sqrt{2E/T}\cos(\omega_1 t + \theta) + n(t)$$
$$H_2: y(t) = G\sqrt{2E/T}\cos(\omega_2 t + \theta) + n(t), \qquad 0 \le t \le T \tag{9.122a}$$

where E is the energy of the transmitted signal in one bit period and $n(t)$ is white Gaussian noise with double-sided power spectral density $\frac{1}{2}N_0$. It is assumed that $|\omega_1 - \omega_2|/2\pi \gg T^{-1}$ so that the signals are orthogonal. Except for G and θ, which are assumed to be random variables, this problem would be a special case of the M-ary orthogonal signaling case just considered. (Recall also the consideration of coherent and noncoherent FSK in Chapter 7.)

The random variables G and θ represent random gain and phase perturbations introduced by a fading channel. The channel is modeled as introducing a random gain and phase shift during each bit interval. Because the gain and phase shift are assumed to remain constant throughout a bit interval, this channel model is called *slowly fading*. We assume that G is Rayleigh and θ is uniform in $(0, 2\pi)$ and that G and θ are independent.

Expanding (9.122a), we obtain

$$\begin{aligned} H_1&: y(t) = \sqrt{2E/T}\,(G_1 \cos \omega_1 t + G_2 \sin \omega_1 t) + n(t) \\ H_2&: y(t) = \sqrt{2E/T}\,(G_1 \cos \omega_2 t + G_2 \sin \omega_2 t) + n(t), \qquad 0 \le t \le T \end{aligned} \tag{9.122b}$$

where $G_1 = G \cos \theta$ and $G_2 = -G \sin \theta$ are independent, zero-mean, Gaussian random variables (recall Example 4.15). We denote their variances by σ^2. Choosing the orthonormal basis set

$$\left.\begin{aligned} \phi_1(t) &= \sqrt{2/T} \cos \omega_1 t \\ \phi_2(t) &= \sqrt{2/T} \sin \omega_1 t \\ \phi_3(t) &= \sqrt{2/T} \cos \omega_2 t \\ \phi_4(t) &= \sqrt{2/T} \sin \omega_2 t \end{aligned}\right\} \quad 0 \le t \le T \qquad \begin{aligned} &\text{(9.123a)} \\ &\text{(9.123b)} \\ &\text{(9.123c)} \\ &\text{(9.123d)} \end{aligned}$$

the term $y(t)$ can be resolved into a four-dimensional signal space, and decisions may be based on the data vector

$$\mathbf{Z} = (Z_1, Z_2, Z_3, Z_4) \tag{9.124}$$

where

$$Z_i = (y, \phi_i) = \int_0^T y(t)\phi_i(t)\, dt \tag{9.125}$$

Given hypothesis H_1, we obtain

$$Z_i = \begin{cases} \sqrt{E}G_i + N_i, & i = 1, 2 \\ N_i, & i = 3, 4 \end{cases} \tag{9.126}$$

and given hypothesis H_2, we obtain

$$Z_i = \begin{cases} N_i, & i = 1, 2 \\ \sqrt{E}G_{i-2} + N_i & i = 3, 4 \end{cases} \tag{9.127}$$

where

$$N_i = (n, \phi_i) = \int_0^T n(t)\phi_i(t)\, dt, \qquad i = 1, 2, 3, 4 \tag{9.128}$$

are independent Gaussian random variables with zero mean and variance $\frac{1}{2}N_0$. Since G_1 and G_2 are also independent Gaussian random variables with zero mean and variance σ^2, the joint conditional pdf's of Z, given H_1 and H_2, are the products of the respective marginal pdf's. It follows that

$$f_Z(z_1, z_2, z_3, z_4 | H_1) = \frac{\exp\left[-(z_1^2 + z_2^2)/(2E\sigma^2 + N_0)\right] \exp\left[-(z_3^2 + z_4^2)/N_0\right]}{\pi^2(2E\sigma^2 + N_0)N_0} \tag{9.129a}$$

and

$$f_Z(z_1, z_2, z_3, z_4 | H_2) = \frac{\exp\left[-(z_1^2 + z_2^2)/N_0\right] \exp\left[-(z_3^2 + z_4^2)/(2E\sigma^2 + N_0)\right]}{\pi^2(2E\sigma^2 + N_0)N_0} \tag{9.129b}$$

The decision rule that minimizes the probability of error is to choose the hypothesis H_ℓ corresponding to the largest posterior probability $P(H_\ell | z_1, z_2, z_3, z_4)$. But these probabilities differ from (9.129) only by a constant that is independent of ℓ. For a particular observation $\mathbf{Z} = (Z_1, Z_2, Z_3, Z_4)$, the decision rule is

$$f_Z(Z_1, Z_2, Z_3, Z_4 | H_1) \underset{H_2}{\overset{H_1}{\gtrless}} f_Z(Z_1, Z_2, Z_3, Z_4 | H_2) \tag{9.130}$$

which, after substitution from (9.129) and simplification, reduces to

$$R_2^2 \triangleq Z_3^2 + Z_4^2 \underset{H_2}{\overset{H_1}{\gtrless}} Z_1^2 + Z_2^2 \triangleq R_1^2 \tag{9.131}$$

The optimum receiver corresponding to this decision rule is shown in Figure 9.8.

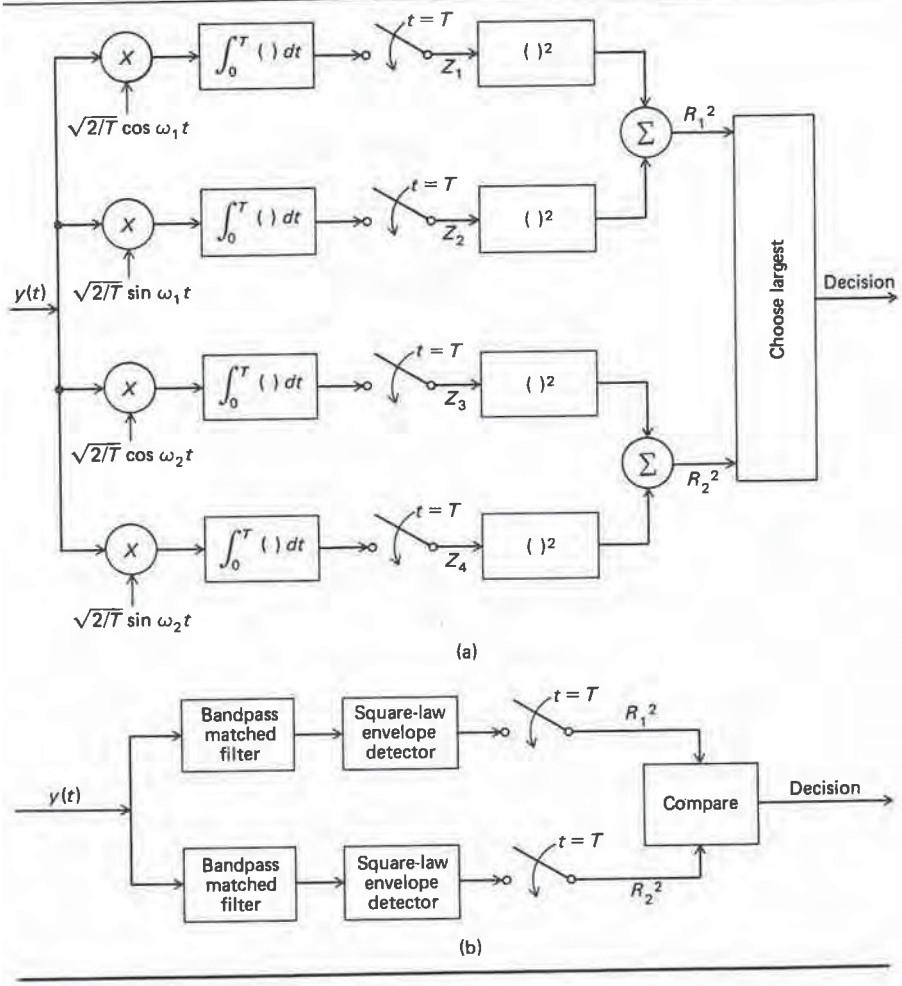
To find the probability of error, we note that both $R_1 \triangleq \sqrt{Z_1^2 + Z_2^2}$ and $R_2 \triangleq \sqrt{Z_3^2 + Z_4^2}$ are Rayleigh random variables under either hypothesis. Given H_1 is true, an error results if $R_2 > R_1$, where the positive square root of (9.131) has been taken. From Example 4.15, it follows that

$$f_{R_1}(r_1 | H_1) = \frac{r_1 e^{-r_1^2/(2E\sigma^2 + N_0)}}{E\sigma^2 + \frac{1}{2}N_0}, \qquad r_1 > 0 \tag{9.132a}$$

and

$$f_{R_2}(r_2 | H_1) = \frac{2r_2 e^{-r_2^2/N_0}}{N_0}, \qquad r_2 > 0 \tag{9.132b}$$

FIGURE 9.8 Optimum receiver structures for detection of binary orthogonal signals in Rayleigh fading. (a) Implementation by correlator and squarer. (b) Implementation by matched filter and envelope detector.

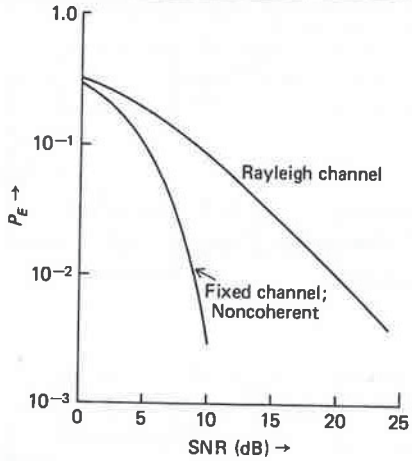


The probability that $R_2 > R_1$, averaged over R_1, is

$$P(E \mid H_1) = \int_0^\infty \left[\int_{r_1}^\infty f_{R_2}(r_2 \mid H_1)\, dr_2 \right] f_{R_1}(r_1 \mid H_1)\, dr_1$$

$$= \frac{1}{2} \frac{1}{1 + \frac{1}{2}(2\sigma^2 E/N_0)} \tag{9.133}$$

FIGURE 9.9 Comparison of P_E versus SNR for Rayleigh and fixed channels with noncoherent FSK signaling



where $2\sigma^2 E$ is the average received signal energy. Because of the symmetry involved, it follows that $P(E|H_1) = P(E|H_2)$ and that

$$P_E = P(E|H_1) = P(E|H_2) \tag{9.134}$$

The probability of error is plotted in Figure 9.9, along with the result from Chapter 7 for constant-amplitude noncoherent FSK (Figure 7.20). Whereas the error probability for nonfading, noncoherent FSK signaling decreases exponentially with the signal-to-noise ratio, the fading channel results in an error probability that decreases only inversely with signal-to-noise ratio.

One way to combat this degradation due to fading is to employ *diversity transmission;* that is, the transmitted signal power is divided among several independently fading transmission paths with the hope that not all of them will fade simultaneously. Several ways of achieving diversity were mentioned in Chapter 7. (See also Problem 9.17.)

9.4 ESTIMATION THEORY

We now consider the second type of optimization problem discussed in the introduction to this chapter—the estimation of parameters from random data. After introducing some background theory here, we will consider several applications of estimation theory to communication systems in Section 9.5.

In introducing the basic ideas of estimation theory, we will exploit several parallels with detection theory. As in the case of signal detection, we have available a noisy observation Z that depends probabilistically on a parameter of interest A.* For example, Z could be the sum of an unknown dc voltage A and an independent noise component N: $Z = A + N$.

Two different estimation procedures will be considered. These are Bayes estimation and maximum-likelihood (ML) estimation. For Bayes estimation, A is considered to be random with a known *a priori* pdf $f_A(a)$, and a suitable cost function is minimized to find the optimum estimate of A. Maximum-likelihood estimation can be used for the estimation of nonrandom parameters or a random parameter with an unknown *a priori* pdf.

Bayes Estimation

Bayes estimation involves the minimization of a cost function, as in the case of Bayes detection. Given an observation Z, we seek the *estimation rule* (or *estimator*) $\hat{a}(Z)$ that assigns a value $\hat{A}$ to A such that the cost function $C[A, \hat{a}(Z)]$ is minimized. Note that C is a function of the unknown parameter A and the observation Z. Clearly, as the absolute error $|A - \hat{a}(Z)|$ increases, $C[A, \hat{a}(Z)]$ should increase, or at least not decrease; that is, large errors should be more costly than small errors. Two useful cost functions are

$$C[A, \hat{a}(Z)] = [A - \hat{a}(Z)]^2 \qquad \text{(squared-error cost)} \tag{9.135a}$$

$$C[A, \hat{a}(Z)] = \begin{cases} 1, & |A - \hat{a}(Z)| > \Delta > 0 \\ 0, & \text{otherwise} \end{cases} \qquad \text{(uniform cost)} \tag{9.135b}$$

where Δ is a suitably chosen constant. For each of these cost functions, we wish to find the decision rule $\hat{a}(Z)$ that minimizes the average cost $E\{C[A, \hat{a}(Z)]\} = \overline{C[A, \hat{a}(Z)]}$. Because both A and Z are random variables, the average cost, or risk, is given by

$$\begin{aligned} \overline{C[A, \hat{a}(Z)]} &= \int_{-\infty}^{\infty} \int_{-\infty}^{\infty} C[a, \hat{a}(z)] f_{AZ}(a, z)\, da\, dz \\ &= \int_{-\infty}^{\infty} \int_{-\infty}^{\infty} C[a, \hat{a}(z)] f_{Z|A}(z \mid a) f_A(a)\, dz\, da \end{aligned} \tag{9.136}$$

where $f_{AZ}(a, z)$ is the joint pdf of A and Z and $f_{Z|A}(z \mid a)$ is the conditional pdf of Z given A. The latter can be found if the probabilistic mechanism that

* For simplicity, we consider the single-observation case first and generalize to vector observations later.

produces Z from A is known. For example, if $Z = A + N$, where N is a zero-mean Gaussian random variable with variance σ_n^2, then

$$f_{Z|A}(z\,|\,a) = \frac{e^{-(z-a)^2/2\sigma_n^2}}{\sqrt{2\pi\sigma_n^2}} \tag{9.137}$$

Returning to the minimization of the risk, we find it more advantageous to express (9.136) in terms of the conditional pdf $f_{A|Z}(a\,|\,z)$, which can be done by means of Bayes' rule, to obtain

$$\overline{C[A, \hat{a}(Z)]} = \int_{-\infty}^{\infty} f_Z(z) \left\{ \int_{-\infty}^{\infty} C[a, \hat{a}(z)] f_{A|Z}(a\,|\,z)\, da \right\} dz \tag{9.138a}$$

where

$$f_Z(z) = \int_{-\infty}^{\infty} f_{Z|A}(z\,|\,a) f_A(a)\, da \tag{9.138b}$$

is the pdf of Z. Since $f_Z(z)$ and the inner integral in (9.138a) are nonnegative, the risk can be minimized by minimizing the inner integral for each z. The inner integral in (9.138a) is called the *conditional risk*.

This minimization is accomplished for the squared-error cost function, (9.135a), by differentiating the conditional risk with respect to $\hat{a}$ for a particular observation Z and setting the result equal to zero. The resulting differentiation yields

$$\begin{aligned} &\frac{\partial}{\partial \hat{a}} \int_{-\infty}^{\infty} [a - \hat{a}(Z)]^2 f_{A|Z}(a\,|\,Z)\, da \\ &\quad = -2 \int_{-\infty}^{\infty} a f_{A|Z}(a\,|\,Z)\, da + 2\hat{a}(Z) \int_{-\infty}^{\infty} f_{A|Z}(a\,|\,Z)\, da \end{aligned} \tag{9.139}$$

which, when set to zero, results in

$$\hat{a}_{se}(Z) = \int_{-\infty}^{\infty} a f_{A|Z}(a\,|\,Z)\, da \tag{9.140}$$

where the fact that $\int_{-\infty}^{\infty} f_{A|Z}(a\,|\,Z)\, da = 1$ has been used. A second differentiation shows that this is a minimum. Note that $\hat{a}_{se}(Z)$, the estimator for a squared-error cost function, is the mean of the pdf of A given the observation Z, or the conditional mean. The values that $\hat{a}_{se}(Z)$ assume, $\hat{A}$, are random since the estimator is a function of the random variable Z.

In a similar manner, we can show that the uniform cost function results in the condition

$$f_{A|Z}(A\,|\,Z)\,\Big|_{A=\hat{a}_{\mathrm{MAP}}(Z)} = \text{maximum} \tag{9.141}$$

for Δ in (9.135b) infinitesimally small. That is, the estimation rule, or estimator, that minimizes the uniform cost function is the maximum of the conditional pdf of A given Z, or the *a posteriori* pdf. Thus this estimator will be referred to as the *maximum a posteriori* (MAP) estimate. Necessary, but not sufficient, conditions that the MAP estimate must satisfy are

$$\frac{\partial}{\partial A} f_{A|Z}(A\,|\,Z)\,\Big|_{A=\hat{a}_{\mathrm{MAP}}(Z)} = 0 \tag{9.142a}$$

and

$$\frac{\partial}{\partial A} \ln f_{A|Z}(A\,|\,Z)\,\Big|_{A=\hat{a}_{\mathrm{MAP}}(Z)} = 0 \tag{9.142b}$$

where the latter condition is especially convenient for *a posteriori* pdf's of exponential type, such as Gaussian.

Often the MAP estimate is employed because it is easier to obtain than other estimates, even though the conditional-mean estimate, given by (9.140), is more general, as the following theorem indicates.

▷THEOREM

If, as a function of a, the *a posteriori* pdf $f_{A|Z}(a\,|\,Z)$ has a single peak, about which it is symmetrical, and the cost function has the properties

$$C(A, \hat{a}) = C(A - \hat{a}) \tag{9.143a}$$

$$C(x) = C(-x) \geq 0 \qquad \text{(symmetrical)} \tag{9.143b}$$

$$C(x_1) \geq C(x_2) \text{ for } |x_1| \geq |x_2| \qquad \text{(convex)} \tag{9.143c}$$

then the conditional-mean estimator is the Bayes estimate.*

Maximum-Likelihood Estimation

We now seek an estimation procedure that does not require *a priori* information about the parameter of interest. Such a procedure is maximum-likelihood (ML) estimation. To explain this procedure, consider the MAP estimation of a random parameter A about which little is known. This lack

* Van Trees (1968), pp. 60–61.

of information about A is expressed probabilistically by assuming the prior pdf of A, $f_A(a)$, to be broad compared with the posterior pdf, $f_{A|Z}(a|Z)$. If this were not the case, the observation Z would be of little use in estimating A. Since the joint pdf of A and Z is given by

$$f_{AZ}(a, z) = f_{A|Z}(a|z)f_Z(z) \tag{9.144}$$

the joint pdf, regarded as a function of a, must be peaked for at least one value of a. By the definition of conditional probability, we also may write (9.144) as

$$\begin{aligned} f_{ZA}(z, a) &= f_{Z|A}(z|a)f_A(a) \\ &\cong f_{Z|A}(z|a) \qquad \text{(times a constant)} \end{aligned} \tag{9.145}$$

where the approximation follows by virtue of the assumption that little is known about A, thus implying that $f_A(a)$ is essentially constant. The ML estimate of A is defined as

$$f_{Z|A}(Z|A)\Big|_{A=\hat{a}_{ML}(Z)} = \text{maximum} \tag{9.146}$$

But, from (9.144) and (9.145), the ML estimate of a parameter corresponds to the MAP estimate if little *a priori* information about the parameter is available. From (9.146), it follows that the ML estimate of a parameter A is that value of A which is most likely to have resulted in the observaton Z; hence the name "maximum likelihood." Since the prior pdf of A is not required to obtain an ML estimate, it is a suitable estimation procedure for random parameters whose prior pdf is unknown. If a deterministic parameter is to be estimated, $f_{Z|A}(z|A)$ is regarded as the pdf of Z with A as a parameter.

From (9.146) it follows that the ML estimate can be found from the necessary, but not sufficient, conditions

$$\frac{\partial f_{Z|A}(Z|A)}{\partial A}\Big|_{A=\hat{a}_{ML}(Z)} = 0 \tag{9.147a}$$

and

$$l(A) \triangleq \frac{\partial \ln f_{Z|A}(Z|A)}{\partial A}\Big|_{A=\hat{a}_{ML}(Z)} = 0 \tag{9.147b}$$

When viewed as a function of A, $f_{Z|A}(z|A)$ is referred to as the *likelihood function*. Both (9.147a) and (9.147b) will be referred to as *likelihood equations*.

From (9.142) and Bayes' rule, it follows that the MAP estimate of a random paramcter satisfies

$$\left[I(A) + \frac{\partial}{\partial A} \ln f_A(A) \right] \Big|_{A=\hat{a}_{\text{MAP}}(Z)} = 0 \tag{9.148}$$

which is useful when finding both the ML and MAP estimates of a parameter.

Estimates Based on Multiple Observations

If a multiple number of observations are available, say $\mathbf{Z} \triangleq (Z_1, Z_2, \ldots, Z_K)$, on which to base the estimate of a parameter, we simply substitute the K-fold joint conditional pdf $f_{\mathbf{Z}|A}(\mathbf{z}|A)$ in (9.146) and (9.147) to find the ML estimate of A. If the observations are independent, when conditioned on A, then

$$f_{\mathbf{Z}|A}(\mathbf{z}|A) = \prod_{k=1}^{K} f_{Z_k|A}(z_k|A) \tag{9.149}$$

where $f_{Z_k|A}(z_k|A)$ is the pdf of the kth observation Z_k given the parameter A. To find $f_{A|\mathbf{Z}}(a|\mathbf{z})$ for MAP estimation, we use Bayes' rule.

▼ **EXAMPLE 9.8** To illustrate the estimation concepts just discussed, let us consider the estimation of a constant-level random signal A embedded in Gaussian noise $n(t)$ with zero mean and variance σ_n^2:

$$z(t) = A + n(t) \tag{9.150}$$

We assume $z(t)$ is sampled at time intervals sufficiently spaced so that the samples are independent. Let these samples be represented as

$$Z_k = A + N_k, \qquad k = 1, 2, \ldots, K \tag{9.151}$$

Thus, *given* A, the Z_k's are independent, each having mean A and variance σ_n^2. Hence the conditional pdf of $\mathbf{Z} \triangleq (Z_1, Z_2, \ldots, Z_K)$ given A is

$$\begin{aligned} f_{\mathbf{Z}|A}(\mathbf{z}|A) &= \prod_{k=1}^{K} \frac{\exp\left[-(z_k - A)^2/2\sigma_n^2\right]}{\sqrt{2\pi\sigma_n^2}} \\ &= \frac{\exp\left[-\sum_{k=1}^{K} (z_k - A)^2/2_n^2\right]}{(2\pi\sigma_n^2)^{K/2}} \end{aligned} \tag{9.152}$$

We will assume two possibilities for A:

1. It is Gaussian with mean m_A and variance σ_A^2.
2. Its pdf is unknown.

In the first case, we will find the conditional-mean and the MAP estimates for A. In the second case, we will compute the ML estimate.

Case 1

If the pdf of A is

$$f_A(a) = \frac{e^{-(a-m_A)^2/2\sigma_A^2}}{\sqrt{2\pi\sigma_A^2}} \tag{9.153}$$

its posterior pdf is, by Bayes' rule,

$$f_{A|\mathbf{Z}}(a\,|\,\mathbf{z}) = \frac{f_{\mathbf{Z}|A}(\mathbf{z}\,|\,a)f_A(a)}{f_{\mathbf{Z}}(z)} \tag{9.154}$$

After some algebra, it can be shown that

$$f_{A|\mathbf{Z}}(a\,|\,\mathbf{z}) = (2\pi\sigma_p^2)^{-1/2} \exp\left(\frac{-\{a - \sigma_p^2[(Km_s/\sigma_n^2) + (m_A/\sigma_A^2)]\}^2}{2\sigma_p^2}\right) \tag{9.155}$$

where

$$\frac{1}{\sigma_p^2} = \frac{K}{\sigma_n^2} + \frac{1}{\sigma_A^2} \tag{9.156}$$

and the sample mean is

$$m_s = \frac{1}{K}\sum_{k=1}^{K} Z_k \tag{9.157}$$

Clearly, $f_{A|\mathbf{Z}}(a\,|\,\mathbf{z})$ is a Gaussian pdf with variance σ_p^2 and mean

$$\begin{aligned} E\{A\,|\,\mathbf{Z}\} &= \sigma_p^2\left(\frac{Km_s}{\sigma_n^2} + \frac{m_A}{\sigma_A^2}\right) \\ &= \frac{K\sigma_A^2/\sigma_n^2}{1 + K\sigma_A^2/\sigma_n^2}\, m_s + \frac{1}{1 + K\sigma_A^2/\sigma_n^2}\, m_A \end{aligned} \tag{9.158}$$

Since the maximum value of a Gaussian pdf is at the mean, this is both the conditional-mean estimate (squared-error cost function, among other convex cost functions) and the MAP estimate (square-well cost function). The

conditional variance var $\{A \mid \mathbf{Z}\}$ is σ_p^2. Because it is not a function of $\mathbf{Z}$, it follows that the average cost, or risk, which is

$$\overline{C[A, \hat{a}(Z)]} = \int_{-\infty}^{\infty} \text{var}\,\{A \mid \mathbf{z}\} f_{\mathbf{z}}(\mathbf{z})\, d\mathbf{z} \tag{9.159}$$

is just σ_p^2.

From the expression for $E(A \mid \mathbf{Z})$, we note an interesting behavior for the estimate of A, or $\hat{a}(Z)$. As $K\sigma_A^2/\sigma_n^2 \to \infty$,

$$\hat{a}(Z) \to m_s = \frac{1}{K} \sum_{k=1}^{K} Z_k \tag{9.160}$$

which says that as the ratio of signal variance to noise variance becomes large, the optimum estimate for A approaches the sample mean. On the other hand, as $K\sigma_A^2/\sigma_n^2 \to 0$ (small signal variance and/or large noise variance), $\hat{a}(\mathbf{Z}) \to m_A$, the *a priori* mean of A. In the first case, the estimate is weighted in favor of the observations; in the latter, it is weighted in favor of the known signal statistics. From the form of σ_p^2, we note that, in either case, the quality of the estimate increases as the number of independent samples of $z(t)$ increases.

Case 2

The ML estimate is found by differentiating $\ln f_{\mathbf{Z}|A}(\mathbf{z} \mid A)$ with respect to A and setting the result equal to zero. Performing the steps, the ML estimate is found to be

$$\hat{a}_{\text{ML}}(\mathbf{Z}) = \frac{1}{K} \sum_{k=1}^{K} Z_k \tag{9.161}$$

We note that this corresponds to the MAP estimate if $K\sigma_A^2/\sigma_n^2 \to \infty$ (that is, if the *a priori* pdf of A is broad compared with the *a posteriori* pdf).

The variance of $\hat{a}_{\text{ML}}(\mathbf{Z})$ is found by recalling that the variance of a sum of independent random variables is the sum of the variances. The result is

$$\sigma_{\text{ML}}^2 = \frac{\sigma_n^2}{K} > \sigma_p^2 \tag{9.162}$$

Thus the prior knowlege about A, available through $f_A(a)$, manifests itself as a smaller variance for the Bayes estimates (conditional-mean and MAP) than for the ML estimate. ▲

Other Properties of ML Estimates

Unbiased Estimates An estimate $\hat{a}(\mathbf{Z})$ is said to be *unbiased* if

$$E\{\hat{a}(\mathbf{Z})\,|\,A\} = A \tag{9.163}$$

This is clearly a desirable property of any estimation rule. If $E\{\hat{a}(\mathbf{Z})\,|\,A\} - A = B \neq 0$, B is referred to as the *bias of the estimate.*

The Cramer-Rao Inequality In many cases it may be difficult to compute the variance of an estimate for a nonrandom parameter. A lower bound for the variance of an unbiased ML estimate is provided by the following inequality:

$$\text{var}\,\{\hat{a}(\mathbf{Z})\} \geq \left(E\left\{ \left[\frac{\partial \ln f_{\mathbf{Z}|A}(\mathbf{Z}\,|\,a)}{\partial a} \right]^2 \right\} \right)^{-1} \tag{9.164a}$$

or, equivalently,

$$\text{var}\,\{\hat{a}(\mathbf{Z})\} \geq \left(-E\left\{ \frac{\partial^2 \ln f_{\mathbf{Z}|A}(\mathbf{Z}\,|\,a)}{\partial a^2} \right\} \right)^{-1} \tag{9.164b}$$

where the expectation is only over $\mathbf{Z}$. These inequalities hold under the assumption that $\partial f_{\mathbf{Z}|A}/\partial a$ and $\partial^2 f_{\mathbf{Z}|A}/\partial a^2$ exist and are absolutely integrable. A proof is furnished by Van Trees (1968). Any estimate satisfying (9.164) with equality is said to be *efficient.*

A sufficient condition for equality in (9.164) is that

$$\frac{\partial \ln f_{\mathbf{Z}|A}(\mathbf{Z}\,|\,a)}{\partial a} = [\hat{a}(\mathbf{Z}) - A]\, g(a) \tag{9.165}$$

where $g(\cdot)$ is a function only of a. If an efficient estimate of a parameter exists, it is the maximum-likelihood estimate.

Asymptotic Qualities of ML Estimates In the limit, as the number of independent observations becomes large, ML estimates can be shown to be *Gaussian, unbiased,* and *efficient.* In addition, the probability that the ML estimate for K observations differs by a fixed amount ϵ from the true value approaches zero as $K \to \infty$; an estimate with such behavior is referred to as *consistent.*

▼ EXAMPLE 9.9 Returning to Example 9.8, we can show that $\hat{a}_{\text{ML}}(\mathbf{Z})$ is an efficient estimate. We have already shown that $\sigma_{\text{ML}}^2 = \sigma_n^2/K$. Using (9.164b), we differentiate in $f_{\mathbf{Z}|A}$ once to obtain

$$\frac{\partial \ln f_{\mathbf{Z}|A}}{\partial a} = \frac{1}{\sigma_n^2} \sum_{k=1}^{K} (Z_k - a) \tag{9.166}$$

A second differentiation gives

$$\frac{\partial^2 \ln f_{\mathbf{Z}|A}}{\partial a^2} = -\frac{K}{\sigma_n^2} \tag{9.167}$$

▲ and (9.164b) is seen to be satisfied with equality.

9.5 APPLICATIONS OF ESTIMATION THEORY TO COMMUNICATIONS

We now consider two applications of estimation theory to the transmission of analog data. The sampling theorem introduced in Chapter 2 was applied in Chapter 3 in the discussion of several systems for the transmission of continuous-waveform messages via their sample values. One such technique is PAM, in which the sample values of the message are used to amplitude-modulate a pulse-type carrier. We will apply the results of Example 9.8 to find the performance of the optimum demodulator for PAM. This is a *linear* estimator because the observations are linearly dependent on the message sample values. For such a system, the only way to decrease the effect of noise on the demodulator output is to increase the SNR of the received signal, since output and input SNR are linearly related.

Following the consideration of PAM, we will derive the optimum ML estimator for the phase of a signal in additive Gaussian noise. This will result in a phase-lock loop structure. The variance of the estimate in this case will be obtained for high input SNR by applying the Cramer-Rao inequality. For low SNRs, the variance is difficult to obtain because this is a problem in *nonlinear* estimation; that is, the observations are nonlinearly dependent on the parameter being estimated.

The transmission of analog samples by pulse-position modulation (PAM) or some other modulation scheme could also be considered. An approximate analysis of its performance for low input SNRs would show the threshold effect of nonlinear modulation schemes and the implications of the tradeoff that is possible between bandwidth and output SNR. This effect was seen previously in Chapter 6 when the performance of PCM in noise was considered.

Pulse-Amplitude Modulation (PAM)

In PAM, the message $m(t)$ of bandwidth W is sampled at T-second intervals, where $T \leq 1/2W$, and the sample values $m_k = m(t_k)$ are used to amplitude-modulate a pulse train composed of time-translates of the basic pulse shape

$p(t)$, which is assumed zero for $t \leq 0$ and $t \geq T_0 < T$. The received signal plus noise is represented as

$$y(t) = \sum_{k=-\infty}^{\infty} m_k p(t - kT) + n(t) \tag{9.168}$$

where $n(t)$ is white Gaussian noise with double-sided power spectral density $\frac{1}{2}N_0$.

Considering the estimation of a single sample at the receiver, we observe

$$y(t) = m_0 p(t) + n(t), \qquad 0 \leq t \leq T \tag{9.169}$$

For convenience, if we assume that $\int_0^{T_0} p^2(t)\, dt = 1$, it follows that a sufficient statistic is

$$\begin{aligned} Z_0 &= \int_0^{T_0} y(t)p(t)\, dt \\ &= m_0 + N \end{aligned} \tag{9.170}$$

where the noise component is

$$N = \int_0^{T_0} n(t)p(t)\, dt \tag{9.171}$$

Having no prior information about m_0, we apply ML estimation. Following procedures used many times before, we can show that N is a zero-mean Gaussian random variable with variance $\frac{1}{2}N_0$. The ML estimation of m_0 is therefore identical to the single-observation case of Example 9.8, and the best estimate is simply Z_0. As in the case of digital data transmission, this estimator could be implemented by passing $y(t)$ through a filter matched to $p(t)$, observing the output amplitude prior to the next pulse, and then setting the filter initial conditions to zero. Note that the estimator is *linearly* dependent on $y(t)$.

The variance of the estimate is equal to the variance of N, or $\frac{1}{2}N_0$. Thus the SNR at the output of the estimator is

$$\begin{aligned} (\text{SNR})_0 &= \frac{2m_0^2}{N_0} \\ &= \frac{2E}{N_0} \end{aligned} \tag{9.172}$$

where $E = \int_0^{T_0} m_0^2 p^2(t)\, dt$ is the average energy of the received signal sample. Thus the only way to increase $(\text{SNR})_0$ is by increasing the energy per sample or by decreasing N_0.

Estimation of Signal Phase: The PLL Revisited

We now consider the problem of estimating the phase of a sinusoidal signal $A \cos(\omega_c t + \theta)$ in white Gaussian noise $n(t)$ of double-sided power spectral density $\frac{1}{2}N_0$. Thus the observed data are

$$y(t) = A \cos(\omega_c t + \theta) + n(t), \qquad 0 \leq t \leq T \tag{9.173}$$

where T is the observation interval. Expanding $A \cos(\omega_c t + \theta)$ as

$$A \cos \omega_c t \cos \theta - A \sin \omega_c t \sin \theta$$

we see that a suitable set of orthonormal basis functions for representing the data is

$$\phi_1(t) = \sqrt{\frac{2}{T}} \cos \omega_c t, \qquad 0 \leq t \leq T \tag{9.174a}$$

and

$$\phi_2(t) = \sqrt{\frac{2}{T}} \sin \omega_c t, \qquad 0 \leq t \leq T \tag{9.174b}$$

Thus we base our decision on

$$z(t) = \sqrt{\frac{T}{2}} A \cos \theta \, \phi_1(t) - \sqrt{\frac{T}{2}} A \sin \theta \, \phi_2(t) + N_1\phi_1(t) + N_2\phi_2(t) \tag{9.175}$$

where

$$N_i = \int_0^T n(t)\phi_i(t) \, dt, \qquad i = 1, 2 \tag{9.176}$$

Because $y(t) - z(t)$ involves only noise, which is independent of $z(t)$, it is not relevant to making the estimate. Thus we may base the estimate on the vector

$$\mathbf{Z} \triangleq (Z_1, Z_2) = \left(\sqrt{\frac{T}{2}} A \cos \theta + N_1, - \sqrt{\frac{T}{2}} A \sin \theta + N_2 \right) \tag{9.177}$$

where

$$Z_i = (y(t), \phi_i(t)) = \int_0^T y(t)\phi_i(t) \, dt \tag{9.178}$$

The likelihood function $f_{\mathbf{Z}|\theta}(z_1, z_2|\theta)$ is obtained by noting that the variance of Z_1 and Z_2 is simply $\frac{1}{2}N_0$, as in the PAM example. Thus the likelihood function is

$$f_{\mathbf{Z}|\theta}(z_1, z_2|\theta) = \frac{\exp\left\{-\frac{1}{N_0}\left[\left(z_1 - \sqrt{\frac{T}{2}}A\cos\theta\right)^2 + \left(z_2 + \sqrt{\frac{T}{2}}A\sin\theta\right)^2\right]\right\}}{\pi N_0}$$

$$= C\exp\left[2\sqrt{\frac{T}{2}}\frac{A}{N_0}(z_1\cos\theta - z_2\sin\theta)\right] \tag{9.179}$$

where the coefficient C contains all factors that are independent of θ. The logarithm of the likelihood function is

$$\ln f_{\mathbf{Z}|\theta}(z_1, z_2|\theta) = \ln C + \sqrt{2T}\frac{A}{N_0}(z_1\cos\theta - z_2\sin\theta) \tag{9.180}$$

which, when differentiated and set to zero, yields a necessary condition for the maximum-likelihood estimate of θ in accordance with (9.147b). The result is

$$-Z_1\sin\theta - Z_2\cos\theta\Big|_{\theta=\hat{\theta}_{ML}} = 0 \tag{9.181}$$

where Z_1 and Z_2 signify that we are considering a particular (random) observation. But

$$Z_1 = (y, \phi_1) = \sqrt{\frac{2}{T}}\int_0^T y(t)\cos\omega_c t\,dt \tag{9.182a}$$

and

$$Z_2 = (y, \phi_2) = \sqrt{\frac{2}{T}}\int_0^T y(t)\sin\omega_c t\,dt \tag{9.182b}$$

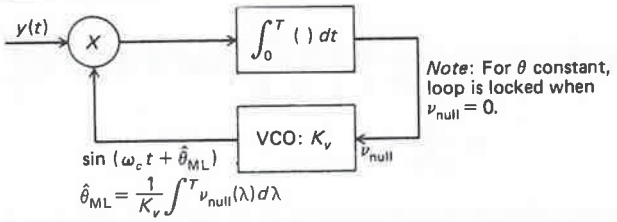
Therefore, (9.181) can be put in the form

$$-\sin\hat{\theta}_{ML}\int_0^T y(t)\cos\omega_c t\,dt - \cos\hat{\theta}_{ML}\int_0^T y(t)\sin\omega_c t\,dt = 0$$

or

$$\int_0^T y(t)\sin(\omega_c t + \hat{\theta}_{ML})\,dt = 0 \tag{9.183}$$

FIGURE 9.10 ML estimator for phase



This equation can be interpreted as the feedback structure shown in Figure 9.10. Except for the integrator replacing a loop filter, this is identical to the phase-locked loop discussed in Chapter 3.

A lower bound for the variance of $\hat{\theta}_{ML}$ is obtained from the Cramer-Rao inequality. Applying (9.164b), we have for the first differentiation, from (9.180),

$$\frac{\partial \ln f_{\mathbf{Z}|\theta}}{\partial \theta} = \sqrt{2T}\frac{A}{N_0}(-Z_1 \sin\theta - Z_2 \cos\theta) \tag{9.184}$$

and for the second,

$$\frac{\partial^2 \ln f_{\mathbf{Z}|\theta}}{\partial \theta^2} = \sqrt{2T}\frac{A}{N_0}(-Z_1 \cos\theta + Z_2 \sin\theta) \tag{9.185}$$

Substituting into (9.164b), we have

$$\text{var}\{\hat{\theta}_{ML}(Z)\} \geq \frac{1}{\sqrt{2T}}\frac{N_0}{A}(E\{Z_1\}\cos\theta - E\{Z_2\}\sin\theta)^{-1} \tag{9.186}$$

The expectations of Z_1 and Z_2 are

$$\begin{aligned} E\{Z_i\} &= \int_0^T E\{y(t)\}\phi_i(t)\,dt \\ &= \int_0^T \sqrt{\frac{T}{2}}A[\cos\theta\,\phi_1(t) - \sin\theta\,\phi_2(t)]\phi_i(t)\,dt \\ &= \begin{cases} \sqrt{\frac{T}{2}}A\cos\theta, & i = 1 \\ -\sqrt{\frac{T}{2}}A\sin\theta, & i = 2 \end{cases} \end{aligned} \tag{9.187}$$

where we used (9.175). Substitution of these results into (9.186) results in

$$\text{var}\,\{\hat{\theta}_{\text{ML}}(Z)\} \geq \frac{1}{\sqrt{2T}}\frac{N_0}{A}\left[\sqrt{\frac{T}{2}}A\,(\cos^2\theta + \sin^2\theta)\right]^{-1}$$
$$= \frac{N_0}{A^2T} \tag{9.188}$$

Noting that the average signal power is $P_s = \frac{1}{2}A^2$ and defining $B_L = (2T)^{-1}$ as the equivalent noise bandwidth* of the estimator structure, we may write (9.188) as

$$\text{var}\,\{\hat{\theta}_{\text{ML}}\} \geq \frac{N_0 B_L}{P_s} \tag{9.189}$$

which is identical to the result given without proof in Table 8.5. As a result of the nonlinearity of the estimator, we can obtain only a lower bound for the variance. However, the bound becomes better as the SNR increases. Furthermore, because ML estimators are asymptotically Gaussian, we can approximate the conditional pdf of $\hat{\theta}_{\text{ML}}$, $f_{\hat{\theta}_{\text{ML}}|\theta}(\alpha|\theta)$, as Gaussian with mean θ ($\hat{\theta}_{\text{ML}}$ is unbiased) and variance given by (9.188).

SUMMARY

1. Two general classes of optimization problems are signal detection and parameter estimation. Although both detection and estimation are often involved simultaneously in signal reception, from an analysis standpoint, it is easiest to consider them as separate problems.

2. Bayes detectors are designed to minimize the average cost of making a decision. They involve testing a likelihood ratio, which is the ratio of the *a posteriori* (posterior) probabilities of the observations, against a threshold, which depends on the *a priori* (prior) probabilities of the two possible hypotheses and costs of the various decision/hypothesis combinations. The performance of a Bayes detector is characterized by the average cost, or risk, of making a decision. More useful in many cases, however, are the probabilities of detection and false alarm P_D and P_F in terms of which the risk can be expressed, provided the *a priori* probabilities and costs are available. A plot of P_D versus P_F is referred to as the receiver operating characteristic (ROC).

* The equivalent noise bandwidth of an ideal integrator of integration duration T is $(2T)^{-1}$ Hz.

3. If the costs and prior probabilities are not available, a useful decision strategy is the Neyman-Pearson detector, which maximizes P_D while holding P_F below some tolerable level. This type of receiver also can be reduced to a likelihood ratio test in which the threshold is determined by the allowed false-alarm level.

4. It was shown that a minimum-probability-of-error detector (that is, the type of detector considered in Chapter 7) is really a Bayes detector with zero costs for making right decisions and equal costs for making either type of wrong decision. Such a receiver is also referred to as a maximum *a posteriori* (MAP) detector, since the decision rule amounts to choosing as the correct hypothesis the one corresponding to the largest *a posteriori* probability for a given observation.

5. The introduction of signal-space concepts allowed the MAP criterion to be expressed as a receiver structure that chooses as the transmitted signal the signal whose location in signal space is closest to the observed data point. Two examples considered were coherent detection of M-ary orthogonal signals and noncoherent detection of binary FSK in a Rayleigh fading channel.

6. For M-ary orthogonal signal detection, zero probability of error can be achieved as $M \to \infty$ provided the ratio of energy per bit to noise spectral density is greater than -1.6 dB. This perfect performance is achieved at the expense of infinite transmission bandwidth, however.

7. For the Rayleigh fading channel, the probability of error decreases only inversely with signal-to-noise ratio rather than exponentially, as for the nonfading case. A way to improve performance is by using diversity.

8. Bayes estimation involves the minimization of a cost function, as for signal detection. The squared-error cost function results in the *a posteriori* conditional mean of the parameter as the optimum estimate, and a square-well cost function with infinitely narrow well results in the maximum of the *a posteriori* pdf of the data, given the parameter, as the optimum estimate (MAP estimate). Because of its ease of implementation, the MAP estimate is often employed even though the conditional-mean estimate is more general, in that it minimizes any symmetrical, convex-upward cost function as long as the posterior pdf is symmetrical about a single peak.

9. A maximum-likelihood (ML) estimate of a parameter A is that value for the parameter, $\hat{A}$, which is most likely to have resulted in the observed data A and is the value of A corresponding to the absolute maximum of

the conditional pdf of Z given A. The ML and MAP estimates of a parameter are identical if the *a priori* pdf of A is uniform. Since the *a priori* pdf of A is not needed to obtain an ML estimate, this is a useful procedure for estimation of parameters whose prior statistics are unknown or for estimation of nonrandom parameters.

10. The Cramer-Rao inequality gives a lower bound for the variance of an ML estimate. In the limit, ML estimates have many useful asymptotic properties as the number of independent observations becomes large. In particular, they are asymptotically Gaussian, unbiased, and efficient (satisfy the Cramer-Rao inequality with equality).

FURTHER READING

Two, by now, classic textbooks on detection and estimation theory at the graduate level are Van Trees (1968) and Helstrom (1968). Both are excellent in their own way, Van Trees being somewhat wordier and containing more examples than Helstrom, which is closely written but nevertheless very readable. Helstrom introduces complex envelope notation at the first and uses it throughout to very effectively include in one volume what Van Trees takes two volumes to accomplish (Volumes 1 and 3; Volume 2 treats nonlinear modulation theory, which Helstrom omits). A concise treatment of detection theory and signal design is the text by Weber (1987), recently reprinted. Shanmugam and Breipohl (1988) and Mendel (1987) are recommended.

At about the same (or somewhat lower) level as Van Trees and Helstrom is the book by Wozencraft and Jacobs (1965), which was the first book in the United States to use the signal-space concepts exploited by Kotel'nikov (1959) in his doctoral dissertation in 1947 to treat digital signaling and optimal analog demodulation. Many other books treat special applications of detection and estimation theory; several were referred to in Chapters 7 and 8 in connection with digital data transmission.

PROBLEMS

Section 9.1

9.1 Consider the hypotheses

$$H_1: Z = N \qquad \text{and} \qquad H_2: Z = S + N$$

where S and N are independent random variables with the pdf's

$$f_S(x) = 2e^{-2x}u(x) \qquad \text{and} \qquad f_N(x) = 10e^{-10x}u(x)$$

(a) Show that

$$f_Z(z|H_1) = 10e^{-10z}u(z)$$

and

$$f_Z(z|H_2) = 2.5(e^{-2z} - e^{-10z})u(z)$$

(b) Find the likelihood ratio $\Lambda(Z)$.

(c) If $P(H_1) = \frac{1}{4}$, $P(H_2) = \frac{3}{4}$, $c_{12} = c_{21} = 5$, and $c_{11} = c_{22} = 0$, find the threshold for a Bayes test.

(d) Show that the likelihood ratio test for part (c) can be reduced to

$$Z \underset{H_1}{\overset{H_2}{\gtrless}} \gamma$$

Find the numerical value of γ for the Bayes test of part (c).

(e) Find the risk for the Bayes test of part (c).

(f) Find the threshold for a Neyman-Pearson test with P_F less than or equal to 10^{-4}. Find P_D for this threshold.

(g) Reducing the Neyman-Pearson test of part (f) to the form

$$Z \underset{H_1}{\overset{H_2}{\gtrless}} \gamma$$

find P_F and P_D for arbitrary γ. Plot the ROC.

9.2 Consider a two-hypothesis decision problem where

$$f_Z(z|H_1) = \frac{\exp(-\frac{1}{2}z^2)}{\sqrt{2\pi}} \quad \text{and} \quad f_Z(z|H_2) = \tfrac{1}{2}\exp(-|z|)$$

(a) Find the likelihood ratio $\Lambda(Z)$.

(b) Letting the threshold η be arbitrary, find the decision regions R_1 and R_2 illustrated in Figure 9.1. Note that both R_1 and R_2 cannot be connected regions for this problem; that is, one of them will involve a multiplicity of line segments.

Section 9.2

9.3 Show that ordinary three-dimensional vector space satisfies the properties listed in the subsection entitled "Structure of Signal Space" in Section 9.2, where $x(t)$ and $y(t)$ are replaced by vectors **A** and **B**.

9.4 Show that the scalar-product definitions given by Equations (9.40a) and (9.40b) satisfy the properties listed in the subsection entitled "Scalar Product" in Section 9.2.

9.5 Using the appropriate definition, calculate (x_1, x_2) for each of the following pairs of signals:

(a) $e^{-|t|}$, $2e^{-5t}u(t)$ (b) $e^{-(2+j3)t}u(t)$, $e^{-(3+j2)t}u(t)$
(c) $\cos 2\pi t$, $\sin^2 2\pi t$ (d) $\cos 2\pi t, 10u(t)$

9.6 Let $x_1(t)$ and $x_2(t)$ be two real-valued signals. Show that the square of the norm of the signal $x_1(t) + x_2(t)$ is the sum of the square of the norm of $x_1(t)$ and the square of the norm of $x_2(t)$ if and only if x_1 and x_2 are orthogonal; that is, $\|x_1 + x_2\|^2 = \|x_1\|^2 + \|x_2\|^2$ if and only if $(x_1, x_2) = 0$. Note the analogy to vectors in three-dimensional space: the Pythagorean theorem applies only to vectors that are orthogonal or perpendicular (zero dot product).

9.7 Evaluate $\|x_1\|$, $\|x_2\|$, $\|x_3\|$, (x_2, x_1), and (x_3, x_1) for the signals in Figure 9.11. Use these numbers to construct a vector diagram and graphically verify that $x_3 = x_1 + x_2$.

9.8 Verify Schwarz's inequality for

$$x_1(t) = \sum_{n=1}^{N} a_n\phi_n(t) \qquad \text{and} \qquad x_2(t) = \sum_{n=1}^{N} b_n\phi_n(t)$$

where the $\phi_n(t)$'s are orthonormal.

9.9 (a) Use the Gram-Schmidt procedure to find a set of orthonormal basis functions corresponding to the signals given in Figure 9.12.
(b) Express s_1, s_2, and s_3 in terms of the orthonormal basis set found in part (a).

FIGURE 9.11

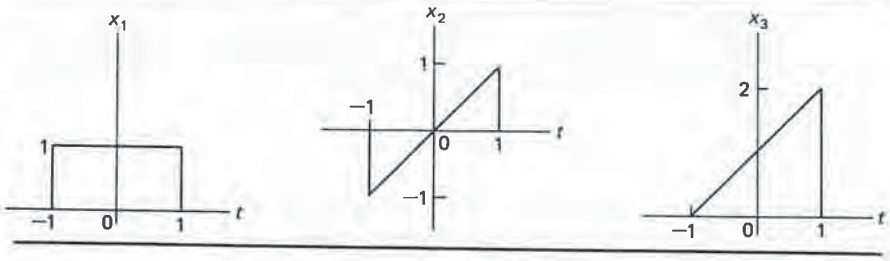
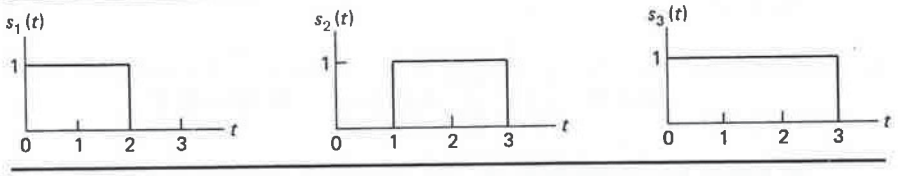


FIGURE 9.12



9.10 Consider the set of signals

$$s_i(t) = \begin{cases} \sqrt{2}\,A\cos\left(2\pi f_c t + \frac{1}{2}i\pi\right), & 0 \le f_c t \le N \\ 0, & \text{otherwise} \end{cases}$$

where N is an integer and $i = 1, 2, 3, 4$.

(a) Find an orthonormal basis set for the space spanned by this set of signals.

(b) Draw a set of coordinate axes, and plot the locations of $s_i(t)$, $i = 1, 2, 3, 4$, after expressing each one as a generalized Fourier series in terms of the basis set found in part (a).

Section 9.3

9.11 For M-ary PSK, the transmitted signal is of the form

$$s_i(t) = A\cos\left(2\pi f_c t + i2\pi/M\right), \quad i = 1, 2, \ldots, M, \text{ for } 0 \le t \le T_s$$

(a) Find a set of basis functions for this signaling scheme. What is the dimension of the signal space? Express $s_i(t)$ in terms of these basis functions and the signal energy, $E = A^2T_s/2$.

(b) Show the optimum partitioning of the observation space according to Equation (9.91).

(c) Sketch a block diagram of the optimum (minimum P_E) receiver.

(d) Write down an expression for the probability of error. Do not attempt to integrate it.

(e) By choosing appropriate half planes in the observation space, find upper and lower bounds for P_E derived in part (d). Sketch them versus SNR for $M = 4$, 8, and 16.

9.12 Consider Equation (9.120) for $M = 2$. Express P_E as a single Q-function. Show that the result is identical to binary, coherent FSK.

9.13 Consider *vertices-of-a-hypercube signaling,* for which the ith signal is of the form

$$s(t) = \sqrt{\frac{E_s}{n}} \sum_{k=1}^{n} \alpha_{ik}\phi_k(t), \qquad 0 \leq t \leq T$$

in which the coefficients α_{ik} are permuted through the values $+1$ and -1, E_s is the signal energy, and the ϕ_k's are orthonormal. Thus $M = 2^n$, where n is an integer. For $M = 8$, $n = 3$, the signal points in signal space lie on the vertices of a cube in three-space.

(a) Sketch the optimum partitioning of the observation space for $M = 8$.

(b) Show that the probability of symbol error is

$$P_E = 1 - P(C)$$

where

$$P(C) = \left[1 - Q\left(\sqrt{\frac{2E_s}{nN_0}}\right)\right]^n$$

(c) Plot P_E versus E_s/N_0 for $n = 1, 2, 3, 4$. Compare with Figure 9.7 for $n = 1$ and 2.

9.14 (a) Referring to the signal set defined by Equation (9.92), show that the minimum possible $\Delta f = \Delta\omega/2\pi$ such that $(s_i, s_j) = 0$ is $\Delta f = 1/(2T_s)$.

(b) Using the result of part (a), show that for a given time-bandwidth product WT_s the maximum number of signals for M-ary FSK signaling is given by $M = 2WT_s$, where W is the transmission bandwidth and T_s is the signal duration. Use null-to-null bandwidth.

(c) For vertices-of-a-hypercube signaling, described in Problem 9.13, show that the number of signals grows with WT_s as $M = 2^{2WT_s}$.

9.15 Go through the steps in deriving Equation (9.133).

9.16 Generalize the fading problem of binary noncoherent FSK signaling to the M-ary case. Let the ith hypothesis be of the form

$$H_i: y(t) = G_i \sqrt{\frac{2E_i}{T_s}} \cos(\omega_i t + \theta_i) + n(t)$$

$$i = 1, 2, \ldots, M; \ 0 \leq t \leq T_s$$

where G_i is Rayleigh, θ_i is uniform in $(0, 2\pi)$, E_i is the energy of the unperturbed ith signal of duration T_s, and $|\omega_i - \omega_j| \gg T_s^{-1}$, for $i \neq j$, so that the signals are orthogonal. Note that $G_i \cos \theta_i$ and $-G_i \sin \theta_i$ are Gaussian with mean zero; assume their variances to be σ^2.

(a) Find the likelihood ratio test and show that the optimum correlation receiver is identical to the one shown in Figure 9.8(a) with $2M$ correlators, $2M$ squarers, and M summers where the summer with the largest output is chosen as the best guess (minimum P_E) for the transmitted signal if all E_i's are equal. How is the receiver structure modified if the E_i's are not equal?

(b) Write down an expression for the probability of symbol error.

9.17 Investigate the use of diversity to improve the performance of binary FSK signaling over the flat fading Rayleigh channel. Assume that the signal energy E_s is divided equally among N subpaths, all of which fade independently. For equal SNRs in all paths, the optimum receiver is shown in Figure 9.13.

(a) Referring to Problem 4.45 of Chapter 4, show that Y_1 and Y_2 are chi-squared random variables under either hypothesis.

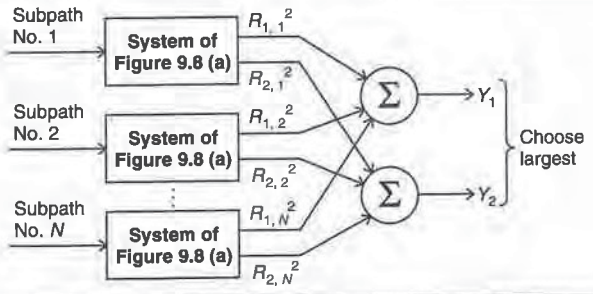
(b) Show that the probability of error is of the form

$$P_E = \alpha^N \sum_{j=0}^{N-1} \binom{N+j-1}{j} (1 - \alpha)^j$$

where

$$\alpha = \frac{\frac{1}{2}N_0}{\sigma^2 E' + N_0} = \frac{1}{2}\frac{1}{1 + \frac{1}{2}(2\sigma^2 E'/N_0)}, \qquad E' = \frac{E_s}{N}$$

FIGURE 9.13



(c) Plot P_E versus SNR $\triangleq 2\sigma^2 E_s/N_0$ for $N = 1, 2, 3, \ldots$, and show that an optimum value of N exists that minimizes P_E for a given SNR.

Section 9.4

9.18 Let an observed random variable Z depend on a parameter λ according to the conditional pdf

$$f_{Z|\Lambda}(z|\lambda) = \begin{cases} \lambda e^{-\lambda z}, & z \geq 0, \lambda > 0 \\ 0, & z < 0 \end{cases}$$

The *a priori* pdf of λ is

$$f_\Lambda(\lambda) = \begin{cases} \dfrac{\beta^m}{\Gamma(m)} e^{-\beta\lambda}\lambda^{m-1}, & \lambda \geq 0 \\ 0, & \lambda < 0 \end{cases}$$

where β and m are parameters and $\Gamma(m)$ is the gamma function. Assume that m is a positive integer.

(a) Find $E\{\lambda\}$ and var $\{\lambda\}$ before any observations are made; that is, find the mean and variance of λ using $f_\Lambda(\lambda)$.

(b) Assume one observation is made. Find $f_{\Lambda|Z}(\lambda|z)$ and hence the minimum mean-square error (conditional-mean) estimate of λ and the variance of the estimate. Compare with part (a). Comment on the similarity of $f_\Lambda(\lambda)$ and $f_{\Lambda|Z}(\lambda|z)$.

(c) Making use of part (b), find the posterior pdf of λ given two observations $f_{\Lambda|Z}(\lambda|z_1, z_2)$. Find the minimum mean-square error estimate of λ based on two observations and its variance. Compare with parts (a) and (b), and comment.

(d) Generalize the preceding to the case in which K observations are used to estimate λ.

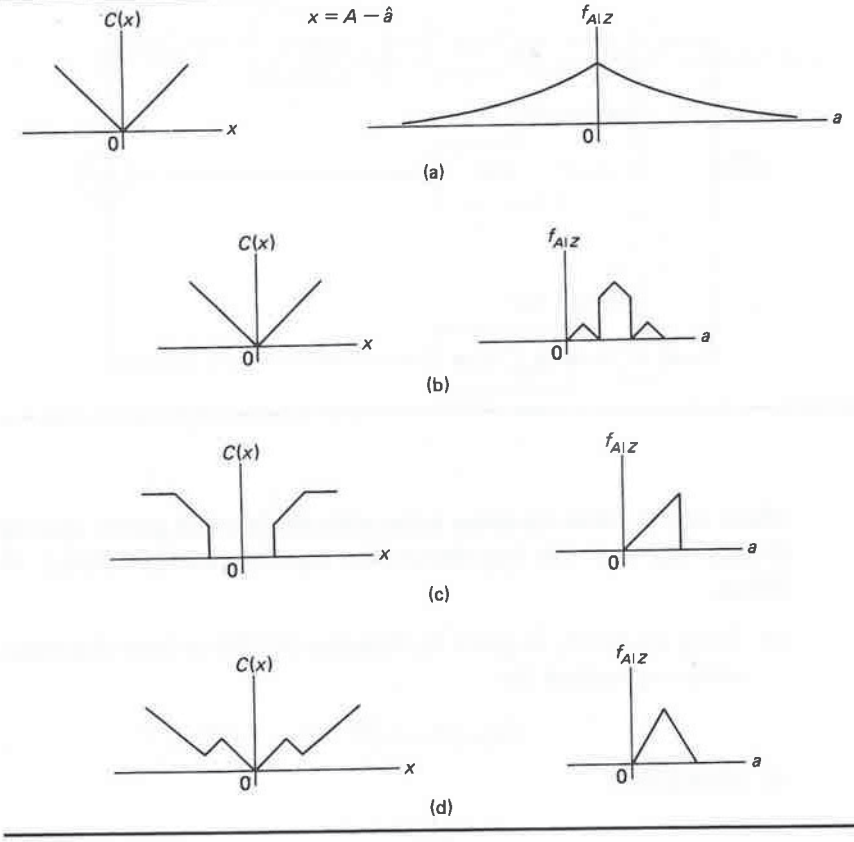
(e) Does the MAP estimate equal the minimum mean-square error estimate?

9.19 For which of the cost functions and posterior pdf's shown in Figure 9.14 will the conditional mean be the Bayes estimate? Tell why in each case.

9.20 Given K independent measurements $(Z_1, Z_2, \ldots, Z_K)$ of a noise voltage $Z(t)$ at the RF filter output of a receiver:

(a) If $Z(t)$ is Gaussian with mean zero and variance σ_n^2, what is the ML estimate of the variance of the noise?

FIGURE 9.14



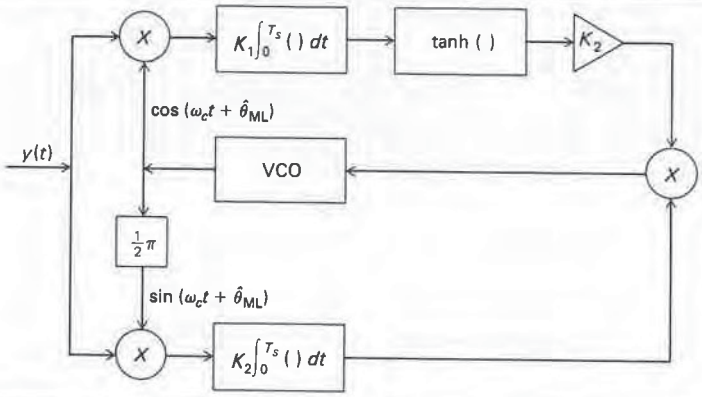
(b) Calculate the expected value and variance of this estimate as functions of the true variance.
(c) Is this an unbiased estimator?
(d) Give a sufficient statistic for estimating the variance of Z.

9.21 Generalize the estimation of a sample of a PAM signal, expressed by Equation (9.169), to the case where the sample value m_0 is a zero-mean Gaussian random variable with variance σ_m^2.

9.22 Consider the reception of a BPSK signal in noise with unknown phase, θ, to be estimated. The two hypotheses may be expressed as

$$H_1: y(t) = \cos(\omega_c t + \theta) + n(t), \qquad 0 \le t \le T_s$$
$$H_2: y(t) = -\cos(\omega_c t + \theta) + n(t), \qquad 0 \le t \le T_s$$

FIGURE 9.15



where $n(t)$ is white Gaussian noise with single-sided power spectral density N_0, and the hypotheses are equally probable [$P(H_1) = P(H_2)$].

(a) Using ϕ_1 and ϕ_2 as given by Equation (9.174) as basis functions, write expressions for

$$f_{\mathbf{Z}|\theta,H_i}(z_1, z_2|\theta, H_i), \qquad i = 1, 2$$

(b) Noting that

$$f_{\mathbf{Z}|\theta}(z_1, z_2|\theta) = \sum_{i=1}^{2} P(H_i) f_{\mathbf{Z}|\theta,H_i}(z_1, z_2|\theta, H_i)$$

show that the ML estimator can be realized as the structure shown in Figure 9.15 by employing Equation (9.147). Under what condition(s) is this structure approximated by a Costas loop? (See Chapter 3, Figure 3.57.)

(c) Apply the Cramer-Rao inequality to find an expression for var $\{\hat{\theta}_{ML}\}$. Compare with the result in Table 8.1.

9.23 Assume a biphase modulated signal in white Gaussian noise of the form

$$y(t) = \sqrt{2P}\sin(\omega_c t \pm \cos^{-1} m + \theta) + n(t), \qquad 0 \le t \le T_s$$

where the $\pm$ signs are equally probable and θ is to be estimated by a maximum-likelihood procedure. In the preceding equation,

T_s = signaling interval
P = average signal power
ω_c = carrier frequency (rad/s)
m = modulation constant
θ = RF phase (rad)

Let the double-sided power spectral density of $n(t)$ be $\frac{1}{2}N_0$.

(a) Show that the signal portion of $y(t)$ can be written as

$$S(t) = \sqrt{2P}\, m \sin(\omega_c t + \theta) \pm \sqrt{2P}\sqrt{1 - m^2}\cos(\omega_c t + \theta)$$

Write in terms of the orthonormal functions ϕ_1 and ϕ_2, given by Equation (9.174).

(b) Show that the likelihood function can be written as

$$L(\theta) = \frac{2m\sqrt{2P}}{N_0}\int_0^{T_s} y(t)\sin(\omega_c t + \theta)dt + \ln\cosh\left[\frac{2\sqrt{2P(1 - m^2)}}{N_0}\int_0^{T_s} y(t)\cos(\omega_c t + \theta)\,dt\right]$$

(c) Draw a block diagram of the ML estimator for θ and compare with the block diagram shown in Figure 9.15.



COMPUTER EXERCISES

9.1 (a) Write a program to plot the receiver operating characteristics for Example 9.2. Use the rational approximation given in Appendix C.6 to evaluate the Q-function.

(b) Repeat for Problem 9.1.

(a) Write a program to plot the curves asked for in Problem 9.13.

(b) Provide a justification for choosing either (8.49) or (8.51) to convert from symbol error probability to bit error probability for vertices-of-a-hypercube modulation. Use (8.52) to convert from symbol energy to bit energy, and plot curves of bit error probability versus E_b/N_0 for this modulation scheme.

(c) Use a solve routine to obtain the value of E_b/N_0, in decibels, required for a desired probability of bit error. Do this for several values of M and note that bit error probability for a given value of E_b/N_0 appears to be independent of M. Provide an explanation for this phenomenon.

9.3 Write a computer program to justify the conclusion drawn in Example 9.6 that a value of τW of 1.4 will ensure that none of the $\phi_k(t)$'s has more than 1/12 of its energy outside the frequency band $|f| < W$.

9.4 Write a computer program to make plots of σ_p^2 versus K, the number of observations, for fixed ratios of σ_A^2/σ_n^2 thus verifying the conclusions drawn at the end of Example 9.8.

9.5 Write a computer simulation of the PLL estimation problem. Do this by generating two independent Gaussian random variables to form Z_1 and Z_2 given by (9.177). Thus for a given θ form the left-hand side of (9.181). Call the first value θ_0. Estimate the next value of θ, call it θ_1, from the algorithm

$$\theta_1 = \theta_0 - \epsilon \tan^{-1}\left(\frac{Z_{2,0}}{Z_{1,0}}\right)$$

where $Z_{1,0}$ and $Z_{2,0}$ are the first values of Z_1 and Z_2 generated and ϵ is a parameter to be varied (choose the first value to be 0.01). Generate two new values of Z_1 and Z_2 (call them $Z_{1,1}$ and $Z_{2,1}$) and form the next estimate according to

$$\theta_2 = \theta_1 - \epsilon \tan^{-1}\left(\frac{Z_{2,1}}{Z_{1,1}}\right)$$

Continue in this fashion, generating several values of θ_i. Plot the θ_i's versus i, the sequence index, to determine if they seem to converge toward zero phase. Increase the value of ϵ by a factor of 10 and repeat. Can you relate the parameter ϵ to a phase-lock loop parameter (see Chapter 3)? This is an example of Monte Carlo simulation.

INFORMATION THEORY AND CODING 10

Information theory provides a different perspective for evaluating the performance of communication systems, and significant insight into the performance characteristics of communication systems can often be gained through the study of information theory. More explicitly, information theory provides a quantitative measure of the information contained in message signals and allows us to determine the capability of a system to transfer this information from source to destination. Coding, a major topic of information theory, will be examined in this chapter in some detail. Through the use of coding, unsystematic redundancy can be removed from message signals so that channels can be used with maximum efficiency. In addition, through the use of coding, systematic redundancy can be induced into the transmitted signal so that errors caused by nonperfect practical channels can be corrected.

Information theory also provides us with the performance characteristics of an *ideal*, or optimum, communication system. The performance of an ideal system provides a meaningful basis against which to compare the performance of the realizable systems studied in previous chapters. Performance characteristics of ideal systems illustrate the gain in performance that can be obtained by implementing more complicated transmission and detection schemes.

Motivation for the study of information theory is provided by *Shannon's coding theorem*, sometimes referred to as *Shannon's second theorem*, which can be stated as follows: If a source has an information rate less than the channel capacity, there exists a coding procedure such that the source output can be transmitted over the channel with an arbitrarily small probability of error. This is a truly surprising statement. We are being led to believe that transmission and reception can be accomplished with *negligible* error, even in the presence of noise. An understanding of this process called *coding*, and an understanding of its impact on the design and performance of communication systems, requires an understanding of several basic concepts of information theory.

10.1 BASIC CONCEPTS

Consider a hypothetical classroom situation occurring early in a course at the end of a class period. The professor makes one of the following statements to the class:

A. I shall see you next period.
B. My colleague will lecture next period.
C. Everyone gets an A in the course, and there will be no more class meetings.

What is the relative information conveyed to the students by each of these statements, assuming that there had been no previous discussion on the subject? Obviously, there is little information conveyed by statement (A), since the class would normally assume that their regular professor would lecture; that is, the probability, $P(A)$, of the regular professor lecturing is nearly unity. Intuitively, we know that statement (B) contains more information, and the probability of a colleague lecturing $P(B)$ is relatively low. Statement (C) contains a vast amount of information for the entire class, and most would agree that such a statement has a very low probability of occurrence in a typical classroom situation. It appears that the lower the probability of a statement, the greater is the information conveyed by that statement. Stated another way, the students' surprise on hearing a statement seems to be a good measure of the information contained in that statement.

We next define information mathematically in such a way that the definition is consistent with the preceding intuitive example.

Information

Let x_j be an event that occurs with probability $p(x_j)$. If we are told that event x_j has occurred, we say that we have received

$$I(x_j) = \log_a \frac{1}{p(x_j)} = -\log_a p(x_j) \tag{10.1}$$

units of information. This definition is consistent with the previous example, since $I(x_j)$ increases as $p(x_j)$ decreases.

The base of the logarithm in (10.1) is quite arbitrary and determines the units by which we measure information. R. V. Hartley,* who first suggested the logarithmic measure of information in 1928, used logarithms to the base 10, and the measure of information was the hartley. Today it is standard to use logarithms to the base 2, and the unit of information is the binary unit,

* Hartley (1928).

or bit. Logarithms to the base e are sometimes utilized, and the corresponding unit is the nat, which stands for natural unit.

There are several reasons for us to be consistent in using the base 2 logarithm to measure information. The simplest random experiment that one can imagine is an experiment with two equally likely outcomes, such as the flipping of an unbiased coin. Knowledge of each outcome has associated with it one bit of information. Also, since the digital computer is a binary machine, each logical 0 and each logical 1 has associated with it one bit of information, assuming that each of these logical states are equally likely.

▼ **EXAMPLE 10.1** Consider a random experiment with 16 equally likely outcomes. The information associated with each outcome is

$$I(x_j) = -\log_2 \tfrac{1}{16} = \log_2 16 = 4 \text{ bits} \tag{10.2}$$

where j ranges from 1 to 16. The information is greater than one bit, since the probability of each outcome is much less than one-half. ▲

Entropy

In general, the *average information* associated with the outcome of an experiment is of interest rather than the information associated with each particular event. The average information associated with a discrete random variable X is defined as the entropy $H(X)$. Thus

$$H(X) = E\{I(x_j)\} = -\sum_{j=1}^{n} p(x_j) \log_2 p(x_j) \tag{10.3}$$

where n is the total number of possible outcomes. Entropy can be regarded as average uncertainty and therefore should be maximum when each outcome is equally likely.

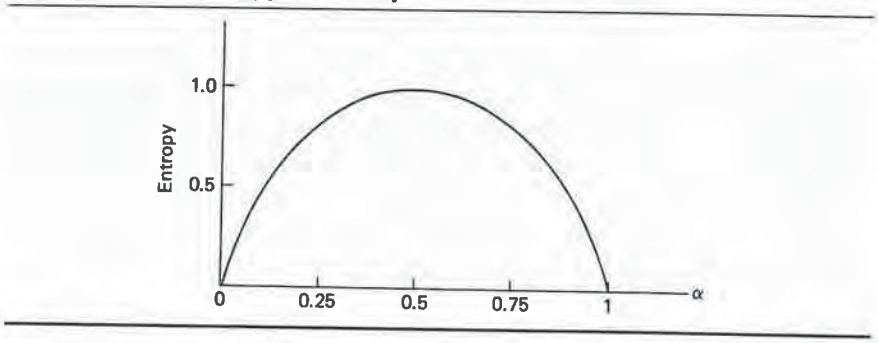
▼ **EXAMPLE 10.2** For a binary source, $p(1) = \alpha$ and $p(0) = 1 - \alpha = \beta$. Derive the entropy of the source as a function of α, and sketch $H(\alpha)$ as α varies from zero to 1.

SOLUTION From (10.3),

$$H(\alpha) = -\alpha \log_2 \alpha - (1 - \alpha) \log_2 (1 - \alpha) \tag{10.4}$$

This is sketched in Figure 10.1. We should note the maximum. If $\alpha = \frac{1}{2}$, each symbol is equally likely, and our uncertainty is a maximum. If $\alpha \neq \frac{1}{2}$,

FIGURE 10.1 Entropy of a binary source



one symbol is more likely to occur than the other, and we are less uncertain as to which symbol appears on the source output. If α or β is equal to zero, our uncertainty is zero, since we know exactly which symbol will occur.

From Example 10.2 we conclude, at least intuitively, that the entropy function has a maximum, and the maximum occurs when all probabilities are equal. This fact is of sufficient importance to warrant a more complete derivation.

Assume that a chance experiment has n possible outcomes and that p_n is a dependent variable depending on the other probabilities. Thus

$$p_n = 1 - (p_1 + p_2 + \cdots + p_k + \cdots + p_{n-1}) \tag{10.5}$$

where p_j is concise notation for $p(x_j)$. The entropy associated with the chance experiment is

$$H = -\sum_{i=1}^{n} p_i \log_2 p_i \tag{10.6}$$

In order to find the maximum value of entropy, the entropy is differentiated with respect to p_k, holding all probabilities constant except p_k and p_n. This gives a relationship between p_k and p_n that yields the maximum value of H. Since all derivatives are zero except the ones involving p_k and p_n,

$$\frac{dH}{dp_k} = \frac{d}{dp_k}(-p_k \log_2 p_k - p_n \log_2 p_n) \tag{10.7}$$

by using (10.5) and since

$$\frac{d}{dx} \log_a u = \frac{1}{u} \log_a e \frac{du}{dx} \tag{10.8}$$

we obtain

$$\frac{dH}{dp_k} = -p_k \frac{1}{p_k} \log_2 e - \log_2 p_k + p_n \frac{1}{p_n} \log_2 e + \log_2 p_n \qquad (10.9)$$

or

$$\frac{dH}{dp_k} = \log_2 \frac{p_n}{p_k} \qquad (10.10)$$

which is zero if $p_k = p_n$. Since p_k was arbitrarily chosen,

$$p_1 = p_2 = \cdots = p_n = \frac{1}{n} \qquad (10.11)$$

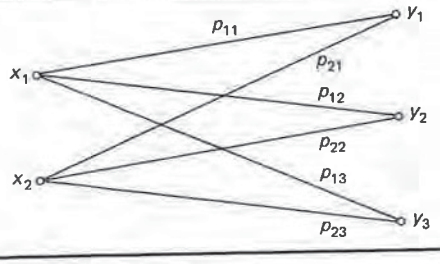
To show that the preceding condition yields a maximum and not a minimum, note that when $p_1 = 1$ and all other probabilities are zero, entropy is zero. From (10.6), the case where all probabilities are equal yields $H = \log_2 n$.

Channel Representations

Throughout most of this chapter we will assume the communications channel to be *memoryless*. For such channels, the channel output at a given time is a function of the channel input *at that time* and is not a function of previous channel inputs. Memoryless discrete channels are completely specified by the set of conditional probabilities that relate the probability of each output state to the input probabilities. An example illustrates the technique. A diagram of a channel with two inputs and three outputs is illustrated in Figure 10.2. Each possible input-to-output path is indicated along with a conditional probability p_{ij}, which is concise notation for $p(y_j \mid x_i)$. Thus p_{ij} is the conditional probability of obtaining output y_j given that the input is x_i and is called a *channel transition probability*.

We can see from Figure 10.2 that the channel is completely specified by

FIGURE 10.2 Channel diagram



the complete set of transition probabilities. Accordingly, the channel is often specified by the matrix of transition probabilities $[P(Y|X)]$, where, for the channel of Figure 10.2,

$$[P(Y|X)] = \begin{bmatrix} p(y_1|x_1) & p(y_2|x_1) & p(y_3|x_1) \\ p(y_1|x_2) & p(y_2|x_2) & p(y_3|x_2) \end{bmatrix} \tag{10.12}$$

Since each input to the channel results in some output, each new row of the channel matrix must sum to unity.

The channel matrix is useful in deriving the output probabilities given the input probabilities. For example, if the input probabilites $P(X)$ are represented by the row matrix

$$[P(X)] = [p(x_1) \quad p(x_2)] \tag{10.13}$$

then

$$[P(Y)] = [p(y_1) \quad p(y_2) \quad p(y_3)] \tag{10.14}$$

which is computed by

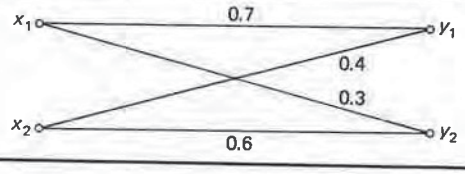
$$[P(Y)] = [P(X)][P(Y|X)] \tag{10.15}$$

If $[P(X)]$ is written as a diagonal matrix, (10.15) yields a matrix $[P(X, Y)]$. Each element in the matrix has the form $p(x_i)p(y_j|x_i)$ or $p(x_i, y_j)$. This matrix is known as the *joint probability matrix*, and the term $p(x_i, y_j)$ is the joint probability of transmitting x_i *and* receiving y_j.

EXAMPLE 10.3 Consider the binary input-output channel shown in Figure 10.3. The matrix of transition probabilities is

$$[P(Y|X)] = \begin{bmatrix} 0.7 & 0.3 \\ 0.4 & 0.6 \end{bmatrix} \tag{10.16}$$

FIGURE 10.3 Binary channel



If the input probabilities are $P(x_1) = 0.5$ and $P(x_2) = 0.5$, the output probabilities are

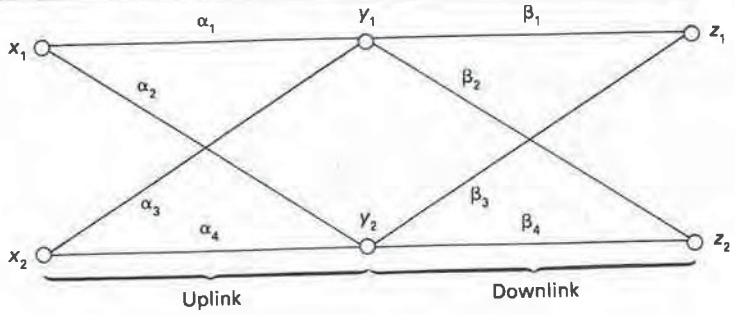
$$[P(Y)] = [0.5 \quad 0.5] \begin{bmatrix} 0.7 & 0.3 \\ 0.4 & 0.6 \end{bmatrix} = [0.55 \quad 0.45] \tag{10.17}$$

and the joint probability matrix is

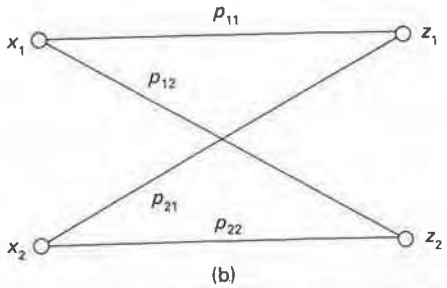
$$[P(X, Y)] = \begin{bmatrix} 0.5 & 0 \\ 0 & 0.5 \end{bmatrix} \begin{bmatrix} 0.7 & 0.3 \\ 0.4 & 0.6 \end{bmatrix} = \begin{bmatrix} 0.35 & 0.15 \\ 0.2 & 0.3 \end{bmatrix} \tag{10.18}$$

As first seen in Chapter 8, a binary satellite communication system can often be represented by the cascade combination of two binary channels. This is illustrated in Figure 10.4(a), in which the first binary channel represents the uplink and the second binary channel represents the downlink. These channels can be combined as shown in Figure 10.4(b).

FIGURE 10.4 Two-hop satellite system. (a) Binary satellite channel. (b) Composite satellite channel.



(a)



(b)

By determining all possible paths from x_i to z_j, it is clear that the following probabilities define the overall channel illustrated in Figure 10.4(b):

$$p_{11} = \alpha_1\beta_1 + \alpha_2\beta_3 \tag{10.19a}$$

$$p_{12} = \alpha_1\beta_2 + \alpha_2\beta_4 \tag{10.19b}$$

$$p_{21} = \alpha_3\beta_1 + \alpha_4\beta_3 \tag{10.19c}$$

$$p_{22} = \alpha_3\beta_2 + \alpha_4\beta_4 \tag{10.19d}$$

Thus the overall channel matrix

$$[P(Z|X)] = \begin{bmatrix} p_{11} & p_{12} \\ p_{21} & p_{22} \end{bmatrix} \tag{10.20}$$

can be represented by the matrix multiplication

$$[P(Z|X)] = \begin{bmatrix} \alpha_1 & \alpha_2 \\ \alpha_3 & \alpha_4 \end{bmatrix} \begin{bmatrix} \beta_1 & \beta_2 \\ \beta_3 & \beta_4 \end{bmatrix} \tag{10.21}$$

The right-hand side of the preceding expression is simply the uplink channel matrix multiplied by the downlink channel matrix.

Joint and Conditional Entropy

If we use the input probabilities $p(x_i)$, the output probabilities $p(y_j)$, the transition probabilities $p(y_j|x_i)$, and the joint probabilities $p(x_i, y_j)$, we can define several different entropy functions for a channel with n inputs and m outputs. These are

$$H(X) = -\sum_{i=1}^{n} p(x_i) \log_2 p(x_i) \tag{10.22}$$

$$H(Y) = -\sum_{j=1}^{m} p(y_j) \log_2 p(y_j) \tag{10.23}$$

$$H(Y|X) = -\sum_{i=1}^{n}\sum_{j=1}^{m} p(x_i, y_j) \log_2 p(y_j|x_i) \tag{10.24}$$

and

$$H(X, Y) = -\sum_{i=1}^{n}\sum_{j=1}^{m} p(x_i, y_j) \log_2 p(x_i, y_j) \tag{10.25}$$

Another useful entropy, $H(X|Y)$, which is sometimes called *equivocation*, is defined as

$$H(X|Y) = -\sum_{i=1}^{n}\sum_{j=1}^{m} p(x_i, y_j)\log_2 p(x_i|y_j) \tag{10.26}$$

These entropies are easily interpreted. $H(X)$ is the average uncertainty of the source, whereas $H(Y)$ is the average uncertainty of the received symbol. Similarly, $H(X|Y)$ is a measure of our average uncertainty of the transmitted symbol after we have received a symbol. The function $H(Y|X)$ is the average uncertainty of the received symbol given that X was transmitted. The joint entropy $H(X, Y)$ is the average uncertainty of the communication system as a whole.

Two important and useful relationships, which can be obtained directly from the definitions of the various entropies, are

$$H(X, Y) = H(X|Y) + H(Y) \tag{10.27}$$

and

$$H(X, Y) = H(Y|X) + H(X) \tag{10.28}$$

These are developed in Problem 10.12.

Channel Capacity

Consider for a moment an observer at the channel output. The observer's average uncertainty concerning the channel input will have some value before the reception of an output, and this average uncertainty of the input will usually decrease when the output is received. In other words, $H(X|Y) \leq H(X)$. The decrease in the observer's average uncertainty of the transmitted signal when the output is received is a measure of the average transmitted information. This is defined as *transinformation*, or *mutual information* $I(X; Y)$. Thus

$$I(X; Y) = H(X) - H(X|Y) \tag{10.29}$$

It follows from (10.27) and (10.28) that we can also write (10.29) as

$$I(X; Y) = H(Y) - H(Y|X) \tag{10.30}$$

It should be observed that transinformation is a function of the source probabilities as well as of the channel transition probabilities.

It is easy to show mathematically that

$$H(X) \geq H(X|Y) \tag{10.31}$$

by showing that

$$H(X|Y) - H(X) = -I(X; Y) \leq 0 \tag{10.32}$$

Substitution of (10.26) for $H(X|Y)$ and (10.22) for $H(X)$ allows us to write $-I(X; Y)$ as

$$-I(X; Y) = \sum_{i=1}^{n} \sum_{j=1}^{m} p(x_i, y_j) \log_2 \frac{p(x_i)}{p(x_i|y_j)} \tag{10.33}$$

Since

$$\log_2 x = \frac{\ln x}{\ln 2} \tag{10.34}$$

and

$$\frac{p(x_j)}{p(x_i|y_j)} = \frac{p(x_i)p(y_j)}{p(x_i, y_j)} \tag{10.35}$$

we can write $-I(X; Y)$ as

$$-I(X; Y) = \frac{1}{\ln 2} \sum_{i=1}^{n} \sum_{j=1}^{m} p(x_i, y_j) \ln \frac{p(x_i)p(y_j)}{p(x_j, y_j)} \tag{10.36}$$

In order to carry the derivation further, we need the often-used inequality

$$\ln (x) \leq x - 1 \tag{10.37}$$

which we can easily prove by considering the function

$$f(x) = \ln (x) - (x - 1) \tag{10.38}$$

The derivative of $f(x)$

$$\frac{df}{dx} = \frac{1}{x} - 1 \tag{10.39}$$

is equal to zero at $x = 1$. It follows that $f(1) = 0$ is the maximum value of $f(x)$, since we can make $f(x)$ as small as we wish by choosing x sufficiently large.

Using the inequality (10.37) in (10.36) results in

$$-I(X; Y) \leq \frac{1}{\ln 2} \sum_{i=1}^{n} \sum_{j=1}^{m} p(x_i, y_j) \left[\frac{p(x_i)p(y_j)}{p(x_i, y_j)} - 1 \right] \tag{10.40}$$

which yields

$$-I(X;\,Y) \leq \frac{1}{\ln 2}\left[\sum_{i=1}^{n}\sum_{j=1}^{m} p(x_i)p(y_j) - \sum_{i=1}^{n}\sum_{j=1}^{m} p(x_i,\,y_j)\right] \tag{10.41}$$

Since both the double sums equal 1, we have the desired result

$$-I(X;\,Y) \leq 0 \tag{10.42}$$

Thus we have shown that mutual information is always nonnegative and, consequently, that $H(X) \geq H(X\,|\,Y)$.

The *channel capacity* C is defined as the maximum value of transinformation, which is the maximum average information *per symbol* that can be transmitted through the channel. Thus

$$C = \max\,[I(X;\,Y)] \tag{10.43}$$

The maximization is with respect to the source probabilities, since the transition probabilities are fixed by the channel. However, the channel capacity is a function of only the channel transition probabilities, since the maximization process eliminates the dependence on the source probabilities. The following examples illustrate the method.

▼ **EXAMPLE 10.4** Find the channel capacity of the noiseless discrete channel illustrated in Figure 10.5.

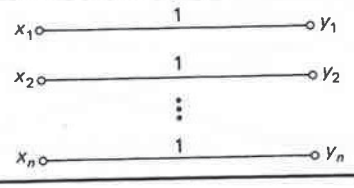
SOLUTION We start with

$$I(X;\,Y) = H(X) - H(X\,|\,Y)$$

and write

$$H(X\,|\,Y) = -\sum_{i=1}^{n}\sum_{j=1}^{n} p(x_i,\,y_j)\log_2 p(x_i\,|\,y_j) \tag{10.44}$$

FIGURE 10.5 Noiseless channel



For the noiseless channel, all $p(x_i, y_j)$ and $p(x_i|y_j)$ are zero unless $i = j$. For $i = j$, $p(x_i|y_j)$ is unity. Thus $H(X|Y)$ is zero for the noiseless channel, and

$$I(X; Y) = H(X) \tag{10.45}$$

We have seen that the entropy of a source is maximum if all source symbols are equally likely. Thus

$$C = \sum_{i=1}^{n} \frac{1}{n} \log_2 n = \log_2 n \tag{10.46}$$

EXAMPLE 10.5 Find the channel capacity of the *binary symmetric channel* illustrated in Figure 10.6.

SOLUTION This problem has considerable practical importance in the area of binary digital communications. We will determine the capacity by maximizing

$$I(X; Y) = H(Y) - H(Y|X)$$

where

$$H(Y|X) = -\sum_{i=1}^{2} \sum_{j=1}^{2} p(x_i, y_j) \log_2 p(y_j|x_i) \tag{10.47}$$

Using the probabilities defined in Figure 10.6, we obtain

$$H(Y|X) = -\alpha p \log_2 p - (1 - \alpha)p \log_2 p - \alpha q \log_2 q - (1 - \alpha)q \log_2 q \tag{10.48}$$

or

$$H(Y|X) = -p \log_2 p - q \log_2 q \tag{10.49}$$

Thus

$$I(X; Y) = H(Y) + p \log_2 p + q \log_2 q \tag{10.50}$$

FIGURE 10.6 Binary symmetrical channel

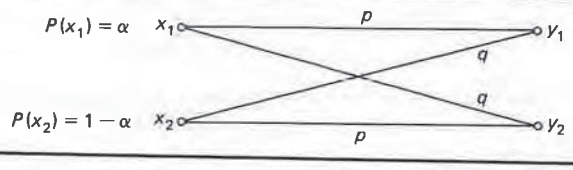
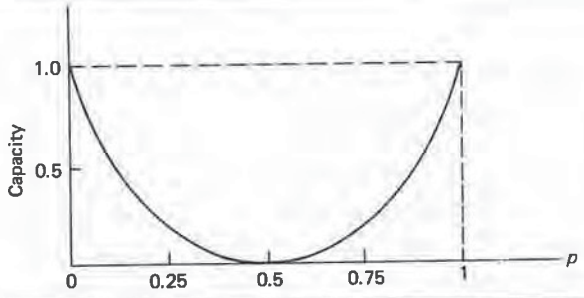


FIGURE 10.7 Capacity of a binary symmetric channel



which is maximum when $H(Y)$ is maximum. Since the system output is binary, $H(Y)$ is maximum when each output has a probability of $\frac{1}{2}$ and is achieved for *equally likely inputs*. For this case, $H(Y)$ is unity, and the channel capacity is

$$C = 1 + p \log_2 p + q \log_2 q = 1 - H(p) \tag{10.51}$$

▲ where $H(p)$ is as defined in (10.4).

The capacity of a binary symmetric channel is sketched in Figure 10.7. As expected, if $p = 0$ or 1, the channel output is completely determined by the channel input, and the capacity is 1 bit per symbol. If p is equal to $\frac{1}{2}$, an input symbol yields either output with equal probability, and the capacity is zero.

It is worth noting that the capacity of the channel illustrated in Figure 10.5 is most easily found by starting with (10.29), while the capacity of the channel illustrated in Figure 10.6 is most easily found starting with (10.30). Choosing the appropriate expression for $I(X; Y)$ can often save considerable effort. It sometimes takes insight and careful study of a problem to choose the expression for $I(X; Y)$ that yields the capacity with minimum computational effort.

The error probability P_E of a binary symmetric channel is easily computed. From

$$P_E = \sum_{i=1}^{2} p(e \mid x_i)p(x_i) \tag{10.52}$$

where $p(e \mid x_i)$ is the error probability given input x_i, we have

$$P_E = qp(x_1) + qp(x_2) \tag{10.53}$$

Thus

$$P_E = q \tag{10.54}$$

which states that the *unconditional error probability* P_E is equal to the conditional error probability $p(y_j|x_i)$, $i \neq j$.

In Chapter 7 we showed that P_E is a decreasing function of the energy of the received symbols. Since the symbol energy is the received power multiplied by the symbol period, it follows that *if the transmitter power is fixed, the error probability can be reduced by decreasing the source rate.* This can be accomplished by removing the redundancy at the source through a process called *source encoding.*

EXAMPLE 10.6 In Chapter 7 we showed that for binary coherent FSK systems, the probability of symbol error is the same for each transmitted symbol. Thus a binary symmetrical channel model is a suitable model for FSK transmission. Assume that the transmitter power is 1000 W and that the attenuation in the channel from transmitter to detector input is 30 dB. Also assume that the source rate r is 10,000 symbols per second and that the noise power spectral density N_0 is 2×10^{-5} W/Hz. Determine the channel matrix.

SOLUTION Since the attenuation is 30 dB, the signal power P_R at the input to the detector is

$$P_R = (1000)(10^{-3}) = 1 \text{ W} \tag{10.55}$$

This corresponds to a received energy per symbol of

$$E_S = P_R T = \frac{1}{10{,}000} = 10^{-4} \text{ J} \tag{10.56}$$

From Chapter 7, Equation (7.83), the error probability for an FSK receiver is

$$P_E = \text{Q}\left(\sqrt{\frac{E_s}{\text{N}_0}}\right) \tag{10.57}$$

which, with the given values, is $P_E = 0.0127$. Thus the channel matrix is

$$[P(Y|X)] = \begin{bmatrix} 0.9873 & 0.0127 \\ 0.0127 & 0.9873 \end{bmatrix} \tag{10.58}$$

It is interesting to compute the change in the channel matrix resulting from moderate reduction in source symbol rate with all other parameters held constant. If the source symbol rate is reduced 25% to 7500 symbols per second, the received energy per symbol is

$$E_s = \frac{1}{7500} = 1.333 \times 10^{-4} \text{ J} \tag{10.59}$$

With the other given parameters, the symbol error probability becomes $P_E = 0.0049$, which yields the channel matrix

$$[P(Y|X)] = \begin{bmatrix} 0.9951 & 0.0049 \\ 0.0049 & 0.9951 \end{bmatrix} \tag{10.60}$$

Thus the 25% reduction in source symbol rate results in an improvement of the system symbol error probability by a factor of almost 3. ▲

In Section 10.2 we will investigate a technique that sometimes allows the source symbol rate to be reduced without reducing the source information rate.

10.2 SOURCE ENCODING

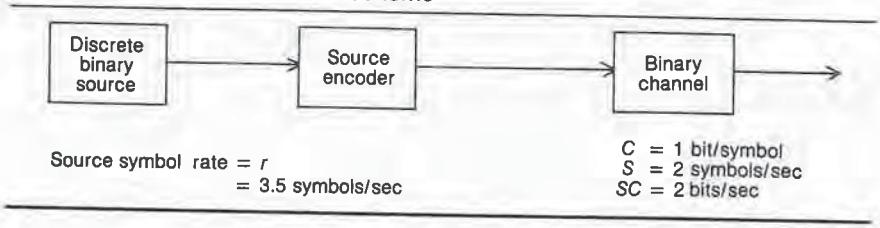
We determined in the preceding section that the information from a source that produced different symbols according to some probability scheme could be described by the entropy $H(X)$. Since entropy has units of bits per symbol, we also must know the symbol rate in order to specify the source information rate in bits per second. In other words, the source information rate R_s is given by

$$R_s = rH(X) \text{ bits/sec} \tag{10.61}$$

where $H(X)$ is the source entropy in bits per symbol and r is the symbol rate in symbols per second.

Let us assume that this source is the input to a channel with capacity C bits per symbol or SC bits per second, where S is the available symbol rate for the channel. An important theorem of information theory, the *noiseless coding theorem*, sometimes referred to as *Shannon's first theorem*, is stated: *Given a channel and a source that generates information at a rate less than the channel capacity, it is possible to encode the source output in such a manner that it can be transmitted through the channel.* A proof of this theorem is beyond the scope of this introductory treatment of information theory and can be found in

FIGURE 10.8 Transmission scheme



any of the standard information theory textbooks.* However, we demonstrate the theorem by a simple example.

An Example of Source Encoding

Let us consider a discrete binary source that has two possible outputs A and B that have probabilities 0.9 and 0.1, respectively. Assume also that the source rate r is 3.5 symbols per second. The source output is connected to a binary channel that can transmit a binary 0 or 1 at a rate of 2 symbols per second with negligible error, as shown in Figure 10.8. Thus, from Example 10.5 with $p = 1$, the channel capacity is 1 bit per symbol, which, in this case, is an information rate of 2 bits per second.

It is clear that the source *symbol* rate is greater than the channel capacity, so the source symbols cannot be placed directly into the channel. However, the source entropy is

$$H(X) = -0.1 \log_2 0.1 - 0.9 \log_2 0.9 = 0.469 \text{ bits/symbol} \quad (10.62)$$

which corresponds to a source *information* rate of

$$rH(X) = 3.5(0.469) = 1.642 \text{ bits/s} \quad (10.63)$$

Thus, the *information* rate is less than the channel capacity, so transmission is possible.

Transmission is accomplished by the process called *source encoding*, whereby codewords are assigned to n-symbol groups of source symbols. The shortest codeword is assigned to the most probable group of source symbols, and the longest codeword is assigned to the least probable group of source symbols. Thus source encoding decreases the average symbol rate, which allows the source to be matched to the channel. The n-symbol groups of source symbols are known as the nth-order extension of the original source.

* See, for example, Gallagher (1968).

TABLE 10.1 First-Order Extension

Source Symbol	$P(\ )$	Codeword	$[P(\ )] \cdot$ [Number of Code Symbols]
A	0.9	0	0.9
B	0.1	1	0.1
			$\bar{L} = 1.0$

Table 10.1 illustrates the first-order extension of the original source. Clearly, the symbol rate of the encoder is equal to the symbol rate of the source. Thus the symbol rate at the channel input is still larger than the channel can accommodate.

The second-order extension of the original source is formed by taking the source symbols two at a time, as illustrated in Table 10.2. The average word length $\bar{L}$ for this case is

$$\bar{L} = \sum_{i=1}^{2^n} p(x_i) l_i = 1.29 \tag{10.64}$$

where $p(x_i)$ is the probability of the ith symbol of the extended source and l_i is the length of the codeword corresponding to the ith symbol. Since the source is binary, there are 2^n symbols in the extended source output, each of length n. Thus, for the second-order extension,

$$\frac{\bar{L}}{n} = \frac{1.29}{2} = 0.645 \text{ code symbols/source symbol} \tag{10.65}$$

and the symbol rate at the encoder output is

$$r\frac{\bar{L}}{n} = 3.5(0.645) = 2.258 \text{ code symbols/second} \tag{10.66}$$

TABLE 10.2 Second-Order Extension

Source Symbol	$P(\ )$	Codeword	$[P(\ )] \cdot$ [Number of Code Symbols]
AA	0.81	0	0.81
AB	0.09	1 0	0.18
BA	0.09	1 1 0	0.27
BB	0.01	1 1 1	0.03
			$\bar{L} = 1.29$

which is still greater than the 2 symbols per second that the channel can accept. It is clear that the symbol rate has been reduced, and this provides motivation to try again.

Table 10.3 shows the third-order extension. For this case, the source symbols are grouped three at a time. The average word length $\bar{L}$ is 1.598, and

$$\frac{\bar{L}}{n} = \frac{1.598}{3} = 0.533 \text{ code symbols/source symbol} \tag{10.67}$$

The symbol rate at the encoder output is

$$r\frac{\bar{L}}{n} = 3.5(0.533) = 1.864 \text{ code symbols/second} \tag{10.68}$$

This rate can be accepted by the channel.

It is worth noting in passing that if the source symbols appear at a constant rate, the code symbols at the encoder output do not appear at a constant rate. As is apparent in Table 10.3, the source output *AAA* results in a single symbol at the encoder output, whereas the source output *BBB* results in five symbols at the encoder output. Thus symbol buffering must be provided at the encoder output if the symbol rate into the channel is to be constant.

Figure 10.9 shows the behavior of $\bar{L}/n$ as a function of n. One can see that $\bar{L}/n$ always exceeds the source entropy and converges to the source entropy for large N. This is a fundamental result of information theory.

To illustrate the method used to select the codewords in this example, let us look at the general problem of source encoding.

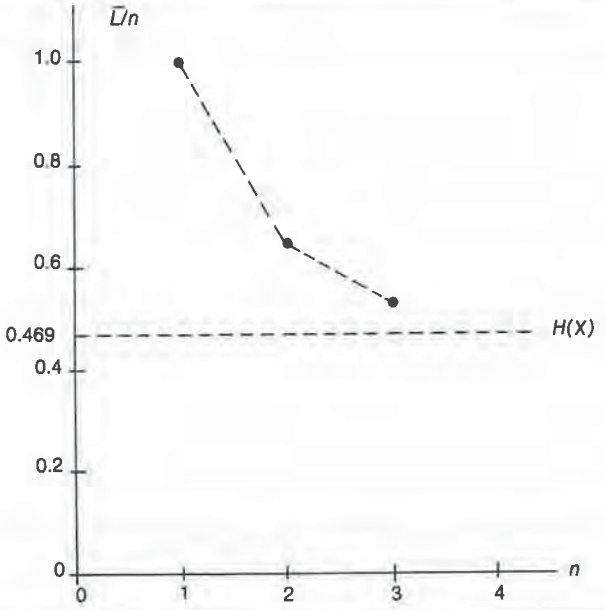
Several Definitions

Before we discuss in detail the method of deriving codewords, we pause to make a few definitions that will clarify our work.

TABLE 10.3 Third-Order Extension

Source Symbol	$P(\ )$	Codeword	$[P(\ )] \cdot$ [Number of Code Symbols]
AAA	0.729	0	0.729
AAB	0.081	1 0 0	0.243
ABA	0.081	1 0 1	0.243
BAA	0.081	1 1 0	0.243
ABB	0.009	1 1 1 0 0	0.045
BAB	0.009	1 1 1 0 1	0.045
BBA	0.009	1 1 1 1 0	0.045
BBB	0.001	1 1 1 1 1	0.005
			$\bar{L} = 1.598$

FIGURE 10.9 Behavior of $\bar{L}/n$



Each codeword is constructed from an *alphabet* that is a collection of symbols used for communication through a channel. For example, a binary codeword is constructed from a two-symbol alphabet, wherein the two symbols are usually taken as 0 and 1. The *word length* of a codeword is the number of symbols in the codeword.

There are several major subdivisions of codes. For example, a code can be either *block* or *nonblock*. A block code is one in which each block of source symbols is encoded into a fixed-length sequence of code symbols. A *uniquely decipherable* code is a block code in which the codewords may be deciphered without using spaces. These codes can be further classified as *instantaneous* or *noninstantaneous,* according to whether or not it is possible to decode each word in sequence without reference to succeeding code symbols. Alternatively, noninstantaneous codes require reference to succeeding code symbols, as illustrated in Figure 10.10. It should always be remembered that a noninstantaneous code can be uniquely decipherable.

A useful measure of goodness of a source code is the *efficiency,* which is defined as the ratio of the minimum average word length of the codewords $\bar{L}_{\min}$ to the average word length of the codeword $\bar{L}$. Thus

$$\text{Efficiency} = \frac{\bar{L}_{\min}}{\bar{L}} = \frac{\bar{L}_{\min}}{\sum_{i=1}^{n} p(x_i) l_i} \tag{10.69}$$

FIGURE 10.10 Instantaneous and noninstantaneous codes

Source symbols	Code 1 (noninstantaneous)	Code 2 (instantaneous)
x_1	0	0
x_2	01	10
x_3	011	110
x_4	0111	1110

where $p(x_i)$ is the probability of the ith source symbol and l_i is the length of the codeword corresponding to the ith source symbol. It can be shown that the minimum average word length is given by

$$\bar{L}_{\min} = \frac{H(X)}{\log_2 D} \tag{10.70}$$

where $H(X)$ is the entropy of the message ensemble being encoded and D is the number of symbols in the encoding alphabet. This yields.

$$\text{Efficiency} = \frac{H(X)}{\bar{L} \log_2 D} \tag{10.71}$$

or

$$\text{Efficiency} = \frac{H(X)}{\bar{L}} \tag{10.72}$$

for a *binary* alphabet. It is worth noting that if the efficiency of a code is 100%, the average word length $\bar{L}$ is equal to the entropy, $H(X)$.

Entropy of an Extended Binary Source

In many problems of practical interest, the efficiency is improved by coding the nth-order extension of a source. This is exactly the scheme used in the example of source encoding in a previous subsection. Computation of the efficiency of each of the three schemes used involves calculating the efficiency of the extended source. The efficiency can, of course, be calculated directly, using the symbol probabilities of the extended source, but there is an easier method.

The entropy of the nth-order extension of a discrete memoryless source $H(X^n)$ is given by

$$H(X^n) = nH(X) \tag{10.73}$$

This is easily shown by representing a message sequence from the output of the nth source extension as $(i_1, i_2, \ldots, i_n)$, where i_k can take on one of two states with probability p_{i_k}. The entropy of the nth-order extension of the source is

$$H(X^n) = -\sum_{i_1=1}^{2}\sum_{i_2=1}^{2}\cdots\sum_{i_n=1}^{2}(p_{i_1}p_{i_2}\cdots p_{i_n})\log_2(p_{i_1}p_{i_2}\cdots p_{i_n}) \quad (10.74)$$

or

$$H(X^n) = -\sum_{i_1=1}^{2}\sum_{i_2=1}^{2}\cdots\sum_{i_n=1}^{2}(p_{i_1}p_{i_2}\cdots p_{i_n})(\log_2 p_{i_1} + \log_2 p_{i_2} + \cdots + \log_2 p_{i_n}) \quad (10.75)$$

We can write the preceding expression as

$$\begin{aligned} H(X^n) = &-\sum_{i_1=1}^{2} p_{i_1}\log_2 p_{i_1}\left[\sum_{i_2=1}^{2} p_{i_2}\sum_{i_3=1}^{2} p_{i_3}\cdots\sum_{i_n=1}^{2} p_{i_n}\right] \\ &-\left[\sum_{i_1=1}^{2} p_{i_1}\right]\sum_{i_2=1}^{2} p_{i_2}\log_2 p_{i_2}\left[\sum_{i_3=1}^{2} p_{i_3}\cdots\sum_{i_n=1}^{2} p_{i_n}\right]\cdots \\ &-\left[\sum_{i_1=1}^{2} p_{i_1}\sum_{i_2=1}^{2} p_{i_2}\cdots\sum_{i_{n-1}=1}^{2} p_{i_{n-1}}\right]\sum_{i_n=1}^{2} p_{i_n}\log_2 p_{i_n} \end{aligned} \quad (10.76)$$

Each term in brackets is equal to 1. Thus

$$H(X^n) = -\sum_{k=1}^{n}\sum_{i_k=1}^{2} p_{i_k}\log_2 p_{i_k} = \sum_{k=1}^{n} H(X) \quad (10.77)$$

which yields

$$H(X^n) = nH(X)$$

The efficiency of the extended source is therefore given by

$$\text{Efficiency} = \frac{nH(X)}{\bar{L}} \quad (10.78)$$

If efficiency tends to 100% as n approaches infinity, it follows that $\bar{L}/n$ tends to the entropy of the extended source. This is exactly the observation made from Figure 10.9.